SANDIA REPORT
SAND2006-7676
Unlimited Release
Printed December 2006

Integrated System Dynamics Toolbox For Water Resources Planning

Vincent C. Tidwell, Leonard A. Malczynski, Howard D. Passell, William J. Peplinski, Marissa D. Reno, Janie Chermak, David Brookshire, Jennifer Thacher, Kristine Grimsrud, Craig Broadbent, Jason Hanson, Jesse F. Roach, Enrique Vivoni, Carlos Aragon, Heather Hallett, Kristan Cockerill, and Don Coursey

Prepared by
Sandia National Laboratories
Albuquerque, New Mexico 87185 and Livermore, California 94550

Sandia is a multiprogram laboratory operated by Sandia Corporation,
a Lockheed Martin Company, for the United States Department of Energy's
National Nuclear Security Administration under Contract DE-AC04-94AL85000.

Issued by Sandia National Laboratories, operated for the United States Department of Energy by Sandia Corporation.

Available to DOE and DOE contractors from
U.S. Department of Energy
Office of Scientific and Technical Information
P.O. Box 62
Oak Ridge, TN 37831

Telephone: (865) 576-8401
Facsimile: (865) 576-5728
E-Mail: reports@adonis.osti.gov
Online ordering: http://www.osti.gov/bridge

Available to the public from
U.S. Department of Commerce
National Technical Information Service
5285 Port Royal Rd.
Springfield, VA 22161

Telephone: (800) 553-6847
Facsimile: (703) 605-6900
E-Mail: orders@ntis.fedworld.gov
Online order: http://www.ntis.gov/help/ordermethods.asp?loc=7-4-0#online

SAND2006-7676
Unlimited Release
Printed December 2006

Integrated System Dynamics Toolbox For Water Resources Planning

Vincent Tidwell, Len Malczynski,
Howard Passell, Will Peplinski,
Marissa Reno, and Jesse Roach
Geohydrology Department 6313
Sandia National Laboratories
P.O. Box 5800
Albuquerque, NM 87185-0735

Janie Chermak, David Brookshire,
Jennifer Thacher, Kristine Grimsrud,
Craig Broadbent, and Jason Hanson
The University of New Mexico
Department of Economics
1915 Roma NE/ Economics Building
Albuquerque, NM 87131-1101

Enrique Vivoni, Carlos Aragon,
and Heather Hallett
New Mexico Tech, Department of
Earth and Environmental Sciences
801 Leroy Place, MSEC 244
Socorro, NM 87801

Kristan Cockerill
Cockerill Consulting
207 Cecil Miller Rd #2
Boone, NC 28607

Don Coursey
University of Chicago
Graduate of Public Policy Studies, 130 Harris
5801 South Ellis
Chicago, IL 60637

Abstract

Public mediated resource planning is quickly becoming the norm rather than the exception. Unfortunately, supporting tools are lacking that interactively engage the public in the decision-making process and integrate over the myriad values that influence water policy. In the pages of this report we document the first steps toward developing a specialized decision framework to meet this need; specifically, a modular and generic resource-planning "toolbox."

The technical challenge lies in the integration of the disparate systems of hydrology, ecology, climate, demographics, economics, policy and law, each of which influence the supply and demand for water. Specifically, these systems, their associated processes, and most importantly the constitutive relations that link them must be identified, abstracted, and quantified. For this reason, the toolbox forms a collection of process modules and constitutive relations that the analyst can "swap" in and out to model the physical and social systems unique to their problem. This toolbox with all of its modules is developed within the common computational platform of system dynamics linked to a Geographical Information System (GIS).

Development of this resource-planning toolbox represents an important foundational element of the proposed interagency center for Computer Aided Dispute Resolution (CADRe). The Center's mission is to manage water conflict through the application of computer-aided collaborative decision-making methods. The Center will promote the use of decision-support technologies within collaborative stakeholder processes to help stakeholders find common ground and create mutually beneficial water management solutions. The Center will also serve to develop new methods and technologies to help federal, state and local water managers find innovative and balanced solutions to the nation's most vexing water problems. The toolbox is an important step toward achieving the technology development goals of this center.

ACKNOWLDEGEMENTS

The authors wish to acknowledge the support, help, and review provided by a wide range of individuals throughout the duration of this project. Specific reference is made to individuals at the end of the chapters to which they contributed. The authors also wish to acknowledge that funding for this project was provided by Sandia National Laboratories' Laboratory Directed Research and Development Program.

TABLE OF CONTENTS

LIST OF FIGURES

LIST OF TABLES

ACRONYMS

ACS	*American Community Survey*
AF	acre feet
amsl	above mean sea level
BDA	Bosque del Apache
BLS	Bureau of Labor Statistics
BoR	Bureau of Reclamation
CADRe	Computer Aided Dispute Resolution
CDWR	Colorado Department of Water Resources
cfs	cubic feet per second
CRS	Captive Release Scenario
CVM	contingent valuation method
DM	demographic model
EAC	elevation-area-capacity
EBID	Elephant Butte Irrigation District
EPA	Environmental Protection Agency
ET	evapotranspiration
ETTB	ET Toolbox
GDD	growing degree day
GIS	Geographical Information System
GW	groundwater
HLH	Hi-Lo-Hi
HRU	hydrologic response unit
I/O	input/output
LFCC	low flow conveyance channel
MAF	million acre feet
MRG	Middle Rio Grande
MRGCD	Middle Rio Grande Conservancy District
NAICS	North American Industry Classification System
NASS	National Agricultural Statistics Service
NCDC	National Climatic Data Center
NMCC	New Mexico Climate Center
NMICA	*New Mexico Information for Community Assessment*

RGSM	Rio Grande silvery minnow
RMSE	root mean square error
RR	Reference Run
SA	sensitivity analysis
SAC	SA coefficient
SAHRA	Semi-Arid Hydrology and Riparian Areas
SJC	San Juan Chama
SOC	Standard Occupations Classification System
SSWRP	South Side Water Reclamation Plant
SW	surface water
TCM	travel cost method
URGWOM	Upper Rio Grande Water Operations Model
USACE	U.S. Army Corps of Engineers
USGS	United States Geological Survey
VIC	Variable Infiltration Capacity
WTP	willingness to pay

1. PROJECT DESCRIPTION AND BACKGROUND

Vincent Tidwell, Sandia National Laboratories

1.1 Justification

Persistent conflict between competing interests is becoming more common in water resources management today. Such conflict often results in gridlock (i.e., no decision, continuation of the status-quo) or a protracted and inefficient decision process that is too often resolved through litigation, resulting in only marginal change while imposing exceedingly high transaction costs. In many cases, it simply takes too long and costs too much to make major water resources decisions – and after all that, we often fail to achieve broad consensus in the decisions. Such difficulties arise because of both the complexity of the natural system and the disparity with which water is valued within the community. Finding solutions to these complex problems requires interdisciplinary and multivalued thinking. No single person or institution has a complete knowledge or experience base from which to tackle these problems. For this reason, a process is needed that brings the entire community together so as to expand the collective thinking. Just as the old Jewish proverb states:

"Plans fail for lack of counsel, but with many advisors they succeed."

Beyond the collaborative process there is a need for tools to help structure group thinking and to provide a vehicle for communicating joint understanding within and external to the team. Integration of collaborative processes with interactive decision-support tools provides a venue where group learning can take place, and leads to the identification of mutual gain solutions.

Previous efforts demonstrate the value of applying technically informed collaborative planning and management methods. These methods involve open, collaborative decision-making processes (Connick and Innes 2003; Spash 2001; Claussen 2001; Susskind et al. 2001; Serageldin 1995; Potapchuk 1991) supported by transparent computer models (Tidwell et al. 2004, in press; Costanza and Ruth 1998; van den Belt 1998; Palmer 1993; Johnson 1990; Wallace and Sancar 1988; Jordão et al. 1997). In fact, most water management processes today incorporate some degree of public involvement and collaboration, and most use computer modeling to support analysis and decision making. However, there is still room for improvement in the way traditional planning, public collaboration, and decision-support computer modeling are integrated. Specifically, we suggest an approach that is different in two important ways. First, public collaboration is encouraged in every aspect of the planning process including data gathering and model development so as to establish a foundation of full disclosure and transparency. Giving stakeholders and public representatives more control over technical analysis and the resulting decision-support models builds trust in the process that can help avoid battles of "dueling science." Second, the cooperatively developed tools provide a portal in which resource managers, decision makers, and stakeholders alike can personally interact with the best available science. In this way, stakeholders can jointly or independently formulate and evaluate new management options, identify tradeoffs, and gain understanding of system behavior. Incorporating rigorous yet accessible analytical tools into collaborative processes empowers stakeholders with greater responsibilities to tackle difficult problems, something often lacking in collaborative decision making today.

Although both a desire for collaboration and the use of computer models are fairly standard in resource management, collaborative modeling methods are relatively new. Various government and nongovernmental organizations have made initial efforts at combining collaboration and modeling but only a few techniques have been developed and relatively few tools have been tailored toward these kinds of techniques. As such, a new generation of computer-aided decision tools are needed that interactively engage the public in the decision-making process and integrate over the myriad values that influence water policy. Specifically, modules of both physical and social processes are needed that can be linked together to capture the unique dynamics of a watershed within the context of a transparent, stakeholder-accessible system dynamics model.

1.2 Objective

Our objective is to develop a resource-planning toolbox to support collaborative watershed management and foster communication between water professionals, decision-makers, and the public. This decision toolbox will integrate the broad physical and social dynamics that define the balance between water supply and demand. The toolbox will be formulated in a fully generic context allowing application to a wide variety of watersheds across the United States and abroad.

1.3 Approach

To create a truly multidisciplinary model requires the assemblage of a multidisciplinary team united in their systems thinking. The team included hydrologists, economists, ecologists, aquatic chemists, watershed scientists, policy analysts, water attorneys, and system modelers. The team was comprised of expertise found both within Sandia and from external sources, including a private consulting firm, the University of New Mexico, New Mexico Institute of Mining and Technology, the University of Arizona, and the University of Chicago.

The team's first task was to develop a "toolbox" conceptual model. This was necessary to organize the overall system into interacting subsystems, while defining the basic processes and constitutive relations which comprise them. Critical subsystems include land surface processes, which encompass precipitation (snow and rain) runoff relations subject to varying vegetation cover and land use practices; surface water hydrology including river routing, tributary inflow and irrigation diversions; groundwater hydrology, subject to river leakage, groundwater pumping and recharge; water quality subject to point and non-point source loading; and environmental health, which tracks the dynamics of riparian and aquatic communities in the basin. In turn, these subsystems are influenced by the temporally variable demands represented by irrigated agriculture, municipal consumption, riparian evapotranspiration, and open-water evaporation subject to applicable legal and political constraints. Finally, alternative water use strategies are integrated as a unique subsystem to allow evaluation of how effectively the alternative can utilize the available water and to quantify its resulting economic and environmental benefit to the region.

It is important to note that these systems are not static in time but rather behave dynamically, expressing the complex interplay of processes that underlie these systems. Additionally, these systems do not operate independently but in complex networks characterized by numerous feedbacks and time delays. That is, the dynamics of one process may depend on the behavior of

one or more related processes. Thus, a second aspect of this task, and the most challenging, was to identify the constitutive relations linking disparate processes comprising the water budget. This involved understanding the strength of cause-and-effect relationships, and determining whether the response is immediate or delayed in time.

The next task in the model development effort involved quantifying and structuring the component processes identified in the model conceptualization phase. Furthermore, this disparate set of processes needed to be integrated within a unified framework under a single computational platform. To maintain a tractable solution to this problem, we adopted a system dynamics platform for creating the resource planning toolbox. More detail on system dynamics is given below.

Another important aspect of this work was creating an interface that effectively conveys results to policy-makers and the public. To accomplish this desire, we created an interactive modeling environment comprised of a number of user-friendly interfaces. The interfaces allow the user to easily change external factors influencing water supply (e.g., climate, population growth), policies governing water allocations, and alternative water use strategies. Additional interfaces then convey model output in terms of shifts in water use among different water use sectors, ability to meet legal obligations, changes to in-stream flows, and others.

The final phase of modeling involved calibrating and testing the resource planning toolbox. Specifically, toolbox modules were structured according to the physical and social system governing flows in the Middle Rio Grande Basin, defined here as the stretch of Rio Grande between the Colorado/New Mexico border and Elephant Butte Reservoir. The model was implemented and parameterized according to the best available data. Subsequently, model simulations were calibrated against measured basin data on a monthly basis for a 25-year period of time (1975–1999).

1.4 Model Architecture

Selection of an appropriate architecture for the toolbox model is based on two criteria. First, an environment is needed that provides an "integrated" view of the watershed — one that couples the complex physics governing water supply with the diverse social and environmental issues driving water demand. Second, a modeling environment is needed that can be taken directly to the public for involvement in the decision process and for educational outreach. For these reasons we have adopted an approach based on the principles of system dynamics (Forrester 1990; Sterman 2000). System dynamics provides a unique framework for integrating the disparate physical and social systems important to water resource management, while providing an interactive environment for engaging the public.

System dynamics is a systems-level modeling methodology developed at the Massachusetts Institute of Technology in the 1950s as a tool for business managers to analyze complex issues involving the stocks and flows of goods and services. System dynamics is formulated on the premise that the structure of a system – the network of cause-and-effect relations between system elements – governs system behavior (Sterman 2000). "The systems approach is a discipline for seeing wholes, a discipline for seeing the structures that underlie complex domains. It is a

framework for seeing interrelationships rather than things, for seeing patterns of change rather than static snapshots, and for seeing processes rather than objects" (Simonovic and Fahmy 1999).

In system dynamics a problem is often decomposed into a temporally dynamic, spatially aggregated system. The scale of the domain can range from the inner workings of a human cell to the size of global markets. Systems are modeled as a network of stocks and flows. For example, the change in volume of water stored in a reservoir is a function of the inflows less the outflows. Key to this framework is the feedback between the various stocks and flows comprising the system. In our reservoir example, feedback occurs between evaporative losses and reservoir storage through the volume/surface area relation for the reservoir. Feedback is not always realized immediately but may be delayed in time, representing another critical feature of dynamic systems.

There are a number of commercially available, object-oriented simulation tools that provide a convenient environment for constructing system dynamics models. For purposes of this effort, the resource planning toolbox is developed in Studio Expert 2005, produced by Powersim, Inc. (www.powersim.com). Model construction proceeds in a graphical environment, using objects as building blocks. These objects are defined with specific attributes that represent individual physical or social processes. These objects are networked together so as to mimic the general structure of the system. In this way, these tools provide a structured and intuitive environment for model development.

1.5 Summary of Results

The result of this work is a generic resource-planning toolbox to support collaborative watershed management and foster communication between water professionals, decision makers, and the public. Within this toolbox resides the overall framework by which an analyst can build a basin-specific model. Comprising the toolbox are subsystem modules and constitutive relations that the analyst can "swap" in and out to capture the physical and social systems important to their problem. This modularity allows the creation of sophisticated, highly integrated models that water professionals can use as well as simplified models aimed at public outreach. This modular toolbox is formulated in system dynamics and subsequently linked to a Geographical Information System (GIS) interface. Toolbox applications are possible at the aggregate watershed scale or the subwatershed scale in which key systems (i.e., land surface, groundwater, surface water) are spatially discretized. Temporal resolution of the toolbox is equally flexible, with options ranging from daily to annual.

This toolbox provides a comprehensive resource planning framework that integrates the disparate systems of hydrology, ecology, climate, population, economics, policy, and water law into a coherent decision-support system that is fully generic, allowing application to a wide variety of watersheds spanning a broad range of scales. The intention is that in time the model will be adopted by resource managers at the local, state, and federal levels as their tool of choice for resolving difficult water allocation problems. Finally, development of this resource-planning toolbox represents an important foundational element of the proposed interagency center for Computer Aided Dispute Resolution (CADRe). The Center's mission is to manage water

conflict through the application of computer-aided collaborative decision-making methods. The Center will promote the use of decision-support technologies within collaborative stakeholder processes to help stakeholders find common ground and create mutually beneficial water management solutions. The Center will also to serve to develop new methods and technologies to help federal, state and local water managers find innovative and balanced solutions to the nation's most vexing water problems. The toolbox is an important step toward achieving the technology development goals of this center.

1.6 Report Outline

The technical content of this report is organized according to a set of stand-alone papers that will be submitted to individual peer-reviewed journals over the next several months. Each chapter contains a separate paper, each dealing with a unique subsystem or set of subsystems that comprise the toolbox. However, these chapters are related to one another through the common toolbox development theme as well as a common basis for model demonstration and testing (i.e., the Middle Rio Grande). In the following, a brief description of each chapter and associated subsystem modules is given.

Surface Water Process Modules: This chapter covers the basic elements pertaining to river routing, including reservoir processes, reservoir operations, open water evaporation, irrigation diversions and conveyance processes, crop and riparian evapotranspiration, municipal waste water returns, and surface-groundwater interaction. Modeling is structured according to a reach-based approach with reaches defined by gages or other key inflows/diversions.

Groundwater Process Modules: Groundwater flow processes are covered in this chapter. Processes include groundwater flow, recharge, surface-groundwater interaction, riparian evapotranspiration, groundwater pumping, and spatially varying groundwater head distributions. A spatially distributed, unstructured computational grid approach forms the overarching framework for this modeling.

Land Surface Process Modules: The surface water and groundwater systems receive tributary inflows and recharge, respectively, from precipitation falling on the adjoining watersheds. The land surface model quantifies these precipitation-runoff-recharge processes. The model treats individual watersheds, disaggregating the system into hydrologic response units. Within each unit falling precipitation (as snow or rain) is partitioned into canopy capture, runoff, direct evaporation, infiltration, change in soil moisture, evapotranspiration, interflow, or deep recharge.

Water Quality Modules: A description of modules used to simulate the transport of conservative solutes is detailed in this chapter. Sources, sinks and mixing both in the surface and groundwater systems are addressed. Chloride and bromide concentrations measured in the Rio Grande are used to calibrate and verify the model.

Ecologic Process Modules: In this chapter a fish ecology module is developed and tested. The model considers fish fertility and mortality as influenced by river discharge and ammonium concentration. The model also considers ease of fish migration and the impact of stocking from

off-stream refugia on the fish population. Application is drawn with the Rio Grande Silvery Minnow.

Economic Process Modules: This chapter explores the relation between water and the economy. There are two economic levels that are included in the model: micro-level components and the overall, regional macro economy. Within the micro theme area, we consider the following sectors: urban residential, agricultural, commercial, industrial, institutional, shoreline use, birding, and non-use values (instream use). Market microeconomic components impact the regional or macro economy through their impact on productivity and employment. Both levels, in turn, impact the demand for water.

Water Marketing Process Modules: The focus of this chapter is the development of decision-support tools for the exploration and design of water markets. Here we describe the decision-support framework and test the framework through a set of experiments involving stakeholders and the public.

Collaborative Modeling Process: The previous chapters have dealt exclusively with the conceptualization, formulation, and testing of physical and social process modules. This paper describes several collaborative modeling projects that provide a diverse array of experience and lessons learned concerning collaborative modeling processes. The experiences reported here are included to provide insight into how to "do" collaborative modeling.

2. SURFACE WATER PROCESS MODULES

Jesse Roach, University of Arizona
Vincent Tidwell, Sandia National Laboratories

2.1 Introduction

As fresh-water resources in the western United States and the world are pushed beyond their sustainable limits by new and growing demands, increased efficiency in management of water resources is of critical importance if water managers are to reduce social conflict and environmental damages often associated with water scarcity. As pointed out by Jury and Vaux (2005), science can play a role in improving water management efficiency, but the science must be integrated, multidisciplinary, interdisciplinary, basin-scale in scope, and, most important, communicated effectively to water managers. Computer models and simulations can provide a very effective way to integrate interdisciplinary science on large temporal and spatial scales. If the simulations are rapid and user-friendly, the computer model itself becomes a vehicle for informing policy decisions with science. Rapid, basin scale, multidisciplinary computer simulations represent a tremendous tool for informing water management with scientific knowledge.

Models to aid in improved water management efficiency must address dynamics in the surface water, groundwater, and land surface systems and their accompanying feedback. This and the following two chapters, respectively, address these systems. Each of these systems is formulated according to a dynamic water budget. Components contributing to the surface water balance include river routing, reservoir operations, open water evaporation, riparian evapotranspiration, river diversion, return flows, and groundwater interaction. These processes are subject to agricultural, municipal, industrial and environmental demands as managed by the built infrastructure and operated according to defined policies, water rights, and water management institutions.

The objective of this chapter focuses on the development of a physically based monthly timestep model of surface water dynamics that can be used as the hydrologic foundation for real-time scenario evaluation by stakeholders, policy makers, and the interested public. Process modules comprising the model are formulated in a completely generic manner, allowing extension to most any surface water system. However, in efforts to focus development and to provide a basis for verification and testing, surface water process modules are described in the specific context of the Middle Rio Grande.

2.2 Model Development

2.2.1 Spatial and Temporal Extent and Resolution

The physical setting of the model is the Rio Grande system extending from the surface water gage near Lobatos, Colorado (managed by the Colorado State Engineer), 6 miles upstream of the Colorado–New Mexico state line (USACE et al. 2002), to the outlet of Caballo Reservoir, some 363 river miles downstream. Two major tributaries, the Rio Chama and Jemez Rivers, are also modeled. The spatial resolution of the model was defined by surface water gage locations with

periods of significant historic record. Consistent with an existing routing and operations model known as the Upper Rio Grande Water Operations Model (URGWOM) (USACE et al. 2002) the river system was divided into 17 conceptual spatial units referred to as reaches. For a detailed physical description of each reach, consult the URGWOM Physical Model Documentation (USACE et al. 2002). In addition to the river reaches, seven reservoirs are modeled explicitly, three in the Chama drainage (Heron, El Vado, Abiquiu), one on the Jemez River (Jemez), and three on the Rio Grande (Cochiti, Elephant Butte, Caballo). The physical extent of the model, including reservoir and gage locations, is shown in Figure 2-1. The surface water gages used for input and calibration are listed in Table 2-1 and Table 2-2 respectively, along with relevant physical information.

The model runs on a monthly timestep, and uses the period from 1975 to 1999 for calibration, 2000 to 2006 for validation, and runs forward from 2006 in scenario evaluation mode. During the calibration period, parameters in the model are manipulated to match observed stream flows at gages listed in Table 2-2 as closely as possible at each timestep, and with no net error for the 25-year calibration period. During the validation period, the calibrated model is run using observed hydrologic and climatic conditions as inputs, and the behavior of the model is compared to observations at the internal stream gages (Table 2-2). This comparison sheds some light on the relative certainty of the model for making predictions with a set of known inputs. Finally, the scenario evaluation mode is used to run the model several decades into the future with user-determined hydrologic and climatic inputs, with the goal of exploring possible hydrologic outcomes to a variety of user-determined scenarios. The monthly timestep allows the model to be small enough and fast enough to run multiyear scenarios in a matter of seconds on a personal computer, while still capturing the seasonal variability that characterizes the surface water system.

Inputs will be discussed in more detail in Section 2.2.3; however, an overview of temporally varying inputs is provided here. Major temporally varying inputs include total gaged surface water flows at the model boundary (Table 2-1), and monthly climate data including temperature (average max, average min, and mean), mean relative humidity, mean windspeed, total solar radiation, total precipitation, reservoir ice cover, and reservoir pan evaporation. Observed historic values for these data are used for calibration and validation input, and are shuffled by historic year to generate coupled hydrologic and climatic inputs for scenario evaluation. Human groundwater extraction and wastewater returns to the river are based on historic data for the calibration and validation period, and modeled as a function of human water use patterns during scenario evaluation. Other temporally varying input data include agricultural and riparian areas by plant type. In this case, estimates of historic values are used during calibration and validation, while user inputs determine the values for future runs. Treatment of human water use patterns is described in Chapter 7. Mountain front and tributary recharge inputs to the groundwater system are essentially constant for all periods.

As will be evident throughout this paper, development of this monthly model of the surface water system was aided tremendously by the data collection and conceptual model development of URGWOM. Coordinated development of this tool with the URGWOM team has occurred to create a fast, simple, and interactive complement to their daily model.

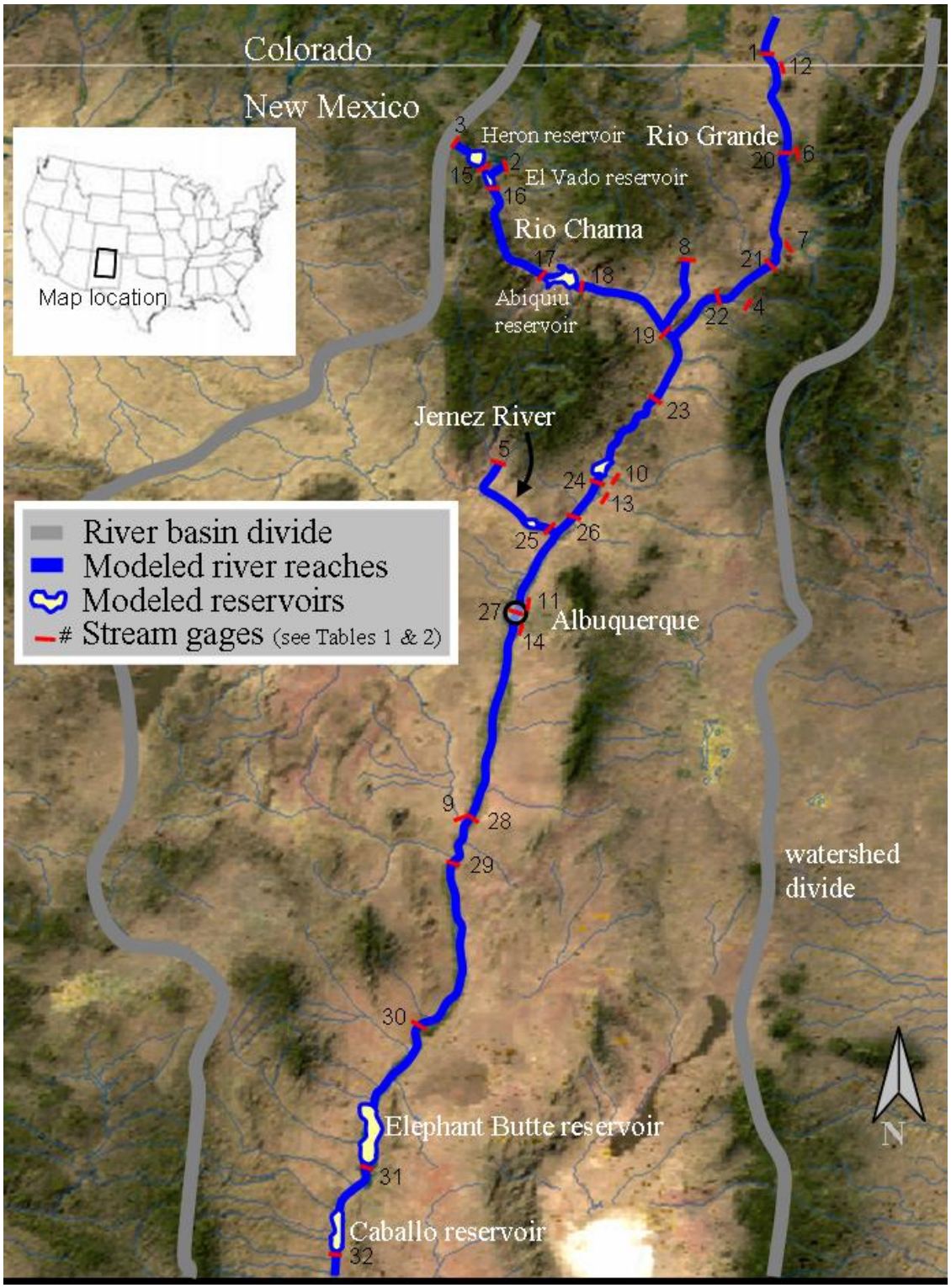

Figure 2-1. Physical extent of model and reach locations as defined by gage locations. Gages are identified with numbers corresponding to specific gage information in Tables 2-1 and 2-2. Gages numbered 1–14 provide input to the model, and are numbered beginning with the largest 1975–1999 input to the model, followed by the second largest, etc. Gages numbered 15–32 provide movement and calibration information within the model extent.

Table 2-1. Gages used for input.
The numbers in the final column refer to the gage locations as shown in Figure 2-1. The Rio Grande near Lobatos gage is operated by the Colorado Department of Water Resources (CDWR), and the Azotea tunnel outlet gage is operated by the United States Bureau of Reclamation (BoR). All other gages are operated by the United States Geological Survey (USGS). Data from www.usgs.gov and URGWOM documentation (USACE et al. 2002).

Gage	USGS Gage#	Average Annual Input 1975-99 [af/yr]	% of Gaged Inputs [%]	Contrib Drainage Area [mi^2]	Datum Elev [ft amsl]	~Lat [dd]	~Long [dd]	Fig 2-1 ID#
Rio Grande near Lobatos	CDWR	386200	34%					1
Rio Chama near La Puente	8284100	295300	26%	480	7083	36.66	106.63	2
Azotea tunnel outlet	BoR	97100	9%					3
Embudo Creek at Dixon	8279000	72500	6%	305	5859	36.21	105.91	4
Jemez River near Jemez	8324000	65100	6%	470	5622	35.66	106.74	5
Red River below Fish Hatchery	8266820	58300	5%	185	7105	36.68	105.65	6
Rio Pueblo de Taos below Los Cordovas	8276300	57900	5%	380	6650	36.38	105.67	7
Rio Ojo Caliente at La Madera	8289000	56900	5%	419	6359	36.35	106.04	8
Rio Puerco near Bernardo	8353000	23100	2%	6220	4722	34.41	106.85	9
Santa Fe River above Cochiti	8317200	8700	1%	231	5505	35.55	106.23	10
North Floodway Channel near Alameda	8329900	7300	1%	88	5015	35.20	106.60	11
Costilla Creek near Garcia	8261000	6500	1%	200	7821	36.99	105.53	12
Galisteo Creek Below Galisteo Dam	8317950	4200	0%	597	5450	35.46	106.21	13
Tijeras Arroyo near Albuquerque	8330600	300	0%	128	4999	35.00	106.65	14

Table 2-2. Gages used for calibration.
The numbers in the final column refer to the gage locations as shown in Figure 2-1.
The Willow Creek below Heron and Rio Grande below Caballo gages are operated by the United States Bureau of Reclamation (BoR). All other gages are operated by the United States Geological Survey (USGS). Data from www.usgs.gov and URGWOM documentation (USACE et al. 2002).

Gage	USGS Gage#	Contrib Drainage Area [mi^2]	Datum Elev [ft amsl]	Average Annual Flow 1975-99 [af/yr]	River Mile (above mouth) [mile]	~Lat dd	~Long dd	Fig 2-1 ID#
Willow Creek below Heron	BoR			96900				15
Rio Chama below El Vado	8285500	777	6696	373900	76	36.58	106.72	16
Rio Chama abv Abiquiu Reservoir	8286500	1500	6280	396700	47	36.32	106.60	17
Rio Chama below Abiquiu Dam	8287000	2047	6040	414800	31	36.24	106.42	18
Rio Chama near Chamita	8290000	3044	5654	464500	3	36.07	106.11	19
Rio Grande near Cerro	8263500	5500	7110	418700	1693	36.74	105.68	20
Rio Grande blw Taos Junction Bridge	8276500	6790	6050	619100	1658	36.32	105.75	21
Rio Grande at Embudo	8279500	7460	5789	685200	1643	36.21	105.96	22
Rio Grande at Otowi	8313000	11360	5488	1200600	1614	35.87	106.14	23
Rio Grande below Cochiti	8317400	11960	5226	1095300	1588	35.62	106.32	24
Jemez River blw Jemez Canyon Dam	8329000	1038	5096	54900		35.39	106.53	25
Rio Grande at San Felipe	8319000	13160	5116	1166600	1573	35.44	106.44	26
Rio Grande at Albuquerque	8330000	14500	4946	1072300	1540	35.09	106.68	27
Rio Grande Floodway nr Bernardo	8332010	19230	4723	953300	1487	34.42	106.80	28
Rio Grande Floodway at San Acacia	8354900	23830	4655	838600	1473	34.26	106.89	29
Rio Grande Floodway at San Marcial	8358400	24760	4242	779100	1425	33.68	106.99	30
Rio Grande blw Elephant Butte Dam	8361000	26510	4241	757500	1382	33.15	107.21	31
Rio Grande blw Caballo Dam	BoR			752400				32

2.2.2 Conceptual Model

The upper Rio Grande river system is fed primarily by snow melt from the San Juan and Sangre de Cristo mountains, which define the northwestern and eastern boundaries of the basin respectively. Water moves into the river system via surface water inflows and return flows, groundwater seepage, and direct precipitation onto open water. Water is also diverted from the San Juan river system, through tunnels under the continental divide and into the Rio Chama system. This interbasin water, moved from the Colorado Basin to the Rio Grande Basin, is known as San Juan Chama (SJC) water. Water is lost from the river system by surface water diversions, leakage to the groundwater system, and open water evaporation to the atmosphere. Riparian evapotranspiration (ET) removes water from a shallow groundwater system, which is in rapid exchange with the river. Water diverted for agricultural irrigation use can be lost to the groundwater system through conveyance system leakage (ditches and canals) and crop seepage, and lost to the atmosphere via crop ET and open water evaporation. In some reaches groundwater discharges to the surface water system by seepage into agricultural drains.

With respect to water balance, land use, and groundwater use, the river system within the model extent is significantly different above Cochiti Reservoir than it is below. In general, the reaches upstream of Cochiti Reservoir tend to gain water from groundwater and tributary inflows faster than it is lost to the atmosphere, while in the reaches downstream of Cochiti atmospheric losses are greater and tributary inputs modest. As a result, flows tend to increase above Cochiti and decrease below, as shown in Figure 2-2. Perhaps partially as a result of this change from gaining to losing, the groundwater system south of Cochiti is fairly well studied and characterized, while the characterization of the groundwater system upstream, especially upstream of the confluence of the Rio Chama and Rio Grande, is more limited. Finally, the majority of land within the model extent that is practicably irrigable by surface water diversion and gravity application lies below Cochiti Reservoir, resulting in significant amounts of water moving through agricultural conveyance systems (canals, ditches, and drains) below that point, as shown in Table 2-3.

2.2.3 Mathematical Model

2.2.3.1 Governing Equations

2.2.3.1.1 River Reach Mass Balance

Employing mass balance, the amount of water that flows out of a given river reach can be expressed mathematically as a function of inflows, outflows, and change in storage within the reach. At a monthly timestep, the change in storage in a river reach is assumed to be negligible with respect to the other flows through the reach, and precipitation gains to open water are also assumed to be negligible. The governing equation for a generic reach (j) is shown in Equation 2-1 below.

$$Q^{j}_{msout} = Q^{j}_{m\sin} + Q^{j}_{sw} + Q^{j}_{gwsw} - Q^{j}_{evap} \qquad (2\text{-}1)$$

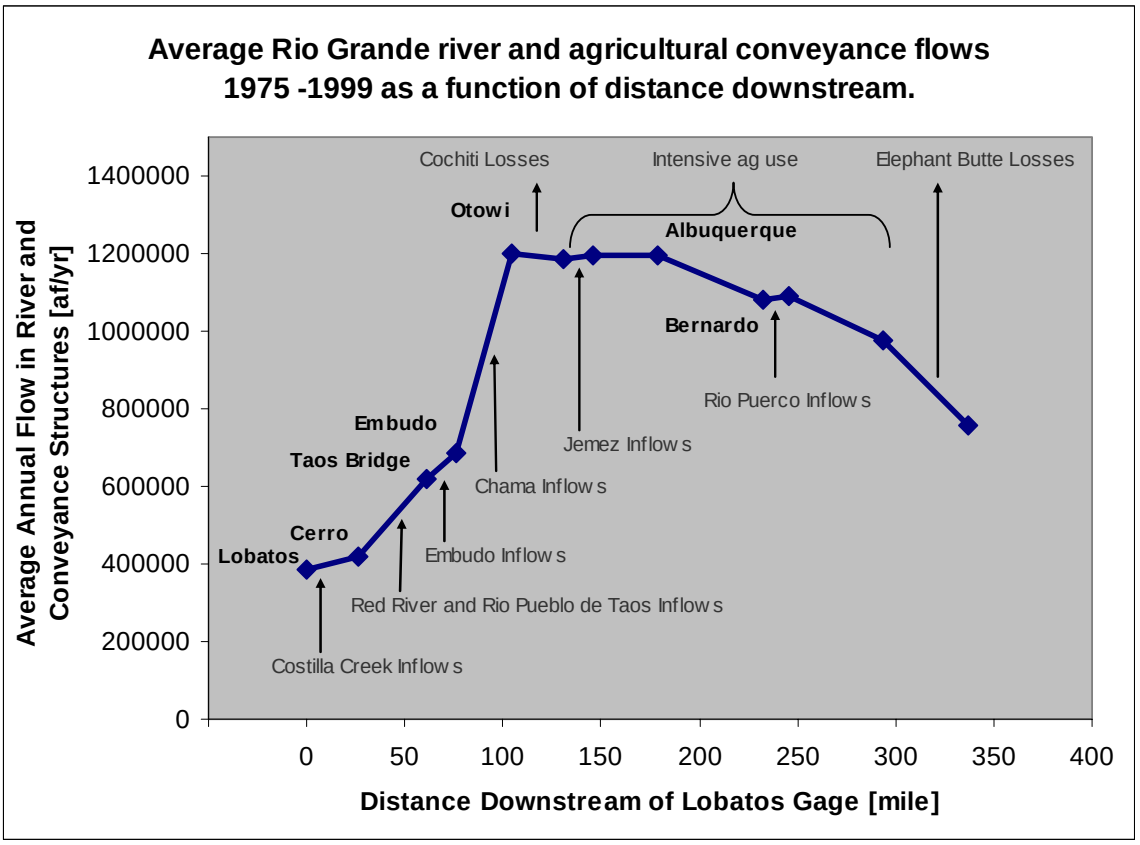

Figure 2-2. Average river and agricultural conveyance flows along Rio Grande 1975–1999. In general, river gains above Cochiti and loses below. Otowi to below Cochiti reach appears to lose because of Cochiti Reservoir losses.

Table 2-3. Percent of total flow past points south of Cochiti Reservoir that is in agricultural conveyance system. Irrigation season is March – October. Flows in the conveyance system are a largest percent of total in the late summer and fall as river flows drop, but agricultural demand remains high. Data from USGS gages listed in Table 2-2, as well as combined conveyance flow data from URGWOM model data (USACE et al. 2002).

Location	Irrigation season % flows in conveyance system 1975-99	August - October % flows in conveyance system 1975-99
Cochiti Pueblo	9%	19%
San Felipe	3%	6%
Albuquerque	12%	27%
Bernardo	13%	32%
San Acacia	22%	26%
San Marcial	19%	34%
Average	13%	23%

In Equation 2-1, Q^j_{msout} represents mainstem flow out of the bottom of reach j, which is the location of the gage representing the lower end of the reach. The term $Q^j_{m\sin}$ represents mainstem flow into reach *j*, from the reach above or a gage on the model boundary. If reach *i* is immediately above reach *j*, the flow out of reach *i* is the same as the flow into reach *j*: $Q^i_{msout} = Q^j_{m\sin}$. The term Q^j_{gwsw} represents the net sum of all interactions between the river and groundwater system in the reach, and is positive for a groundwater gaining reach, and negative for a groundwater losing reach. The term Q^j_{evap} represents open water evaporative losses. The term Q^j_{sw} represents the net sum of all surface water inflows into and diversions out of the reach, as shown in Equation 2-2 below. The surface water inflows, diversions, and returns, may be gaged or ungaged.

$$Q^j_{sw} = Q^j_{swgaged} + Q^j_{swungaged} - Q^j_{swdiversion} + Q^j_{swreturn} \tag{2-2}$$

The terms $Q^j_{swgaged}, Q^j_{swungaged}, Q^j_{swdiversion}, Q^j_{swreturn}$ represent gaged and ungaged surface water inflows (tributaries) and surface water diversions and returns respectively. Below Cochiti Reservoir, the agricultural conveyance system is modeled as a parallel unit of mass balance to the river system. For these reaches, the diversion and return flow terms in Equation 2-2 serve as inflows and outflows for the conveyance system. Assuming that direct evaporation losses from conveyance features is negligible, mass balance in the conveyance system south of Cochiti Reservoir is modeled using Equation 2-3.

$$Q^j_{swdiversion} + Q^i_{convtf} = Q^j_{cropET} + Q^j_{convgw} + Q^j_{swreturn} + Q^j_{convtf} \tag{2-3}$$

Equation 2-3 states that surface water can enter the conveyance system by diversion from the associated reach ($Q^j_{swdiversion}$), or by through flow from the conveyance system immediately upstream (Q^i_{convtf}). Water is lost from the conveyance system to the atmosphere by ET from crops (Q^j_{cropET}). Conveyance water moves to the groundwater system as seepage from crops and canals, or moves from the groundwater system back to the conveyance system as seepage into drains. The groundwater exchange terms are lumped into a single conveyance to groundwater term (Q^j_{convgw}) in Equation 2-3 that can be positive or negative depending on the relative magnitude of the conveyance to groundwater system exchanges. Surface water flows out of the conveyance system to the river ($Q^j_{swreturn}$), or to the downstream conveyance system (Q^j_{convtf}).

As will be described in more detail in the following sections, the general strategy used to solve reach based mass balance (Equation 2-1) during the calibration period is to set the mainstem inflow term ($Q^j_{m\sin}$) using historic gage data. Open water evaporation losses (Q^j_{evap}) are estimated using channel geometry information and a reference ET from historic climate data input to a modified Penman Montieth equation. The groundwater exchange (Q^j_{gwsw}) is based either on a static exchange based on historic winter gage data or a coupled, dynamic groundwater model, depending on data available for a given reach. The surface water term (Q^j_{sw}) is found

using Equation 2-2, whose terms are set to historic gage values where available, and modeled otherwise. Crop ET losses for all reaches (Q^{j}_{cropET}) are modeled with a Penman Monteith based reference ET. In most reaches, the ungaged surface water inflow term ($Q^{j}_{swungaged}$) is used as a closure and calibration term. Downstream of Cochiti, the conveyance system is modeled using historic diversion ($Q^{j}_{swdiversion}$) and through flow (Q^{i}_{convtf}, Q^{j}_{convtf}) data, solving for unknown return flows ($Q^{j}_{swreturn}$) after evaporative losses and groundwater exchanges are accounted for. Groundwater to conveyance system flows (Q^{j}_{convgw}) are modeled with a coupled groundwater model, leaving return flows ($Q^{j}_{swreturn}$) as the only unknown in Equation 2-3. In reaches where the river system and conveyance system are coupled to a groundwater model, calibration involves a combination of ungaged surface inflows and/or parameter adjustments associated with the surface water groundwater connection, to best match historic gage data. Table 2-4 summarizes important information associated with the modeled reaches, including degree of groundwater coupling. The carriage water factor is explained in Section 2.2.3.2.8.

During validation and scenario evaluation, main stem flows into the reach ($Q^{j}_{m\sin}$) are set to gage data for reaches beginning on the model boundary, and to outflows from the reach above otherwise. Surface water diversions ($Q^{j}_{swdiversion}$) are modeled based on agricultural demand and historic diversion patterns. Water available to return ($Q^{j}_{swreturn}$) or flow into the next conveyance reach (Q^{i}_{convtf}, Q^{j}_{convtf}) is partitioned based on reach specific historic proportions. All other terms in Equations 2-1 through 2-3 are calculated as in the calibration period.

2.2.3.1.2 Reservoir Mass Balance

Seven reservoirs are included in the model. Table 2-5 summarizes basic information associated with the reservoirs. Reservoir mass balance is calculated according to Equation 2-4.

$$\Delta S^{r} = Q^{r}_{sw} + Q^{r}_{precip} - Q^{r}_{gw} - Q^{r}_{evap} - Q^{r}_{release} \qquad (2\text{-}4)$$

The change in storage for a given timestep at reservoir *r* (ΔS^{r}) is the sum of inflows minus outflows. Inflows include gaged and ungaged surface water inflows (Q^{r}_{sw}) to the reservoir, and gains from precipitation that falls directly on the reservoir surface (Q^{r}_{precip}). Outflows may include groundwater leakage from the reservoir (Q^{r}_{gw}), evaporation from the reservoir (Q^{r}_{evap}), and all releases (including spills) ($Q^{r}_{release}$) from the reservoir. In general, as will be discussed in more detail in the following sections, reservoirs were calibrated with historic gaged surface water inflows and releases, and calculated precipitation, evaporation, and groundwater leakage. Reservoir releases were set to historic for the calibration period, and modeled with operation rules for the validation and scenario evaluation periods.

Table 2-4. Reach summary table.
Irrigated agricultural acreage is an average of 1975–1999 values reported in URGWOM physical model documentation (USACE et al. 2002) and information from Rio Chama watermaster report 2002 (Wells 2002). See Table 2-9 for crop type distribution upstream of Cochiti. The carriage water factor is explained in Section 2.2.3.2.9. Riparian acreage is calculated from remotely sensed data for reaches above Cochiti and URGWOM values below, with the exception of Jemez, which uses values from a regional groundwater model of the Albuquerque Basin by Doug McAda and Peggy Barroll (2002).

Reach	Length [miles]	Gaged Tributaries	Irrigated Ag Acreage Modeled [acres]	Carriage Water Factor [%]	Riparian Acreage Modeled [acres]	Modeled Ag Convey-ance System	Coupled GW Model
Chama: Willow Creek to Heron	12	Azotea Tunnel (San Juan Chama)	0		0		None
Chama: Heron to El Vado	6	Rio Chama	0		1		None
Chama: El Vado to Abiquiu	29		300		20		Static
Chama: Abiquiu to Chamita	29	Ojo Caliente	4,540		80		Static
Lobatos to Cerro	26	Costilla Creek	0		300		Static
Cerro to Taos Junction Bridge	35	Red River Rio Pueblo de Taos	0		0		Static
Taos Junction Bridge to Embudo	15	Rio Embudo	190		100		Static
Embudo to Otowi	29		4,670		165		Dynamic
Otowi to Cochiti	27		0		1		Dynamic
Cochiti to San Felipe	15	Galisteo Creek	4,520	0.85	4,055	**X**	Dynamic
Jemez: Jemez Pueblo to Reservoir	30		5,370	0.2	3,985	**X**	Dynamic
San Felipe to Albuquerque	33	North Flood Channel	12,680	0.65	6,747	**X**	Dynamic
Albuquerque to Bernardo	53	South Flood Channel	53,700	0.4	20,114	**X**	Dynamic
Bernardo to San Acacia	14	Rio Puerco	680	0.2	6,639	**X**	Dynamic
San Acacia to San Marcial	48		10,490	0.2	21,591	**X**	Dynamic
San Marcial to Elephant Butte	42		0		7,635	**X**	Dynamic
Elephant Butte to Caballo	18		0		0		None

Table 2-5. Modeled reservoirs summary information.
Numbers from URGWOM (USACE 2002) with the exception of the El Vado capacity, which is the maximum historic storage 1975–1999 (May and October 1986).

	Year Completed [AD]	Capacity [AF]	Dam Crest Elevation [ft amsl]	Primary functions
Heron	1971	401,300	7199	Storage San Juan Chama (SJC) water.
El Vado	1935	189,500	6914.5	Storage native and SJC water for irrigation.
Abiquiu	1963	1,198,500	6381	Flood control and storage SJC water.
Cochiti	1973	589,200	5479	Flood control.
Jemez	1953	262,500	5271.6	Flood and sediment control.
Elephant Butte	1916	2,023,400	4407	Storage for irrigation.
Caballo	1938	326,700	4190	Storage for irrigation.
Total		4,991,100		

The following sections describe each of the terms in Equations 2-1 through 2-4 in more detail.

2.3.2.2 Evapotranspiration

2.2.3.2.1 Reservoir Evaporation

For the 1975–1999 period, pan evaporation was measured for April through October for all reservoirs, and during all months for Elephant Butte and Caballo where evaporation pans do not freeze. For the five upper reservoirs, where pan evaporation cannot be consistently measured from November through March, winter evaporation rate is estimated by Equation 2-5.

$$E^{r,m} = \frac{T_{\max}^{r,m} + T_{\min}^{r,m}}{2} * k^{r,m} \tag{2-5}$$

where

$E^{r,m}$ = evaporation rate from reservoir *r* during month *m* [L/T]
$T_{\max}^{r,m}$ = average daily maximum temperature for *r* during *m* [degree]
$T_{\min}^{r,m}$ = average daily minimum temperature for *r* during *m* [degree]
$k^{r,m}$ = coefficient of proportionality for *r* during *m* [L/(degree*T)]

For the five upper reservoirs from April through October, and Elephant Butte and Caballo during all months, the evaporation rate is estimated with Equation 2-6.

$$E^{r,m} = 0.7 * E_{pan}^{r,m} \tag{2-6}$$

where

$E^{r,m}$ = evaporation rate from reservoir *r* during month *m* [L/T]
$E_{pan}^{r,m}$ = pan evaporation measured at reservoir *r* during *m* [L/T]

Volume and edge effects result in pan evaporation typically overestimating actual open water evaporation. To correct for this effect, actual open water evaporation rate is estimated by multiplying measured pan evaporation by a pan coefficient less than unity. URGWOM uses a pan coefficient of 0.7 for all reservoirs. The methodology represented by Equations 2-5 and 2-6 for a monthly timestep is the same as used by URGWOM at a daily timestep (USACE et al. 2002).

2.2.3.2.2 Reference Evapotranspiration Rate

Where pan evaporation is not measured, crop and open water evaporation are calculated using a reference ET rate. The daily timestep URGWOM model uses daily reference ET rates calculated by a United States Bureau of Reclamation (BoR) product developed specifically for the Rio Grande south of Cochiti, called the ET Toolbox (Brower 2004). The monthly model uses the same modified Penman Monteith equation used by the ET Toolbox:

$$ET_{ref} = \frac{\frac{\Delta}{\Delta+\gamma} * SR \quad + \quad \frac{\gamma}{\gamma+\Delta} * U * D}{LHV * \rho_w} \tag{2-7}$$

where:

ET_{ref}	=	reference ET rate [L/T]
Δ	=	vapor pressure/temperature gradient [M/LT^{2}degree]
γ	=	psychrometric constant [M/LT^{2}degree]
SR	=	net solar radiation [M/T^3]
U	=	wind speed function = 15.36(1+0.0062*U2m) [L/T]
U2m	=	wind speed in km/day measured at 2 meters [L/T]
D	=	vapor pressure deficit [M/LT^2]
LHV	=	latent heat of vaporization for water [L^2/ T^2]
ρ_w	=	water density [M/L^3]

The numerator on the right side of Equation 2-7 has two terms, representing energy available per unit area per time for ET from solar- and gradient-driven evaporation respectively. The denominator converts the energy to water volume per unit area (depth) per time. Equation 2-7 represents reference ET as a function of climatic conditions. For the monthly model, each term above is specific to a given reach in a given month.

As explained in the ET Toolbox documentation (Brower 2004, page 52), the majority of the historic, daily climate data used in the ET Toolbox was derived from a combination of Los Lunas and Alcalde weather stations for all reaches between Cochiti and Elephant Butte reservoirs. For reaches south of Cochiti, ET Toolbox daily data were averaged to monthly for use in the model. North of Cochiti, historic climate data were used from weather stations at El Vado dam, Abiquiu dam, Cerro, Alcalde, and Cochiti dam as available. Where nearby data were not available, historic monthly average values were substituted. Table 2-6 summarizes climate stations used for historic data for reaches north of Cochiti.

Table 2-6. Historic climate data sources used for reaches above Cochiti. Reaches below Cochiti use ET Toolbox data set (Brower 2004).

Reach	Temperature Station	Temperature 1st Replacement	Temperature 2nd Replacement	RH, Wind, and Solar Radiation Station	RH, Wind, and Solar Radiation 1st Replacement
Chama: Willow Creek to Heron	El Vado Dam			Alcalde	Alcalde historic average
Chama: Heron to El Vado	El Vado Dam			Alcalde	Alcalde historic average
Chama: El Vado to Abiquiu	Abiquiu Dam			Alcalde	Alcalde historic average
Chama: Abiquiu to Chamita	Abiquiu Dam			Alcalde	Alcalde historic average
Lobatos to Cerro	Cerro	Cerro historic average		Alcalde	Alcalde historic average
Cerro to Taos Junction Bridge	Cerro	Cerro historic average		Alcalde	Alcalde historic average
Taos Junction Bridge to Embudo	Alcalde	Espanola	Alcalde historic average	Alcalde	Alcalde historic average
Embudo to Otowi	Alcalde	Espanola	Alcalde historic average	Alcalde	Alcalde historic average
Otowi to Cochiti	Cochiti Dam	Cochiti historic average		Alcalde	Alcalde historic average

2.2.3.2.3 Plant Coefficients

Reference ET is modified by empirically determined unitless coefficients to scale reference ET to a particular plant or environment type. Evaporation coefficients for riparian and crop vegetation were derived according to ET Toolbox methodology, which uses either a growing degree or monthly average method to estimate crop coefficients. The monthly average method always applies the same crop coefficient to a given crop in a given month. The growing degree method is used to track the energy that can contribute to plant growth and development through the growing season, and is essentially a model of plant growth through a growing season as a function of air temperature. Using the growing degree method, a given crop ET will be greater in a warm year than a cool year. The growing degrees available for plant utilization in a given month *m* by plant type *p* can be calculated as:

$$GD^{m,p} = \left(\frac{(T_{\max}^{m,p} + T_{\min}^{m,p})}{2} - T_{base}^{p} \right) * days^{m} \qquad (2\text{-}8)$$

where:

$GD^{m,p}$ = growing degrees in month *m* for plant type *p* [degrees/T]

$T_{\max}^{m,p}$ = the average maximum monthly temperature for month *m*, or plant maximum temperature cutoff parameter for plant type *p*, whichever is smaller [degrees/T]

$T_{\min}^{m,p}$ = the average minimum monthly temperature for month *m*, or $T_{base}^{m,p}$, whichever is larger [degrees/T]

$T_{base}^{m,p}$ = the base temperature parameter for plant type *p* [degrees/T]

$days^{m}$ = the number of days in month *m* [-]

ET Toolbox derived relationships between growing degree days and plant ET coefficient as a function of plant species were used to go from growing degree days to plant coefficient (Brower 2004). Regardless of coefficient method, ET is only applied during the growing season of a given plant type. Table 2-7 summarizes the crop and plant types represented in the model, the method used for calculation of crop coefficients, the growing degree parameters for the plant type where applicable, and the beginning and end months of growing season of the plant type.

2.2.3.2.4 Open Water Coefficients

Where pan evaporation is not directly measured, open water evaporation can be predicted by multiplying reference ET by a unitless open water evaporation coefficient, an approach that is analogous to the method described above for vegetation. The open water coefficient method is used to estimate direct evaporation from a river reach. The ET Toolbox uses monthly open water coefficients developed by M. E. Jensen in the lower Colorado system (Jensen 1998). To develop local open water coefficients, the reference ET calculated for each reach above a reservoir was compared to the pan evaporation measured at the reservoir. As discussed previously, URGWOM uses a pan coefficient of 0.7 for all New Mexico reservoirs. Thus, open water evaporation coefficients can be estimated with pan evaporation and reference ET:

$$C_{ow}^{r,m} = \frac{0.7 * E_{pan}^{r,m}}{ET_{ref}^{j,m}} \tag{2-9}$$

where:

$C_{ow}^{r,m}$ = implied open water coefficient associated with reservoir *r* in month *m* [-]

$E_{pan}^{r,m}$ = pan evaporation measured at reservoir *r* during month *m* [L/T]

$ET_{ref}^{j,m}$ = reference ET in reach *j* immediately upstream of reservoir *r* in month *m* [L/T]

Table 2-7. Plant types represented in the model, method for determining crop coefficients, associated growing degree parameters, and growing season start and end month.

	Plant Type	Coefficient Method	Base Temp GD (F)	Max Temp Cutoff GD (F)	Start Month	Stop Month
Agricultural	Alfalfa	Growing Degree Day	5	50	Jan	Oct
	Chile Peppers	= Corn	10	30	May	Nov
	Corn	Growing Degree Day	10	30	May	Nov
	Cotton	Growing Degree Day	12	30	May	Oct
	Grapes	Growing Degree Day	10	30	April	Oct
	Melons	Monthly Table			April	Aug
	Misc. Fruit	Monthly Table			Jan	Dec
	Misc. Vegetables	= Corn	10	30	May	Nov
	Nursery Stock	Monthly Table			Jan	Dec
	Oats	= Spring Barley	5	30	April	July
	Pasture Grass	0.65		50	March	Sept
	Sorghum	Growing Degree Day	7	50	June	Dec
	Spring Barley	Growing Degree Day	5	30	May	Oct
	Tree Fruit	Monthly Table			Jan	Dec
	Wheat	Growing Degree Day	4	27	April	July
Riparian	Bosque	Growing Degree Day	15.5	50	April	Nov
	Cottonwood	Growing Degree Day	15.5	50	April	Nov
	Marsh	Monthly Table			Jan	Dec
	Misc. Grass	0.65	5	50	Jan	Dec
	Salt Cedar	Growing Degree Day	15.5	50	April	Nov

Figure 2-3 shows average open water coefficient values for each reservoir in each month of the year. Pan evaporation was not recorded at Heron or El Vado for winter months in the 1975–1999 calibration period. The summer coefficients are lower for upper reservoirs (Heron and El Vado) in part because pan evaporation is measured at the reservoir, but reference ET is calculated based on nonrepresentative climate data from climate stations at lower elevations. To arrive at a single coefficient for each month, Heron and El Vado values were excluded, and the remaining monthly measurements averaged and rounded to the nearest tenth. Table 2-8 shows the adopted open water coefficients for this model, as well as the coefficients from Jensen. The two are fairly close except December through March when the Jensen coefficients are significantly lower than the adopted upper Rio Grande coefficients.

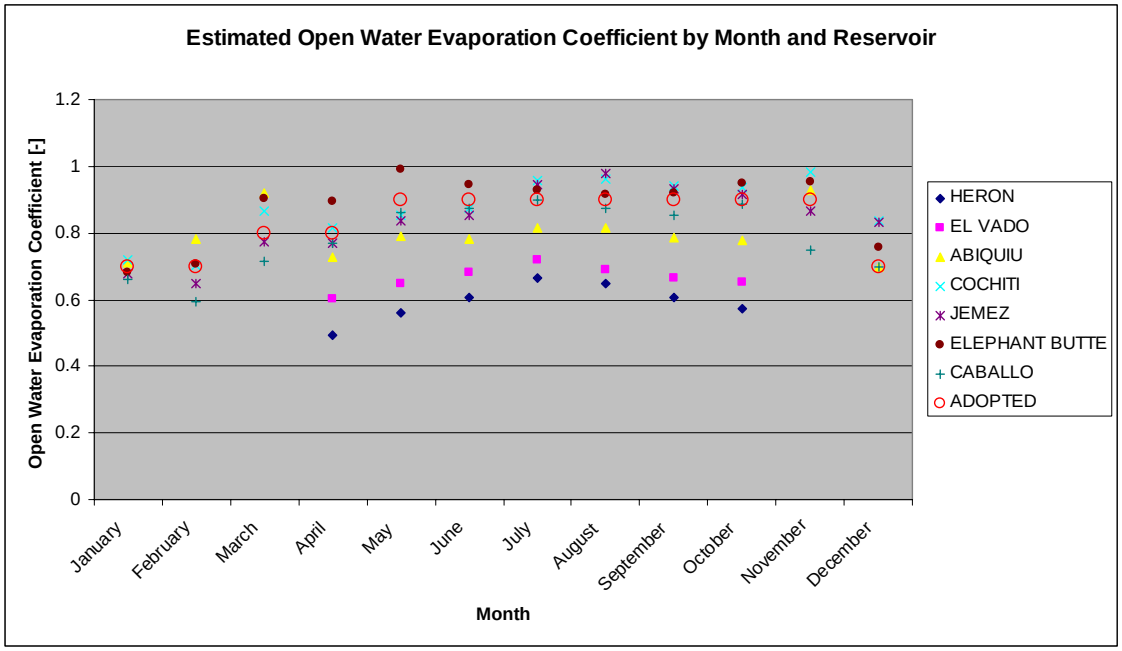

Figure 2-3. Inverse estimations of open water coefficients based on pan evaporation rates measured at reservoirs.

Table 2-8. Open water evaporation coefficients derived for the upper Rio Grande as compared to coefficients derived by Jensen (1998) in the lower Colorado River. The latter are used by ET Toolbox (Brower 2004), while the former are used in the monthly timestep model described in this report. These coefficients are multiplied by reference ET to estimate open water evaporation.

Month	Open Water Evaporation Coefficient Upper Rio Grande	Open Water Evaporation Coefficient Jensen
January	0.7	0.52
February	0.7	0.57
March	0.8	0.67
April	0.8	0.79
May	0.9	0.84
June	0.9	0.89
July	0.9	0.89
August	0.9	0.85
September	0.9	0.89
October	0.9	0.86
November	0.9	0.87
December	0.7	0.57

2.2.3.2.5 Volumetric Evapotranspiration

Reference ET is multiplied by a plant or open water coefficient as described above to get the ET rate for a specific plant type or open water. This value must be multiplied by the associated area of plant or water to get volumetric ET for plants and volumetric evaporation for open water.

$$Q_{evap}^{r} = E^{r,m} * A^{r,m} * (1 - \mathrm{cov}^{r,m}) \quad \text{(2-10a)}$$

$$Q_{cropET}^{j} = ET_{ref}^{j,m} * \sum_{p} C^{j,m,c} * A^{j,m,c} \quad \text{(2-10b)}$$

$$Q_{evap}^{j} = ET_{ref}^{j,m} * C_{ow}^{m} * A^{j,m,w} \quad \text{(2-10c)}$$

$$Q_{ripET}^{j} = ET_{ref}^{j,m} * \sum_{p} C^{j,m,r} * A^{j,m,r} \quad \text{(2-10d)}$$

where:

Q_{evap}^{r}	=	evaporation from reservoir *r* as defined in Equation 2-4 [L^3/T]
Q_{cropET}^{j}	=	crop ET in reach *j* as defined in Equation 2-3 [L^3/T]
Q_{evap}^{j}	=	open water evaporation in reach *j* as defined in Equation 2-1 [L^3/T]
Q_{ripET}^{j}	=	riparian ET in reach j for groundwater balance [L^3/T]
$E^{r,m}$	=	evaporation rate from reservoir *r* during month *m* [L/T]
$ET_{ref}^{j,m}$	=	reference ET in reach *j* during month *m* [L/T]
$C^{j,m,p}$	=	ET coefficient in reach *j* during month *m* for plant *p* [-]
C_{ow}^{m}	=	open water evaporation coefficient during month *m* [-]
$A^{r,m}$	=	surface area of reservoir *r* during month *m* [L^2]
$A^{j,m,c}$	=	crop area in reach *j* during month *m* for agricultural crop *c* [L^2]
$A^{j,m,w}$	=	open water area in reach *j* during month *m* [L^2]
$A^{j,m,r}$	=	riparian vegetation area in reach *j* during month *m* for plant *r* [L^2]
$\mathrm{cov}^{r,m}$	=	percent of reservoir *r* covered by ice during month *m* [%]

Reservoir areas ($A^{r,m}$) are calculated based on storage volume in the reservoir using Elevation-Area-Capacity (EAC) relationships specific to each reservoir (tables from Roberta Ball, USACE personal communication 2003). Ice cover on a given reservoir ($\mathrm{cov}^{r,m}$) is a historically measured value, taken from the daily URGWOM data set and averaged to monthly.

2.2.3.2.6 Crop Acreage

Vegetation areas for irrigated agricultural crops are taken from three different sources. Crop acreages along the Rio Chama are taken from the Watermaster's Report for the Rio Chama Mainstream 2002, with crop type percentages from the Rio Chama Watermaster at the time (Stermon M. Wells, personal communication July 2003). For acreages above Cochiti along the Rio Grande, approximate acreages of 200 and 5,000 acres for the reaches Taos Junction Bridge to Embudo and Embudo to Otowi respectively are taken from the URGWOM Physical Model Documentation (USACE et al. 2002). The same crop distribution as used for the Chama is assumed for the Rio Grande above Cochiti. Table 2-9 summarizes crop acreage assumed for reaches above Cochiti for 1975–1999. Over 50,000 acres of agricultural land are irrigated by surface water below Cochiti Reservoir and above Elephant Butte Reservoir (USACE et al. 2002, PHYMOD-65). Irrigated crop acreages for the reaches in this "middle Rio Grande" stretch are taken from URGWOM Physical Model Documentation (*ibid*), which tabulated the data from the Middle Rio Grande Conservancy District (MRGCD) sources, and broke it into river reach based units. Based on this rich dataset, the model represents irrigated crop types and acreages in the middle Rio Grande that are different for each year from 1975–1999. For the validation period (2000–2006), 1999 crop acreage values are used, and the scenario evaluation period uses user input to determine crop acreages, with 1999 acreages as a default.

2.2.3.2.7 Riparian Vegetation Acreage

Vegetation areas for riparian vegetation upstream of Cochiti were calculated by the authors from remotely sensed data. Some values were modified slightly during calibration based on qualitative ground observations. The riparian vegetation areas north of Cochiti result in losses that are small within the context of the overall water budget between gages, so no time has been spent validating or improving the calculated values. Downstream of Cochiti, with the exception of the Jemez and San Acacia to San Marcial reach, riparian acreages from the URGWOM Physical Model Documentation (*ibid*) were used. URGWOM does not use riparian area in the Jemez reach, so the Jemez riparian values were taken from the McAda and Barroll (2002) Albuquerque basin regional groundwater model. Gage data suggest losses in the San Acacia to San Marcial reach that were about 13,000 acre feet (AF)/yr greater than predicted with the model using URGWOM riparian and crop acreages. Gage error may be part of the unexpectedly high water loss, especially during the 1985 –1988 period when losses in the reach seem unusually high, or it may be a result of active wetlands management in the Bosque del Apache wildlife refuge, which effectively sits at the end of the agricultural irrigation system. For modeling purposes we are assuming that gage error is distributed normally about zero during the calibration period, so no attempt was made to evaluate unusual gage error. Calibration was achieved by increasing riparian acreage between San Acacia and San Marcial by 33% from 16,000 acres to 22,000 acres. Additional work will be necessary to discover the source of this error. Riparian acreages used in the model are reported in Table 2-4.

Table 2-9. Irrigated crop acreages for river reaches above Cochiti Reservoir. The assumed crop distribution for each crop type is based on Rio Chama adjudicated crop distribution patterns (Stermon Wells, personal communication July 2003). Chama total acreage from the 2002 Chama Watermaster's report. Rio Grande total acreage from URGWOM Physical Model Documentation (USACE et al. 2002). ETTB Category is the ET Toolbox vegetation category to which each crop type was applied for determination of crop coefficients.

Crop Type	ETTB Category	Assumed Crop Distribution %	El Vado to Abiquiu Reservoir Acres	Abiquiu Reservoir to Chamita Acres	Taos Junction Bridge to Embudo Acres	Embudo to Otowi Acres
Total	Total	100.0%	317	4862	200	5000
Alfalfa	Alfalfa	22.5%	71	1094	45	1125
Hay & Pasture	Pasture Grass	39.1%	124	1902	78	1956
Corn	Corn	10.7%	34	522	21	537
Orchard	Tree Fruit	10.7%	34	519	21	534
Grain	Wheat	6.4%	20	311	13	320
Garden	Misc Veg	4.0%	13	193	8	199
Fallow	None	6.6%	21	321	13	330

2.2.3.2.8 River Channel Open Water Area

The open water area associated with each reach of the river channel is a function of flow rate and channel cross-section geometry. Above Cochiti, the relationship between stream width and flow associated with each gage is used as a proxy for the relationship in associated reaches. Channel geometry at gage locations is not likely representative of the entire reach above or below the gage, but additional data are not available, and surface evaporation from the upper reaches is conceptually a relatively small term, so this assumption is considered acceptable. Cross-sectional area at each gage as a function of flow rate is reported in the URGWOM Physical Model Documentation (USACE et al. 2002). Stage as a function of flow rate is a key relationship associated with surface water gages, and is available indirectly from field measurement data published online for each gage operated by the United States Geological Survey (USGS).[1] With stage and cross-sectional area available as a function of flow rate, a trapezoidal channel cross section was assumed, and a base width and bank slope selected to fit the relationships between flowrate, stage, and cross-sectional area observed at the gages. Table 2-10 summarizes cross-sectional relationships adopted for select gages above Cochiti. A trapezoidal channel did not satisfactorily describe historic field measurements of stage and flow at either the Rio Grande gage below Taos Junction Bridge or the Chama gage near Chamita, and so these gages were not included. Chama reaches from below El Vado Reservoir and all Rio Grande reaches above Cochiti were assumed to follow the cross-sectional relationships of the gages defining the beginning or end of the reach, or an average of both as available. For example, in the reach from Lobatos to Cerro, for an average monthly flow rate of 100 cubic feet per second (cfs), the calculated river stage using the Cerro gage relationship would be $0.2145*100^{0.4742} = 1.9$ feet. The calculated width of the river would be 56 feet (base width parameter) plus 6.5 (bank slope parameter)*1.9 feet, or 68.35 feet. This width is then multiplied

[1] E.g., for Rio Grande near Cerro gage: http://nwis.waterdata.usgs.gov/nm/nwis/measurements/?site_no=08263500&agency_cd=USGS

by the length of the reach (26 miles, see Table 2-4) to get a total open water area of 0.34 mile^2 for Lobatos to Cerro at 100 cfs flowrate ($A^{j,m,w}$ in Equation 2-10c).

Table 2-10. Channel geometry relationships adopted at selected gages, used to estimate stage and area as a function of flow rate in reaches above Cochiti Reservoir. Reaches between gages in this table used an average of both; other reaches used upper or lower gage data as available.

Gage	Stage [ft] from Q[cfs]	Cross Sectional Area [ft^2] from Q[cfs]	Fitted Base Width Parameter [ft]	Fitted Bank Slope Parameter (run/rise) [-]
Rio Chama below El Vado	$0.27*Q^{0.37}$	$13*Q^{0.48}$	75	8
Rio Chama above Abiquiu Reservoir	$0.35*Q^{0.36}$	$11.5*Q^{0.47}$	50	5
Rio Chama below Abiquiu Dam	$0.4*Q^{0.33}$	$7*Q^{0.54}$	28	12
Rio Grande near Cerro	$0.2145*Q^{0.4742}$	$4.2943*Q^{0.6976}$	56	6.5
Rio Grande at Embudo	$0.15*Q^{0.48}$	$5.1771*Q^{0.593}$	61	3
Rio Grande at Otowi	$0.2*Q^{0.41}$	$3.2959*Q^{0.6628}$	40	16

2.2.3.2.9 Potential Versus Actual ET in Model

Equations 2-10b through 2-10d use reference ET to calculate the potential ET for agricultural, channel surface, and riparian ET. The potential ET is the maximum ET expected for a given set of climatic conditions and growing history of a plant (if using growing degree day (GDD) approach). The actual ET observed is less than potential if water availability is limiting. In the case of riparian vegetation, depth to groundwater can limit riparian ET. This is discussed in detail in Chapter 3. In the case of agricultural ET, crops are often grown in a moisture deficit state, that is, with less water applied than could potentially be transpired. Actual water delivery is based on permitted water deliveries set by the State Engineer, and restricted in timing and magnitude based on delivery infrastructure and social institutions. The actual agricultural ET calculated in the model is reduced from potential ET based on availability. A calibration factor of carriage water required to deliver water for use was used in middle valley reaches to reduce available water for agricultural ET to agricultural ET values predicted by URGWOM. The calibrated carriage water requirements are shown in Table 2-4, and decrease as water moves downstream in the conveyance system. For example, the 85% requirement between Cochiti and San Felipe suggests that only 15% of the water in the conveyance system is used to satisfy agricultural ET demand, and the rest moves down to the next reach for use there. Without this calibration factor, the model would satisfy potential demand at the top of the conveyance system to the detriment of downstream users, which is not the observed tendency.

2.2.3.3 Groundwater Surface Water Interactions

2.2.3.3.1 Groundwater Contributions Upstream of Rio Chama/Rio Grande Confluence

Relevant studies of the geohydrology of the groundwater system associated with the Rio Grande and Rio Chama river systems north of their confluence include a characterization of the aquifer

geology by Wilkins (1986), a mass balance characterization of the Rio Grande system above Embudo by Hearne and Dewey (1988), and a regional groundwater model of the Taos area by Barroll and Burck (2005). The reaches above the Rio Chama/Rio Grande confluence tend to be gaining reaches (see Figure 2-2); however, quantitative estimates of the magnitude of that gain are limited. Hearne and Dewey (1988) constrained overall contributions with surface gage data, while Barroll and Burck (2005) calibrated groundwater flows to the Rio Grande between Arroyo Hondo and Rio Pueblo de Taos (part of the Cerro to Taos Bridge surface water reach, see Figure 2-1 and Table 2-2) using estimates based on direct stream flow measurements. Because the Hearne and Dewey work is spatially lumped above the Embudo gage and the Barroll and Burck work is spatially limited, additional data were developed for this modeling effort.

The magnitude of groundwater contributions for reaches upstream of the Rio Chama Rio/Grande confluence was estimated by analyzing winter gage flows. Historic gage data was filtered for winter months (November–February) when agricultural diversions and riparian ET are assumed negligible such that surface water losses are limited to direct evaporation from the river surface. Evaporative losses from the river channel for winter months during the calibration period (1975–1999) were calculated with Equation 2-10c described in Section 2.2.3.2. In a given reach between an upstream and downstream gage, the calculated evaporative losses were removed from the upstream gaged flow, and gaged tributary flows, if any, including wastewater return flows (Espanola), were added to the upstream gaged flow. This "corrected" flow at the downstream gage was compared to the gaged flow to get a residual (observed–corrected) for each calibration winter month for each reach. The residual is positive when the downstream gage reading is larger than the corrected estimate. These residuals represent a combination of gage error, error in loss approximation, and ungaged gains between the gages. If gage and model errors are not overwhelming, the residuals should represent a proxy to ungaged inflows. No meaningful relationship was discovered between these ungaged inflow approximations and precipitation, snow pack, reservoir stage (Chama reaches), or stream flow. The ungaged groundwater inflows were set to constant values that result in an approximately equal number of negative and positive residuals in each reach for winter months 1975–1999. The mathematical details and an example calculation are shown below.

The uncorrected winter residual for a given reach in a given month is the difference between the upstream gage plus tributary flow (inflows) and the downstream gage reading plus calculated evaporative losses (outflows):

$$R_{uw}^{j,m} = (Q_{down}^{j,m} + Q_{loss}^{j,m}) - (Q_{up}^{j,m} + Q_{trib}^{j,m}) \qquad (2\text{-}11)$$

where:

$R_{uw}^{j,m}$ = the uncorrected winter residual for reach j in month m [L^3/T]
$Q_{down}^{j,m}$ = the gaged flow at the bottom of reach j in month m [L^3/T]
$Q_{loss}^{j,m}$ = the modeled loss for reach j in month m [L^3/T]
$Q_{up}^{j,m}$ = the gaged flow at the top of reach j in month m [L^3/T]
$Q_{trib}^{j,m}$ = the gaged tributary input to reach j in month m [L^3/T]

For example, the January 1975 Lobatos (upstream gage) to Cerro (downstream gage) uncorrected winter residual was 15%.

$$R_{uw}^{LBT2CROJan1975} = (Q_{down}^{j,m} + Q_{loss}^{j,m}) - (Q_{up}^{j,m} + Q_{trib}^{j,m}) = 198.8cfs + 0.5cfs - 170.3cfs - 0cfs = 29cfs$$

The uncorrected winter residuals for the Lobatos to Cerro reach are shown in Figure 2-4a, and suggest that the reach is gaining. To estimate groundwater contribution magnitude, a constant groundwater inflow is added to the reach to get a corrected winter residual that is negative approximately as often as positive during the calibration period.

$$R_{cw}^{j,m} = (Q_{down}^{j,m} + Q_{loss}^{j,m}) - (Q_{up}^{j,m} + Q_{trib}^{j,m} + Q_{base}^{j}) \quad (2\text{-}12)$$

where:

$R_{uw}^{j,m}$ = the corrected winter residual for reach *j* in month *m* [L^3/T]

Q_{base}^{j} = the base flow added to reach *j* in all months [L^3/T]

Figure 2-4b shows the corrected residual distribution for Lobatos to Cerro resulting from the addition of 39 cfs of constant base flow to the reach. Figures 2-5 through 2-9 show the uncorrected and corrected residual distributions for the other reaches extending above the Rio Chama/Rio Grande confluence. The remainder of this section contains further explanation of the results for the three reaches along the Rio Grande from Cerro to Otowi, and a summary of adopted base flow values.

The 34-mile reach from Cerro to Taos Junction Bridge includes a 17-mile stretch from below the Arroyo Hondo tributary to above the Rio Pueblo de Taos tributary that was the subject of seepage studies by the United States Geological Survey in 1963–1964, and TetraTech, Inc., in 2003. These studies estimated groundwater surface water interactions by measuring surface flows at several cross sections along the reach. TetraTech estimated a net groundwater gain in the Rio Grande from Arroyo Hondo to Taos Junction Bridge of approximately 22 cfs for the 17-mile stretch (1.3 cfs/mile), while the USGS estimated gains of 17, 15, and 7.5 cfs for the same stretch in August 1963, October 1963, and October 1964 respectively (1, 0.9, and 0.4 cfs/mile) (TetraTech 2003). As a result of these analyses, Barroll and Burck (2005) calibrated groundwater leakage to the Rio Grande between Arroyo Hondo and Rio Pueblo de Taos to be approximately 1 cfs/mile. These estimates are quite a bit lower per mile than the 94 cfs total inflow to the 35-mile reach (2.7 cfs/mile) suggested by the winter gage analysis for the encompassing Cerro to Taos Bridge reach (see Figure 2-5b). There are two main reasons for the discrepancy.

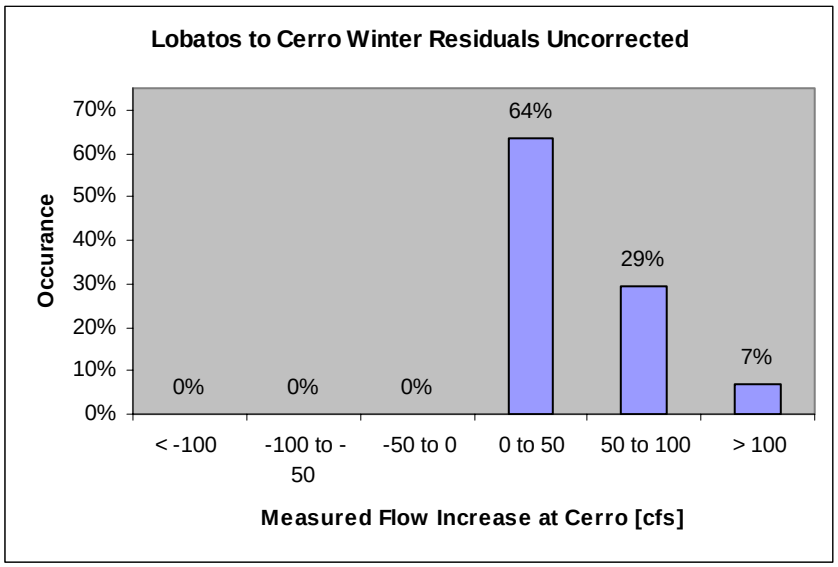

Figure 2-4a. Uncorrected winter residuals for Lobatos to Cerro reach 1975–1999.

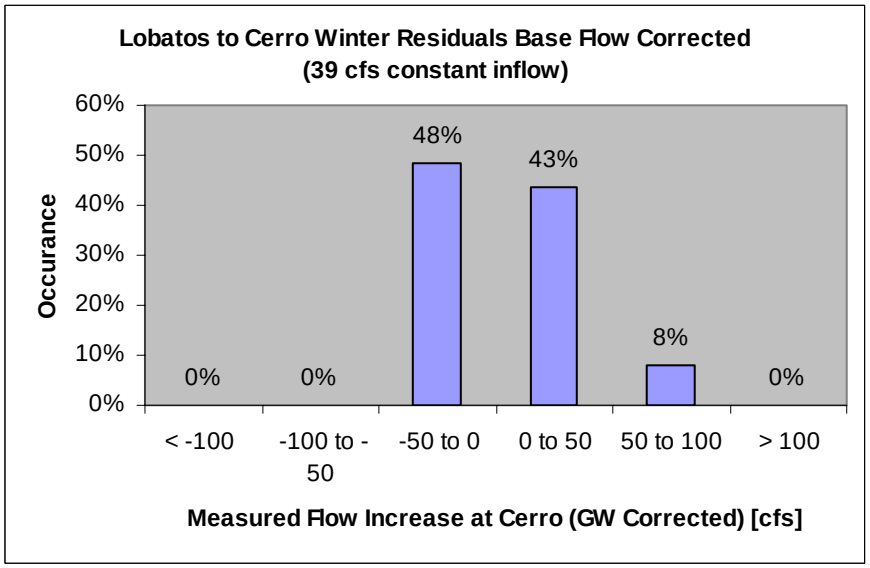

Figure 2-4b. Corrected winter residuals for Lobatos to Cerro reach 1975–1999 associated with a constant 39 cfs base flow addition.

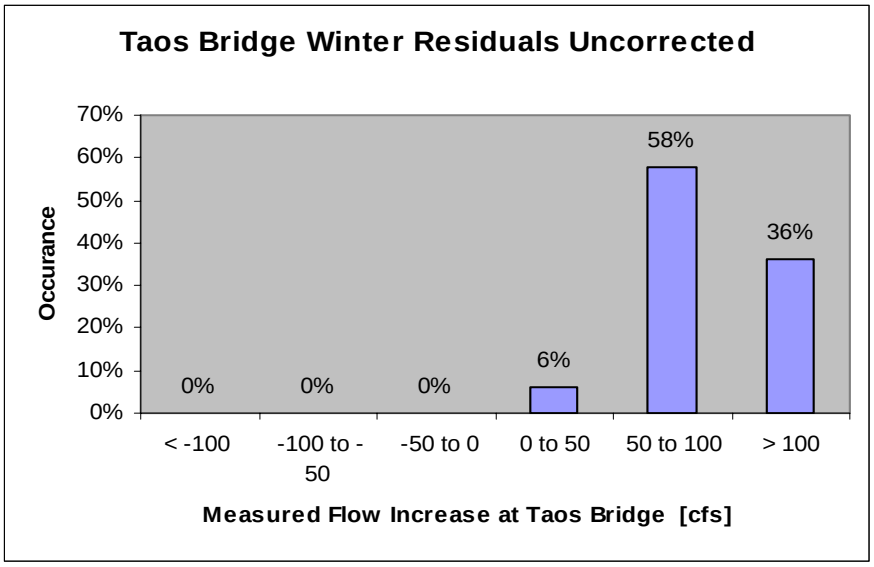

Figure 2-5a. Uncorrected winter residuals for Cerro to Taos Junction Bridge reach 1975–1999.

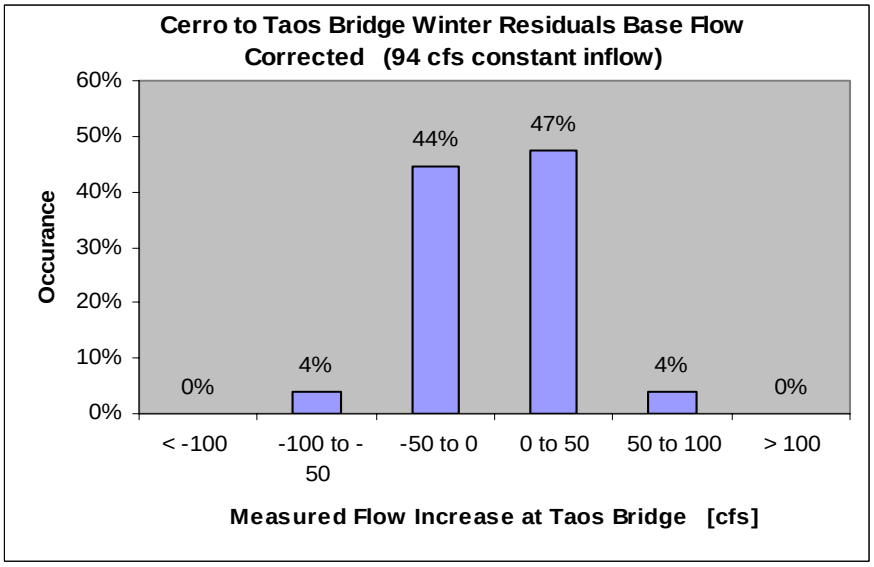

Figure 2-5b. Corrected winter residuals for Cerro to Taos Junction Bridge reach 1975–1999 associated with a constant 94 cfs base flow addition.

Although it was not used to define a reach because of an incomplete historic record, the USGS operated a gage on the Rio Grande below the Arroyo Hondo confluence from March 1963 to September 1996, and from July 2002 to September 2004. Applying the same winter residual method described above to the reach from Cerro to Arroyo Hondo suggests that 78 cfs of base flow enters the Rio Grande in that stretch, leaving 16 cfs to enter the river between Arroyo Hondo and Taos Junction Bridge, a distance of 19 miles. This value compares well with the seepage studies and adopted value used by Barroll and Burck (2005). The 78 cfs of calculated base flow in the 16-mile stretch from Cerro to Arroyo Hondo is high because it includes tributary inputs from the Arroyo Hondo. Because of incomplete historic record, this tributary is not included as gaged inflow to the reach, but the USGS did operate a gage on the Arroyo Hondo near the Rio Grande confluence from 1912 to 1985.[2] Data from that gage suggest that average winter flows of the Arroyo Hondo are about 17 cfs. This reduces the estimated groundwater input to the Cerro to Arroyo Hondo stretch to approximately 60 cfs in 19 miles, a high value at 3.2 cfs/mile, but plausible for the area. The adopted groundwater contribution to the Cerro to Taos Bridge reach is 77 cfs, with the remaining 17 cfs attributed to surface water inflow from Arroyo Hondo.

The uncorrected winter residual distribution for the Taos Bridge to Embudo reach was centered about zero, so no groundwater correction was added to this reach (Figure 2-6). The corrected winter residual distribution for Embudo to Otowi suggests a very large winter base flow of 71 cfs for the 29 mile reach. This number seems too large to local hydrologists (Dr. Nabil Shafike, Senior Hydrologist, New Mexico Interstate Stream Commission, personal communication 2006). Consistent with this notion, a regional groundwater model underlying the Rio Grande from the Rio Chama/Rio Grande confluence to Cochiti Reservoir (see Section 2.2.3.3.2) calculates groundwater inflows between the confluence and Otowi gage of approximately 9 cfs (~ 0.6 cfs/mile) (Frenzel 1995). It is possible that the high winter gains between Embudo and Otowi includes significant ungaged surface water inflow from the Santa Cruz and Pojaque Rivers, and Santa Clara Creek. For the purposes of this study, 1 cfs/mile of groundwater inflow was assumed along the Rio Grande between Embudo and the Rio Chama confluence, for a total of 15 cfs above the confluence, and including the 9 cfs estimated below the confluence, 24 cfs total groundwater contribution to the Embudo to Otowi reach. The remaining 47 cfs of ungaged inflows suggested by the winter residual analysis (Figure 2-7b) was attributed to ungaged surface water inflows (described below).

Adopted base flow values for each reach are summarized in Table 2-11. These numbers are the best available, but are approximate. Because of potential ungaged surface runoff during historic winter months, the groundwater base flow estimates may include some fraction of ungaged surface flows. Base flow values shown in Table 2-11 are used during all model periods.

[2] USGS gage ID number 08268500.

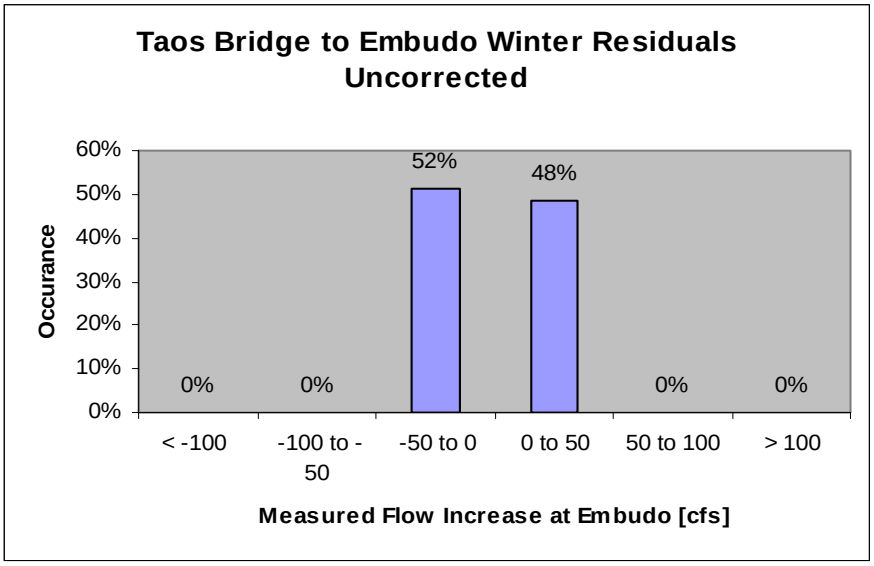

Figure 2-6. Uncorrected winter residuals for Taos Junction Bridge to Embudo reach 1975–1999. The uncorrected residuals are approximately distributed about zero, so no base flow was added in this reach.

Table 2-11. Base flow contribution added to modeled river reaches upstream of Rio Chama Rio Grande confluence. Values are based on winter gaged flows.

	Reach	Adopted Ungaged GW Contribution [cfs]	Reach Length [mile]	GW Contribution per Mile [cfs/mile]	Adopted Ungaged SW Contribution [cfs]
Chama	El Vado to Abiquiu	8	29	0.3	
	Abiquiu to Chamita	17	29	0.6	
	Chama Total	25	58	0.4	
Rio Grande	Lobatos to Cerro	39	26	1.5	
	Cerro to Taos Bridge	77	35	2.2	17
	Taos Bridge to Embudo	0	15	0.0	
	Embudo to Otowi	24	29	0.8	47
	Rio Grande Total	140	105	1.3	64

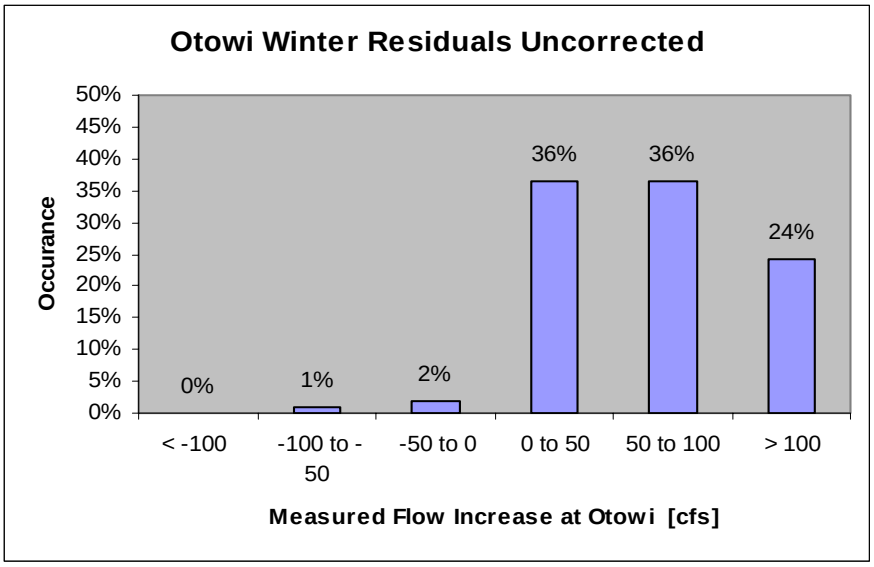

Figure 2-7a. Uncorrected winter residuals for Embudo to Otowi reach 1975–1999.

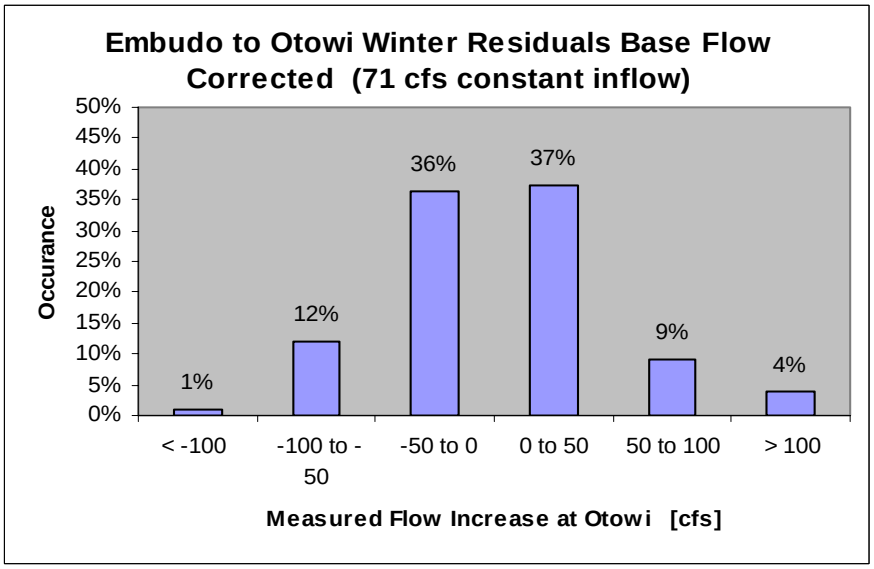

Figure 2-7b. Corrected winter residuals for Embudo to Otowi reach 1975–1999 associated with a constant 71 cfs base flow addition.

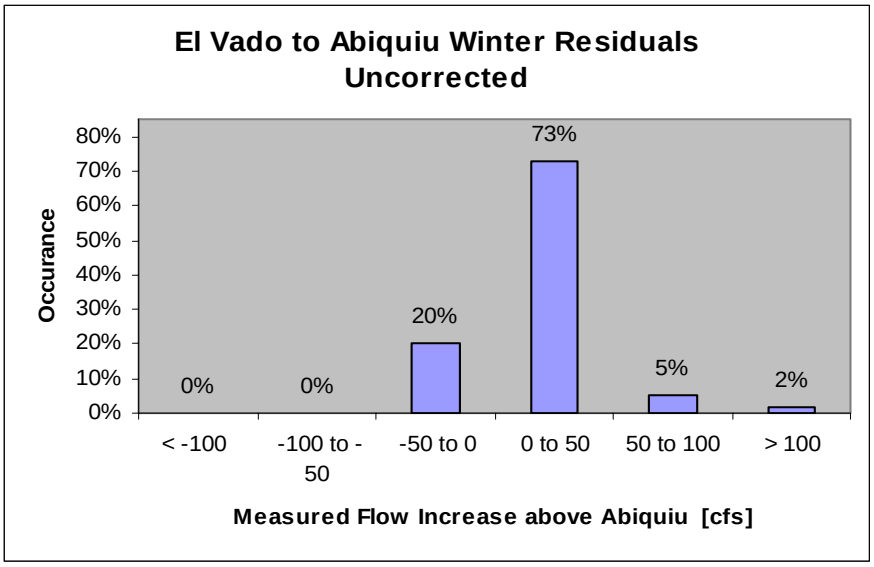

Figure 2-8a. Uncorrected winter residuals for below El Vado to above Abiquiu reach 1975–1999.

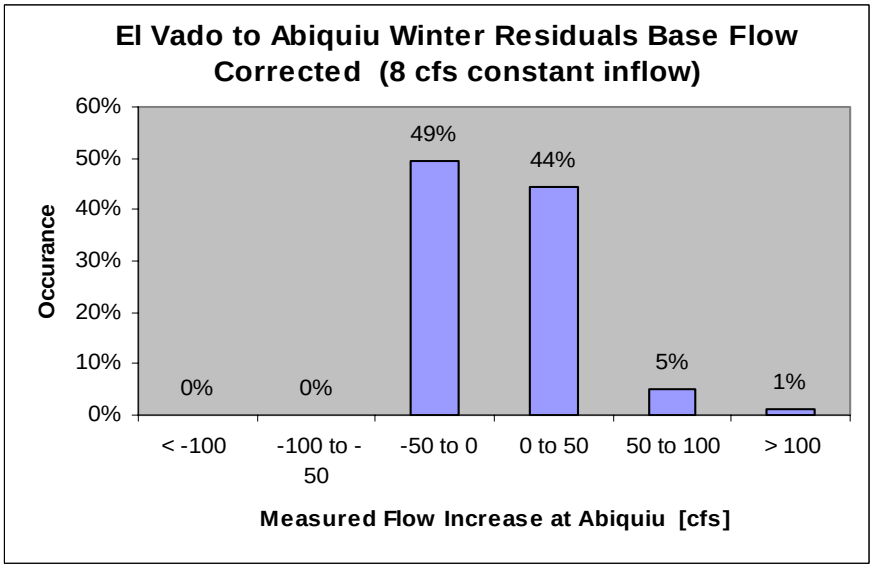

Figure 2-8b. Corrected winter residuals for below El Vado to above Abiquiu reach 1975–1999 associated with a constant 8 cfs base flow addition.

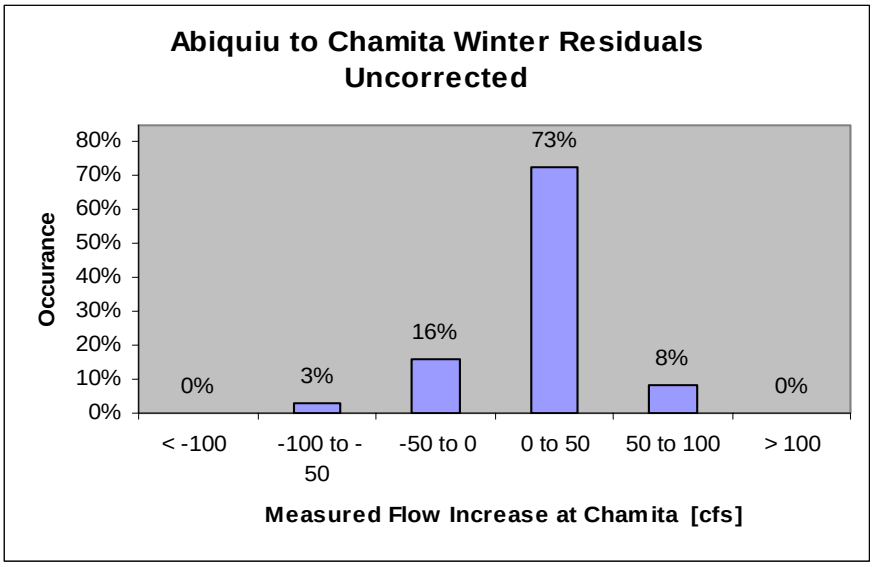

Figure 2-9a. Uncorrected winter residuals for below Abiquiu to Chamita reach 1975–1999.

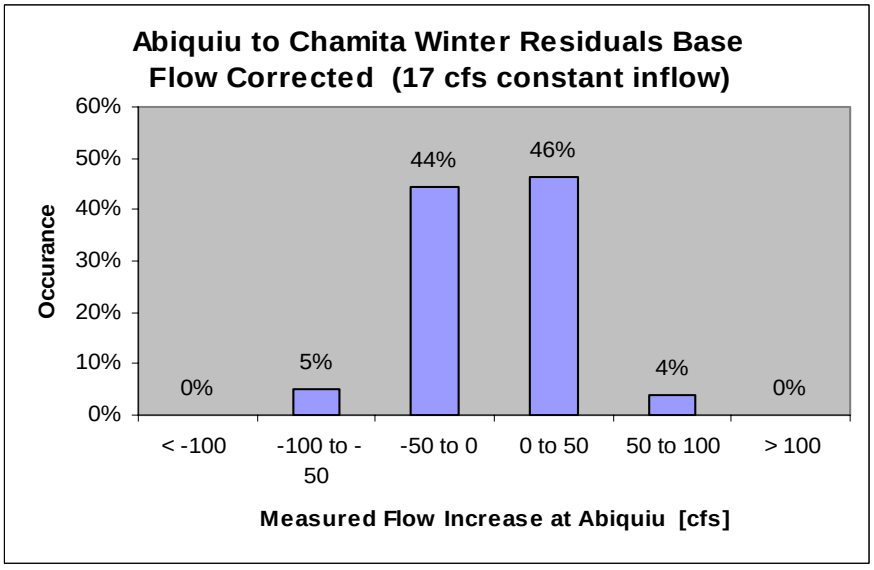

Figure 2-9b. Corrected winter residuals for below Abiquiu to Chamita reach 1975–1999 associated with a constant 17 cfs base flow addition.

2.2.3.3.2 Groundwater Surface Water Interactions Below Rio Chama Confluence

Understanding of the groundwater system downstream of the Rio Chama/Rio Grande confluence is far greater than that upstream. Regional groundwater models have been created for the Espanola Basin (Frenzel 1995), Albuquerque Basin (McAda and Barroll 2002), and the Socorro Basin (Shafike 2005). Together these groundwater models incorporate the regional Rio Grande river system from the Rio Chama confluence to Elephant Butte Reservoir. As described in the next chapter of this report, spatially aggregated, explicit finite difference groundwater flow models were created to capture the salient groundwater behavior represented by the Frenzel, McAda/Barroll, and Shafike models. The spatially aggregated versions run more rapidly than their spatially distributed counterparts, and are set up to run at a monthly timestep to facilitate connection to the surface water system described here. This section summarizes issues of coupling and calibration associated with connecting the groundwater models to the surface water, but for a more detailed description of model behavior the reader is referred to Chapter 3. Model parameters calculated during calibration were used during validation and scenario evaluation runs.

2.2.3.3.2.1 Espanola Basin Groundwater System

The Espanola Basin groundwater model created by Peter Frenzel (1995) covers the river system roughly from the Rio Grande/Rio Chama confluence to Cochiti Reservoir, and focuses specifically on pumping effects of the Los Alamos and Santa Fe well fields. Irrigated agriculture effects are not explicitly represented. Transient flows from the Frenzel model were used to calibrate a spatially aggregated 16-zone model that was linked dynamically to a similar Albuquerque basin groundwater model to the south, as well as to surface water reaches from the Rio Grande/Rio Chama confluence to Cochiti Reservoir. River stage was calculated as a function of monthly average flow in the Embudo to Otowi and Otowi to Cochiti reaches using the gage-based stage to flow relationships described in Section 2.2.3.2.8 and shown in Table 2-10. The modeled river leakage was calibrated to match the Frenzel values as closely as possible.

2.2.3.3.2.2 Albuquerque Basin Groundwater System

The Albuquerque basin regional groundwater model created by Douglas McAda and Peggy Barroll (2002) simulates regional groundwater flow associated with the Rio Grande river system roughly from Cochiti Reservoir to San Acacia. Transient flows from that model were used to calibrate a spatially aggregated 51-zone model that was linked dynamically to the 16-zone Espanola basin groundwater model, Jemez and Cochiti reservoirs, and surface water reaches from Cochiti to San Acacia. The Albuquerque groundwater basin does not communicate to any significant extent with the Socorro groundwater basin to the south in either the McAda/Barroll or Shafike models. Surface water stages in the river, canal, and drains are calculated with Manning's equation, and the spatially aggregated groundwater system is calibrated to match the McAda and Barroll model. The overall riparian ET combines atmospheric constraints on ET (reference ET) from the surface model with depth to groundwater constraints from the groundwater model using a calibration factor as described in the next chapter of this report. Values were calibrated to fall between the McAda/Barroll and URGWOM predicted values for

the middle Rio Grande. Total mass balance was achieved for reaches above Bernardo by adding ungaged surface inflows. From Bernardo to San Acacia, calibration was achieved by manipulation of surface water groundwater exchanges.

2.2.3.3.2.3 Socorro Basin Groundwater System

The Socorro basin regional groundwater model created by Nabil Shafike (2005) simulated regional groundwater flow associated with the Rio Grande river system from San Acacia to Elephant Butte Reservoir. As described in detail in the next chapter of this report, steady state values for the Shafike model were used to calibrate a spatially aggregated 12-zone model that is dynamically linked to the surface water reaches from San Acacia to Elephant Butte. The Socorro groundwater basin does not communicate to any significant extent with the Albuquerque groundwater basin to the north in either the McAda/Barroll or Shafike models. Surface water stages in the river, canal, and drains are calculated with Manning's equation. San Acacia to San Marcial was calibrated by increasing the riparian acreage by 40%. See Section 2.2.3.2.7 for further discussion of this change. The San Marcial to Elephant Butte reach was calibrated to 1975–1999 gage values by manipulation of surface water groundwater exchanges.

2.2.3.4 Surface Water Flows

2.2.3.4.1 Gaged Streams

The majority of water enters the surface water system as gaged inflows, with the largest of these occurring at the top of the Rio Grande (Rio Grande near Lobatos gage) and Rio Chama (Rio Chama near La Puente gage), which together are responsible for 60% of gaged inflows to the model. Other tributary gages are included as reach inflows where they are available close to the confluence with any river reach. Relevant gaged tributary flows are added to the model during all model periods, with future run values based on historic year reshuffle as described in Section 2.2.1.

Flows from the gages in Table 2-1 are used as direct input into the model with three exceptions: the Ojo Caliente at La Madera gage, the Chama at La Puente gage, and the Embudo at Dixon gage. The La Madera gage is located 20 miles from the confluence of the Ojo Caliente and Chama, and gage readings are reduced by modeled potential losses between the gage and confluence. In the case of the La Puente gage, estimating flow at the gage with El Vado Reservoir behavior (see Section 2.2.3.5.4) and comparing to gaged flows suggests that the La Puente gage tends to overestimate high flows. In the case of the Embudo creek gage, 1975–1999 gage readings suggest that on average, more gaged water enters the Taos Bridge to Embudo reach (855 cfs in Rio Grande at Taos Bridge and 100 cfs from Embudo Creek for a total of 955 cfs) than leaves (946 cfs in Rio Grande at Embudo gage). Either losses in the 15-mile canyon reach are dramatically underestimated, or inflows are overestimated. The latter seems more likely. Flows from both the La Puente and Embudo Creek gages over a certain threshold are reduced by a calibrated percentage to result in flows consistent with downstream observations.

2.2.3.4.2 Gaged Municipal Wastewater Returns

Gaged wastewater return flows from municipal sources are included in the model for the cities of Espanola, Bernalillo, Rio Rancho, Albuquerque, Los Lunas, Belen, Socorro, and Truth or Consequences. 1975–1999 wastewater flow data are taken from URGWOM. Taos wastewater data are available; however, the Taos wastewater is assumed to discharge to the groundwater system, or the Rio Pueblo de Taos, which is a gaged tributary in the model. Los Alamos County and Los Alamos National Laboratory wastewater data are also available; however, they are assumed to be accounted for in the groundwater contribution to the Otowi to Cochiti reach, which as discussed in Chapter 3 was based on seepage studies within that river reach (Frenzel 1995). Historic municipal wastewater data is used for calibration and validation, while future runs use returns based on human water use patterns based on historic trends and user input. For further discussion on modeling of human use patterns, see Chapter 7.

2.2.3.4.3 Surface Water Diversions and Returns

Surface water diversion for agricultural irrigation is a historic and socially important use of water in river systems in New Mexico, and represents the largest traditional user of water supplies. Along the Rio Grande proper, surface water is diverted from the river into agricultural conveyance systems for irrigation use in most reaches below Taos Junction Bridge. The same is true to some extent of all modeled reaches along the Rio Chama and Jemez River.

Along the Chama, historic diversion data are available; the diversion is set to historic, consumptive use is the potential crop ET up to diversion amount, and the return is the diversion less the consumptive use. Along the Rio Grande above Cochiti, and along the Jemez, historic diversion data are not readily available. For these reaches during all periods, as well as the Chama reaches during validation and scenario evaluation periods, we assume that half of the diversion is lost, and half returns to the system. The diversion amount is calculated as double the potential crop ET (see Section 2.2.3.2) up to available water, and the return is the diversion less the consumptive losses. Consumptive loss is the potential crop ET up to diversion amount.

Below Cochiti along the Rio Grande, calibration period diversions and conveyance through flows are based on historic data. During validation and scenario evaluation periods, diversions are based on 1975–1999 average diversions at each diversion point up to available. The exception is the low flow conveyance channel (LFCC), which was originally designed to reduce conveyance losses between San Acacia and Elephant Butte. Utilized heavily between 1950 and 1986, growing awareness of endangered species requirements and sediment buildup at its terminus have resulted in essentially zero diversions to the LFCC since the late 1980s (Shafike 2005). Default diversion targets for each diversion point are summarized in Table 2-12. These defaults may change as a function of irrigated crop acreage and user inputs as the model is enhanced for scenario evaluation.

Table 2-12. Surface water diversion target to agricultural conveyance system below Cochiti for validation and scenario evaluation periods. Values are 1975–1999 average diversions rounded to the nearest 100 AF/mo. Low flow conveyance default diversions are assumed to be zero; however, this value can be changed by the user.

Diversion Target for Validation and Scenario Evaluation Periods [AF/mo]						
	Diversion name in reach	Cochiti CTI2SFP	Angostura SFP2ALB	Isleta ALB2BDO	San Acacia BDO2SA	LFCC BD02SA
Month	January	0	200	0	200	0
	February	100	300	0	100	0
	March	8300	11100	18700	6500	0
	April	11200	14900	26000	8500	0
	May	12300	17200	28400	8400	0
	June	12100	17100	28900	8500	0
	July	12000	18300	25500	7300	0
	August	11700	16800	20200	4600	0
	September	11100	16000	18300	3300	0
	October	11200	15100	14600	3700	0
	November	300	1100	200	300	0
	December	0	100	0	300	0

South of Cochiti, exchanges between the surface water agricultural conveyance system and the groundwater system are calculated as described in Section 2.2.3.3.2, and loss to the atmosphere is potential crop ET up to available, limited by carriage water requirements as discussed previously (Section 2.2.3.2.9) and summarized in Table 2-4. This is true for all modeling periods. After these interactions are considered, the water available to return to the river either flows through to the downstream agricultural conveyance system or returns to the river. A historically based fixed percentage of available water continues to the conveyance system in the next reach, and the rest returns to the river. The canal through flow percentages for each Rio Grande reach below Cochiti are summarized in Table 2-13. During the calibration period, the conveyance inflows are set to gage data, so the conveyance system effectively resets at each reach; however, during validation and scenario evaluation the conveyance through flows from an upstream reach (Q^{i}_{convtf} in Equation 2-3) become the conveyance inflows for the next reach downstream (Q^{j}_{convtf} in Equation 2-3).

2.2.3.4.4 Ungaged Surface Water Inflows

Combining Equations 2-1 and 2-2, and solving for ungaged surface water inflows:

$$Q^{j}_{swungaged} = Q^{j}_{msout} - Q^{j}_{m\sin} - Q^{j}_{swgaged} + Q^{j}_{swdiversion} - Q^{j}_{swreturn} - Q^{j}_{gwsw} + Q^{j}_{evap} \qquad (2\text{-}13)$$

Table 2-13. Amount of water in the agricultural conveyance system assumed to leave the reach in the conveyance system rather than returning to the river. Average of 1975–1999 observations.

Reach	Conveyance % Through Flow
Cochiti to San Felipe	23%
San Felipe to Albuquerque	63%
Albuquerque to Bernardo	45%
Bernardo to San Acacia	47%
San Acacia to San Marcial	58%
San Marcial to Elephant Butte	100%

The previous sections have defined all terms on the right side of Equation 2-13. After all terms on the right of Equation 2-13 have been considered, most reaches and reservoirs north of Bernardo need additional water to be consistent with the observed gage data. These reaches and reservoirs were calibrated to have no net error between the gages during 1975–1999 by adding a modeled ungaged surface water inflow term. The term was estimated as a percentage of a nearby gaged tributary. Using this approach, input data for ungaged surface water inflows are based on available gages, and an explicit error term can be calculated. Table 2-14 lists the reaches and reservoirs to which ungaged surface water inflows were added as a calibration term, and the associated gage and calibration factor for the reach. This ungaged inflow is in addition to any ungaged baseflow into the reach attributed to surface water as described in Section 2.2.3.3.1 and shown in Table 2-11. For reaches upstream of Cochiti, this term was only added during non-winter months (March through October). The reach from Elephant Butte to Caballo includes only gaged releases from Elephant Butte, and whatever ungaged surface inflow is necessary to get net zero error in observed storage at Caballo compared to modeled for the calibration period. The ungaged surface inflow is added as a function of average precipitation rate at Elephant Butte and Caballo reservoirs.

2.2.3.5 Reservoir Behavior

Section 2.2.3.1.2 and Table 2-5 give an overview of the characteristics of the major reservoirs within the model extent, and Equation 2-4 outlines the governing mass balance equation for reservoirs. Section 2.2.3.2 discusses how the evaporation term is calculated for the reservoirs. This section will consider the leakage terms, the precipitation terms, and the inflow and outflow terms for the seven modeled reservoirs.

2.2.3.5.1 Reservoir Groundwater Leakage

Groundwater flow into Elephant Butte Reservoir is modeled from the Socorro Basin groundwater system. See Chapter 3. Reservoir leakage is modeled for Heron, Cochiti, and Jemez reservoirs. Leakage from Heron is modeled according to URGWOM (USACE et al. 2002) methodology.

$$Q_{gw}^{Heron} = (z^{Heron,m} - 7100\,ft) * 0.2134 \frac{ft^2}{s} + 0.76 \frac{ft^3}{s} \qquad (2\text{-}14)$$

Table 2-14. Dynamic ungaged surface water inflows to modeled river reaches. Added to close the mass balance. These values are in addition to any baseflow assigned to the reach (see Section 2.2.3.3.1 and Table 2-11). No ungaged inflows are added to reaches north of Cochiti during winter months (November through February).

Reach or Reservoir	Ungaged Inflow Added?	Ungaged Inflow Factor	Comments
Chama: Willow Creek to Heron	Yes	6.7%	Rio Chama near La Puente, Mar – Oct only
Chama: Heron to below El Vado	No		
Chama: El Vado to above Abiquiu Reservoir	Yes	36%	Rio Ojo Caliente at La Madera
Chama: below Abiquiu to Chamita	Yes	2.5%	Rio Ojo Caliente at La Madera
Lobatos to Cerro	No		
Cerro to Taos Junction Bridge	Yes	39%	Rio Pueblo de Taos below Los Cordovas
Taos Junction Bridge to Embudo	No		
Embudo to Otowi	Yes	165%	Rio Nambe below dam (USGS 08294210)
Otowi to below Cochiti	No		
Below Cochiti to San Felipe	Yes	300%	Galisteo creek below Galisteo dam
Jemez: Jemez Pueblo to Reservoir	Yes	70%	Flows < 200 cfs at Jemez River near Jemez
Jemez continued		10%	Flows > 200 cfs at Jemez River near Jemez
San Felipe to Albuquerque	Yes	400%	North floodway channel near Alameda
Albuquerque to Bernardo	Yes	75%	Rio Puerco near Bernardo
Bernardo to San Acacia	No		
San Acacia to San Marcial	No		
San Marcial to below Elephant Butte	No		
Below Elephant Butte to Caballo	Yes	26,800 acres	Multiplied by average of EB and Caballo precipitation values (L/T)

where

Q_{gw}^{Heron} = groundwater leakage out of Heron Reservoir [L^3/T].

$z^{Heron,m}$ = the greater of 7,100 feet or the stage of Heron in feet for month *m* [L].

Reservoir leakage from Cochiti and Jemez reservoirs are calculated as a function of reservoir stage and underlying aquifer head as described in Chapter 3.

2.2.3.5.2 Reservoir Precipitation

Reservoir precipitation gains for all reservoirs are calculated as the measured precipitation depth in a given timestep multiplied by the reservoir area in that timestep.

$$Q^{r}_{precip} = P^{r,m} * A^{r,m} * (1 - \mathrm{cov}^{r,m}) \quad (2\text{-}15)$$

where

Q^{r}_{precip} = precipitation gains to reservoir *r* as defined in equation 4 [L^3/T]
$P^{r,m}$ = precipitation rate measured at reservoir *r* during month *m* [L/T]
$A^{r,m}$ = the area of reservoir *r* during month *m* [L^2]
$\mathrm{cov}^{r,m}$ = percent of reservoir *r* covered by ice during month *m* [%]

As discussed in Section 2.2.3.2.5, reservoir areas ($A^{r,m}$) are calculated based on storage volume in the reservoir using EAC relationships specific to each reservoir (tables from Roberta Ball, USACE personal communication 2003). Ice cover on a given reservoir ($\mathrm{cov}^{r,m}$) is a historically measured value, taken from the daily URGWOM data set and averaged to monthly. For scenario evaluation runs, the ice cover is calculated using a simple regression relationship to average temperature during the previous month.

2.2.3.5.3 Reservoir Surface Water Inflows and Releases

Inflows to El Vado from Heron and Abiquiu from the Chama are set to appropriate gage data for the calibration period, and modeled for validation and scenario runs. Inflows to Heron from the SJC diversion tunnel (see Section 2.2.2), El Vado from the Rio Chama, Cochiti from the Rio Grande, Jemez Reservoir from the Jemez River, and Elephant Butte and Caballo reservoirs from the Rio Grande are modeled based on reach behavior between the nearest upstream gage and the reservoir. If the nearest upstream gage is a calibration gage (Table 2-2), it is set to observed values for the historic calibration period, and modeled values for validation and scenario evaluation. Input gages (Table 2-1) are set to observed values for all periods, with scenario values from a reshuffle of historic data. Reservoir inflows from modeled but ungaged reaches are calculated within the model for all periods. Ungaged inflows were added to Heron and Abiquiu reservoirs for calibration purposes as discussed in Section 2.2.3.4.4. In addition to modeled or gaged reservoir inflows, an error inflow (positive or negative at each timestep but net zero over time after calibration) is added to the reservoirs at each calibration timestep to force the modeled storage to observed storage. This error term is added to the reservoir to avoid compounding errors and maintain reservoir storage at historic observed levels during the calibration period.

Reservoir releases for the 1975–1999 calibration period are set to observed historic releases. Reservoir releases for the validation and scenario evaluation periods are modeled using reservoir operation rules. The seven major reservoirs within the model extent are operated according to a complex set of legal and physical constraints with a broad range of objectives including interstate compact delivery requirements, downstream flood control, storage for agricultural and municipal demand, electric generation, and minimum stream flow. The full extent of operational requirements is represented in URGWOM. Predicted behavior of reservoirs under specific hydrologic scenarios by URGWOM was used to develop a simplified set of rules for operations. The reservoir operations rules that determine releases in the validation and scenario evaluation periods are summarized by reservoir in the next seven subsections.

2.2.3.5.3.1 Heron Reservoir Release Rules

Heron Reservoir is operated by the BoR to store SJC water diverted from the Colorado river basin into the Rio Grande Basin (see Section 2.2.2) for use by entities with contracts to the water. There are currently 17 contractors with rights to almost all 96,200 AF of annual allocation of SJC water (USDoI 2006). For simplicity, the URGWOM planning run and the monthly model consider three of the contractors specifically: the City of Albuquerque, with annual rights to 48,200 AF; the MRGCD, with annual rights to 20,900 AF; and the Cochiti Recreation Pool, with annual rights up to 5,000 AF. All other contractors are lumped into a "combined" contractor account with annual rights to 21,100 AF. The final 1,000 AF is unallocated water reserved for future Native American water rights settlements and not considered in the model. In January of each year, the contractor allocation of SJC water in Heron available for use in that year is set to the annual right. Any amount not used by the end of the year reverts to the general pool from which the allocations are reset at the beginning of the next year. In practice, to avoid a dramatic release of unused contractor water from Heron at the end of the year, there is some flexibility in release date granted to the contractors to allow releases of the previous year's water in the first few months of the next year. In simple terms then, Heron is modeled to pass through all native water, and release SJC water based on modeled requests from contractors up to their annual allocation. The legal framework of SJC operations mean that evaporative losses are not charged to a given contractor, so the annual allocation of water is available to the contractor at any time in the year. In other reservoirs where the contractors may be allowed to store SJC water, the water is subject to evaporative losses. The result of this is that contractors are assumed to prefer to leave their allocation of water in Heron until they have use for it downstream, only moving it into downstream storage to avoid losing the water to the general pool at the end of the year.

2.2.3.5.3.2 El Vado Reservoir Release Rules

El Vado Reservoir is operated by the MRGCD primarily to store native spring runoff to augment irrigation supplies later in the season when natural flows are low. The irrigation served includes native American lands with rights that are prior and paramount to all other irrigation rights. Article VII of the Rio Grande compact prohibits additions to non prior and paramount native storage in El Vado if the total project water[3] stored in Elephant Butte and Caballo is less than 400,000 AF. MRGCD can also store its SJC water in El Vado, and lease space for storage of SJC water to other contractors. For modeling purposes, when irrigation demands below Cochiti are satisfied by Rio Grande flows, El Vado is operated to capture all native inflows that are physically and legally allowed, less a minimum release for irrigation demands on the Chama. If Rio Grande flows are not sufficient to cover irrigation demands below Cochiti, native water is released from El Vado if available to satisfy those demands. If native water is insufficient, MRGCD-owned SJC water is released, and when that is gone also MRGCD calls for SJC releases directly from Heron Reservoir. Any MRGCD SJC allocation remaining in Heron at the end of the year is moved to El Vado. All releases of SJC water from Heron not intended for storage in El Vado are passed through. Combined SJC contractor storage in El Vado is allowed as a user input to the model.

[3] Project water in Elephant Butte and Caballo is all water in the reservoirs, less any SJC water in Elephant Butte for recreation pool purposes, and less any credit water from New Mexico or Colorado deliveries to Elephant Butte in excess of legal requirements. It is basically required delivery water from New Mexico.

2.2.3.5.3.3 Abiquiu Reservoir Release Rules

Abiquiu Reservoir is operated by the United States Army Corps of Engineers (USACE) primarily as a flood control reservoir, though storage of SJC water, primarily by Albuquerque, has become a significant part of operations. Native water is stored in Abiquiu only temporarily to prevent flows downstream from exceeding flows of 1,800 cfs, 3,000 cfs, and 10,000 cfs below the reservoir, at the confluence with the Ojo Caliente, and at the confluence with the Rio Grande respectively. When the stored native flood water can be released, it is with an exception called carryover storage. To ensure that flood waters that would have been largely unused had they not been stored are not used to supplement irrigation, if flows in the Rio Grande at Otowi are less than 1,500 cfs at any point after July 1 in an irrigation season, then stored flood water from that irrigation season is delivered downstream after the irrigation season is over. For modeling purposes, native water is not stored except for flood control purposes, and released downstream as soon as possible within the constraints of carryover storage. There is some discussion of native water storage at Abiquiu for stream augmentation purposes in the future, and this option is allowed as a user input. The model allows Albuquerque, MRGCD, and the combined contractor to store 130,000 AF, 2,000 AF, and 11,000 AF respectively in Abiquiu based on URGWOM values (Marc Sidlow, USACE personal communication 2006). This storage space is used by the contractors as available to avoid losses of allocated water in Heron at the beginning of each new year, and vacated first by the contractors when there is need for it downstream.

2.2.3.5.3.4 Cochiti Reservoir Release Rules

Cochiti Reservoir, like Abiquiu upstream, is operated by the USACE primarily as a flood control reservoir. The only native storage allowed in Cochiti is native flood control storage to maintain downstream flows below 7,000 cfs. This storage is temporary and evacuated as quickly as possible subject to the same carryover storage requirements described in Section 2.2.3.5.3.3. The only SJC storage allowed in Cochiti is that amount necessary to maintain approximately 1,200 acres of reservoir area for recreation purposes. The 5,000 AF/yr SJC allocation to the Cochiti Recreation Pool is used to offset evaporative losses to the recreation pool in Cochiti. Additional storage is disallowed in Cochiti in part because large storage volumes in the reservoir lead to high leakage with adverse consequences to agricultural lands downstream of the dam (e.g., Smith 2001).

2.3.1.1.1 Jemez Reservoir Release Rules

Jemez Reservoir, like Abiquiu and Cochiti, is operated by the USACE primarily for flood control. The reservoir also acts as a sediment barrier to prevent sediment from discharging to the Rio Grande. For model purposes, the only storage allowed in Jemez is native flood control to aid in maintaining Rio Grande flows between Cochiti and Elephant Butte from exceeding 7,000 cfs. Flood storage in Jemez is subject to the same carryover storage requirements described in Section 2.2.3.5.3.3.

2.2.3.5.3.6 Elephant Butte Reservoir Release Rules

Elephant Butte Reservoir is operated by the Elephant Butte Irrigation District (EBID) to store water delivered from New Mexico to Texas under the requirements of the Rio Grande compact. The water is released for irrigation in southern New Mexico and western Texas. The water released from Elephant Butte (and then Caballo) is consumed outside of the model boundary, so for future releases, a target release table is used. The available water up to the target value is released for each month. Available water includes water in the reservoir less SJC and New Mexico or Colorado credit water (water delivered to Elephant Butte from upstream in excess of contract obligation). The model release targets from Elephant Butte by month are shown in Table 2-15.

Table 2-15. Target releases used for Elephant Butte and Caballo reservoirs to determine releases in validation and scenario evaluation modes.

	Elephant Butte [AF]	**Caballo [AF]**
January	23600	7500
February	52100	28100
March	82700	109100
April	102700	89500
May	122800	101800
June	133000	128900
July	117500	135100
August	81000	107400
September	42100	67100
October	14600	15500
November	6600	0
December	18300	0
Total	797000	790000

2.2.3.5.3.7 Caballo Reservoir Release Rules

Caballo Reservoir, like the larger Elephant Butte just upstream, is also operated by EBID. Caballo serves largely as additional storage to moderate releases from Elephant Butte and add flexibility to EBID operations. There are no irrigation diversions between Elephant Butte and Caballo, and in many ways, Caballo is simply an extension of the larger Elephant Butte Reservoir. Release targets used in the model for Caballo Reservoir are shown in Table 2-15.

2.2.3.5.4 Reservoir Calibration

A given reservoir, or more commonly a reach-reservoir combination, was calibrated so that the error inflow described in Section 2.2.3.5.3 was net zero for the 1975–1999 calibration period. Heron and Jemez reservoirs were calibrated by adding ungaged inflows to the upstream reach as described in Section 2.2.3.4.4.

El Vado Reservoir was calibrated by reducing peak flows at the Rio Chama near La Puente gage. This strategy was pursued after it was observed that from 1975 through 1999, the amount of water that modeled El Vado dynamics suggested should be flowing into the reservoir was less than the sum of gages below Heron and on the Chama at La Puente. The distribution errors at La Puente gage implied by El Vado behavior is skewed towards an overestimate of inflows as shown in Figure 2-10a, and the skew in the distribution is a strong function of flow rates observed at La Puente gage as shown in Figure 2-10b. This analysis suggests that if Equations 2-10a, 2-14, and 2-15 and associated parameters accurately represent behavior in El Vado Reservoir, the Rio Chama near La Puente gage tends to overestimate large flows. El Vado was calibrated by reducing the portion of observed flows at La Puente gage greater than 2,000 cfs by 35%.

Abiquiu Reservoir was calibrated by adding ungaged inflows to the reservoir. The magnitude and timing of these inflows were calculated as 53% of gaged flows on the Jemez River near Jemez. The Jemez River was chosen as representative of the Jemez mountain tributaries (including the Rio Puerco and Canones drainages) assumed largely responsible for ungaged inflows to Abiquiu Reservoir. Cochiti Reservoir was calibrated with leakage to the groundwater system as described in detail in the next chapter.

2.2.3.6 Calibration and Validation Summary Information

This section serves only to summarize and aggregate information that is scattered throughout this chapter up to this point. As discussed in the previous sections, Equations 2-1 through 2-4 are used to model mass balance between surface water gages along the river, the agricultural conveyance system, and in reservoirs. The mass balances described in each of these spatial units are calibrated to match 1975–1999 observations by adding ungaged surface water inflows, adjusting riparian and agricultural ET, reducing gaged inflows, or changing reservoir leakage to the groundwater system. Table 2-16 summarizes the reach calibration method utilized for each reach and reservoir, and the 25-year average flow represented by the calibration term.

As has been mentioned throughout this report, certain terms that are utilized or calculated in one way during the 1975–1999 calibration period are calculated differently during the 2000–2006 validation period and 2006 forward scenario evaluation period. The most important of these are calibration gages (Table 2-2), which are used to reset the model flows in each reach during calibration, but are only used for comparison purposes in validation, and are not used at all in scenario evaluation. Another major change is in the use of input gages (Table 2-1) and input climate data. These data are historical for the calibration and validation period, and from a reshuffle of historic years for the scenario evaluation period. Reservoir releases are from historic observations for the calibration period, and based on rules for the validation and scenario evaluation periods. Table 2-17 summarizes variables in the model whose treatment changes in different model periods.

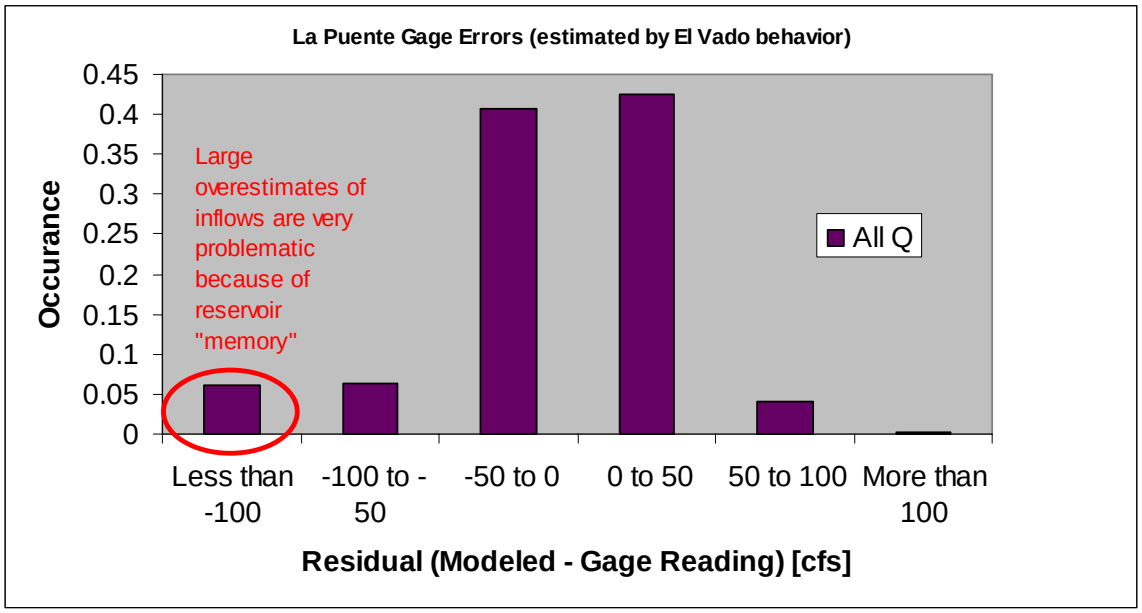

Figure 2-10a. La Puente gage errors.
If El Vado behavior is modeled with inflows from La Puente and Heron, too much water ends up in the reservoir between 1975 and 1999. If we estimate La Puente flows with El Vado historic storage, and compare to actual La Puente flows, we can derive a distribution of gage errors as shown here. The residuals below 100 cfs stand out from an otherwise relatively normal distribution.

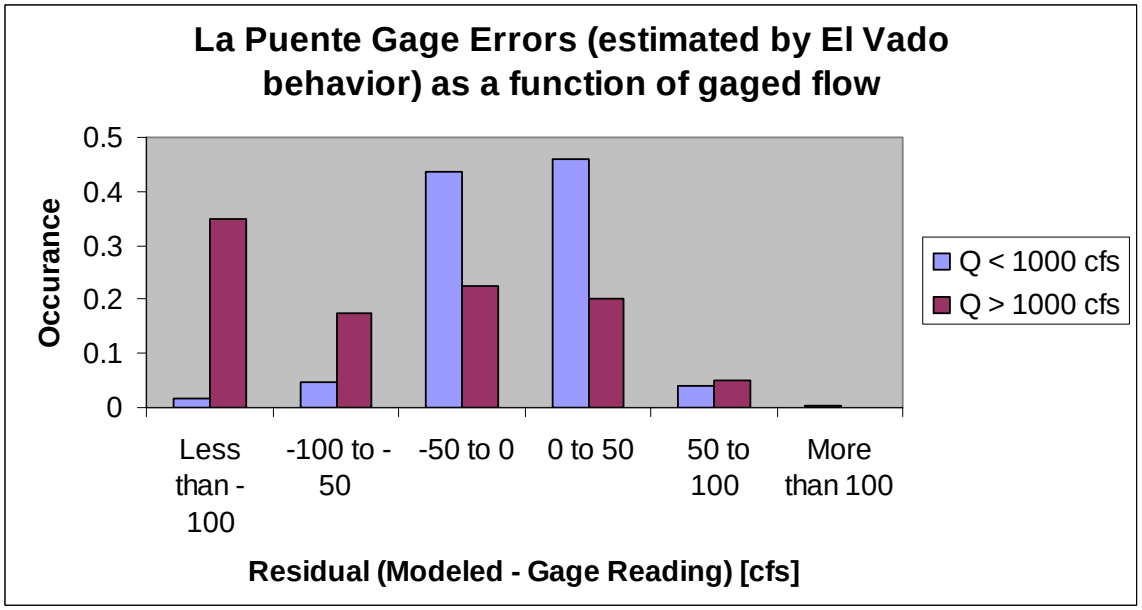

Figure 2-10b. La Puente gage errors as a function of gaged flow.
The residuals shown in Table 2-10b are a strong function of measured flows at La Puente. This distribution suggests that high flows at La Puente tend to be overestimated by the gage.

Table 2-16. Calibration summary for reaches and reservoirs in model extent. The type of calibration employed for each reach or reservoir and the total magnitude of the calibration term is included.

Reach or Reservoir	Calibration Term	Average Magnitude 1975-1999 [cfs]
Chama: Willow Creek to Heron	Ungaged SW inflow	26
Chama: Heron to El Vado	Gaged SW reduction	-17
Chama: El Vado to Abiquiu	Ungaged SW inflow	26
Abiquiu Reservoir	Ungaged SW inflow	48
Chama: Abiquiu to Chamita	Ungaged SW inflow	2
Lobatos to Cerro	none	0
Cerro to Taos Junction Bridge	Ungaged SW inflow	42
Taos Junction Bridge to Embudo	Gaged SW reduction	-7
Embudo to Otowi	Ungaged SW inflow	71
Otowi to Cochiti	Reservoir leakage	-31
Cochiti to San Felipe	Ungaged SW inflow	18
Jemez: Jemez Pueblo to Reservoir	Ungaged SW inflow	51
San Felipe to Albuquerque	Ungaged SW inflow	41
Albuquerque to Bernardo	Ungaged SW inflow	24
Bernardo to San Acacia	Riparian ET	-21
San Acacia to San Marcial	Riparian ET	-86
San Marcial to Elephant Butte	Riparian ET	-31
Elephant Butte to Caballo	Ungaged SW inflow	35

Table 2-17. Summary of variables with a change in treatment between calibration (1975–1999) and validation and scenario evaluation periods (2000 forward).

Variable	Calibration	Validation and Scenario Evaluation
Gaged inflows (Table 1)	Observed	Observed for validation, historic reshuffle for scenario evaluation.
Climate data	Observed	Observed for validation, historic reshuffle for scenario evaluation.
Mainstem SW inflow	Observed	Observed at model boundary, inflows from upstream reach outflows otherwise.
Reservoir outflows	Observed	Reservoir release rules.
Reservoir error inflows	Calculated	None.
Reservoir ice cover	Observed	Calculated based on regression to previous months temperature.
Conveyance through flow	Observed	Percent of available.
Surface water diversions	Observed	Modeled based on demand or historic average.
Agricultural acreage	Observed	1999 data for validation, user input from 1999 defaults for scenario evaluation.
Riparian acreage	Observed	1999 data for validation, user input from 1999 defaults for scenario evaluation.
Municipal wastewater	Observed	Function of modeled human water use patterns.

2.3 Results

2.3.1 Calibration Residuals

One way to evaluate model performance is to look at errors, or residuals, at points of historic observation. The points of observation to which we can compare surface water model performance during the calibration period include stream flows at gages and reservoir storage. Ideally, the calibration residuals will be normally distributed about zero, and comparable to the distribution of uncertainty associated with the observations themselves. Gage error distribution estimates were developed for the 1975–1999 period by plotting stage versus measured flow for all field measurements at the gage locations between 1975 and 1999. A single best fit rating curve was fit to the measurements at each location, and error assumed to be equal to the difference between the measured values and the single best fit rating curve. This method overestimates gage error, however, because it does not incorporate incremental adjustments to the rating curve through time. Current efforts to rework the gage error distribution estimates by assigning a gage error at each field measurement based on the rating curve shift incorporated as a result of the field measurement are under way.

Currently the model is calibrated to San Acacia, with reach calibration for the San Acacia to San Marcial, San Marcial to Elephant Butte, and Elephant Butte to Caballo reaches and reservoir calibration for Elephant Butte and Caballo reservoirs under way. The residuals for river gages at the bottom of reaches above San Acacia for the 1975–1999 calibration period are shown in Figures 2-11 through 2-20. In general, model performance degrades as distance downstream increases. This is a combination of increases in system complexity with distance downstream, and decreases in gage accuracy as a result of shifting channel geometries associated with sand-dominated riverbeds characteristic of lower reaches. Storage residuals for reservoirs above Elephant Butte for the same time period are shown in Figures 2-21 through 2-25.

2.3.2 Mass Balance in Each Reach and Reservoir Compared to URGWOM

This analysis is under way, and has been delayed by complexities associated with interpretation of URGWOM inputs, outputs, and calculations.

2.3.3 Future Results

As mentioned in Section 2.2.3.1, estimates of gage error distribution are being reworked with a slightly different methodology. Validation residuals shown in Figures 2-11 through 2-20 will be compared to estimates of gage reliability at each observation point for the calibration period. Mass balance comparisons to the URGWOM model will be included. Additionally, as validation data (2000–2006) gathering is completed and verified, additional results will include validation residuals and resulting error analysis for scenario runs. Finally, other potential results will include sensitivity analysis of important model inputs and parameters.

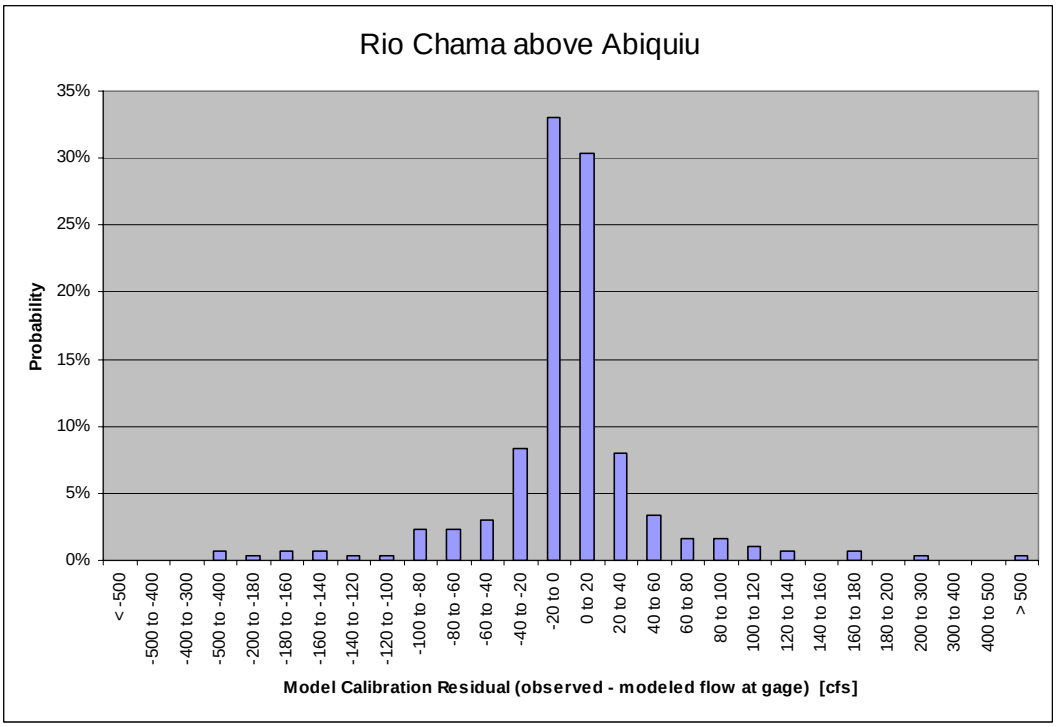

Figure 2-11. Model residual (observed – modeled) distribution for the surface water gage on the Chama above Abiquiu Reservoir (USGS Gage ID 8286500) for the 1975–1999 calibration period. Ideally, modeled residuals are normally distributed tightly about zero.

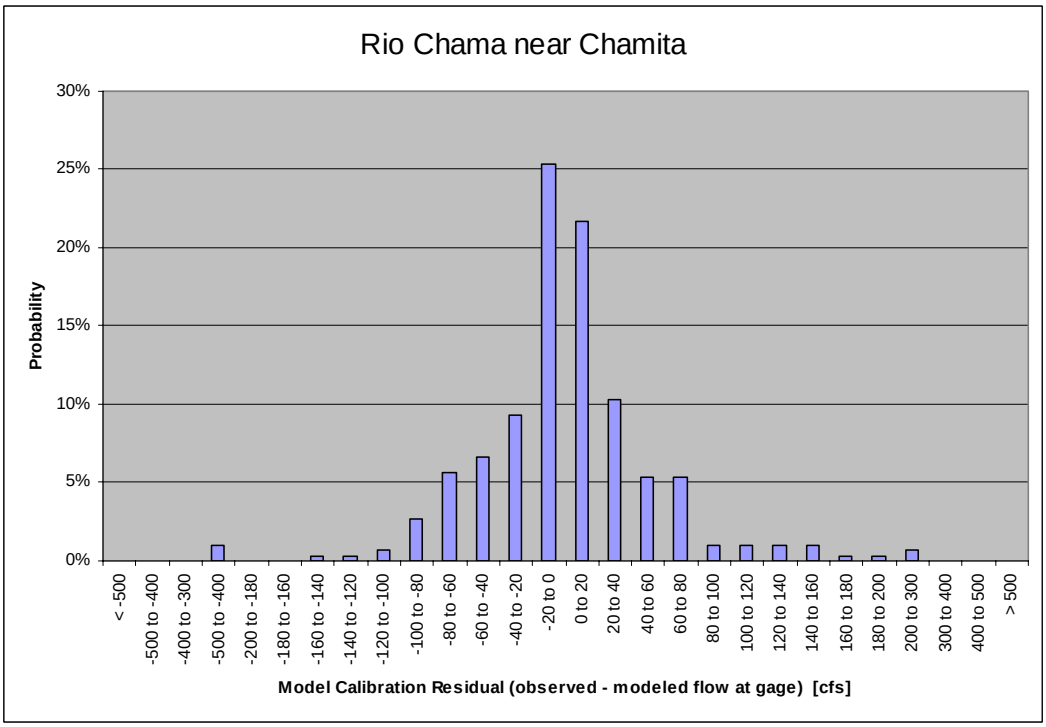

Figure 2-12. Model residual (observed – modeled) distribution for the surface water gage on the Chama near Chamita (USGS Gage ID 8290000) for the 1975–1999 calibration period. Ideally, modeled residuals are normally distributed tightly about zero.

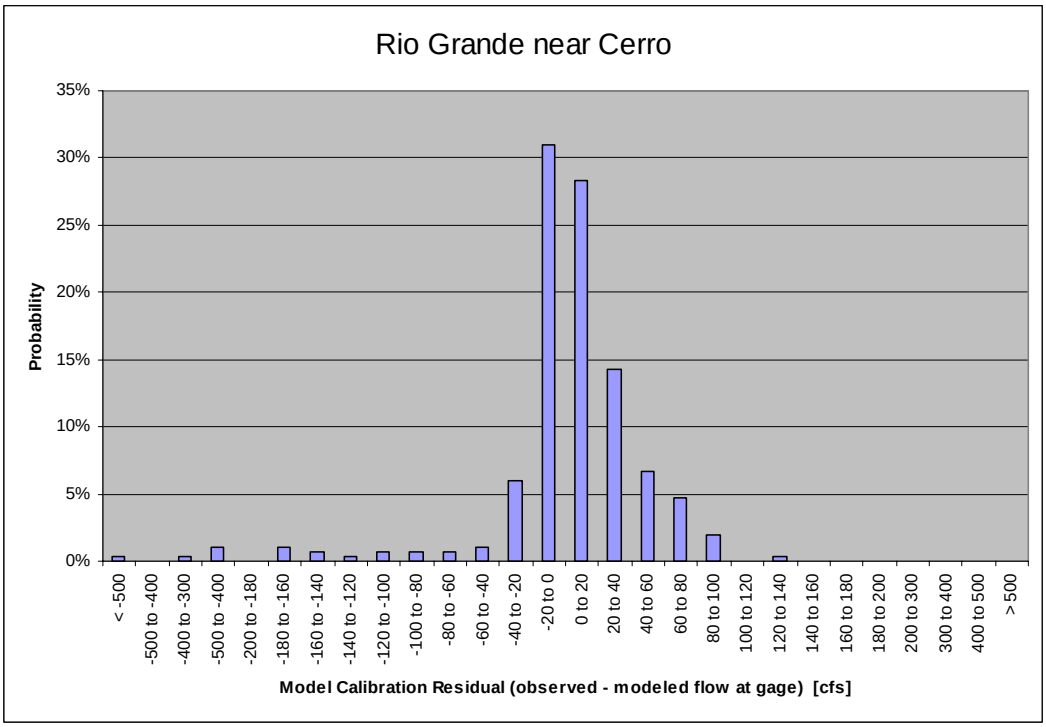

Figure 2-13. Model residual (observed – modeled) distribution for the surface water gage on the Rio Grande near Cerro (USGS Gage ID 8263500) for the 1975–1999 calibration period. Ideally, modeled residuals are normally distributed tightly about zero.

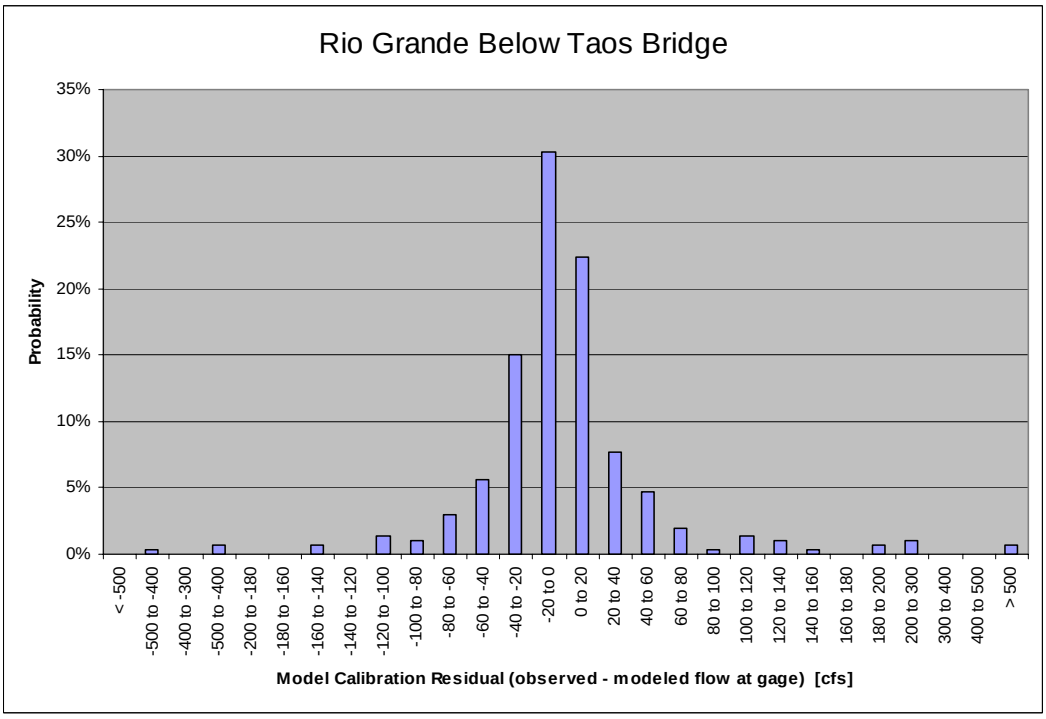

Figure 2-14. Model residual (observed – modeled) distribution for the surface water gage on the Rio Grande below Taos Bridge (USGS Gage ID 8276500) for the 1975–1999 calibration period. Ideally, modeled residuals are normally distributed tightly about zero.

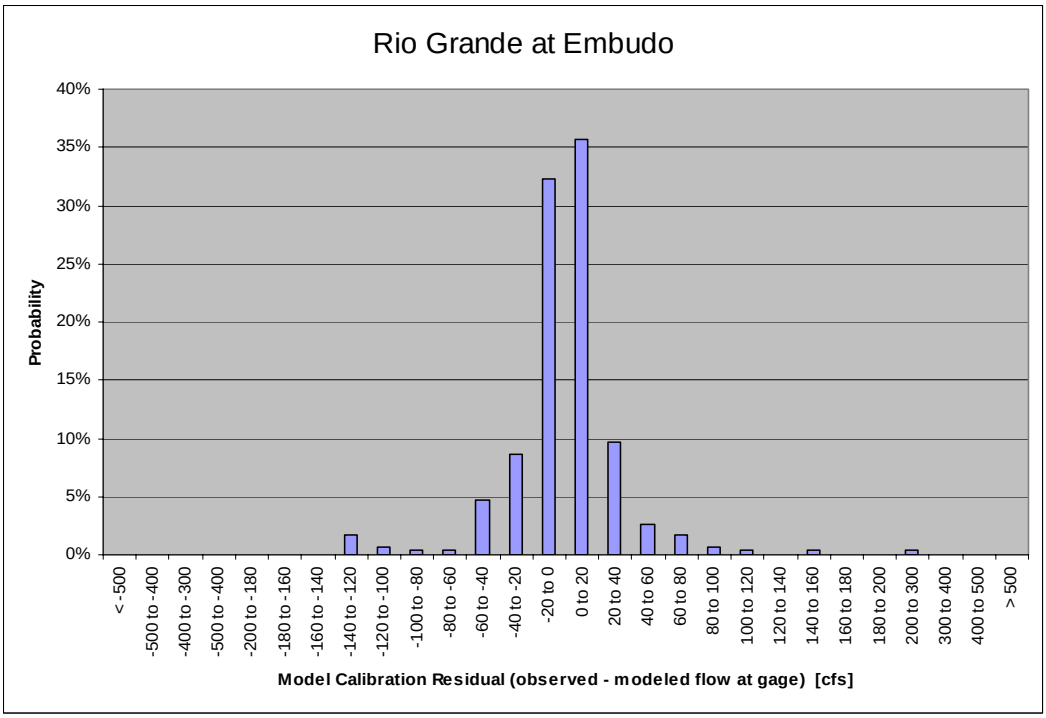

Figure 2-15. Model residual (observed – modeled) distribution for the surface water gage on the Rio Grande at Embudo (USGS Gage ID 8279500) for the 1975–1999 calibration period. Ideally, modeled residuals are normally distributed tightly about zero.

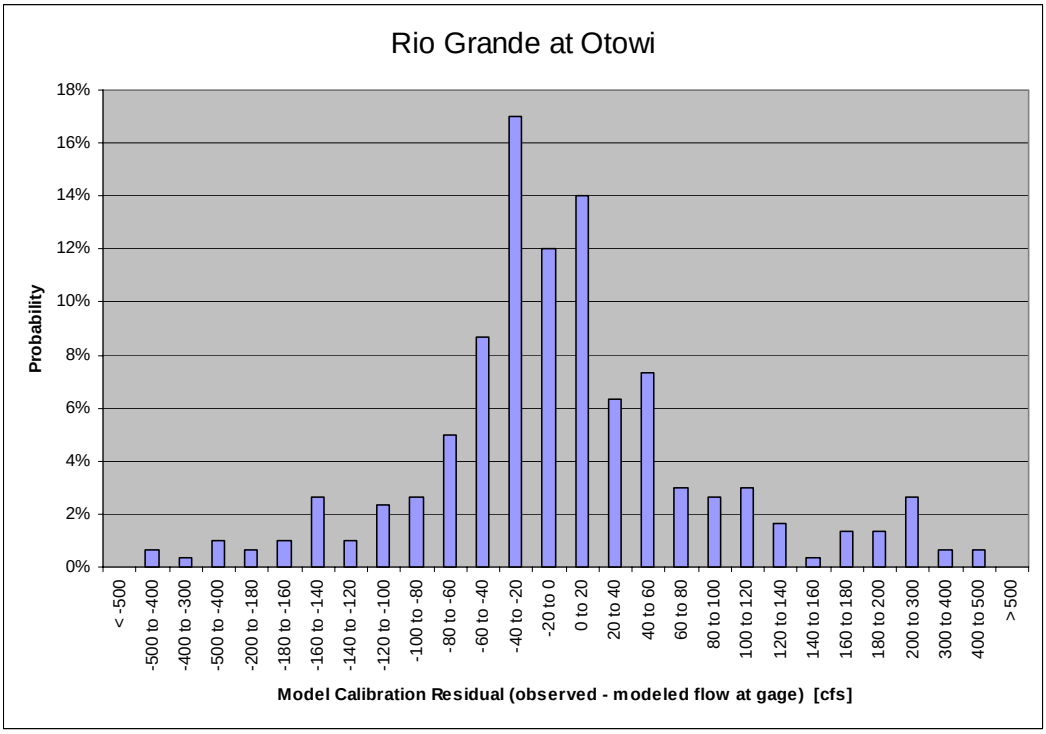

Figure 2-16. Model residual (observed – modeled) distribution for the surface water gage on the Rio Grande at Otowi (USGS Gage ID 8313000) for the 1975–1999 calibration period. Ideally, modeled residuals are normally distributed tightly about zero.

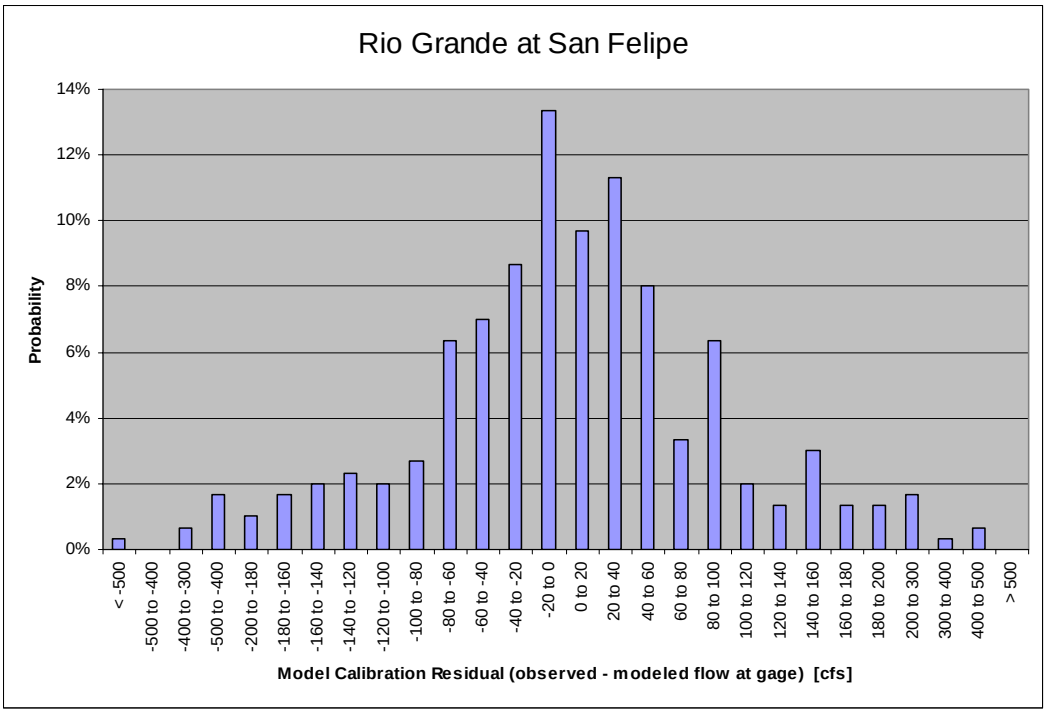

Figure 2-17. Model residual (observed – modeled) distribution for the surface water gage on the Rio Grande at San Felipe (USGS Gage ID 8319000) for the 1975–1999 calibration period. Ideally, modeled residuals are normally distributed tightly about zero.

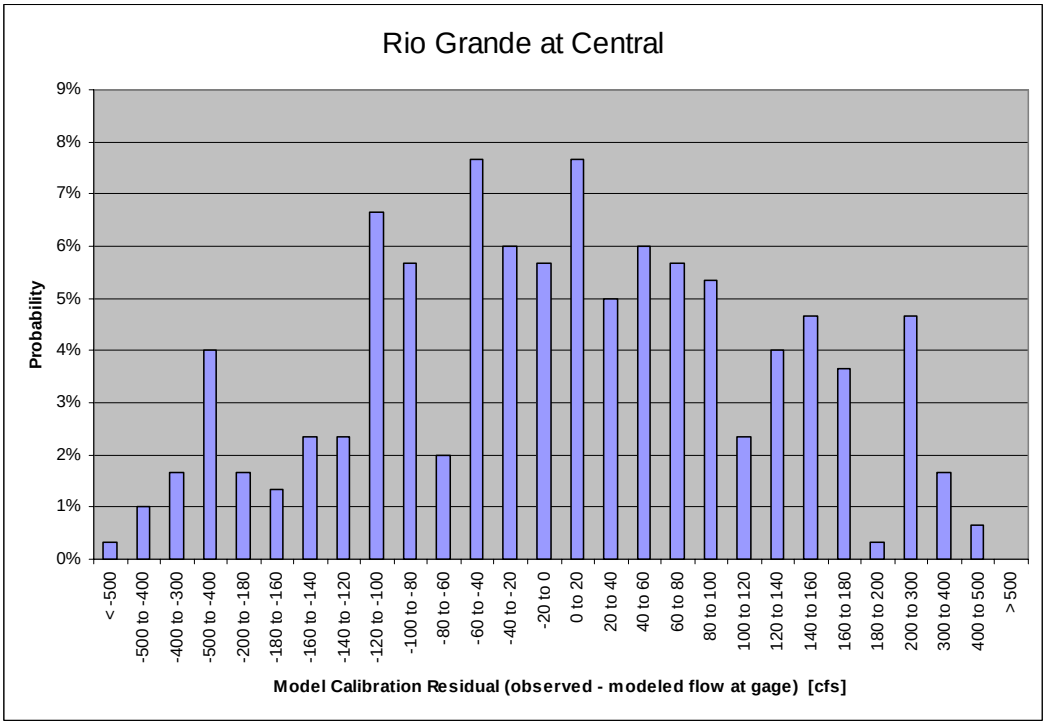

Figure 2-18. Model residual (observed – modeled) distribution for the surface water gage on the Rio Grande at Central bridge in Albuquerque (USGS Gage ID 8330000) for the 1975–1999 calibration period. Ideally, modeled residuals are normally distributed tightly about zero.

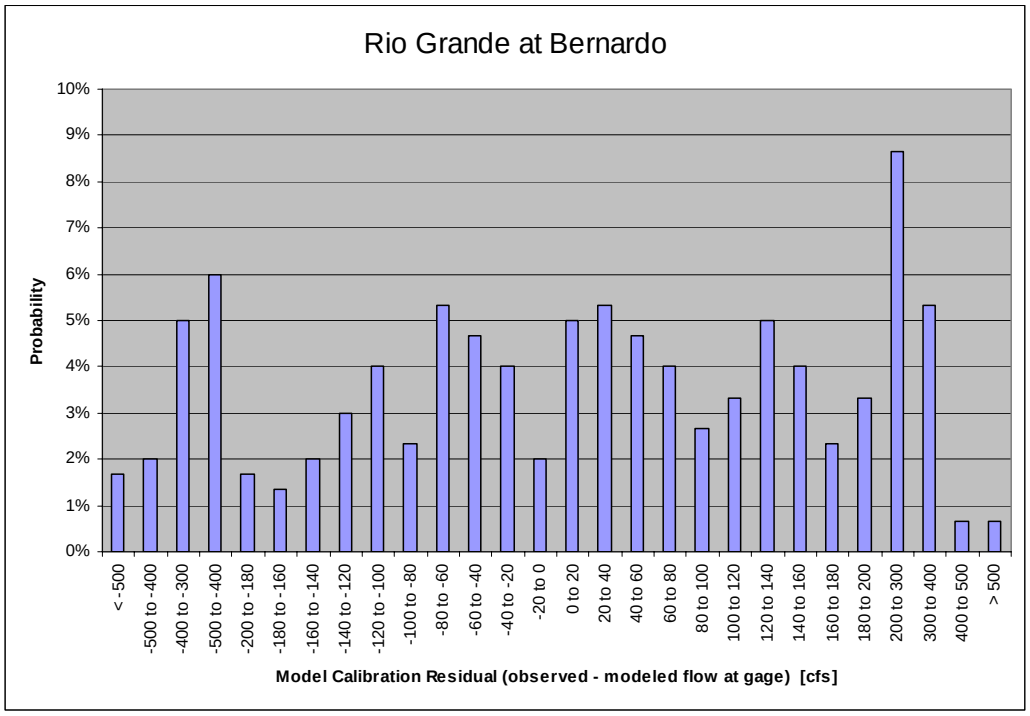

Figure 2-19. Model residual (observed – modeled) distribution for the surface water gage on the Rio Grande floodway at Bernardo (USGS Gage ID 8332010) for the 1975–1999 calibration period. Ideally, modeled residuals are normally distributed tightly about zero.

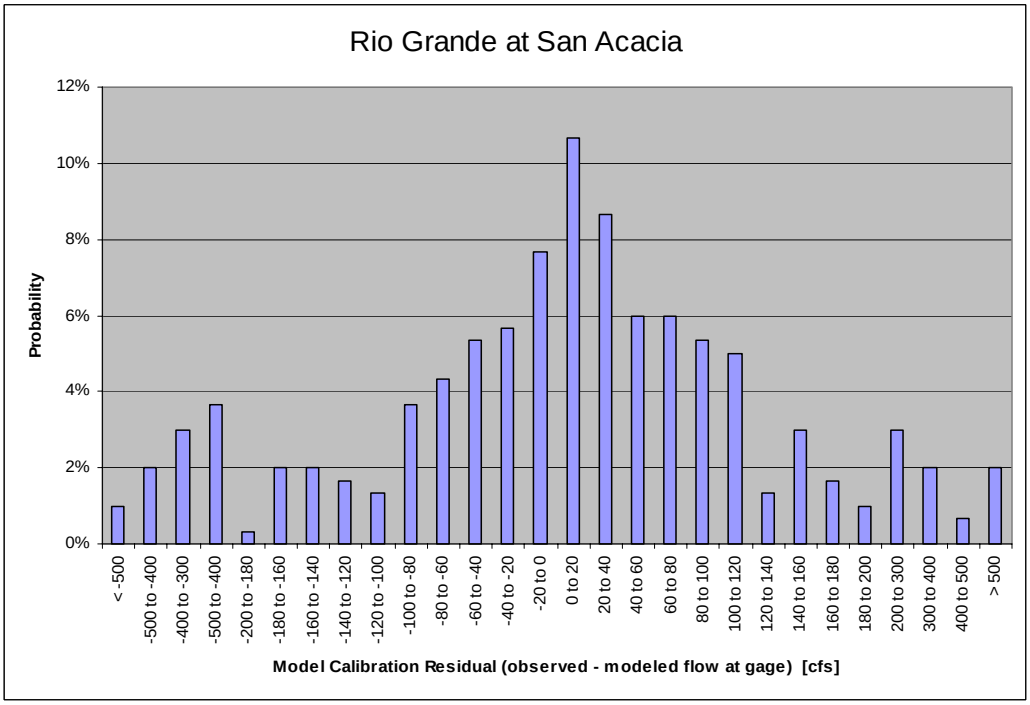

Figure 2-20. Model residual (observed – modeled) distribution for the surface water gage on the Rio Grande floodway at San Acacia (USGS Gage ID 8354900) for the 1975–1999 calibration period. Ideally, modeled residuals are normally distributed tightly about zero.

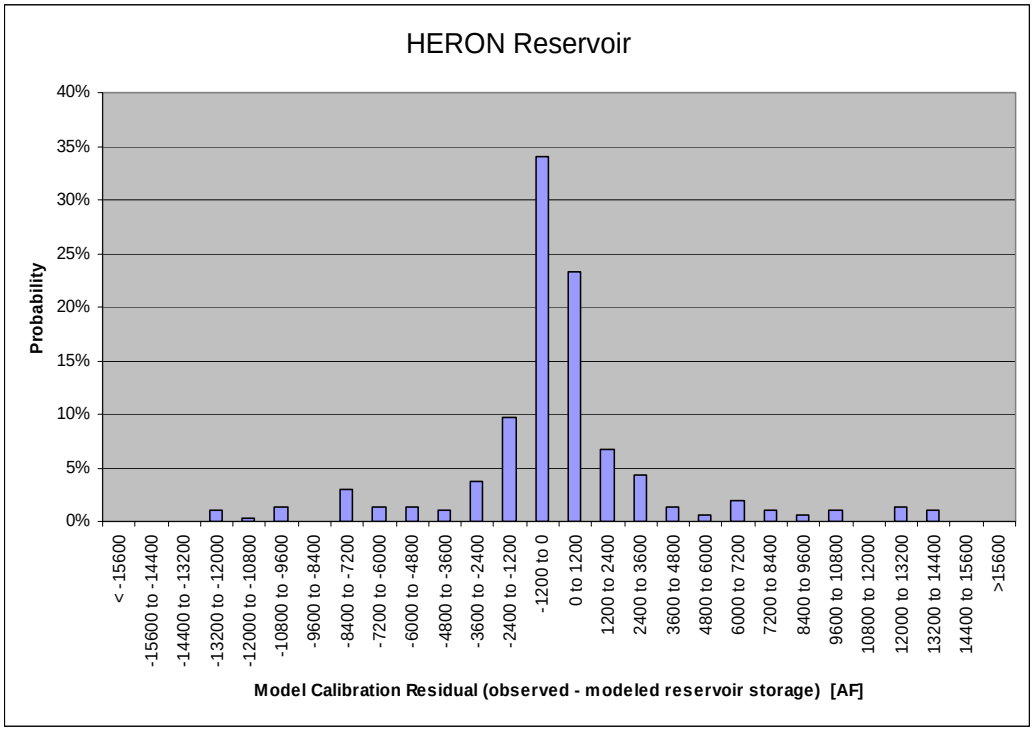

Figure 2-21. Model residual (observed – modeled) distribution for storage in Heron Reservoir for the 1975–1999 calibration period. Ideally, modeled residuals are normally distributed tightly about zero.

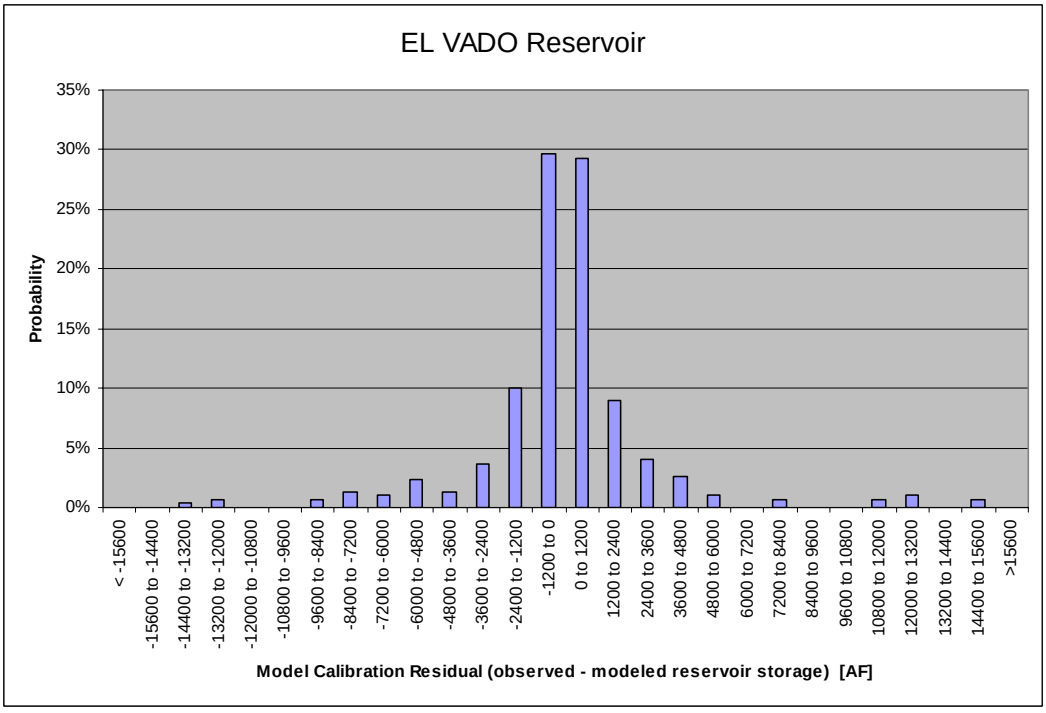

Figure 2-22. Model residual (observed – modeled) distribution for storage in El Vado Reservoir for the 1975–1999 calibration period. Ideally, modeled residuals are normally distributed tightly about zero.

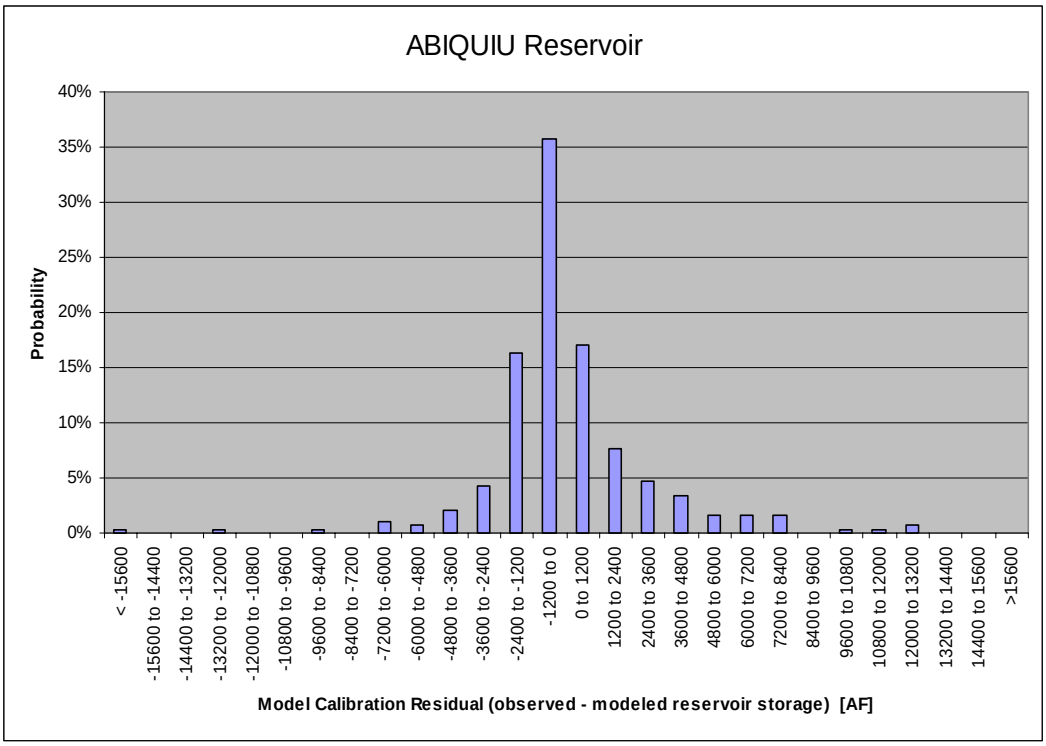

Figure 2-23. Model residual (observed – modeled) distribution for storage in Abiquiu Reservoir for the 1975–1999 calibration period. Ideally, modeled residuals are normally distributed tightly about zero.

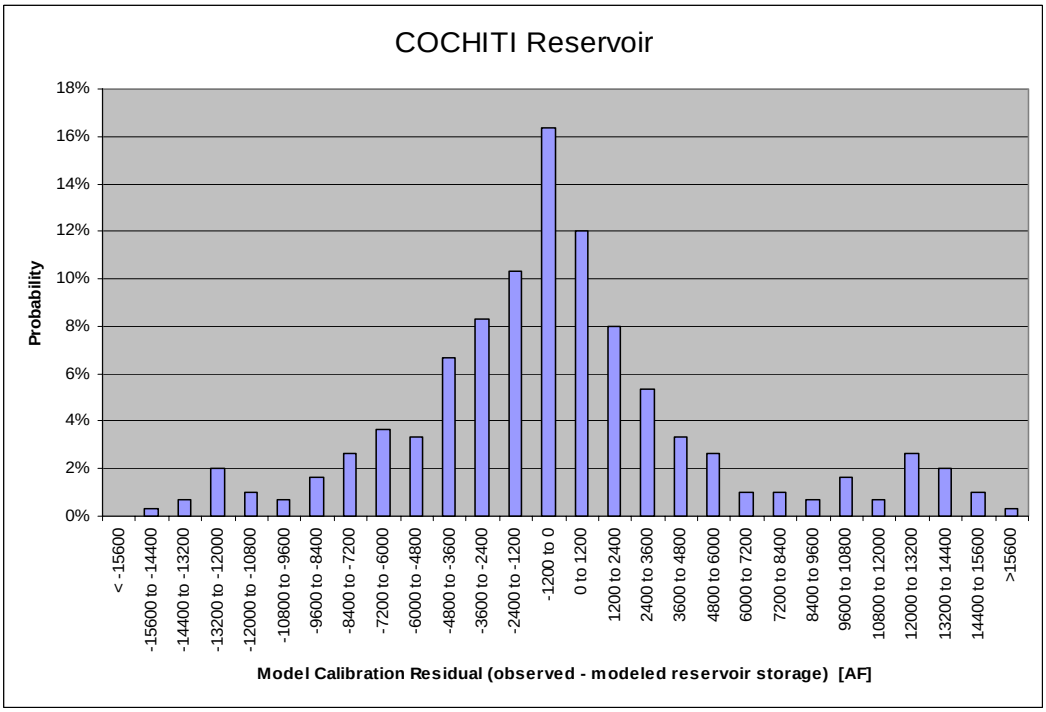

Figure 2-24. Model residual (observed – modeled) distribution for storage in Cochiti Reservoir for the 1975–1999 calibration period. Ideally, modeled residuals are normally distributed tightly about zero.

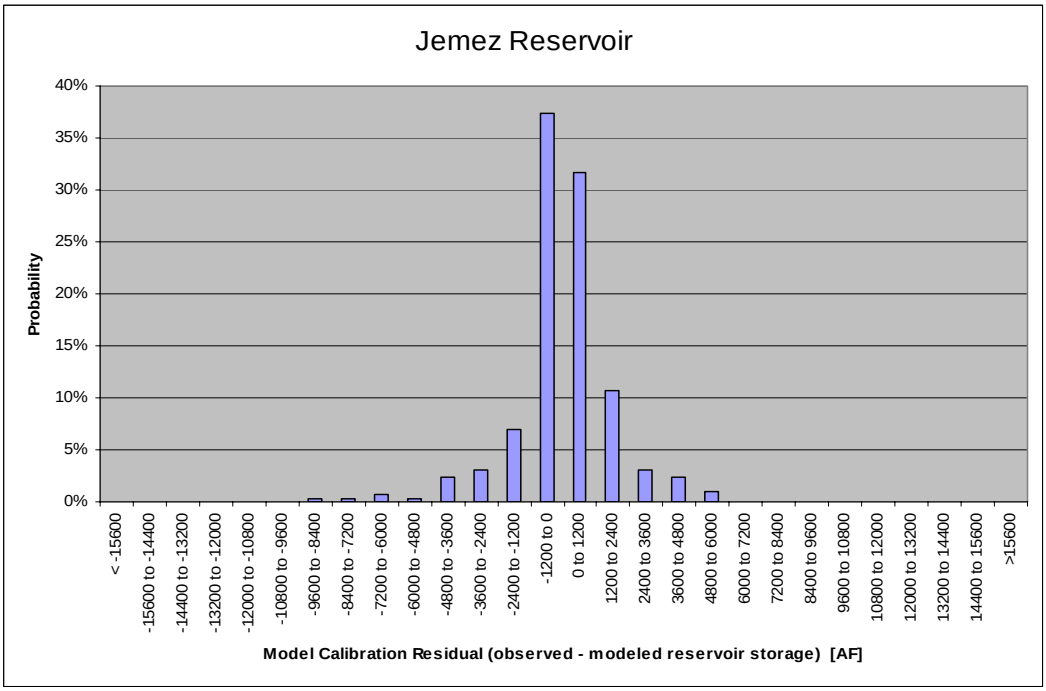

Figure 2-25. Model residual (observed – modeled) distribution for storage in Jemez Reservoir for the 1975–1999 calibration period. Ideally, modeled residuals are normally distributed tightly about zero.

2.4 Conclusion

Initial work suggests that a monthly timestep mass balance based model is largely able to capture the surface water dynamics of the Rio Grande river system in New Mexico between 1975 and 1999. Validation using 2000–2006 data will provide insight into the confidence with which the model can be used to evaluate future hydrologic conditions in the basin under different scenarios, which is after all the ultimate goal of this modeling exercise. A system dynamics approach to the surface water system provides a useful foundation for a fast, multidisciplinary, and basin scale model of the myriad of systems whose interactions through time affect how water moves through the Rio Grande.

2.5 Acknowledgments

The authors would like to express their gratitude to the many people who have helped in the development of this work, including our colleagues at the University of Arizona, SAHRA, and Sandia, as well as Al Brower of the Bureau of Reclamation, Doug McAda and Dave Wilkins of the USGS, and Peggy Barroll and Buck Wells of the New Mexico Office of the State Engineer, all of whom provided insight and clarification in response to unsolicited questions. Special thanks to the URGWOM technical team, which in the (currently ongoing) process of reviewing the monthly timestep model has provided many important insights and helpful criticism. Mistakes are certainly ours, but the quality of the model has been improved due to time and energy from the URGWOM tech team, especially Marc Sidlow of the Army Corps of Engineers, and Nabil Shafike of the New Mexico Interstate Stream Commission, who have been particularly generous and patient in responding to our questions.

3. GROUNDWATER PROCESS MODULES

Jesse Roach, University of Arizona
Vincent Tidwell, Sandia National Laboratories

3.1 Introduction

A common goal of system dynamics modeling is a high-level model that can capture the salient behavior of a system without sacrificing computational speed. To model groundwater flow, the majority of numerical model schemes rely on a fixed-grid finite difference approximation to the governing groundwater flow equations (e.g., MODFLOW, McDonald and Harbaugh 1998). The fixed-grid approach allows for a very systematic and thus numerically efficient approach to development and solution of the driving finite difference equations, but can be cumbersome for modeling large, heterogeneous basins, because the most detailed spatial resolution required in any one part of the model is carried throughout the spatial extent of the model. If runtime is not an issue, a groundwater model can likely be created most easily and quickly with an off-the-shelf fixed-grid approach. However, where runtime is important and fixed-grid inefficiencies are significant, finite element, variable-grid finite difference, and compartmental approaches may reduce model size significantly by utilizing spatial units of varying size.

This chapter will explore the use of a compartmental modeling approach for rapid, reduced resolution groundwater modeling. Compartmental models have been used extensively in the literature to model steady state groundwater flow as a function of hydrochemical data when hydrologic parameter data are sparse (e.g., Campana and Simpson 1983; Adar and Neuman 1986; Adar et al. 1988), but not to model groundwater flow as a function of head. A close exception to this rule appears in Adar and Sorek (1989) where hydrochemical data are used to solve for quasi steady state flows between compartments, which are then combined with available head data to estimate transmissivities based on Darcy's law. In this chapter we use similar concepts to create a head-based groundwater flow model between zones of irregular size and shape.

3.2 Conceptual Model: Compartmental Groundwater Model

Compartmental groundwater models are referred to interchangeably in the literature as compartmental, cell, or mixing-cell models, and are used most commonly to constrain bulk groundwater movement using available groundwater chemistry data (Campana et al. 2001). Compartmental models can also be thought of as a spatially distributed and communicating set of "lumped-parameter" models (models that do not use spatial coordinates (Gelhar and Wilson 1974)), and compartmental models with explicit development of hydrologic parameters have been referred to as distributed parameter models (e.g., Adar and Sorek 1989). The irregular shapes common to a compartmental approach can be convenient for describing areas of hydrologic uniformity, but render a rigorous finite difference approximation to the governing flow equations tedious. Thus, the distributed parameters are typically not derived mathematically from hydrolgeologic data, but rather empirically as an inverse modeling exercise. Flow and head values must be independently obtained in order to solve for transmissivities. Model quality is limited by the choice of representative groundwater compartments, especially as

spatial resolution is reduced. Choice of representative compartments is discussed in greater detail in the next section of this paper. Assuming that they have been well chosen, consider the irregular spatial groundwater compartments shown in Figure 3-1.

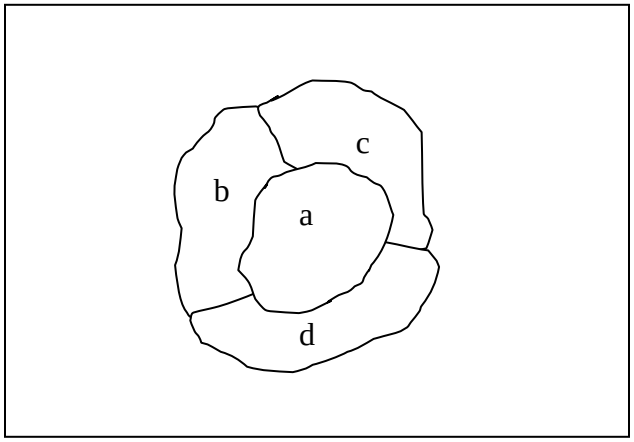

Figure 3-1. Example groundwater compartments.

Applying conservation of mass to compartment *a*, the change in storage in compartment *a* is equal to the sum of flows into *a* less the sum of flows out of *a*. Mathematically,

$$\frac{dS_a}{dt} = Q_{ab} + Q_{ac} + Q_{ad} + Q_{aS} \tag{3-1}$$

where $\frac{dS_a}{dt}$ is the change in storage through time in compartment *a*; Q_{ab}, Q_{ac}, Q_{ad} are net flows into compartment *a* from compartments *b*, *c*, and *d* respectively; and Q_{aS} is the net sum of all groundwater interior source and boundary flows into compartment *a* from external sources including, for example, evapotranspiration, well extraction or injection, recharge, stream leakage, and drain capture. Q terms are positive for flow into compartment *a*, and negative for flow out. Applying Darcy's law for flow between compartments,

$$Q_{ab} \cong \frac{-K_{ab} A_{ab}}{L_{ab}} (h_a - h_b) \tag{3-2}$$

where K_{ab} is an effective saturated hydraulic conductivity between compartments *a* and *b*; A_{ab} is an effective cross-sectional area between compartments *a* and *b* normal to net flow between the compartments; L_{ab} is an effective distance between compartments *a* and *b*; and h_a, h_b are representative heads in compartment *a* and *b* respectively. A key assumption in compartmental modeling when dealing with hydrochemical data is that a given compartment is fully mixed, such that a singe concentration represents the concentration throughout the compartment. The analogous assumption implicit in Equation 3-2 is that a single head value is representative of

head throughout the compartment. Obviously this approximation improves as compartment size and heterogeneity decrease.

In an unconfined aquifer, the cross-sectional area between compartments will change as head changes in either compartment, making flow between compartments a nonlinear function of head. For compartmental model applications, spatial scale is usually relatively large compared to head changes, meaning that the variation of A_{ab} through time will be very small. In these cases, it is reasonable to assume that A_{ab} is constant, particularly given the overall accuracy loss accepted with reduced resolution groundwater modeling. The remainder of this development employs this assumption; however, it is important to point out that the development of the model without this assumption would be analogous though slightly more complex.

With the assumption that A_{ab} is constant with respect to head, Equation 3-2 can be simplified to a linear description of flow as a function of head:

$$Q_{ab} \cong \alpha_{ab} (h_b - h_a) \tag{3-3}$$

where

$$\alpha_{ab} \equiv \frac{Keff_{ab} A_{ab}}{L_{ab}} \tag{3-4}$$

Substituting Equation 3-3, and analogous terms for compartments *c* and *d*, Equation 3-1 can be rewritten as

$$\frac{dS_a}{dt} = \alpha_{ab}(h_b - h_a) + \alpha_{ac}(h_c - h_a) + \alpha_{ad}(h_d - h_a) + Q_{aS} \tag{3-5}$$

Using a finite timestep approximation for storage change, and adding superscript notation to specify time, Equation 3-5 can be rewritten to solve for storage in aquifer compartment *a* at time *t+1* as a function of storage and head values at time *t*

$$S_a^{t+1} = S_a^t + \Delta t\left[\alpha_{ab}\Delta h_{ab}^t + \alpha_{ac}\Delta h_{ac}^t + \alpha_{ad}\Delta h_{ad}^t + Q_{aS}\right] \tag{3-6}$$

where S^t is aquifer storage at time *t*, Δt is timestep duration, and Δh_{ab}^t is the head in compartment *b* minus the head in compartment *a* at time *t*. Equation 3-6 is a forward difference explicit solution to the Darcy-based, compartmental groundwater flow equation.

In matrix form for all groundwater compartments

$$\underline{S_i^{t+1}} = \underline{S_i^t} + \Delta t\left[\sum_{i=1}^{n}\left(\underline{\underline{Q_{ij}^t}}\right) + \underline{Q_{iS}^t}\right] \tag{3-7}$$

where for *n* groundwater compartments, the vectors (indicated by a single line under the variable) in Equation 3-7 have length of *n*, and the matrices (double line) are *n* by *n*. The $\underline{\underline{Q_{ij}^t}}$ matrix represents flow to *i* from *j* at timestep *t* for all *i* and *j*, and is summed across all *i* to result in an array of total internal flows to each compartment as shown below.

$$\underline{Q_{ij}^t} = \sum_{i=1}^{n} \sum_{j=1}^{n} \left(\alpha_{ij} * \Delta h_{ij}^t \right) \tag{3-8}$$

α_{ij} is the conductance value (Equation 3-4) between compartment *i* and *j* (zero for compartments that are not hydrologically connected), and Δh_{ij}^t represents the term $h_j - h_i$. If all source flows ($\underline{Q_{iS}^t}$) are either known or a function of aquifer heads, the $\underline{\underline{\alpha_{ij}}}$ matrix is known, and storage and head conditions at the beginning of the timestep are known, we end up with a system of *n* equations and *n* unknowns whose solution describes groundwater movement at a given model timestep (Equation 3-8) and aquifer storage at the beginning of the next timestep (Equation 3-7). The new aquifer storage is used to calculate a new aquifer head using the following relationship between storage and head in an unconfined aquifer:

$$S_i = (h_i - zbot_i) * F_i * sy_i \tag{3-9}$$

where F_i and sy_i are the horizontal (footprint) area and specific yield of compartment *i* respectively. Equation 3-9 is used to update the heads so that Equation 3-7 may be solved for at the next timestep, thereby modeling groundwater movement and storage through time.

3.2.1 Stability Criteria

Because the forward difference explicit formulation predicts the future state of a system based on the present state of that system, the system of equations can be unstable if the timestep is too long relative to the spatial scale and rate of movement of water between compartments. Conditional stability for Equation 3-6 (and by analogy the set of equations represented by Equation 3-7) is satisfied for an unconfined aquifer if the following stability criterion is met.

$$\Delta t \sum_{j=1}^{n} \alpha_{ij} \leq F_i sy_i \tag{3-10}$$

The term on the left side of the equation is equal to the maximum amount of water that could move into compartment *i* in one timestep if the head in *i* is one unit less than the head in all other connected compartments. The term on the right side of the equation is the storage capacity available in compartment *i* for the same head differences before flow would switch directions. This is analogous to the well-known unconditional stability criteria for a forward difference explicit 2d square grid solution: $\Delta t \left[2T_x + 2T_y \right] \leq F * sy$ where T_x, T_y are transmissivities in the x and y direction, and are doubled because there are two faces in each direction through which water can reach the square cell of interest (modified from Bear and Verruijt (1987), eq. 9.3.5).

3.2.2 Boundary and Source Terms

Having characterized groundwater flow between compartments with the $\underline{\underline{Q_{ij}^t}}$ matrix of Equation 3-7, we must describe the boundary and source fluxes to each groundwater compartment through time (Q_{iS}^t). In a dynamic systems framework, the source fluxes and boundary terms are coupling points between systems, in particular the surface water system, atmospheric system, land surface system, socio-economic system, and other groundwater basins. The source and boundary fluxes can be prescribed head (Dirichlet or Type 1), prescribed flux (Neumann or Type 2), or mixed (Cuachy or Type 3) boundary conditions. For boundary or source flows described by prescribed flow, the appropriate boundary flow rate (Q_{iS}^t) is substituted into Equation 3-7. Mathematically,

$$Q_{iS}^t = Q_p \tag{3-11a}$$

where Q_p is a prescribed flow rate. For boundary or source flow described by prescribed head on the boundary, with or without a leaky membrane condition, flow across the boundary of zone *i* can be modeled as

$$Q_{iS}^t = \alpha_{iB}(h_B^t - h_i^t) \tag{3-11b}$$

where α_{iB} is a coefficient of proportionality describing flow across the boundary as a function of boundary head h_B^t and head in compartment *i* h_i^t. This coefficient may be head dependent. If there are data to warrant it, and the boundary flux can be described with Darcy's law, the α_{iB} coefficient can be resolved into component parts

$$\alpha_{iB} \cong \frac{K_{iB}A_{iB}}{b_{iB}} \tag{3-11c}$$

where K_{iB} is effective conductivity across the boundary, A_{iB} represents the area through which that flow occurs, and b_{iB} is the representative distance across which the driving head change occurs.

3.2.3 Groundwater Compartment Delineation

An effective compartmental groundwater model should capture the first-order behavior of a groundwater system with relatively low complexity. Such a model provides the ability to capture basic system behavior with minimal runtime. The amount of complexity that should be built into a compartmental model depends on the balance between model requirements and the runtime that can be afforded. The advantage of a simplified approach is strengthened if the relationship between model complexity and the ability of the model to describe the physical system is strongly nonlinear as diagrammed theoretically in Figure 3-2. In these situations, once the first order behavior has been captured, relatively modest model improvements require significant increases in complexity. When this is true and runtime is important (as it is in systems models designed for interactive use), complexity should be limited to the point at which salient system behavior is captured in the model.

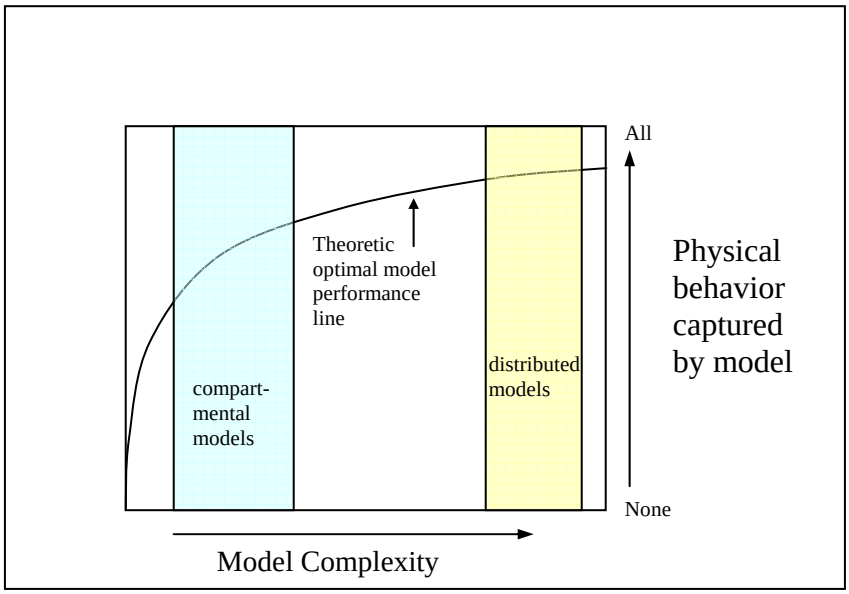

Figure 3-2. Theoretical relationship between model complexity and physical behavior captured by the model.

In the context of a compartmental groundwater model, the choice of appropriate compartments to capture system behavior is the key to development of a meaningful model. Physically meaningful compartments will represent areas of relatively homogenous aquifer properties and groundwater behavior. According to Campana et al. (2001, p. 37), compartment differentiation depends on "hydrogeological uniformity, the availability of data, the degree of resolution desired, and constraints imposed by numerical solutions" (e.g., stability criteria as mentioned above). The resolution desired will depend on the questions being addressed by the model, as well as spatial resolution required to meaningfully couple to other modeled systems. Choosing the spatial resolution requires, as with any modeling effort, a good conceptual model of the groundwater system, especially for basins with limited data availability. If reliable spatially distributed models of the basin in question exist, they can be used to help choose representative groundwater compartments and calibrate a simplified model. As implied above, even with an excellent spatially distributed model available for a given basin, run time and dynamic input and output considerations can make a compartmental model more appropriate than a large spatially distributed model for certain applications. The following section outlines a method for compartment selection and model calibration when a reliable MODFLOW model of the basin already exists.

3.3 Compartmental Model Development Using a MODFLOW Model

If a reliable, spatially distributed MODFLOW model exists, fixed Cartesian grid inefficiencies make it likely that a spatially aggregated, compartmental, groundwater model of the type described above can be developed that will capture a large amount of the MODFLOW model behavior with a fraction of the complexity. A trial-and-error iterative process using the software package ZONEBUDGET for model development is described below. Future research into

automation and optimization of compartment delineation holds promise for streamlining this otherwise tedious step.

3.3.1 Define Groundwater Compartments

As discussed above, groundwater compartments should be chosen based on hydrogeologic uniformity, data availability, and resolution desired, which within the context of systems modeling will depend on model purpose as well as on resolution of linked systems. When using a MODFLOW model to develop and calibrate a compartmental model, we are essentially modeling a model. The simplified model can only be as good as the spatially distributed model, with the implicit assumption being that the more complex model represents reality. This is a key assumption to keep in mind when validating and running the simplified model, because even a well-developed MODFLOW model based on an accurate conceptual model is an imperfect and non-unique representation of reality. With that weakness in mind, the strength of the approach lies in the rich dataset provided by the MODFLOW model input and output files. MODFLOW input files can be used to define areas of uniform hydrologic parameters, as well as areas of acute forcings (e.g., recharge and well pumping). MODFLOW output files can be used to define areas of uniform head values, steep head gradients, and large transient drawdown. Using these fields and an overall understanding of the conceptual groundwater model they describe, compartments should be chosen that are representative of uniform groundwater behavior. The goal is to choose the number, size, and shape of the compartments so that at steady state, or on average through the transient run, MODFLOW flows between the compartments are from compartments of higher average head to compartments of lower average head. This step sounds trivial, but depending on the degree of simplification desired can be both challenging and tedious because flow at a relatively small compartmental interface is being predicted based on the head average for the entire two compartments sharing that interface. Future work on automating and optimizing the selection of zone sizes and shapes might help streamline what is now the most time-intensive step in creation of a spatially aggregated groundwater model from an existing distributed model. Once the compartments have been defined, the process for checking the behavior of the flow between compartments is outlined below.

3.3.2 Describe Head-Dependent Groundwater Flow Between Compartments

MODFLOW modeled groundwater flow between spatially lumped compartments can be tracked using the United States Geological Survey (USGS) computer program ZONEBUDGET (Harbaugh 1990). To start, a cell-by-cell water budget output file for the calibration period of interest must be generated with the MODFLOW model. This cell-by-cell budget is specific to the MODFLOW model, and will serve as input to the ZONEBUDGET routine for all aggregation trials. Once spatially aggregated compartments have been defined, the average head in each compartment at each timestep in the MODFLOW model must be calculated. This can be done by defining the initial compartment storage, tracking storage changes through time with ZONEBUDGET storage change output, and relating storage at each timestep to average compartment head, or by using MODFLOW head fields from each timestep to define average compartment head. Next, ZONEBUDGET is used to find the groundwater flow between compartments at each timestep. Finally, rearranging Equation 3-3 and adding explicit timestep notation, we obtain an equation for the linear flow parameter that equates differences in head between compartments to flow between those compartments.

$$\alpha_{ij}^{t} \cong \frac{Q_{ij}^{t}}{(h_j^t - h_i^t)} \tag{3-12a}$$

Physically meaningful flow occurs from compartments of higher head to compartments of lower head meaning that the linear flow parameter α_{ij} cannot be negative.

$$\alpha_{ij}^{t} \geq 0 \tag{3-12b}$$

Recall that Q_{ij}^{t} is groundwater flow from compartment *j* into compartment *i* at timestep *t* such that a negative *Q* value means flow is into *j* from *i*. h_j^t and h_i^t represent average head in compartment *j* and compartment *i* at timestep *t*. It is important to note that poor spatial aggregation can lead to situations where a compartment of average higher head flows to a compartment of lower average head because the average head is not representative of the contact area between compartments. For this reason we evaluate Equation 3-12 through time. Solving Equation 3-12a at each timestep for each compartment and checking the distribution of α_{ab}^{t} for all compartment pairs through time, including frequency of violation of Equation 3-12b provides metrics that can be used to evaluate the quality of compartment delineation. For example, one criteria for acceptable compartment delineation would be that for all compartment pairs, the arithmetic average of the α_{ab}^{t} values for all timesteps is greater than or equal to zero. In other words, on average groundwater moves from compartments of higher head to compartments of lower head. If the acceptability criterion is not met, compartment size, shape, and/or number must be manipulated appropriately, and the process repeated until a satisfactory compartment delineation is achieved. This iterative process is diagramed in Figure 3-3. The acceptable spatial aggregation is used to derive the alpha matrix ($\underline{\underline{\alpha_{ij}}}$) of Equation 3-8, either by simply taking the temporal averages of each compartment pair flow parameter array ($\overline{\alpha_{ab}^{t}}$ for all t), or by optimization to match flows in the compartmental model to flows in the MODFLOW model, constrained by Equation 3-12b.

3.3.3 Calibrate Boundary and Source Flows

With the alpha matrix defining groundwater connectivity and head-dependent flow, the boundary and source flow terms can be added. The MODFLOW packages typically used to model source and boundary terms include the recharge package, the well package, the evaportranspiration (ET) package, the river package, the stream-aquifer package, and the drain package, of which the recharge and well package model specified flux terms, while the others model head-dependent fluxes. Because of the interdependence of fluxes, especially head-dependent fluxes, as a general rule, the constant or specified boundary and source flows should be calibrated or added first, followed by groundwater head-dependent fluxes, followed by groundwater head- and surface-water-dependent fluxes as applicable.

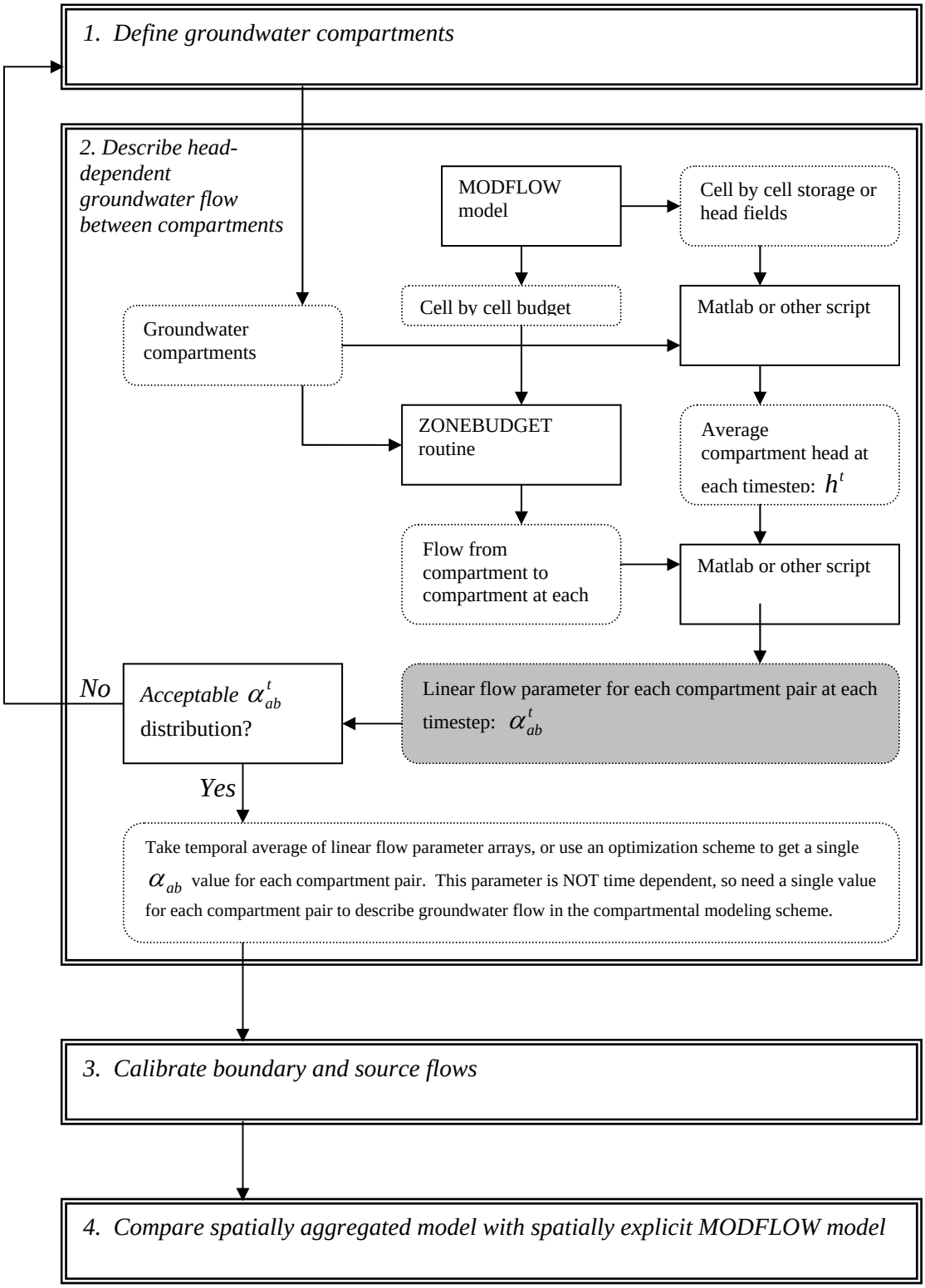

Figure 3-3. Visual representation of compartmental model development from more spatially distributed MODFLOW model, with emphasis on description of head-dependent groundwater flow parameters.

In practice this usually means starting with recharge and well fluxes, then moving to ET, and finally to the more complex river and drain interactions, with iterations through the more complex calibrations until the overall calibration is satisfactory.

3.3.3.1 Specified Flux Terms

If the atmospheric and land surface systems are being modeled, natural recharge can be calculated independently and linked dynamically to the appropriate groundwater compartments. If human behavior and demand systems are being modeled, artificial and crop recharge, and well use can also be calculated and linked dynamically to the appropriate groundwater compartments. If these systems are not being modeled to a sufficient degree to estimate recharge or well demand, these terms can be specified with values from the associated MODFLOW input files. In all cases, the trivial equation 11a is used to populate the specified flux terms.

3.3.3.2 Head-Dependent Flux Terms

Head- and/or stage-dependent flux terms describing interaction between surface and groundwater systems including river leakage/gain and drain capture can be calculated using Equation 3-11b when the systems are hydrologically connected and Equation 3-11a otherwise. Calibration of head-dependent flux terms as modeled by the compartmental model to the same flux terms modeled by MODFLOW can be done by manipulation of the alpha term as a lumped parameter, or, where appropriate, by calibration of the most poorly understood or measured portions of the constant term (Equation 3-11c). For example, if we are using Equation 3-11b to model river leakage, and the river area (A) is well characterized, we might choose to calibrate the flux by adjusting the sediment conductivity divided by sediment thickness term ($\frac{K}{b}$). If the sediment thickness is well characterized also, we may decide to adjust the bed sediment conductivity value only. Mathematically it makes no difference, but keeping track of the individual components of the constant term and adjusting those that are less well understood has advantages in comparison of calibrated parameters between the spatially aggregated model and the MODFLOW model, as well as in connectivity to other systems that may use the same constants in other calculations. If the lumped calibration approach is used, a new constant should be created in the model structure with no association to the component constants.

Once calibration is complete, the spatially aggregated compartmental model is a stand-alone model of reduced complexity imitating to some degree the groundwater system behavior as represented by the MODFLOW model. The next step in model development is validation, which will determine if the model is sufficient for its designed purpose, or if it should be refined further.

3.3.4 Validate Spatially Aggregated Model

Because spatially distributed groundwater models require three-dimensional parameter and initial condition fields that are rarely if ever experimentally available, calibration of groundwater models is a famously non-unique exercise (e.g., Neuman and Wierenga 2003, pp. 35-36). This problem has led some researchers to argue that complex groundwater models cannot be validated

at all (Konikow and Bredehoeft 1992). Validation of the MODFLOW model, and the associated debate, though important, are beyond the scope of this discussion. Clearly the MODFLOW model being spatially aggregated must be meaningful before any attempt is made to reproduce it at a different spatial scale. Insofar as a reliable MODFLOW model exists that is used and trusted by decision makers, a spatially simplified version can be a very useful part of systems-level interactive modeling. In the case of spatial aggregation of a reliable MODFLOW model, the validation is an exercise to see how well the spatially simplified model can capture the behavior of the MODFLOW model for the calibration period, an independent validation period, and what will be called a robustness analysis period where the magnitudes of forcings (source and boundary fluxes) are different from those of the calibration period. Useful comparison metrics include the magnitude of groundwater flows between compartments through time, drawdown through time, and magnitude of head-dependent source fluxes through time. For the calibration and validation periods, a root mean square error (RMSE) or other error function can be used to evaluate goodness of fit. For the robustness analysis, a range of forcing magnitudes can be reported that are associated with model performance better than a given critical RMSE or other error function. These validation metrics can be summarized in table form as shown in Table 3-1.

Table 3-1. Example validation table for spatially aggregated model in comparison to MODFLOW model.

Comparison Metric	Calibration Period	Validation Period	Robustness Range Stress j: e.g., Wells
Groundwater Flows (Q_{ab}^{t})	RMSE or other error function	RMSE or other error function	RMSE < RMSEcrit for e.g., 0.5j to 1.5j
Drawdown	RMSE or other error function	RMSE or other error function	RMSE < RMSEcrit for e.g., 0.5j to 1.5j
Head-Dependent Flux i: e.g., ET	RMSE or other error function	RMSE or other error function	RMSE < RMSEcrit for e.g., 0.5j to 1.5j

The calibration and independent validation periods are fairly self-explanatory, and typically if a MODFLOW model has a historic calibration and future prediction period, model output from these can be used as the calibration and validation periods respectively for the spatially aggregated model. The robustness analysis can be performed on the calibration or validation periods, or both, and involves changing a single stress systematically and watching the effect on model comparison. For example, pumping from a single well or all wells in a certain area could be multiplied by 0.7, 0.85, 1.15, and 1.30, and for each change the behavior of the MODFLOW and spatially aggregated models compared. This sensitivity analysis to the range of forcing stresses can be plotted separately, or the range of stress deviations resulting in an error different from some critical error can be reported in tabular form as in Table 3-1. The idea of all the validation metrics is to get a sense of to what degree and under what circumstances the spatially aggregated groundwater model can be considered a good representation of the source MODFLOW model.

3.4 Case Studies in the Rio Grande River-Aquifer System in New Mexico

The remainder of this report will discuss application of the spatially aggregated modeling theory described above to three contiguous groundwater basins along the Rio Grande river system in New Mexico. The three basins of interest, the Albuquerque Basin, the Espanola Basin, and the Socorro Basin, underlie the Rio Grande river system from the Rio Chama confluence in the north to Elephant Butte Reservoir in the south. Figure 3-4 shows the spatial relationship of the three basins of interest.

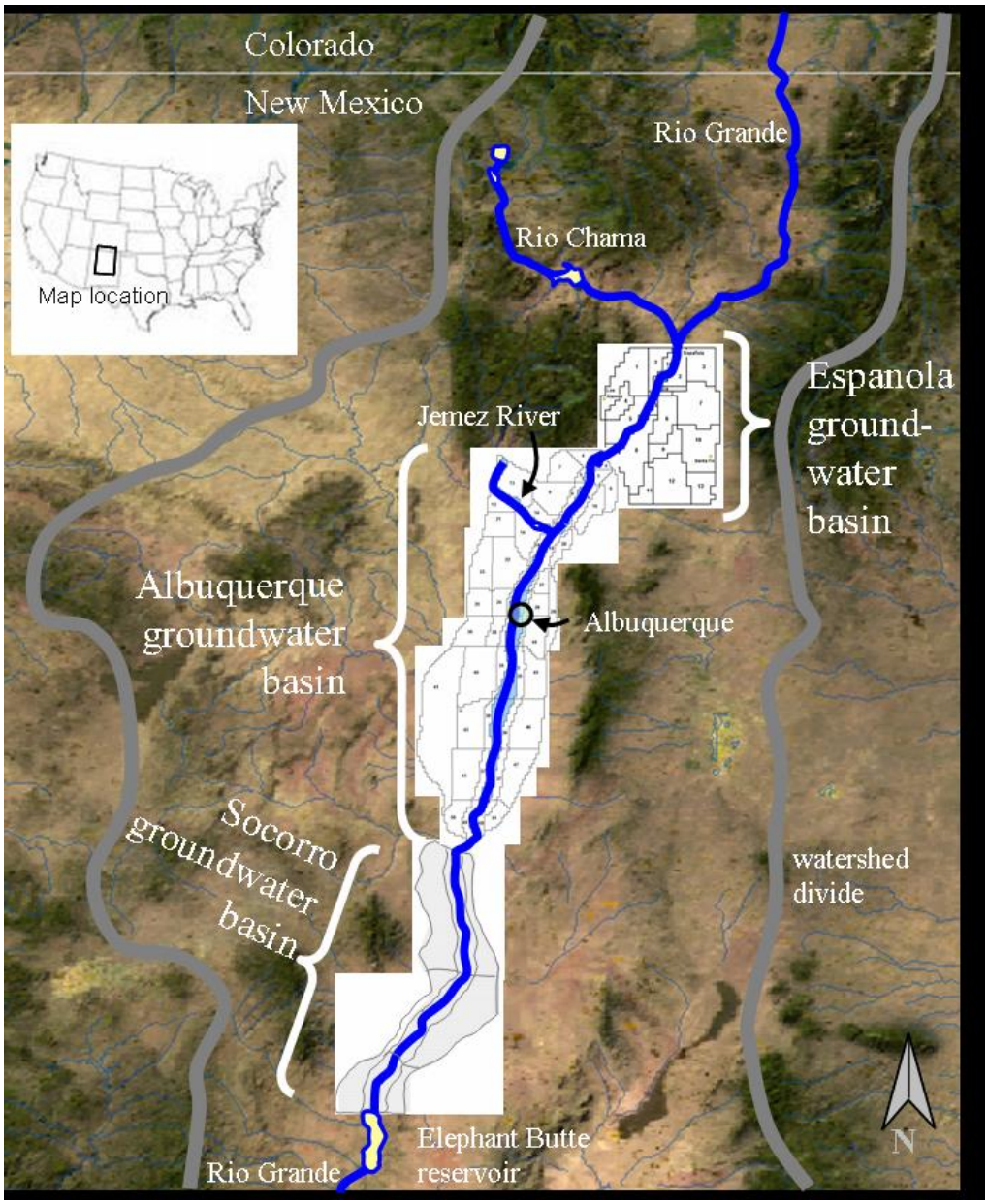

Figure 3-4. Geographic locations and model extent of the spatially aggregated groundwater models of the Espanola, Albuquerque, and Socorro groundwater basins in New Mexico.

3.4.1 Case Study 1: The Albuquerque Groundwater Basin

3.4.1.1 Albuquerque Basin Model Development

Using the techniques described above, a compartmental model with 51 compartments (zones) was developed as a spatially simplified representation of a large (over 100,000 cells) MODFLOW model used to describe groundwater flow in the Albuquerque Basin in New Mexico (McAda and Barroll 2002). The McAda and Barroll MODFLOW model extent is shown in Figure 3-5, and underlies the Rio Grande from above Cochiti Reservoir to San Acacia. The development of a spatially aggregated version of the McAda and Barroll model is described below.

Step 1: Define groundwater compartments (zones)

The sequence of steps necessary for compartmental model development from a MODFLOW model, as shown in Figure 3-3 and discussed previously, begins with delineation of groundwater compartments or zones. Because a driving goal for the reduced spatial resolution groundwater model for Albuquerque Basin was to create dynamic groundwater surface water linkages, groundwater zones were chosen to be coincident with surface water gages. Specifically, the gages of interest for the Albuquerque Basin include the USGS gages located on the Rio Grande below Cochiti Dam (USGS Gage number 08317400), near San Felipe (08319000), in Albuquerque (08330000), near Bernardo (0832010), and near San Acacia (08354900), and the gages located on the Jemez River near Jemez Springs (08324000), and below Jemez Canyon Dam (08329000). Together these gages define five river reaches in which calculated mass balance changes can be compared to gage readings. A second factor used in initial zone demarcation is the presence of high-conductivity sediments located in close proximity to the river. These alluvial sediments are relatively dynamic from a groundwater perspective, with a strong seasonal signal as water is gained from river, canal, and crop seepage, and lost to agricultural drain capture and riparian vegetation ET. These hydrologically active alluvial sediments act differently enough from the rest of the aquifer that they can be conceptualized as a shallow alluvial aquifer on top of a more stable regional aquifer. The first two layers of the MODFLOW model near the river were set up to be coincident with these high-conductivity sediments (McAda and Barroll 2002, p. 20), and spatial aggregation efforts defined the shallow aquifer to include only the top two MODFLOW layers. Initial efforts to create a compartmental model for description of the groundwater flow system broke the basin into four zones per river reach, a shallow alluvial zone, and three regional zones, for a total of 20 zones. Once these zones were chosen (step 1 in Figure 3-3), the alpha matrix ($\underline{\underline{\alpha_{ij}}}$) was calculated for the zones as follows.

Step 2: Alpha matrix determination

Using Equation 3-12a, at each model timestep the ratio of flows to head difference can be calculated for each zone pair.

$$Q_{ij} = \alpha_{ij}(h_j - h_i) \Rightarrow \alpha_{ij} = \frac{Q_{ij}}{h_j - h_i} \qquad \text{Units of } \alpha_{ij} \text{ are } [L^2/\text{time}] \qquad (3\text{-}13)$$

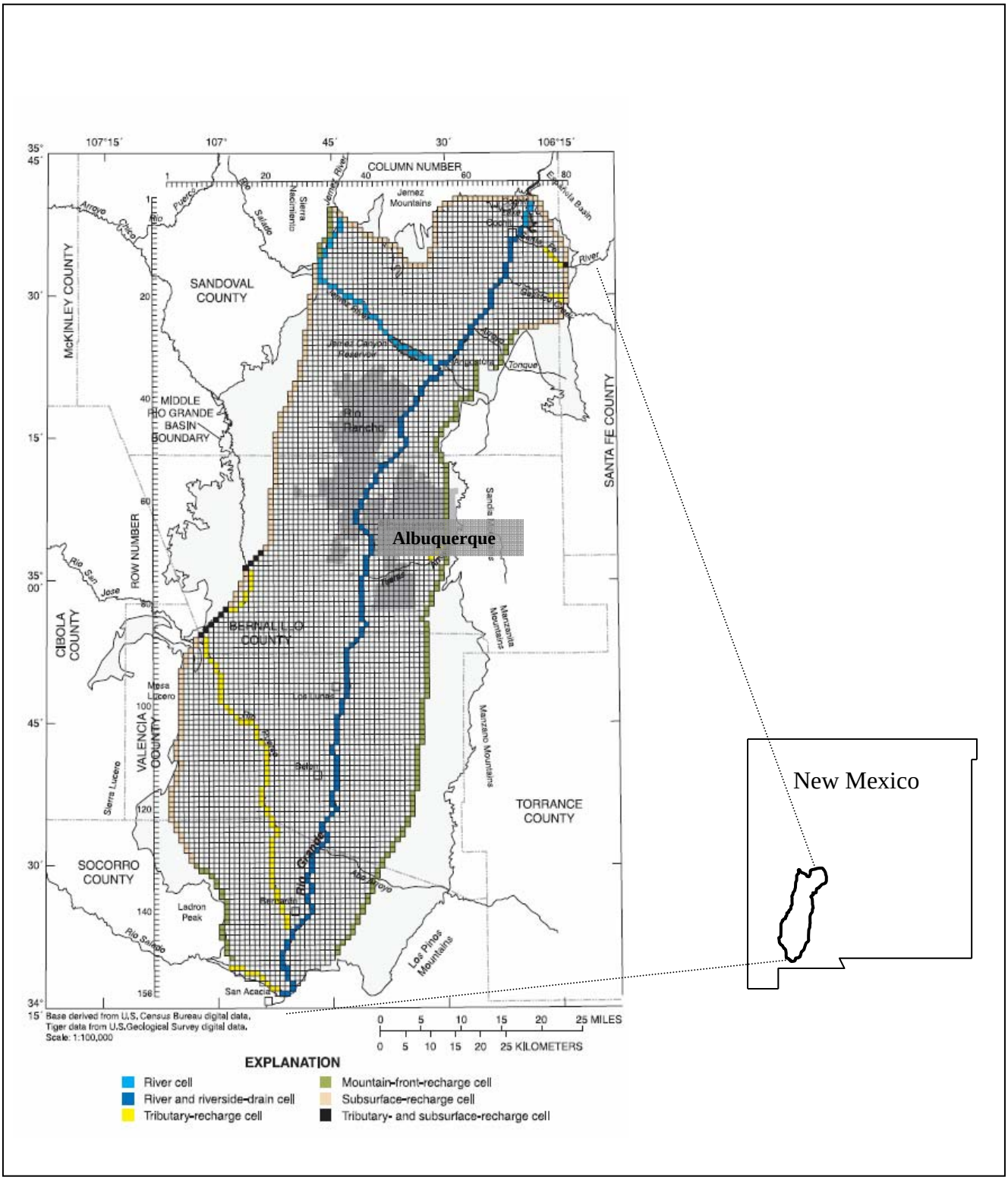

Figure 3-5. Albuquerque Basin MODFLOW model extent. Modified from McAda and Barroll (2002), Figure 7.

A non-negative time averaged value suggests that on average, MODFLOW flow is from a zone of higher average head to a zone of lower average head (see previous discussion associated with derivation of Equation 3-12). The zonal geometry was altered in search of a zone geometry that would result in non-negative average alpha values over all timesteps for all zone pairs. When the initial 20 zone delineation did not prove satisfactory, additional zones were added using hydrogeological and source flux data to reduce the number of negative time averaged alpha values. This process was accomplished through trial and error, with a 51-zone model finally satisfying the non-negative alpha requirement for all zone pairs except one. The one negative average alpha value was for flow between shallow aquifers north and south of Central Bridge in Albuquerque (near a significant pumping-induced cone of depression), and was set to a positive value based on alpha values and contact areas for other shallow aquifer to shallow aquifer contacts. The final zone geometries for the 51-zone compartmental model are shown in Figure 3-6. The alpha matrix, zone bottom elevations, and January 1975 initial zone heads for the 51-zone model can be found in Appendix A, Tables A-1 and A-2. A specific yield value of 0.2 is used in all compartments, consistent with the McAda and Barroll model.

Step 3: Source and boundary flux definition and calibration

It is important to note that within a systems context, nearly all of the boundary and source terms may be functions of the operation of other interdependent systems. In a fully integrated systems model, systems affecting groundwater source terms include the land surface system (mountain front and tributary recharge), other groundwater basins (subflow), the surface water system (canal recharge, river leakage, drain capture), and the human behavioral system (canal, septic, and crop recharge). A significant advantage to systems-level modeling is that linked systems add constraints to make model realizations less non-unique. The amount of water that moves out of the surface water system into the groundwater system must be considered in both systems. A key purpose of the spatial aggregation described here is to facilitate dynamic linkages to other systems, specifically a previously existing monthly timestep surface water model. For this reason, the spatially aggregated groundwater model was set up to run on a monthly timestep, and fluxes between the surface water and groundwater system were set up to take advantage of monthly surface water information. The integration of the surface water system to the groundwater system necessitated some departures from the McAda and Barroll estimated fluxes between surface water and groundwater, and is discussed later in this chapter. The immediate discussion will focus on initial calibration of the spatially aggregated groundwater model to fluxes from the McAda and Barroll model for purposes of evaluating the performance of the compartmental groundwater model.

Fluxes independent of groundwater head (specified flux boundary conditions)

Albuquerque basin fluxes treated as independent of groundwater head by McAda and Barroll and the initial calibration of the compartmental model include well extraction, specified flux groundwater flow along model margins, and recharge from surface sources that are not connected hydrologically to the aquifer, including recharge from the mountain front, ephemeral and tributary channels, disconnected streams, irrigation canals, irrigated crops, and septic tanks. These terms are applied as appropriate in the compartmental model using Equation 3-11a.

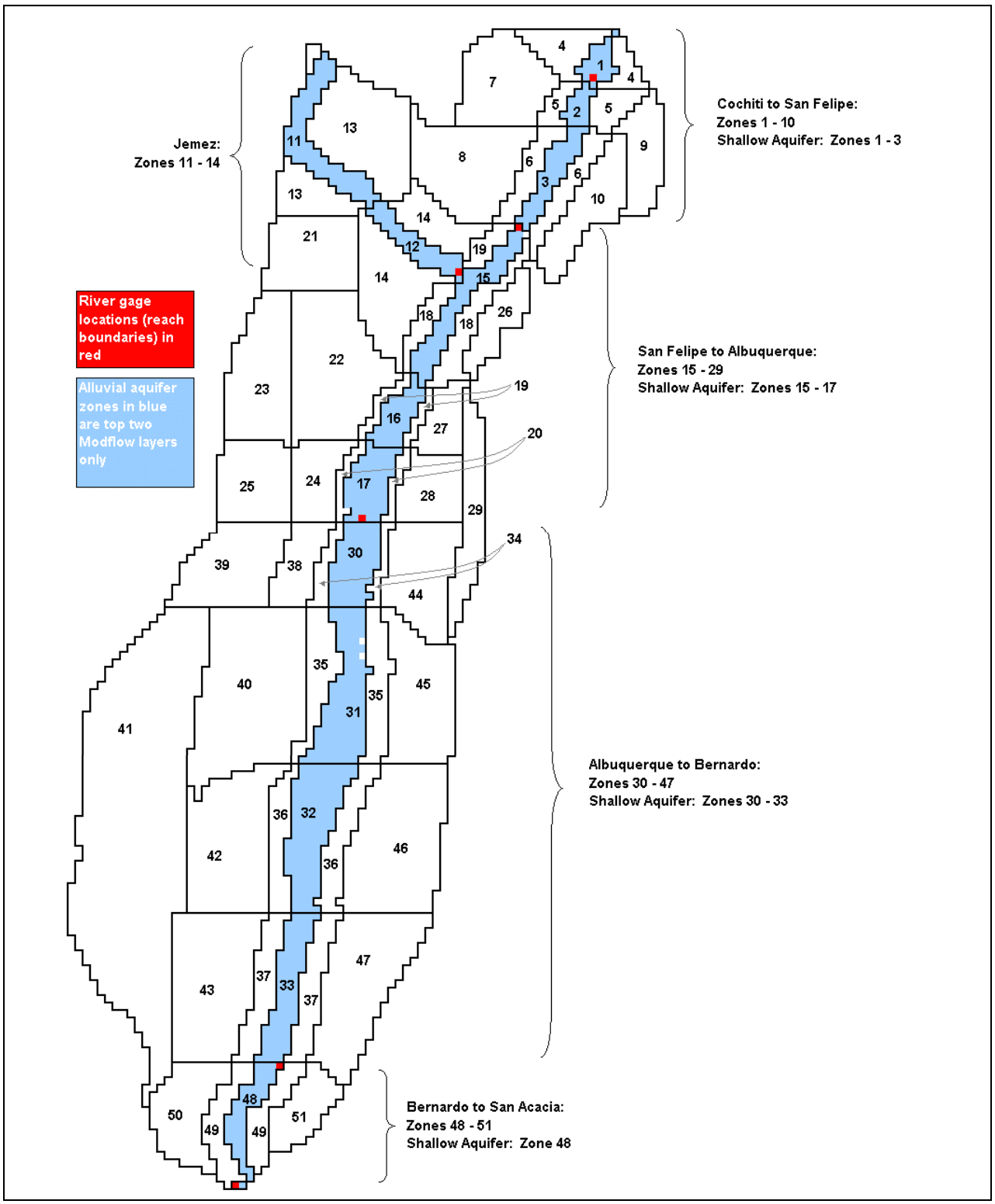

Figure 3-6. Groundwater zones for the spatially aggregated compartmental flow model of the Albuquerque groundwater basin. Zones filled with blue are alluvial aquifer zones, and include only the top two MODFLOW layers. Other zones include all MODFLOW layers.

Fluxes dependent on groundwater head

Source or boundary fluxes modeled as groundwater head dependent by McAda and Barroll include aquifer interaction with hydrologically connected surface water including the Jemez and Rio Grande rivers and the Jemez Canyon and Cochiti Reservoirs, agricultural drains, and ET. These fluxes are also modeled as groundwater head depending in the compartmental model, as is irrigation canal leakage.

River and reservoir leakage

In the 51-zone compartmental model, Jemez and Rio Grande river-aquifer interactions, irrigation canal leakage, and reservoir-aquifer interactions were modeled by combining Equations 3-11b and 3-11c as follows:

$$Q_{i-SWGW} = \frac{K_{i-bed} F_{i-bed}}{b_{i-bed}} (z_{i-sw} - \beta) \begin{cases} \beta = z_{i-bed} & if \quad z_{i-bed} - b_{i-bed} \geq h_i \\ \beta = h_i & if \quad z_{i-bed} - b_{i-bed} < h_i \end{cases} \tag{3-14}$$

where z_{i-sw} is the surface water elevation; z_{i-bed} is the elevation of the top of the bed sediments; b_{i-bed} is thickness of the flow limiting bed sediments; K_{i-bed} is the saturated hydraulic conductivity of the flow limiting bed sediments; h_i is the groundwater head; all terms are specific to compartment *i*; and all head and elevation terms are defined based on a common datum. Equation 3-14 describes hydrologically separate flow when groundwater head is below the flow-limiting sediments, and head-dependent flow to or from the surface water system otherwise, and is consistent with the conceptual approach used by MODFLOW in the river package (McDonald and Harbaugh 1988). For Rio Grande leakage, bed thickness (b_{i-bed}) and bed conductivity (K_{i-bed}) were set to 5 feet and 0.5 feet/day respectively consistent with a value of 0.1 day^{-1} for $\frac{K_{i-bed}}{b_{i-bed}}$ used by McAda and Barroll (2002). For river leakage in the Rio Grande, Equation 3-14 was calibrated with McAda and Barroll parameters for bed thickness and conductivity, and modifying the river bed elevation of each shallow aquifer compartment within an acceptable range. River bed conductivity K_{i-bed} was also adjusted during calibration of the shallow aquifer north of Albuquerque, where spatial aggregation seems to result in larger leakage near the cones of depression than is predicted by the MODFLOW model. For the Jemez River, bed thickness was set to 1 foot consistent with McAda and Barroll, and both bed elevation and river bed conductivity adjusted during calibration. For reservoir leakage, values of river bed thickness and river bed conductivity were adjusted during calibration. Jemez Reservoir was assumed hydrologically separate from the groundwater system. For irrigation canals, canal conductivity was set to 0.15 feet per day consistent with estimates cited by McAda and Barroll (2002), and canal bed thickness to two feet consistent with McAda and Barroll (2002) values after calibration. Calibrated parameters for river and reservoir leakage are shown in Appendix A, Table A-3. Determination of surface water elevations will be described after consideration of drain flows.

Drain capture

In unconfined aquifers where groundwater flow to a surface water sink is predominantly horizontal, and there is no significant seepage face, a Dupuit-Forchheimer-based approach may be used to model flux (e.g., Fetter 1980, eq. 5-59). This approach was used to model groundwater flow to the agricultural drains:

$$Q_{DUP} = \frac{K_{i-a} L_i}{x_i} (h_i^{\,2} - z_{i-sw}^{\,2}) \tag{3-15}$$

where K_{i-a} is the hydraulic conductivity of the aquifer compartment, L_i is the length of the drain, x_i is a characteristic distance beyond which the drain has negligible effect on groundwater head, and all terms are specific to compartment *i*. All other terms are as defined previously. Equation 3-15 is expressed as double the typical Dupuit-Forchheimer equation to represent flow to a drain from two sides. Drain elevations were set to 5 feet below the corresponding river bed elevation, and flow to the drains was calibrated by adjusting aquifer conductivity (K_{i-a}) and characteristic length values (x_i). Calibrated parameter values for the drains are shown in Appendix A.

Surface water stage (z_{sw}) for reservoirs was taken from historic data, while surface water stage for rivers and drains was found at each timestep by iterative solution of Manning's equation for open channel flow:

$$Q_{MAN} = \frac{1.49 \quad A \quad R^{2/3} S^{1/2}}{n} \tag{3-16a}$$

where Q_{MAN} is discharge in cubic feet per second, *S* is the dimensionless drain slope, *n* is the dimensionless Manning coefficient of roughness, *A* is the cross-sectional area of flow in square feet, and *R* is the hydraulic radius in feet (e.g., Grant and Dawson 1997, p. 130). For a channel with vertical sides,

$$A = (z_{sw} - z_{bed}) * W \tag{3-16b}$$

$$R = \frac{A}{2(z_{sw} - z_{bed}) + W} \tag{3-16c}$$

where *W* is the channel width. Groundwater fluxes from the river are small compared to surface water fluxes, and thus have negligible effect on surface water discharge and stage. In the case of drains, however, groundwater movement is the primary source of any surface water flow in the drains. The amount of water that will move to the drain depends on the stage in the drain, which itself determines how much water will move through the drain as surface flow. For this situation, an iterative solution was necessary to find the surface water stage that resulted in surface flow in the drain equivalent to flow to the drain from the groundwater system. In the

Albuquerque basin model, an iterative solution was used to find a drain stage (z_{sw}) that would result in a Dupuit-Forchheimer predicted groundwater flow to the drain (Equation 3-15) equal to a Manning-based surface water flow out of the drain (Equation 3-16a). A Manning coefficient of 0.028 was used for the river and drain channels, and river discharge was from USGS historic gaged flows in the mainstem and associated tributaries.

Evapotranspiration

ET is modeled as a head-dependent flux similar to that of McAda and Barroll. ET is 5 feet/year when water level is at or above the land surface, and decreases linearly to 2 feet/year when depth to groundwater is 9 feet, then decreases linearly from there to 0.75 feet per year when depth to groundwater is 16 feet, then decreases linearly from there to 0 feet/year when depth to groundwater is 30 feet, and is 0 feet/year for all groundwater depths greater than 30 feet below the surface (McAda and Barroll 2002, p. 38). This same relationship is used in the compartmental model. In mathematical form:

$$Q_{iET} = ET_{i-ref} F_{i-ET} * \theta \quad \begin{cases} \theta = 1 \quad if \quad (z_{i-surf} - h_i) < 0\, ft \\ \theta = 1 - \dfrac{2(z_{i-surf} - h_i)}{30} \quad if \quad 0\, ft \le (z_{i-surf} - h_i) \le 9\, ft \\ \theta = 0.4 - \dfrac{(z_{i-surf} - h_i) - 9}{28} \quad if \quad 9\, ft \le (z_{i-surf} - h_i) \le 16\, ft \\ \theta = 0.15 - \dfrac{3(z_{i-surf} - h_i) - 48}{280} \quad if \quad 16\, ft \le (z_{i-surf} - h_i) \le 30\, ft \\ \theta = 0 \quad if \quad (z_{i-surf} - h_i) > 30\, ft \end{cases} \tag{3-17}$$

where ET_{i-ref} is -5 feet/year for all *i*, F_{i-ET} is the area of vegetation using groundwater in compartment *i*, h_i is groundwater head in compartment *i*, and z_{i-surf} is the surface elevation of compartment i, with all elevations defined from the same datum used to define groundwater head. Equation 3-14 was calibrated to McAda and Barroll estimated ET fluxes by adjusting the representative surface elevation (z_{i-surf}) of shallow aquifer compartments containing riparian vegetation (all except shallow aquifer underlying Cochiti Reservoir). Calibrated surface elevations are listed in Appendix A.

Step 4: Validation of spatially aggregated model

Within the context of this discussion, validation refers to ascertaining the extent to which the spatially aggregated model can capture the salient behavior of the spatially distributed McAda and Barroll model in both calibration and predictive periods. This comparison makes up the bulk of Section 3.4.1.2.

3.4.1.2 Albuquerque Basin Results

With the initial goal of replicating the McAda and Barroll (2002) MODFLOW model of the Albuquerque Basin as closely as possible with 51 zones, the reduced resolution Albuquerque basin groundwater model was implemented using Equations 3-7 through 3-9 to describe flow between groundwater zones.

Internal groundwater movement

Spatial aggregation leads to a loss of spatial head distribution information, which affects the ability to predict both internal groundwater flows and head-dependent source and boundary flows. To see the effect on predicted internal groundwater flows alone, the spatially aggregated model was implemented with source terms ($\underline{Q_{iS}^t}$ in Equation 3-7) from the McAda and Barroll model. Figure 3-7 shows the comparison of the two models predicted on 1975 to 2000 groundwater drawdown.

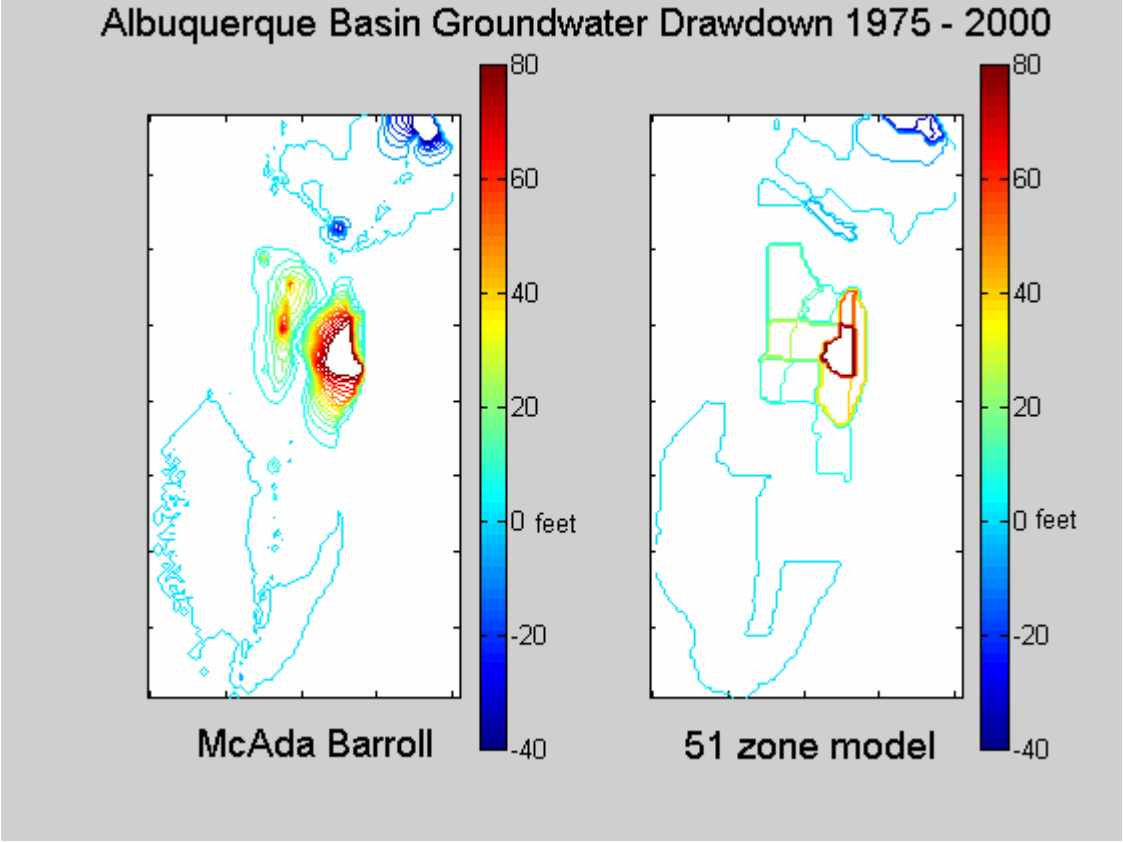

Figure 3-7. Drawdown in the Albuquerque Basin from 1975 to 2000 as modeled by McAda and Barroll (2002), and with the 51-zone compartmental groundwater model. Both models show the dominant patterns of ponding in the north from Cochiti Reservoir, and drawdown in the center due to municipal groundwater use.

Figure 3-8 shows the absolute value of all predicted flows between zones for the 51-zone model with MODFLOW forcings, compared to the absolute value of all flows between the same zones in the McAda and Barroll model. The average difference between total groundwater flows between zones predicted by the two models is less than 1%. In Figure 3-7 we see that the driving changes to the Albuquerque groundwater system between 1975 and 2000 are mounding under the leaky and young (closed in 1975[4]) Cochiti Reservoir in the north, and pumping induced drawdown under Albuquerque and Rio Rancho in the center of the basin. Transient high reservoir storage episodes account for the increased movement "hump" seen between 1985 and 1988 in Figure 3-9, and reservoir-induced recharge and pumping both lead to the trend of increased overall groundwater movement. Seasonal oscillations are seen beginning in 1990 when the MODFLOW model goes from an annual timestep to a biannual timestep based on a 7.5-month growing season, and a 4.5-month nongrowing season. In general, though lacking spatial resolution, the 51-zone compartmental model captures the overall patterns of groundwater movement predicted by McAda and Barroll under the same set of forcings.

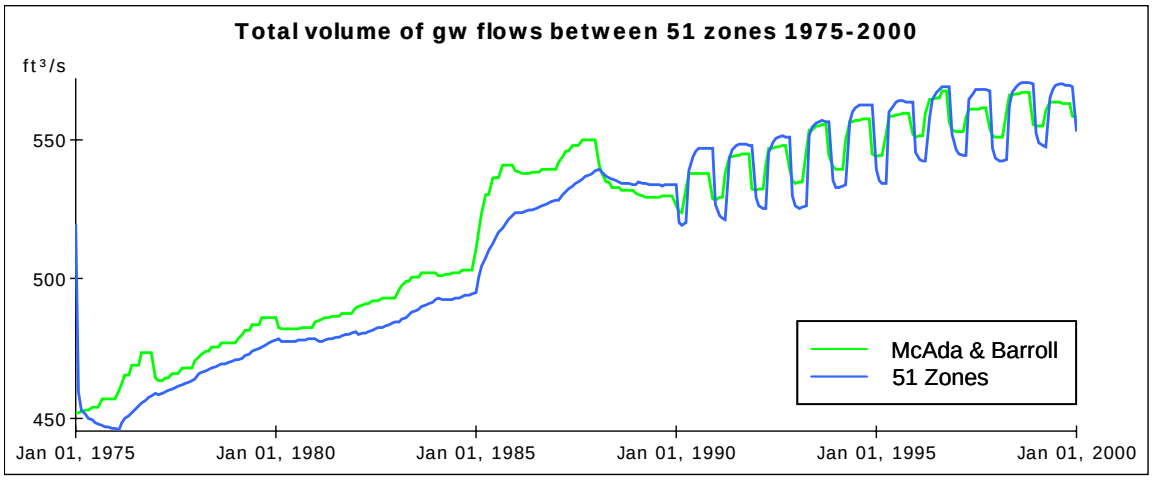

Figure 3-8. Absolute value of predicted flow between 51 zones, MODFLOW compared to McAda and Barroll model. At each timestep, the absolute value of all flows between any two zones is summed as a comparison metric to help evaluate the ability of the 51-zone compartmental model to capture the overall groundwater movement patterns. The average difference between the modeled total flows is less than 1%.

Boundary fluxes

Specified flux terms in the two models are the same. Head-dependent flux terms include river and reservoir leakage, drain capture, and ET, modeled in the 51-zone model with Equations 3-14, 3-15, and 3-17 respectively, with surface stage from Equation 3-16.

[4] http://www.fws.gov/southwest/mrgbi/Resources/Dams/#cochiti

River, irrigation canal, and reservoir leakage

Figure 3-9 shows the head-dependent river leakage simulated by each model from 1975–2000 for the Jemez and Rio Grande rivers. Cumulative leakage for the 25-year period served as the calibration target, and is approximately 8 million acre feet (MAF) for both models. The difference in magnitude of fluctuations is a result of temporal resolution differences between the models, with the compartmental model using monthly data and the MODFLOW model using annual data until 1990, and biannual (growing and nongrowing seasons) data from 1990–2000. River leakage is driven in large part by river stage, which varies significantly at a monthly timestep, to a lesser degree in a biannual timestep, and negligibly when averaged across an entire year.

Simulated Cochiti and Jemez Reservoir leakages are shown in Figures 3-10 and 3-11. Again, the cumulative leakages for the 25-year period (400,000 AF for Cochiti and 60,000 AF for Jemez) served as the calibration targets, and are the same for both models. Differences in temporal resolution are evident; however, the compartmental model does replicate the basic system behavior represented by the McAda and Barroll model.

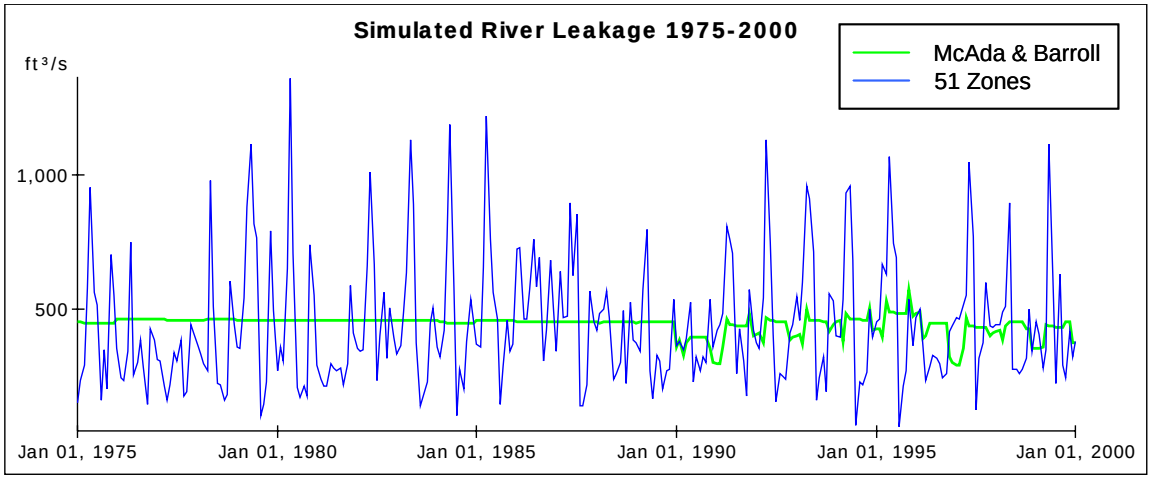

Figure 3-9. Head-dependent river leakage in Jemez River and Rio Grande from below Cochiti Reservoir to San Acacia, as modeled by McAda and Barroll (2002), and 51-zone spatially aggregated model for the period from 1975 to 2000.

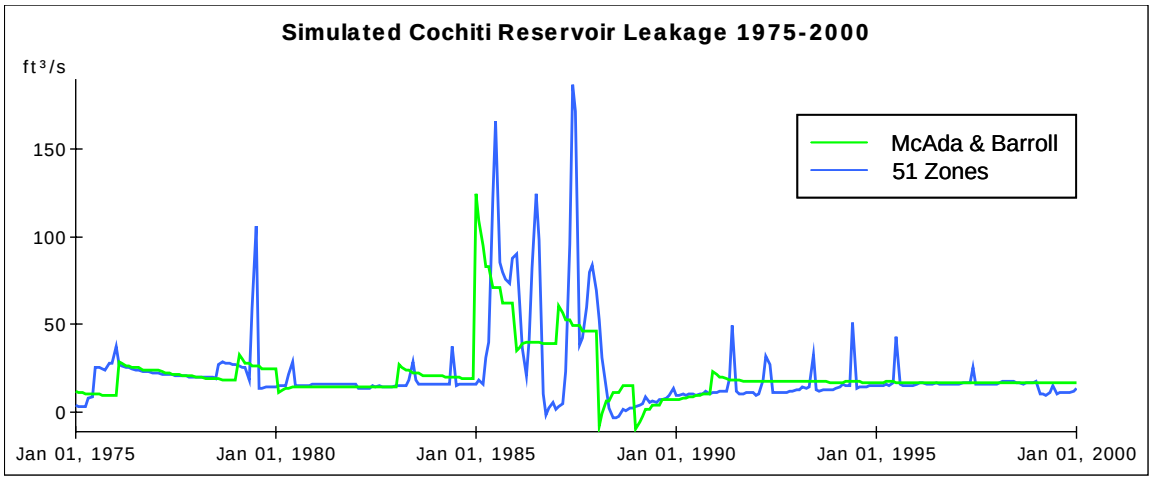

Figure 3-10. Head-dependent reservoir leakage in Cochiti Reservoir, as modeled by McAda and Barroll (2002), and 51-zone spatially aggregated model for the period from 1975 to 2000.

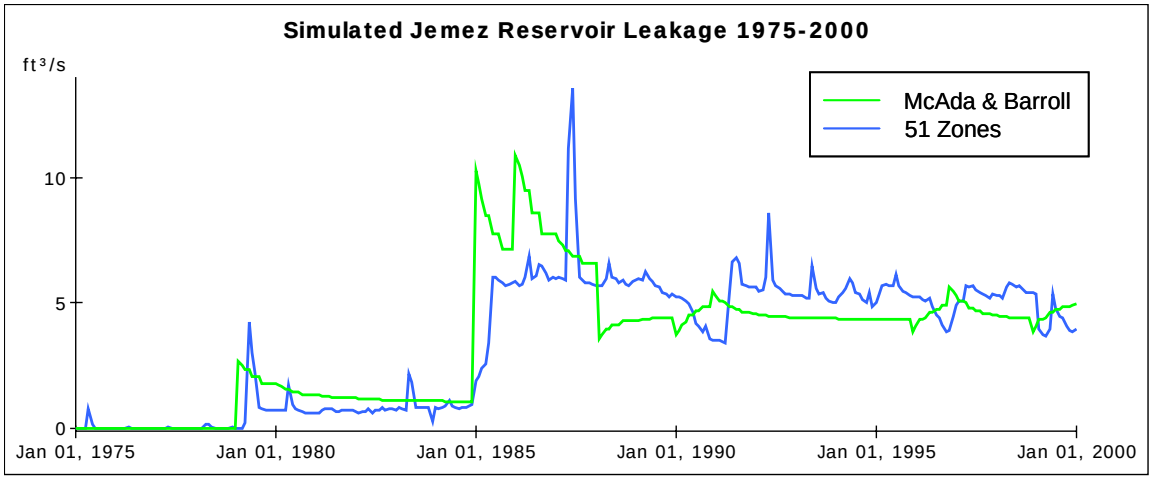

Figure 3-11. Head-dependent reservoir leakage in Jemez Reservoir, as modeled by McAda and Barroll (2002), and 51-zone spatially aggregated model for the period from 1975 to 2000.

Drain flow

Groundwater flow to the drains is modeled in the spatially aggregated model with the Dupuit-Forchheimer approach shown in Equation 3-15, while it is modeled with a flow-limiting bed approach similar to Equation 3-14 in the McAda and Barroll model. Table A-4 in Appendix lists specific parameters used to model drain capture in the Albuquerque basin with Equation 3-15. As shown in Figure 3-12, the Dupuit-Forchheimer approach captures the overall behavior of the groundwater system, with cumulative drain capture in the compartmental model calibrated to match the McAda and Barroll estimate of 9 MAF in 25 years. Seasonal fluctuations again are due to a finer temporal resolution and the shallow aquifer responding to significant seasonal river leakage fluctuations. As is the case in the McAda and Barroll model (2002, p. 62), the drains capture a significant amount of the river leakage, and thus seasonal variations in river leakage are reflected in seasonal variations in drain flow.

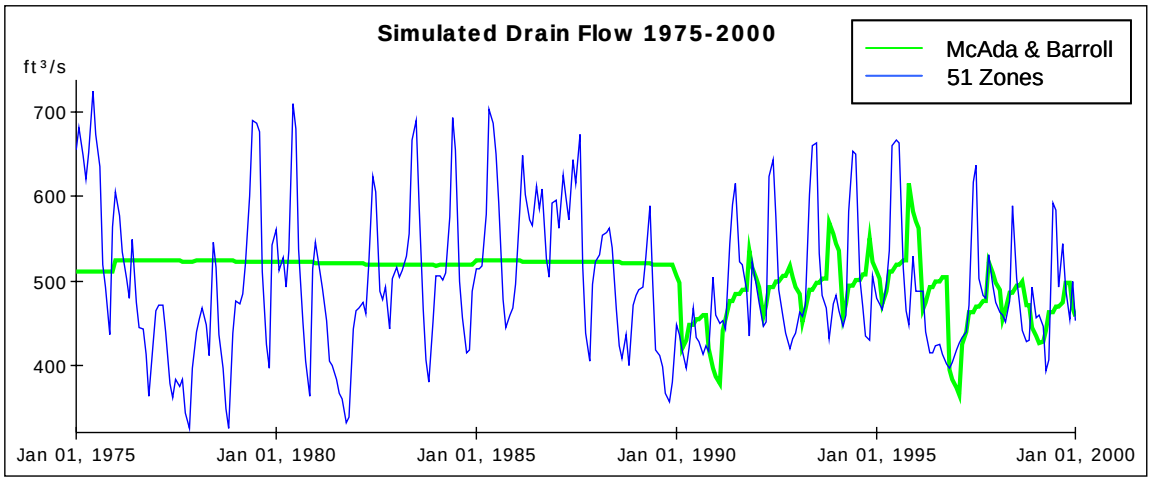

Figure 3-12. Head-dependent flow to drains, as modeled by McAda and Barroll (2002), and 51-zone spatially aggregated model for the period from 1975 to 2000.

Figure 3-13 shows simulated riparian ET in the two models for the 1975 to 2000 calibration period. Surface elevations resulting in the model behavior shown in Figure 3-13 are shown in Table A-5 in Appendix A. ET drops slightly beginning in 1984 because total riparian area before 1984 is estimated with a 1975 United States Bureau of Reclamation (BoR) spatial dataset (~145 km^2), and after 1984 with a 1992 BoR spatial dataset (~126 km^2) (McAda and Barroll 2002, p. 38). The visible match between models is easiest to see after 1990 when the MODFLOW model begins using seasonal data.

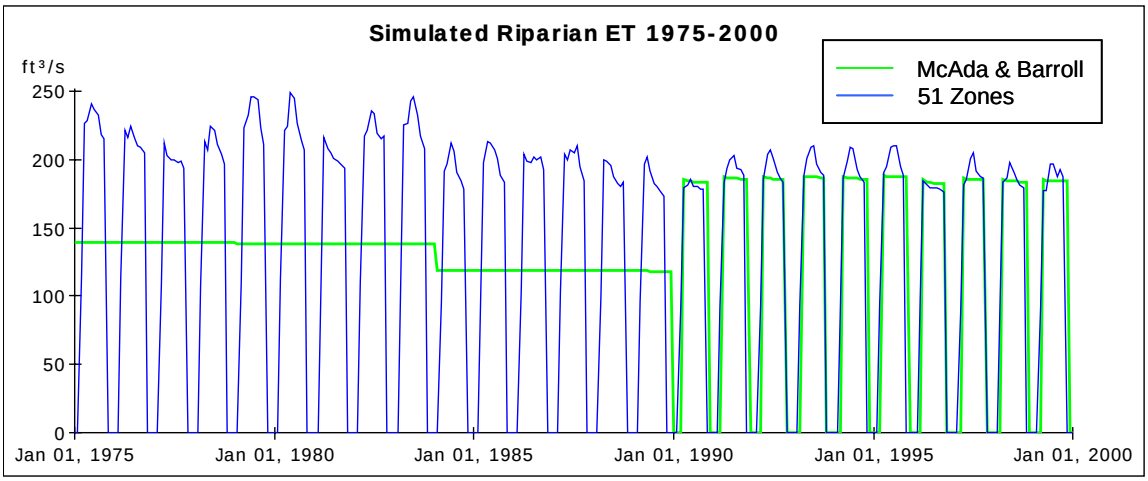

Figure 3-13. Head-dependent riparian ET as modeled by McAda and Barroll (2002), and 51-zone spatially aggregated model for the period from 1975 to 2000.

With head-dependent fluxes calculated based on average compartmental head, the 51-zone model is a stand-alone representation of the Albuquerque basin groundwater system. Figure 3-14, a corollary to Figure 3-8, shows the total groundwater fluxes predicted between zones for the stand-alone model and McAda and Barroll's model. Although the average error between predicted flows is still less than 1%, there is a visible drop-off in how closely the compartmental model tracks the MODFLOW model. Part of that is due to lack of spatial resolution, and part is also due to the increased seasonality of boundary fluxes that can be represented with a monthly timestep. Incorporation of dynamic head-dependent fluxes to the compartmental model does not result in significant changes to the drawdown patterns shown in Figure 3-7 (Figure A-1, Appendix A).

Overall, considering the level of spatial aggregation associated with the 51-zone model, it is able to capture salient groundwater system behavior during the calibration period, and thus provides a reasonable approximation to groundwater system behavior when system forcings are within the range of those seen in the past. The next section describes the behavior of the stand-alone compartmental model compared to the McAda and Barroll model for model forcings outside of the historic range.

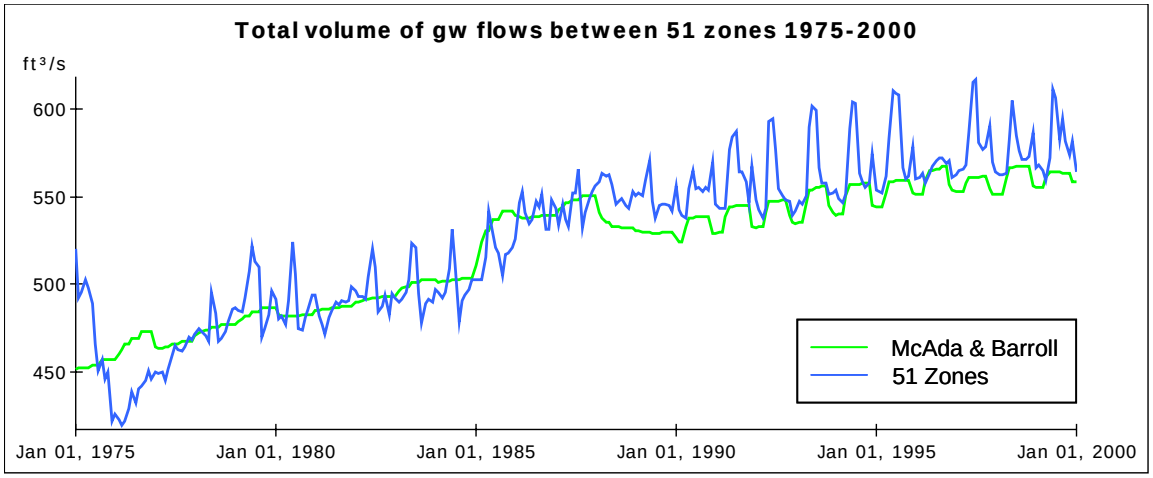

Figure 3-14. Total groundwater fluxes predicted between zones for the stand-alone model and McAda and Barroll model. At each timestep, the absolute value of all flows between any two zones is summed as a comparison metric to help evaluate the ability of the 51-zone compartmental model to capture the overall groundwater movement patterns. The average difference between the modeled total flows is less than 1%. As compared to Figure 3-7, Figure 3-14 tracks simulated flows for the compartmental model with internally calculated head-dependent boundary flux terms.

Robustness Analysis

This section will evaluate the performance of the 51-zone model as compared to the MODFLOW model for future scenario runs with widely varying groundwater pumping.

Integration of Groundwater System with Surface Water and Human Behavioral Systems

Several major changes were made to the calibrated groundwater model described above to allow for connection to a monthly surface water model. It was necessary to increase Cochiti Reservoir leakage to the groundwater system for consistency with the reservoir mass balance. It was also necessary to combine the atmospheric and head dependent constraints on riparian evapotranspiration represented in the surface water and groundwater models respectively, and finally adjustments were made to calibration parameters to balance both the surface water and groundwater systems within the constraints of historic surface water flow data.

Cochiti Reservoir recalibration

When the groundwater leakage for Cochiti Reservoir shown in Figure 3-10 was incorporated into a surface water model of Cochiti storage, the modeled reservoir storage exceeded the historic stage-based estimates, as shown in Figure 3-15. The surface water reservoir mass balance includes estimates of precipitation gains and evaporative losses, and inflows from an upstream gage, modified by modeled losses and groundwater gains from the Espanola Basin (see previous chapter) in the reach between the gage and the reservoir. The excess modeled reservoir storage suggests an underestimate of losses or an overestimate of gains to the reservoir. There are no direct measurements of reservoir leakage; McAda and Barroll (2002) estimated Cochiti leakage with a surface water mass balance (p. 37), but that water balance may not have included groundwater gains from the Espanola Basin of approximately 12 cubic feet per second (cfs) between the Otowi gage and Cochiti Reservoir (see Section 3.4.2) that are included in the surface water model used here. The relative leakiness of Cochiti is supported by anecdotal evidence of waterlogging of fields downstream of Cochiti Reservoir after its completion that necessitated expensive drainage projects and mandates limiting the target storage pool in the reservoir (Smith 2001, p. 98). Of the flows into and out of the reservoir, groundwater leakage and ungaged runoff into the reservoir are the most difficult to quantify. Without considering ungaged runoff, the model has too much water in the reservoir, and so increased groundwater leakage is the most plausible adjustment to be made within the constraints of the surface water balance. Leakage in the reservoir was increased on average by approximately 7,700 AF per year (11 cfs) for the historic period to attain mass balance in the reservoir. The historic calibrated leakage is shown in Figure 3-16. The increased leakage in high-storage events results in drainage of groundwater back to the reservoir when the reservoir volume is rapidly reduced. This is physically plausible, and happens in the MODFLOW model as well.

Interestingly, during calibration of the Albuquerque basin MODFLOW model, McAda and Barroll increased tributary recharge from the nearby Santa Fe River and Galisteo Creek by 1,500 AF per year over initial estimates. It is plausible that underestimates of Cochiti Reservoir leakage in the MODFLOW model led modelers to increase nearby stream recharge. The increased leakage in Cochiti also made calibration of the surface water reach downstream easier.

Evapotranspiration as a function of groundwater head and atmospheric variables

Recall Equation 3-17, rewritten in a simplified form below for convenience:

$$Q_{iET} = ET_{i-ref} F_{i-ET} * \theta \qquad (3\text{-}17)$$

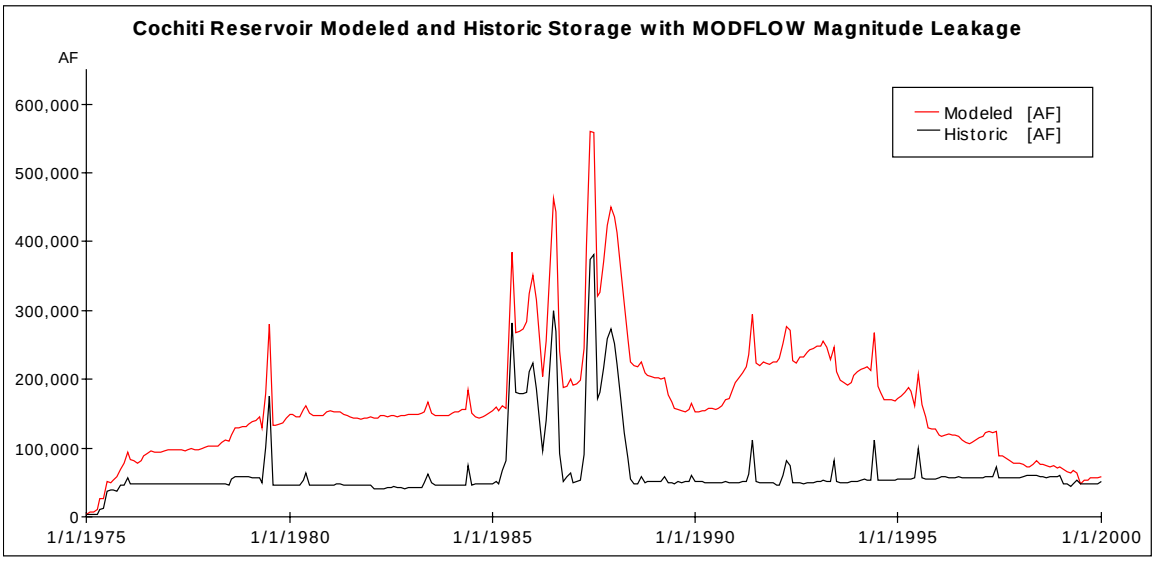

Figure 3-15. Cochiti Reservoir modeled with McAda and Barroll MODFLOW magnitude leakage. Reservoir leakage is likely underestimated, resulting in a model with too much water in the reservoir.

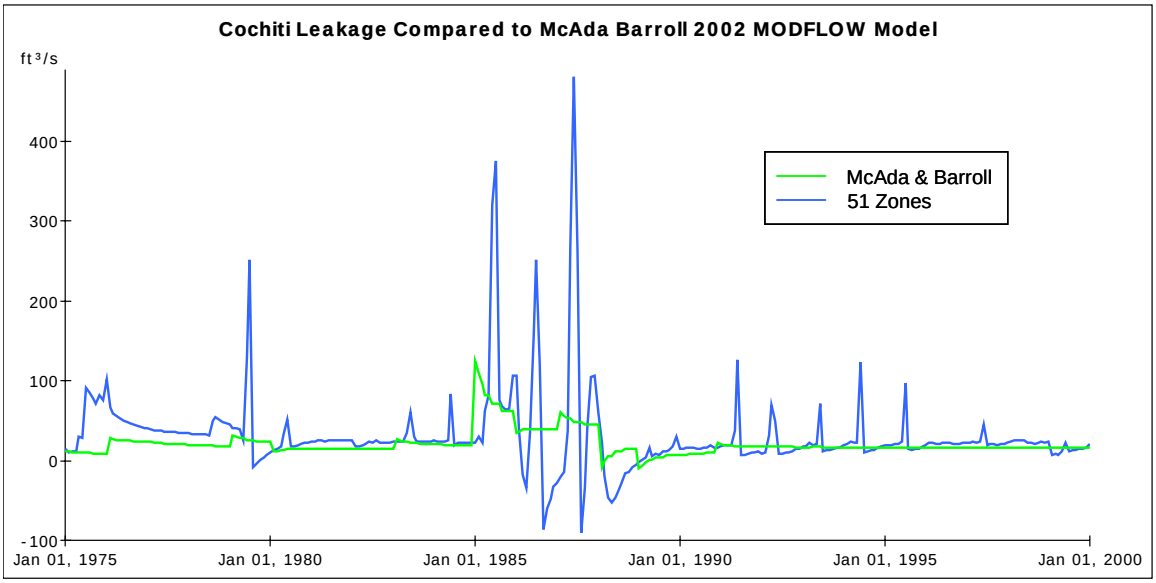

Figure 3-16. Cochiti Reservoir modified (increased) leakage (compare to Figure 3-11) to attain improved mass balance in the reservoir.

ET_{i-ref} is the maximum ET rate possible, F_{i-ET} is the spatial area over which that evaporation occurs, and θ is a groundwater-dependent function that goes from unity when depth to groundwater is zero, to zero when depth to groundwater is greater than the rootzone, which in the McAda and Barroll (2002) MODFLOW model is 30 feet. In the McAda and Barroll model, as in most groundwater models, ET_{i-ref} is a constant, independent of atmospheric conditions or plant type. On the other hand, surface water models often estimate phreatophytic ET based on atmospheric conditions and plant type information, with no regard to groundwater availability. The monthly surface water model to which the 51-zone groundwater model is coupled uses a modified Penman Monteith reference ET equation based on atmospheric conditions, and a plant coefficient based on vegetative properties. This approach is consistent with that of a daily timestep operations model known as the Upper Rio Grande Water Operations Model (URGWOM) (USACE et al. 2002), which makes use of an ET engine called the ET Toolbox (ETTB) (Brower 2004). To make phreatophytic evapotranspiration a function of atmospheric demand, vegetative properties, and groundwater availability, the approaches were combined as follows.

In the surface water model, the maximum predicted riparian (phreatophytic) evaporation for the 1975–1999 monthly average climate conditions averages approximately 3.5 feet per year. In the McAda and Barroll model, ET of 5 ft/yr occurs when depth to the groundwater is zero, and this rate drops linearly to 2 ft/yr when depth to groundwater is 9 feet. Thus the surface water approach is consistent with the MODFLOW approach for an average depth to groundwater of 4.5 feet. This suggests that the surface water model riparian vegetation crop factors may have been developed for riparian vegetation that on average had a depth to water of about 5 feet. The implication of this hypothesis is that when both atmospheric potential and depth to groundwater are constraints to riparian ET, the atmospheric potential rates must be adjusted upward to be consistent with a situation where groundwater levels are not limiting at all to ET rates. For purposes of this modeling effort, a correction factor of 1.3 was found by trial and error, and applied to bosque, cottonwood, and salt cedar riparian crop coefficients in the surface model to account for this effect. Grass and marsh crop coefficients were not changed as it was assumed that these species can only use groundwater resources when depth to groundwater is essentially zero. The ET_{i-ref} term became the maximum potential ET rate for the species in question as calculated in the surface water model, including the calibration adjustment of 1.3 to woody phyreatophte species. Comparison of cumulative riparian ET volumes predicted by the McAda and Barroll groundwater model, the URGWOM surface water model, and the coupled approach for the Rio Grande corridor from Cochiti to San Acacia is shown in Figure 3-17.

Connection to dynamic Espanola groundwater basin model

The Albuquerque groundwater basin is hydrologically connected to the Espanola groundwater basin to the northeast. McAda and Barroll (2002) assume a constant inflow of 10,000 AF per year from the Espanola Basin. As will be described in the next section, a spatially aggregated groundwater model of the Espanola Basin has also been developed. The Espanola and Albuquerque models were connected, allowing dynamic, head-dependent flow between the basins. Details of this connection are presented in the next section.

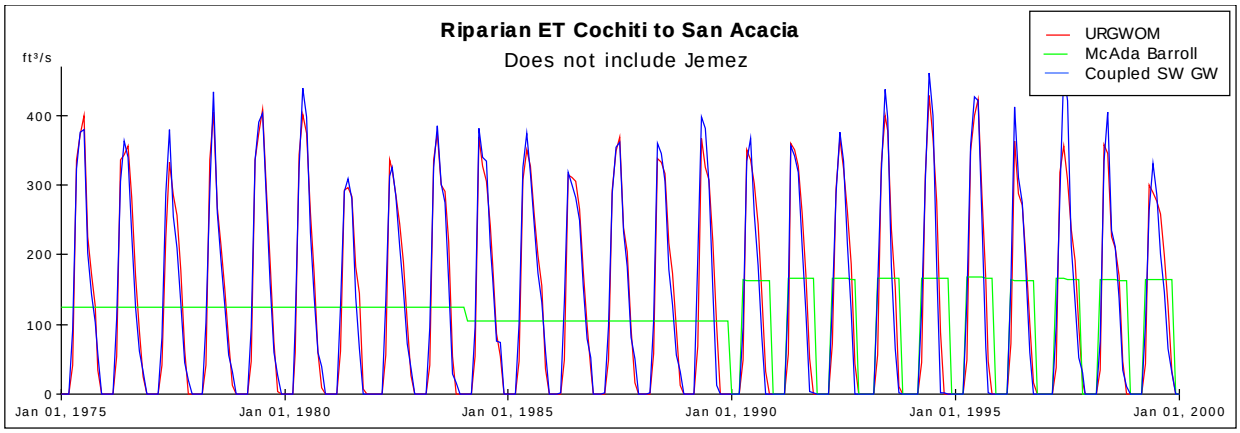

Figure 3-17. Riparian ET 1975–1999 for Rio Grande reaches from Cochiti to San Acacia as modeled by the coupled monthly time step model, the URGWOM surface water model, and the McAda and Barroll (2002) regional groundwater model. Jemez ET is not included in the graph because it is not represented explicitly in URGWOM.

Other adjustments to groundwater fluxes made during calibration of coupled model

Three other changes were made to the groundwater model to bring the fully coupled surface water/groundwater model into calibration with historic stream gage data between 1975 and 1999. For consistency with URGWOM, a value of 8 inches/year was used as a crop seepage constant (compared to 6 inches/year used by McAda and Barroll), depending on water actually delivered to the field. Crop acreages from URGWOM were also used instead of crop acreages used by McAda and Barroll. The approximate average acreages and seepage rates for crop recharge are summarized in Table 3-2; however, the URGWOM values for crop acreage vary with time from 1975–1999 and are broken down by crop type. For more information, see the URGWOM Physical Model Documentation (USACE et al. 2002). Agricultural water actually delivered to the fields was reduced for consistency between the surface water model and URGWOM. This reduction of water applied to the fields resulted in a decrease in crop seepage recharge (see Appendix A, Figure A-2); however, this change in flux was relatively minor compared to overall fluxes from the surface water to the groundwater.

Table 3-2. Approximate irrigated acreages and crop seepage rates used by the URGWOM surface water model, the McAda and Barroll regional groundwater model, and the coupled model described here.

	Middle Valley Ag (acres)	Seepage Rate (inches/yr)	Potential Seepage (AF/yr)
URGWOM	46,000	8	31,000
Coupled	46,000	8	31,000
McAda & Barroll	67,000	6	34,000

Irrigation canals were changed from a constant specified flux in the groundwater model alone to a surface water stage and groundwater head-dependent flux, modeled with Equation 3-14. Surface stage estimates were derived with Manning's equation (Equation 3-16). Canal bed

conductivity was set to 0.15 feet per day consistent with estimates cited by McAda and Barroll (2002), and canal bed thickness to two feet consistent with McAda and Barroll (2002) calibrated values. Canal bed elevation values were set to 5 feet above river channel elevation, effectively eliminating groundwater head dependence.

Figure 3-18 shows canal leakage values estimated by the coupled surface water groundwater model as compared to URGWOM and McAda and Barroll (2002) models.

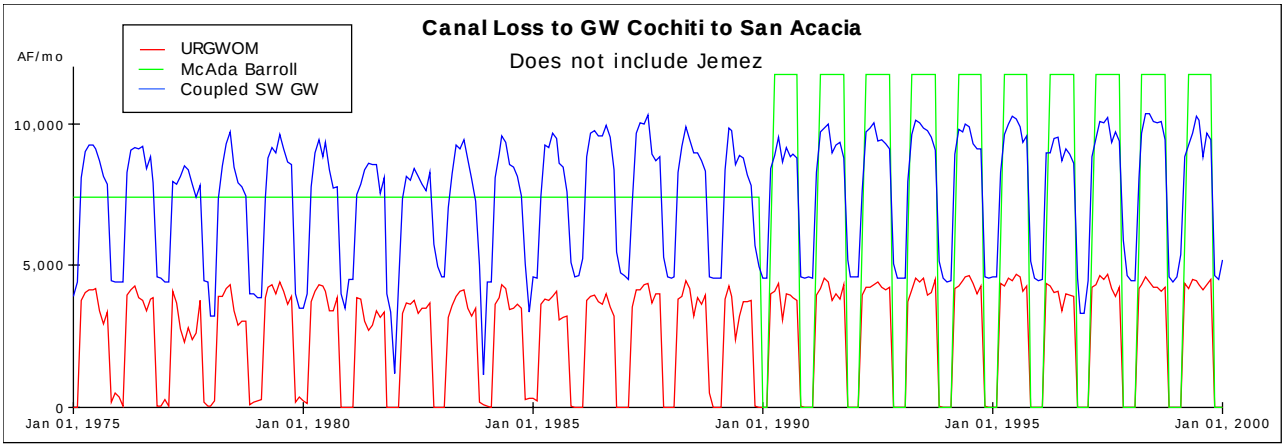

Figure 3-18. Irrigation canal seepage losses to the groundwater aquifer 1975–1999 for Rio Grande reaches from Cochiti to San Acacia as modeled by the coupled monthly timestep model, the URGWOM surface water model, and the McAda and Barroll (2002) regional groundwater model. Jemez canals are not included in the graph because they are not represented in URGWOM.

The spatially aggregated and coupled model estimates are comparable in overall magnitude to the McAda Barroll estimates to which they were calibrated; however, they do not drop to zero in the winter because drain capture results in water flowing in the conveyance system year round, with water captured in the drains in one surface water reach, assumed to be returned to the river or flowing in the irrigation canals in the next reach.

The final change made to the groundwater parameters associated with coupling to the surface water model was to reduce the effective surface elevation for the shallow aquifer *zone between Bernardo* and San Acacia (zone 48) from 4,716.5 feet above mean sea level (amsl) to 4714 feet amsl to increase riparian ET in that reach for consistency with San Acacia stream *and agricultural conveyance gage data between 1975 and 1999.*

Figures 3-19 and 3-20 show the overall fluxes from the surface water to the groundwater systems, and out of the groundwater system as modeled by the URGWOM model, the McAda and Barroll model, and the coupled model described here. Though component terms vary in space and time between the models, the overall fluxes to and from the groundwater system are very consistent for the 1975 to 1999 calibration period. For more information, see the cumulative and timestep-specific component fluxes and summary fluxes compared for the three models shown in Figures A-2 through A-8 in Appendix A.

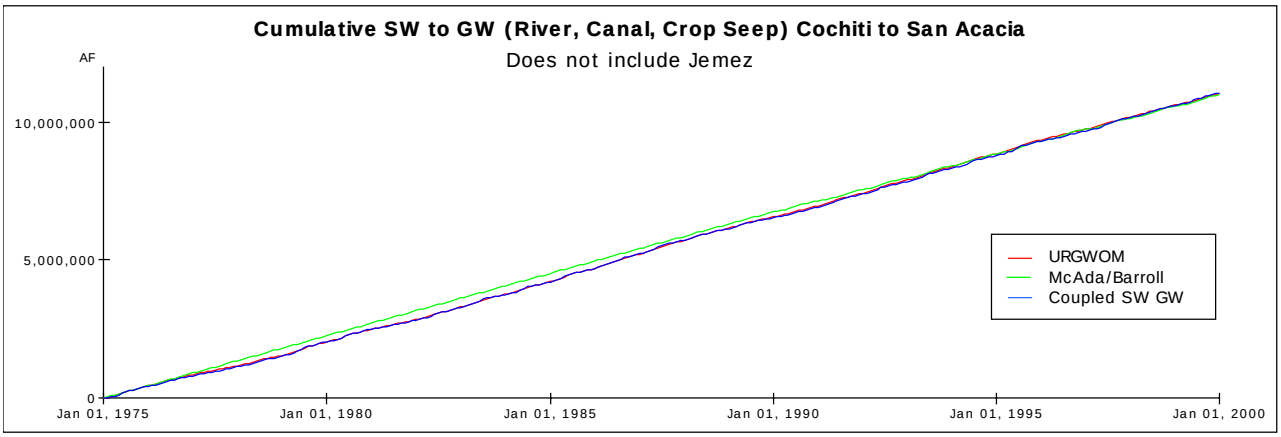

Figure 3-19. Cumulative fluxes to the groundwater system from the surface water system for the Rio Grande reaches from Cochiti to San Acacia as modeled by the coupled monthly timestep model, the URGWOM surface water model, and the McAda and Barroll (2002) regional groundwater model. Jemez is not included because surface water/groundwater fluxes in the Jemez reach are not represented in URGWOM.

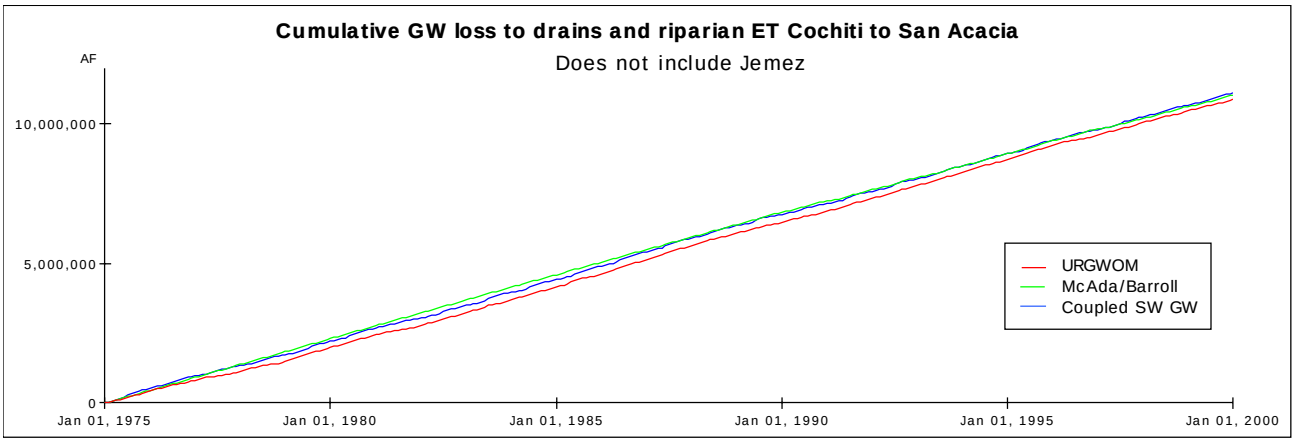

Figure 3-20. Cumulative fluxes out of the groundwater system via drains and riparian ET for the Rio Grande reaches from Cochiti to San Acacia as modeled by the coupled monthly timestep model, the URGWOM surface water model, and the McAda and Barroll (2002) regional groundwater model. Jemez is not included because surface water/groundwater fluxes in the Jemez reach are not represented in URGWOM.

3.4.2 Case Study 2: The Espanola Groundwater Basin

3.4.2.1 Espanola Basin Model Development

The Espanola groundwater basin lies to the north of the Albuquerque Basin (see Figure 3-4), and for the purposes of this analysis interacts with the Rio Grande river system from the Rio Chama/Rio Grande confluence in the north to the beginning of the Cochiti Reservoir maximum pool extent in the south. This spatial extent is based on a MODFLOW regional groundwater model of the area created by Peter Frenzel in 1995 as an enhanced version of a MODFLOW model created by McAda and Wasiolek in 1988. The spatial extent of the Frenzel model is shown in Figure 3-21.

Step 1: Define groundwater compartments (zones)

Using the methodology outlined in Figure 3-3 and discussed above, 16 zones were spatially aggregated from the Frenzel grid. The trial-and-error procedure was analogous to the approach taken in the Albuquerque basin, and proceeded until, on average, MODFLOW estimated flows between the zones chosen traveled from higher average head to lower average head. The 16 zones are shown in Figure 3-22. Three shallow aquifer zones (14–16) were defined to represent the alluvial aquifer sediments associated with the Rio Grande and Pojoaque River. The shallow aquifer zones contain only the top layer of the Frenzel MODFLOW grid. All other aquifer zones contain all eight Frenzel model layers. Zone bottom elevations were assumed to be 200 feet beneath 1975 heads for alluvial zones, and 5,600 feet beneath the 1975 heads for all other zones, based on Frenzel model layer thicknesses for layer 1 and 1-8 respectively. Zone geometry information and 1975 initial head values are shown in Table A-6 of Appendix A. A specific yield of 0.15 is used for all zones, consistent with the Frenzel model.

Step 2: Alpha matrix determination

As was done with the Albuquerque basin model described previously, head values through time from the MODFLOW groundwater model were used to find flow between zones and average head values for the 16 zones for the calibration period 1975–1992 (end of Frenzel historic period) from which average alpha values for each zone pair were calculated by rearranging Equation 3-11b to solve for alpha. The alpha matrix for the 16-zone model is shown in Table A-7 of Appendix A.

Step 3: Source and boundary flux definition and calibration

Modeled groundwater dynamics are less complex in the Espanola basin than the Albuquerque basin. Irrigated agriculture within the Espanola basin model extent is not explicitly connected to the groundwater system by Frenzel or the spatially aggregated model, nor is there a head-dependent ET term modeled.

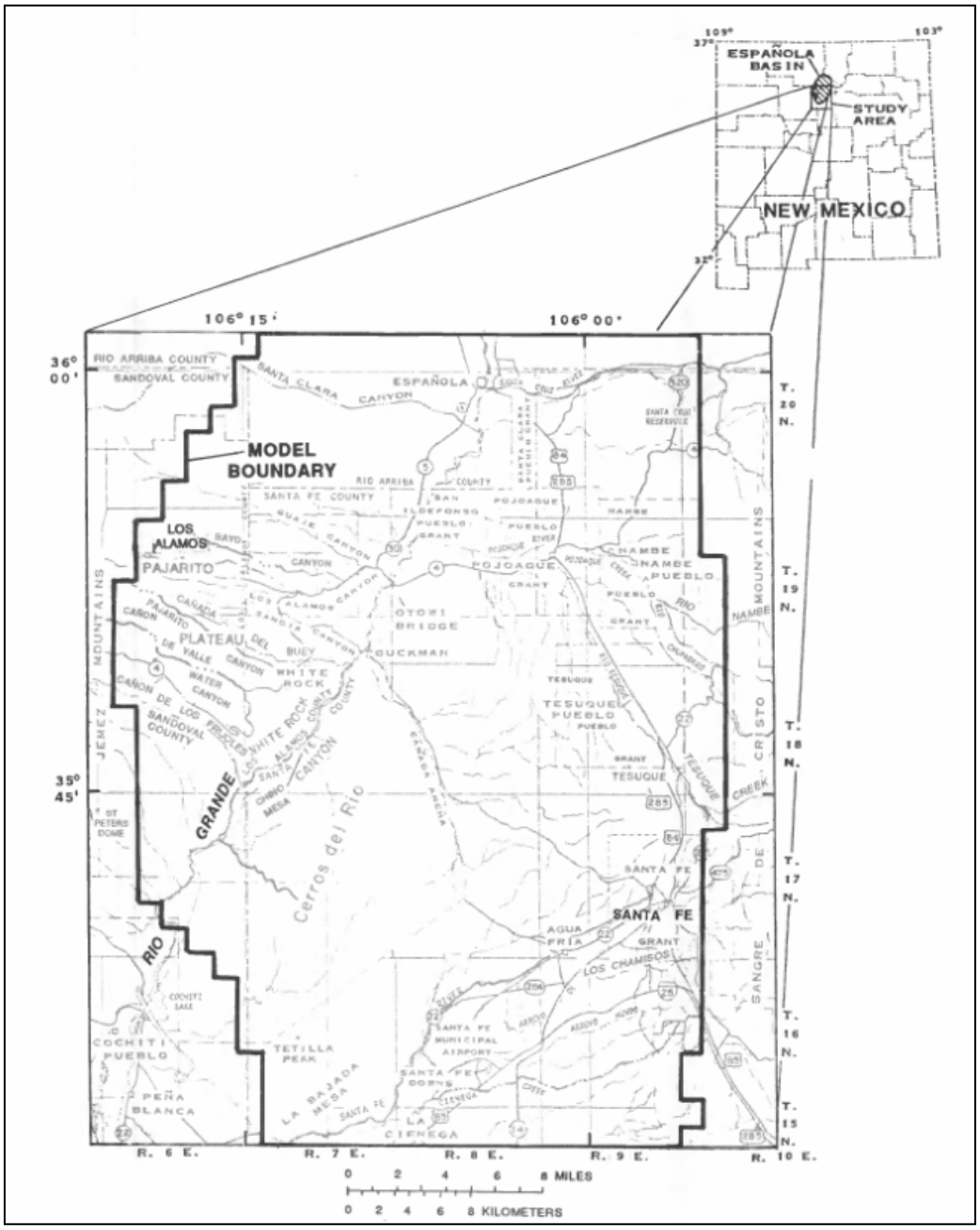

Figure 3-21. Spatial extent of Frenzel (1995) regional groundwater model of the Espanola Basin. Taken from Frenzel (1995), Figure 1.

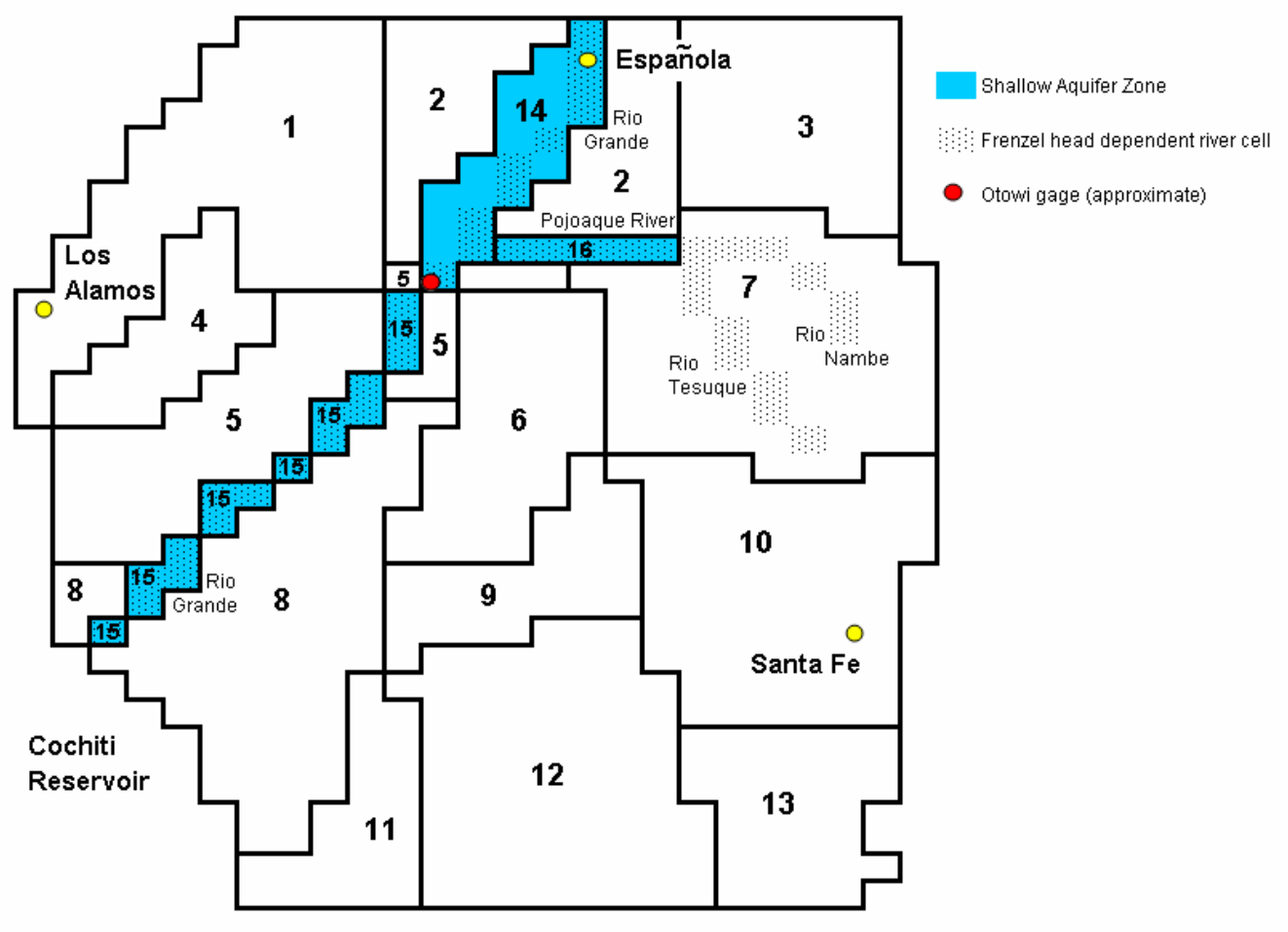

Figure 3-22. Spatially aggregated zones used for simulation of Espanola Basin groundwater system. Shallow aquifer zones (14 through 16) are associated with top two layers of Frenzel (1995) model.

Specified fluxes

Specified flux terms in the Frenzel model were used as specified terms in the 16-zone model as well. Spatial distribution of terms was taken from Frenzel input files. Specified flux terms for the Espanola Basin model are summarized in Table 3-3.

Table 3-3. Specified fluxes to the 16-zone spatially aggregated Espanola Basin groundwater model. Unit of flows is cubic feet per second (cfs) for consistency with Frenzel (1995) report.

Zone	Areal Recharge [cfs]	Mountain Front Recharge [cfs]	Channel Recharge [cfs]	Santa Fe River Recharge [cfs]	La Cienaga Springs [cfs]	South Boundary Flow [cfs]
1	0.0812	8.02				
2	0.0884					
3	0.0449	4.2				
4	0.0333					
5	0.0870	2.06				
6	0.0812					
7	0.1000	6.1	4.3			
8	0.2392					
9	0.0645					
10	0.5393	8.3	5.1	2.2		
11	0.0689					0.28
12	1.7309				-6.5	-1.74
13	0.9785	2.25	0.7			-0.17
14	0.5813					
15	0.0507					
16	0.0072					
Total	4.8	30.9	10.1	2.2	-6.5	-1.6
Frenzel Total	4.8	31	10.1	2.2	-6.5	-2.3

The specified channel recharge includes input from losing stretches of the Rio Nambe, Rio Tesuque, and Arroyo Hondo. The minor disparity in the southern boundary flows may be the result of misinterpretation of the MODFLOW input files, though all other terms extracted from those input files are consistent with the overall Frenzel budget reported in Table 3-2 (Frenzel 1995).

Sewer recharge from the Los Alamos area is not included in the Frenzel model due to lack of information; sewer recharge from the Espanola area is not included in the Frenzel model, and is assumed to return to the surface water system, so it also is not included in the 16-zone model. Sewer recharge from the Santa Fe area recharges the lower Santa Fe river channel, and is treated as a specified time variant flux by Frenzel. Frenzel values are used in the 16-zone model from 1975 to 1992, and thereafter by assuming one half of Santa Fe total demand ends up as sewage effluent. Estimated Santa Fe sewage recharge input values for the 1975–1999 period are shown in Figure 3-23.

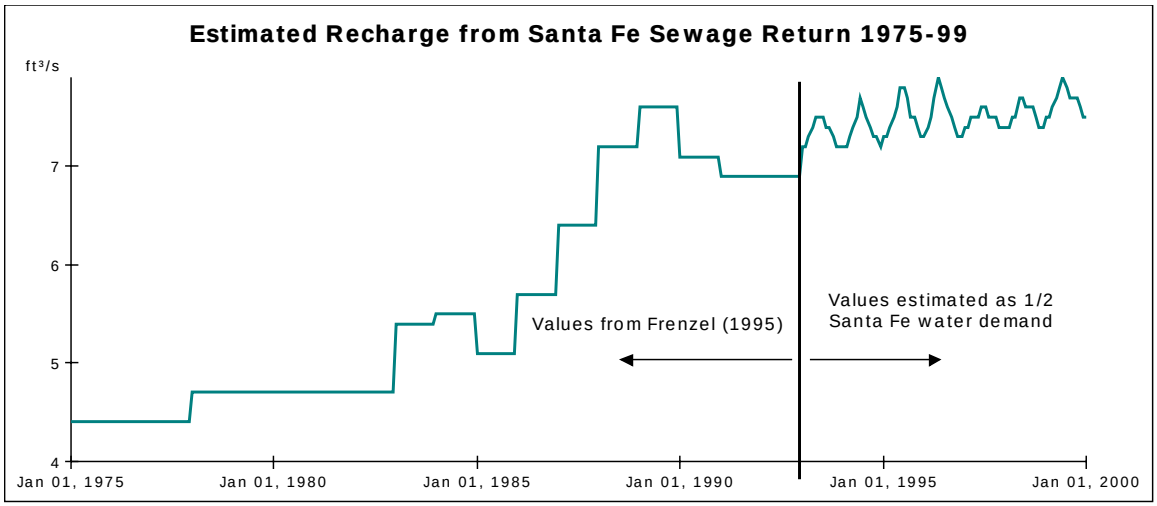

Figure 3-23. Estimated Santa Fe sewage return values 1975–1999. Used as specified flux recharge input data in the Espanola basin groundwater model.

Well data for Los Alamos and Santa Fe well fields were specified based on Frenzel values for the 1975–1992 period, and based on the Jemez y Sangre Water Planning Council's Regional Water Plan (2003) for the 1993–1999 period. Espanola well field pumping is not represented in the Frenzel model, and was taken from the Jemez y Sangre Water Plan as available from 1975 forward for use in the 16-zone model. Private and domestic well data are used from Frenzel for 1975–1992, and increased by 2.4% per year from 1992 values for the 1993–1999 period. Adopted well extraction values for the major well fields in the Espanola basin are shown in Figure 3-24.

Head-dependent fluxes

Consistent with the Frenzel approach, head-dependent terms incorporated into the 16-zone model include a constant head boundary to the north, and river-aquifer interactions for the Rio Grande, Pojoaque River, Rio Tesuque and Rio Nambe. For simplicity and consistency with Frenzel, stream-aquifer interactions were calculated using stream conductance

$$Q_{aq2str} = C_{str}(h_{aq} - z_{str}) \qquad (3\text{-}18)$$

where Q_{aq2str} is volumetric flow from the aquifer to the stream, h_{aq} and z_{str} are the aquifer head and stream stage respectively, and C_{str} is the stream bed conductance, a constant with units of length squared per time, which lumps hydrologic and geometric properties of the stream bed through which flow occurs. Stream stage for the Rio Grande comes from a surface water model that uses channel geometry ratings to estimate stage as a function of flow (see Chapter 2). Stream stage for the other streams is a spatial average of the values used by Frenzel, and is time invariant. Parameters associated with stream-aquifer interactions are summarized in Appendix A, Table A-8.

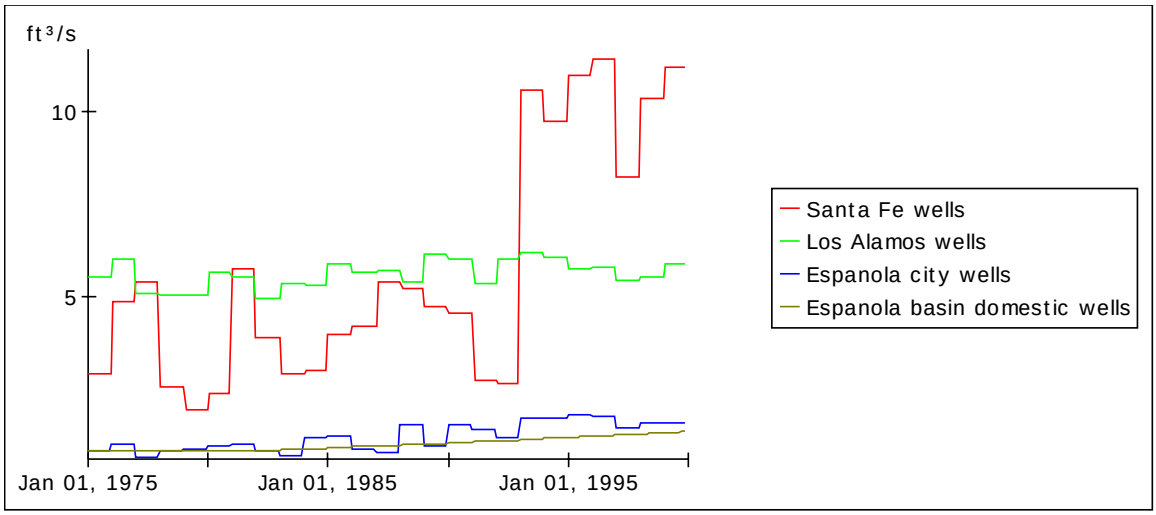

Figure 3-24. Well extraction input data for the Espanola Basin 1975–1999.

The spatially aggregated model incorporates a head-dependent flow from the 16-zone Espanola basin model to the 51-zone Albuquerque basin model to the southwest, which connects the models, replacing a constant head boundary in the Frenzel (1995) model, and a constant flux boundary in the McAda and Barroll (2002) model. Head-dependent flow from the Espanola basin to the Albuquerque basin was implemented by calibrating alpha values to describe total flow from one model to the other consistent with estimates from Frenzel and McAda and Barroll. Alpha values used for boundary flow to the north and southwest are shown in Appendix A, Table A-9.

3.4.2.2 Espanola Basin Results

Head-dependent stream-aquifer interactions for the Rio Grande are compared to the Frenzel values in Figure 3-25. The Frenzel values, which end in 1992, were the overall calibration target, and do not show seasonality because of the annual timestep of the Frenzel model. Seasonality in the spatially aggregated model comes from a monthly stream stage calculated in the coupled surface water model. The seasonality is far greater in the system south of Otowi because the river in this section is within a canyon, and subject to large stage variations as flows change. As described above, stream aquifer interactions for the Pojoaque River and Rio Nambe/Rio Tesuque combination are modeled with fixed stream stage. These interactions are essentially constant at 4.3 and 4.6 cfs flow to the streams respectively, as a result of calibration to associated values in the Frenzel model.

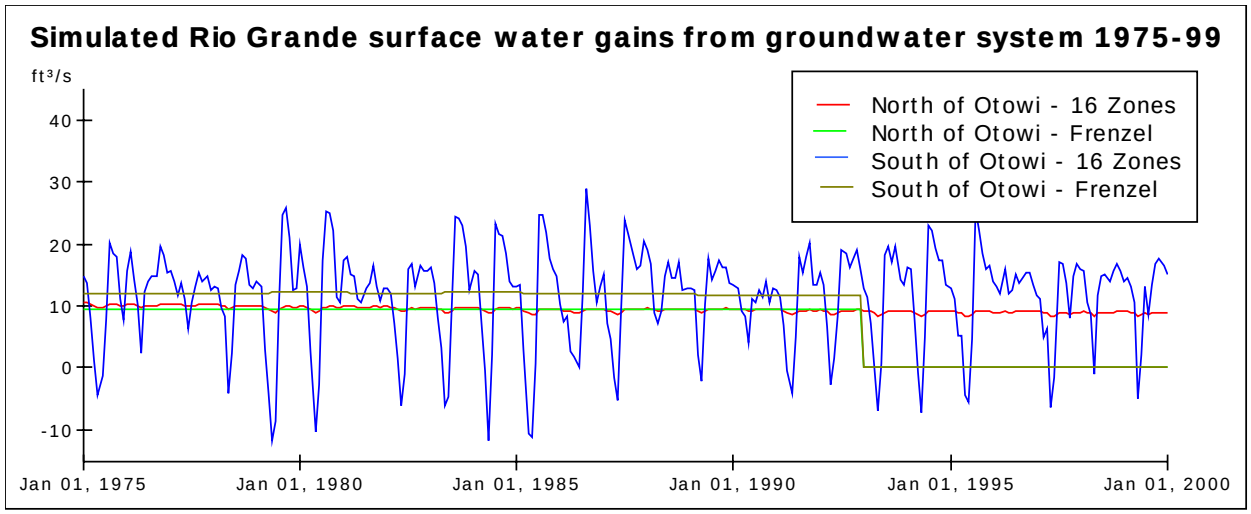

Figure 3-25. Stream-aquifer interactions for the Rio Grande–Espanola Basin groundwater system north of Otowi gage.

Head-dependent flows modeled from the 16-zone Espanola basin model to the 51-zone Albuquerque basin model are compared to the associated specified flows used by Frenzel (1995) as an outflow from the Espanola basin, and McAda and Barroll (2002) as an inflow to the Albuquerque basin in Figure 3-26. The head-dependent flow between basins was calibrated to end up between the Frenzel and McAda and Barroll estimate, and declines initially as leakage from Cochiti Reservoir associated with reservoir operations beginning around 1975 slows groundwater flow from Albuquerque basin to the Espanola basin (see mounding under Cochiti Reservoir in Figure 3-7).

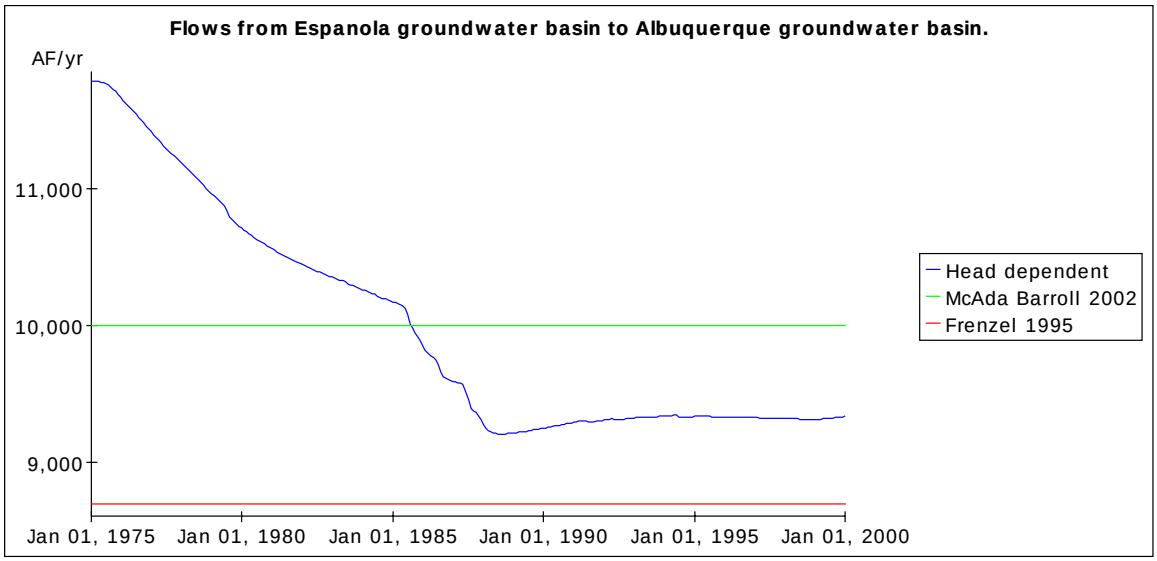

Figure 3-26. Simulated groundwater flows from the Espanola Basin to the Albuquerque Basin from 1975–1999. Combination of the Espanola Basin and Albuquerque Basin spatially aggregated groundwater models allows fixed boundary flows estimated by Frenzel (1995) and McAda and Barroll (2002).

Drawdown in the basin between 1975 and 1999 as simulated by Frenzel and the 16-zone model are shown in Figure 3-27. Another way to compare relative model performance is to look at each timestep at net subsurface flow between any two zones, and then sum all of these flows for all zones. The resulting metric is a measure of how much groundwater movement there is in each model at each timestep. Figure 3-28 shows the net groundwater movement between zones for both models.

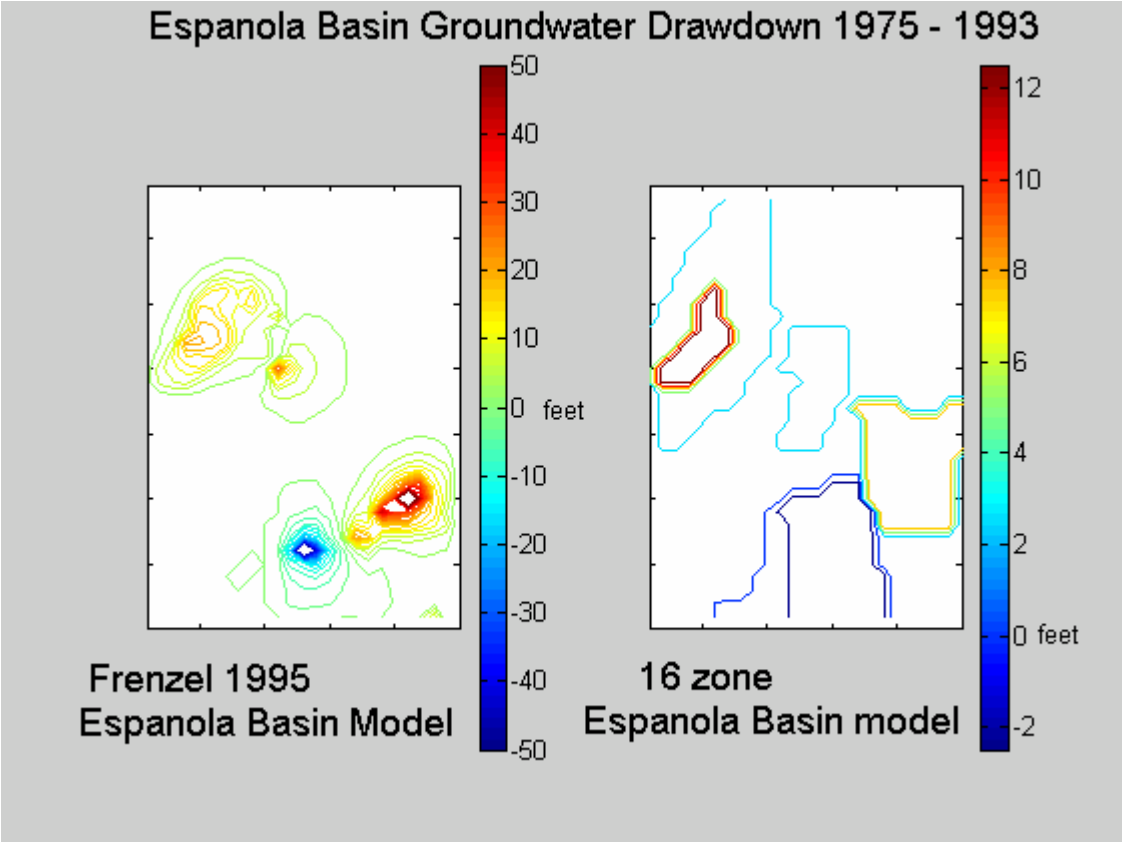

Figure 3-27. Drawdown in the Espanola Basin from 1975 to 1992 as modeled by Frenzel (1995) and the 16-zone compartmental groundwater model. Both models show the dominant patterns of drawdown from Santa Fe and Los Alamos well fields, and ponding from Santa Fe sewage recharge in the southwest.

Figure 3-27 and 3-28 demonstrate that the spatially aggregated Espanola basin model is able to capture the salient behavior of Frenzel's spatially distributed model. In addition, the spatially aggregated model runs rapidly on a desktop computer, and facilitates dynamic connection to the Albuquerque basin spatially aggregated groundwater model as well as an associated surface water model. These features will facilitate integrated, real-time scenario evaluation at a basin scale, something new in the policy analysis toolbox.

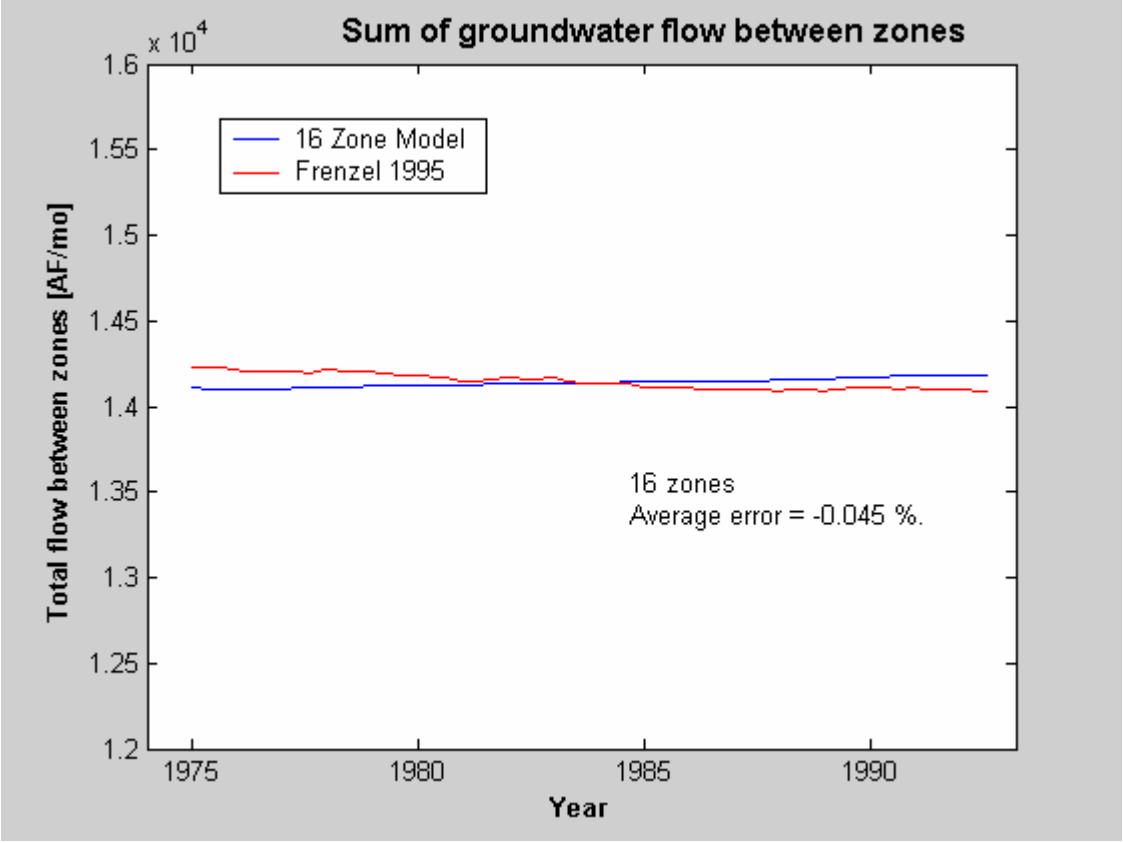

Figure 3-28. Net groundwater movement between zones. At each timestep, the absolute value of all flows between any two zones is summed as a comparison metric to help evaluate the ability of the 16-zone compartmental model to capture the overall groundwater movement patterns. The average difference between the modeled total flows is less than 1%.

3.4.3 Case Study 3: The Socorro Groundwater Basin

3.4.3.1 Socorro Basin Model Development

The Socorro groundwater basin is associated with the Rio Grande river system south of San Acacia. The Albuquerque and Socorro groundwater basins are separated by a basin uplift known as the San Acacia constriction, which effectively separates the two groundwater systems (Shafike 2005). Groundwater pumping in the Socorro basin serves domestic, municipal, and industrial use in sparsely populated Socorro county, (2005 population of 18,000 according to the U.S. Census Bureau), as well as supplemental irrigation demand if surface irrigation supplies are short (Shafike 2005). The relatively small groundwater use associated with these demands compared to overall basin fluxes suggests that the groundwater system can be reasonably approximated assuming steady state (Nabil Shafike, personal communication October 2006). Following this reasoning, Shafike calibrated a spatially explicit model of the basin using steady state flow estimates, and used that parameterization for a one-year transient run using surface

water conditions observed in 2001. Figure 3-29 shows the spatial extent of the Shafike model. Because of the limited timeframe of the transient run and the relative equilibrium of the overall groundwater system, a different approach was used to develop a spatially aggregated groundwater model for the Socorro basin than was used in the Albuquerque and Espanola basins described above. A spatially aggregated groundwater model containing 12 zones was calibrated to the steady state fluxes reported by Shafike for the basin to develop the alpha matrix needed to solve Equation 3-11b. The groundwater model was then run for the 1975–1999 calibration period with dynamic surface water exchanges modeled using Equations 3-14 through 3-17 as in the Albuquerque and Espanola basin models described above. The source fluxes (crop seepage, canal leakage, river leakage, drain capture, and riparian ET) were modified as necessary from the steady state estimates during calibration to result in mass balance for the coupled surface water groundwater system between 1975 and 1999. The remainder of this section describes this procedure in more detail.

Step 1: Define groundwater compartments (zones)

In the 48-mile (USACE et al. 2002) surface water reach from the Rio Grande gage near San Acacia to the Rio Grande gage near San Marcial, surface water diversions largely support irrigated agriculture demands in the top 30 miles (approximate), and wildlife habitat conservation for the Bosque del Apache National Wildlife Refuge in the bottom 18 miles (approximate). For this reason, the spatially aggregated groundwater system model was divided into three major longitudinal sections, the first covering the river system from San Acacia to the northern boundary of Bosque del Apache, the second covering the river system from the northern boundary of Bosque del Apache to San Marcial, and the third covering the river system from San Marcial to the southern extent of the Shafike model in Elephant Butte Reservoir. In each of these sections, the groundwater system is partitioned into four compartments, a narrow and thin shallow aquifer compartment representing high-conductivity alluvial sediments, a central regional aquifer compartment surrounding and underlying the shallow aquifer compartment, and a regional aquifer compartment on each side of the central regional compartment. The groundwater compartments are shown in Figure 3-29.

Step 2: Alpha matrix determination

To estimate the alpha parameters for the spatially aggregated model, steady state groundwater flows between the 12 zones were estimated as follows. First, flow along the river axis from shallow aquifer zone to shallow aquifer zone (1 to 2, 2 to 3, and 3 to south boundary) and from central regional to central regional zone (5 to 8, 8 to 11, and 11 to south boundary) was estimated with Darcy's law using visual inspection of steady state hydraulic gradients from a file of steady state heads provided by Nabil Shafike (personal communication 2005) and average aquifer geometry and hydrologic properties from the Shafike (2005) report. Results of those calculations are shown in Table 3-4.

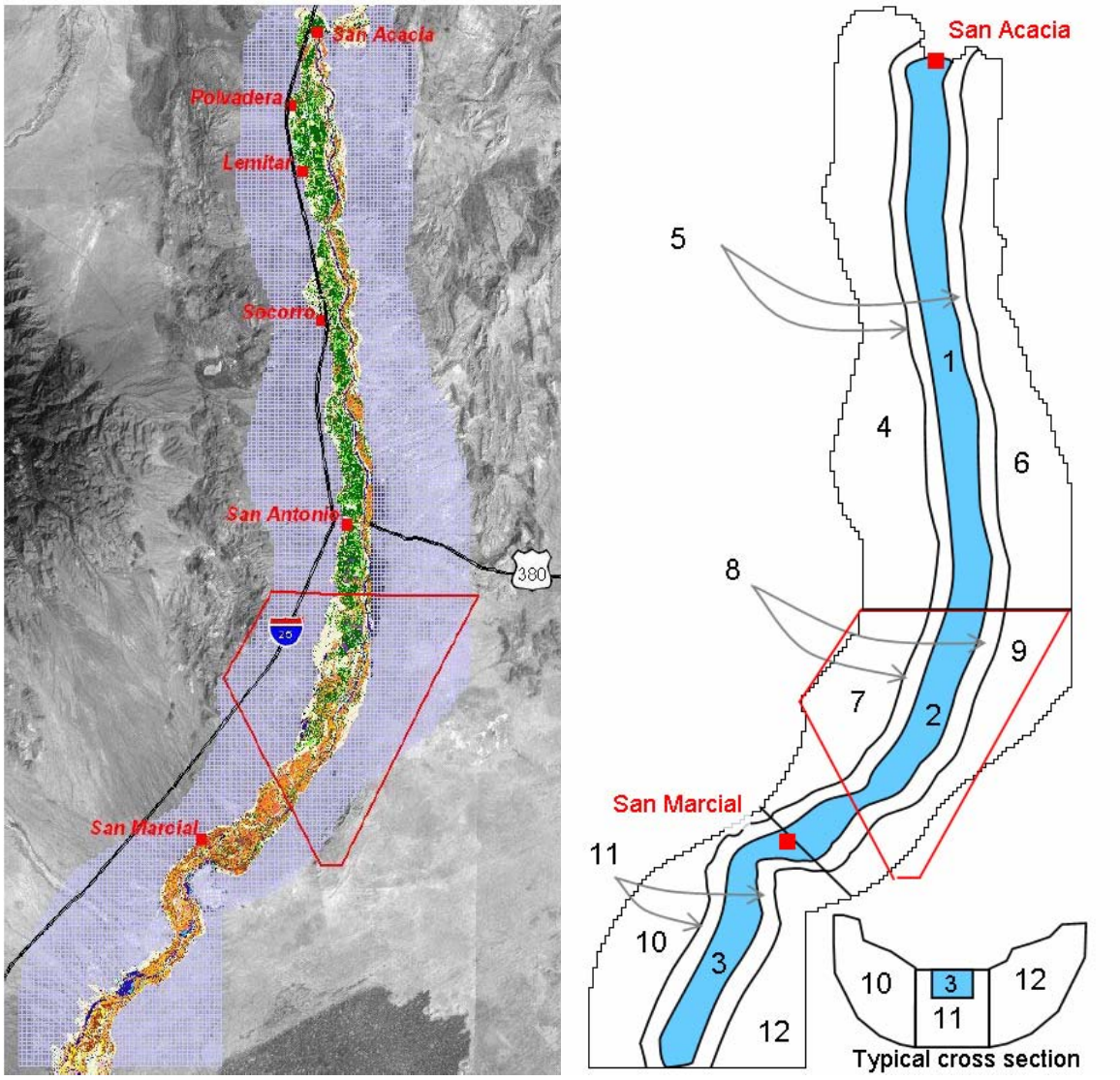

Figure 3-29. Active model grid for Shafike (2005) groundwater model of Socorro Basin (left), and zone delineation for the spatially aggregated model (right). The spatially aggregated model contains shallow aquifer zones (1–3) that roughly coincide with the top layer of the Shafike model within the inner valley. The models extend from San Acacia in the north to Elephant Butte Reservoir in the south. The red outline delineates the Bosque del Apache National Wildlife Refuge. For reference, San Acacia can be seen at the south end of the McAda and Barroll Albuquerque basin grid (Figure 3-5). Left image from Shafike (2005, Figure 11a).

Table 3-4. Darcy-based calculations to estimate steady state flow in north-south direction for shallow and central regional aquifer zones.

	Sub-Reach	Zone	Ksat [ft/da]	Ave Zone Width [ft]	Ave Zone Depth [ft]	SS Hydraulic Gradient [-]	North South SS Flow through Zone [AF/yr]
Shallow Aquifer Zone	San Acacia to Bosque del Apache	1	100	10000	100	0.0008	690
	Bosque del Apache to San Marcial	2	100	10000	100	0.0006	510
	San Marcial to Elephant Butte	3	100	10000	100	0.0006	480
Center Regional Aquifer Zone	San Acacia to Bosque del Apache	5	0.3	20000	4000	0.0008	170
	Bosque del Apache to San Marcial	8	0.3	20000	4000	0.0006	130
	San Marcial to Elephant Butte	11	0.3	20000	4000	0.0006	120

Second, visual inspection of steady state heads led to the rough assumption that of mountain front recharge occurring between San Acacia and Bosque del Apache, 10% flowed south to neighboring regional zones (4 to 7 and 6 to 9), and 90% flowed to zone 5. Groundwater flow between regional aquifer zones on the margins of the model north and south of San Marcial (7 to 10 and 9 to 12) was assumed negligible. Finally, it was assumed that at steady state, flow across the southern boundary of the model from the regional aquifer east of the river (12) was also negligible. With these assumptions, flow between each zone could be specified. For example, the central regional aquifer between San Acacia and Bosque del Apache (zone 5) receives 90% of mountain front recharge from the regional aquifers to the east (zone 6) and west (zone 4) totaling 4,806 AF/yr. As seen in Table 3-4, 170 AF/yr moves to the next central regional aquifer south (zone 8). Thus 4,806 – 170, or 4,636, AF/yr must flow to the overlying shallow aquifer zone (zone 1). The same logic was applied to each zone, resulting in the flow matrix shown in Table 3-5.

Average steady state head values for each zone were estimated by visual inspection of the steady state head distribution file generated by the Shafike model. The steady state average heads adopted for each zone are shown in Table 3-6. With the head values, head differences between all zones were calculated, and Equation 3-11b rearranged to solve for alpha by dividing flows between zones by the head difference between the same zones. The alpha value for 11 to 12 could not be set this way because there is no assumed steady state gradient. $\alpha_{11,12}$ was set at 1 acre/mo by analogy to $\alpha_{8,9}$. The resulting alpha matrix for the 12-zone model is listed in Table A-10 of Appendix A.

Table 3-5. Estimated steady state groundwater flows between Socorro groundwater basin zones, and to south boundary (SB) for 12-zone spatially aggregated model.

		Socorro Basin Estimated SS GW Flows [af/yr]												
		To Zone:												
		1	2	3	4	5	6	7	8	9	10	11	12	SB
From Zone:	1		690			-4636								
	2	-690		510					-4004					
	3		-510									-1620		480
	4					3645		405						
	5	4636			-3645		-1161		170					
	6					1161				129				
	7				-405				3835		0			
	8		4004			-170		-3835		-129		130		
	9						-129		129				0	
	10							0				1610		4830
	11			1620					-130		-1610		0	120
	12									0		0		0
	SB			-480							-4830	-120	0	
	Sum	3946	4184	1650	-4050	0	-1290	-3430	0	0	-6440	0	0	5430

Table 3-6. Adopted zonal heads for Socorro Basin spatially aggregated model. EB is steady state reservoir stage at Elephant Butte.

Zone:	1	2	3	4	5	6	7	8	9	10	11	12	EB
Adopted SS Head:	4580	4500	4460	4640	4590	4600	4560	4510	4520	4850	4440	4440	4430

Step 3: Source and boundary flux definition and calibration

Steady state source terms to and from each of the zones were also estimated. The steady state run evaluated by Shafike (2005) does not include crop irrigation and associated conveyance canal and crop seepage recharge terms, nor does it include well pumping. The steady state run does include flow from the groundwater system into a low-elevation conveyance channel called the Low Flow Conveyance Channel (LFCC), which serves as a drain for the system. To estimate steady state flows between the 12 groundwater zones, steady state basin fluxes reported by Shafike (2005) were distributed to each of the zones.

Socorro Basin steady state groundwater gains

Mountain front recharge was assigned to zones 4, 6, 7, and 10 with locations based on estimated mountain front spatial distributions in the area from Roybal (1991), summing to the 15,210 AF/yr used by Shafike (2005). Values are shown in Table 3-7. Shafike (2005, Figure 14) reports the results of Rio Grande seepage runs, suggesting weighted average river leakage ranging from 224.5 cfs to 500 cfs between San Acacia and Fort Craig, with 61% to 71% of the

leakage occurring between San Acacia and the north boundary of Bosque del Apache, 27% to 37% occurring between the north boundary of Bosque del Apache and San Marcial, and 2% between San Marcial and Fort Craig. For the approximately 6 miles from Fort Craig to Elephant Butte, river leakage was assumed to be the same as from San Marcial to Fort Craig: 1 to 2 cfs/mile. Using these distributions, and the total river leakage of 205,020 AF/yr used by Shafike, steady state river leakage into groundwater zones 1-3 was assigned as shown in Table 3-7.

Socorro Basin assumed steady state groundwater losses

Groundwater leaves the Socorro basin system by flow to the LFCC (drain flow), by riparian ET, and via subflow out the southern boundary of the model. Visual inspection of Shafike (2005, Figure 15) suggests that about 75% of steady state groundwater flows to the LFCC occur north of Bosque del Apache, and essentially 100% occur north of San Marcial. Shafike reports total steady state groundwater flow to the LFCC of 152,140 AF/yr. In the spatially aggregated model 75% of this amount is lost from shallow aquifer zone 1, and the remainder from shallow aquifer zone 2. Values are shown in Table 3-7. Having identified all other steady state flux terms associated with the shallow aquifer zones, riparian ET was solved for using mass balance. For example, in the shallow aquifer zone from San Acacia to Bosque del Apache (zone 1), river leakage adds 135,500 AF/yr to the groundwater system, LFCC losses remove 117,100, and net flows from adjacent aquifer zones add 3,950, leaving 135,500 + 3,950 – 117,100 = 22,350 AF/yr available for removal by ET. Values are summarized in Table 3-7.

Table 3-7. Steady state fluxes adopted for 12-zone Socorro Basin model. The net groundwater flow of -5,410 AF/yr represents groundwater flow out the southern boundary of the model, as calculated by Shafike (2005). Shafike totals listed are from Table 2 of the 2005 report.

GW Zone	GW Gain [AF/yr]		GW Loss [AF/yr]		Implied Subsurface Flows [AF/yr]
	MtnFrnt	Rvr Leak	LFCC	ET	
1	0	135500	117100	22350	3950
2	0	61000	35000	30200	4200
3	0	8600	0	10250	1650
4	4050	0	0	0	-4050
5	0	0	0	0	0
6	1290	0	0	0	-1290
7	3430	0	0	0	-3430
8	0	0	0	0	0
9	0	0	0	0	0
10	6440	0	0	0	-6440
11	0	0	0	0	0
12	0	0	0	0	0
Total	15210	205100	152100	62800	-5410
Shafike SS Totals	15210	205020	152140	63030	-5430

The groundwater model was coupled to the surface water model for the 1975–1999 calibration period in stages. Fluxes across the southern boundary from zones 3 and 11 were modeled as head-dependent on Elephant Butte Reservoir, and fluxes across the southern boundary from zone 10 were modeled as constant flux. Fluxes across the southern boundary from zone 12 were assumed negligible. Initially, river leakage was held constant and LFCC capture and riparian ET implemented as a function of relevant aquifer and surface characteristics using Equations 3-15 through 3-17 as described previously for the Albuquerque basin. Reference ET (1975–1999) from the surface water model modified for use with depth to groundwater as an additional constraint (described previously) was used to drive atmospheric ET demand. LFCC fluxes were calibrated to steady state by manipulation of bed elevation values. ET fluxes were calibrated to steady state by manipulation of average surface elevation of the shallow aquifer zones. Once the LFCC and riparian ET parameters were set, river leakage was implemented using Equation 3-14. Initially, all 1975–1999 flows at San Acacia (floodway and conveyance) were set as flows in the river channel. The river bed conductivity and thickness values were set to 0.5 feet/day and 5 feet respectively, consistent with values used in the Albuquerque basin. River bed elevation values were then manipulated to bring average 1975–1999 river leakage close to steady state estimated values (Table 3-7). Finally, historic diversions into the LFCC and agricultural conveyance system were restored, and non-LFCC canal leakage, crop seepage, well pumping, and historic Elephant Butte stage incorporated into the surface water groundwater interaction. Well pumping is calculated based on simple estimates of the small municipal and industrial demand in the area, and estimates of supplemental water needs when agricultural demand exceeds available water in the irrigation conveyance system. Well pumping values assumed for the Socorro Basin spatially aggregated model are shown in Figure 3-30. Seventy-five percent of the extraction is assumed to occur from the shallow aquifer between San Acacia and the northern boundary of Bosque del Apache (groundwater zone 1), and the remaining 25% from the underlying regional aquifer (groundwater zone 5).

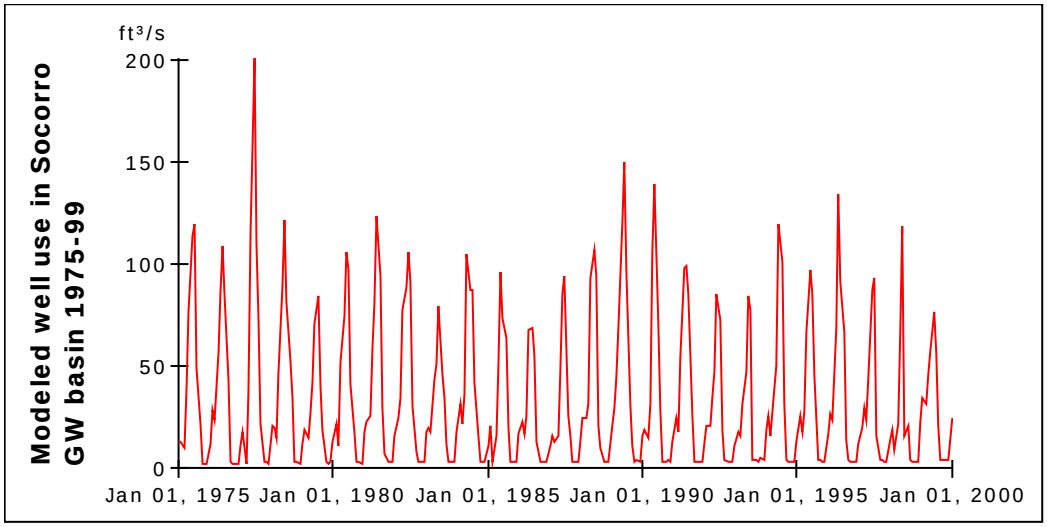

Figure 3-30. Well pumping assumed for Socorro Basin 1975–1999. Based on estimates of municipal and industrial use and supplemental irrigation demand.

Canal bed conductivities were set to 0.2 feet per day consistent with values reported in the URGWOM physical model documentation for canal bed conductivities below San Acacia (USACE et al. 2002). Canal bed thickness values were set to 2 feet based on values used in the Albuquerque basin (see Step 3 in Section 3.4.1.1), and canal bed elevations were set 2 feet above the river channel elevation. Irrigation canals are only included in the model between San Acacia and Bosque del Apache. Steady state parameters were adjusted as necessary to achieve 1975–1999 mass balance between the San Acacia and San Marcial gages, and between the San Marcial and Elephant Butte Reservoir, as estimated by Elephant Butte behavior (see Chapter 2). The major adjustments associated with calibration of the coupled model were an increase in riparian acreage in the San Acacia to San Marcial reach as described in Chapter 2, an adjustment of the shallow aquifer effective surface elevation (controlling depth to groundwater and thus riparian ET) between San Marcial and Elephant Butte, and a limit to the leakage of the LFCC. The LFCC was modeled as a drain according to the Dupuit-Forchheimer approach using Equation 3-15 as described previously. However, unlike drains in the Albuquerque basin, the LFCC can carry thousands of cubic feet per second. When the LFCC is carrying thousands of cubic feet per second, the stage of the water in the LFCC may be greater than that of the surrounding aquifer, leading to leakage to the aquifer. Equation 3-13 seems to do a reasonable job of predicting this leakage as long as the stage in the canal does not get too much larger than the aquifer head, but when this occurs, Equation 3-13 seems to result in excessively large flows from the canal back to the groundwater. This may be a problem inherent to the approach, or a bug in the model code. As this report goes to press, the problem has been temporarily solved by limiting the amount of water that can move from the LFCC back to the aquifer to 300 cfs in each groundwater zone until the cause of the large flows can be ascertained. Table A-11 in Appendix A summarizes calibrated parameters used to model interactions between the aquifer and the LFCC, river, irrigation canals, and riparian vegetation.

3.4.3.2 Socorro Basin Results

As explained above, the spatially aggregated Socorro Basin groundwater model was developed from a spatially explicit but steady state groundwater model developed by Nabil Shafike (2005), and run in a transient mode. Figure 3-31 shows the groundwater heads in the 12 aquifer zones from 1975–1999. There is no trend in any of the zones, suggesting that despite temporal fluctuations in stream aquifer exchanges due to temporally varying surface water conditions the groundwater system is in a quasi-steady state. Zones 1-3 are the shallow aquifer zones, and show noise about a steady average.

LFCC gains from the groundwater system modeled with the coupled model as compared to URGWOM and steady state values from the Shafike (2005) model are shown in Figure 3-32. The LFCC was used significantly until around 1986 (Shafike 2005), and the groundwater gains to the canal are clearly greater after that time in both transient models. The cumulative 25-year groundwater flow to the LFCC modeled by the coupled model falls between the URGWOM prediction, and the steady state prediction, as seen in Figure A-9 in Appendix A.

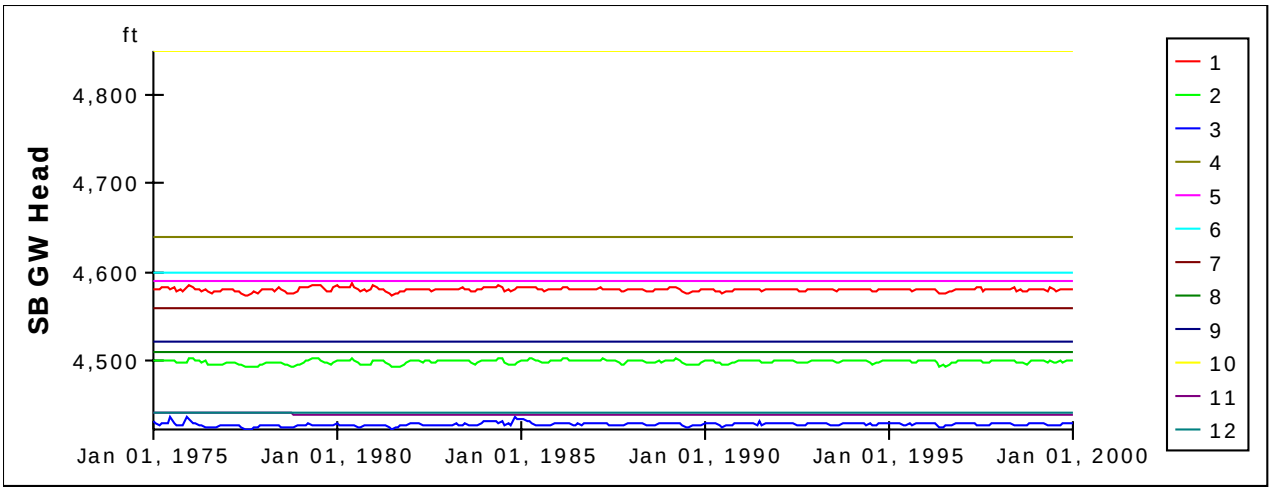

Figure 3-31. Modeled groundwater heads in Socorro Basin by groundwater zone between 1975–1999. Flat trend justifies the steady state assumptions used to develop the groundwater model parameters.

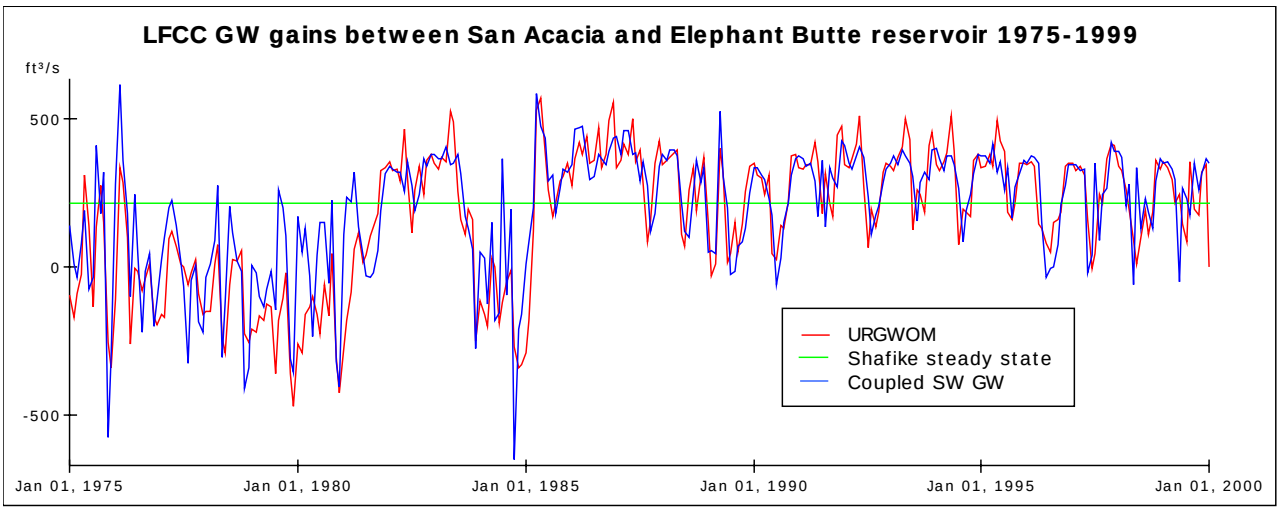

Figure 3-32. Flows from the groundwater system to the LFCC for Rio Grande reaches from San Acacia to Elephant Butte as modeled by the coupled monthly timestep model, the URGWOM surface water model, and steady state values reported by Shafike (2005).

River leakage values from the different models are shown in Figure 3-33. The coupled values and URGWOM values agree well from 1985 on, but not before. Further investigation into URGWOM methodology will be required to understand the reason for this difference. From a cumulative river leakage perspective, the 25-year total river leakage predicted by the coupled model is similar to the steady state cumulative. The URGWOM cumulative value is less, again largely because of the gaining reach tendencies estimated by URGWOM between 1975 and 1985. The cumulative river leakage values are shown in Figure A-10 in Appendix A.

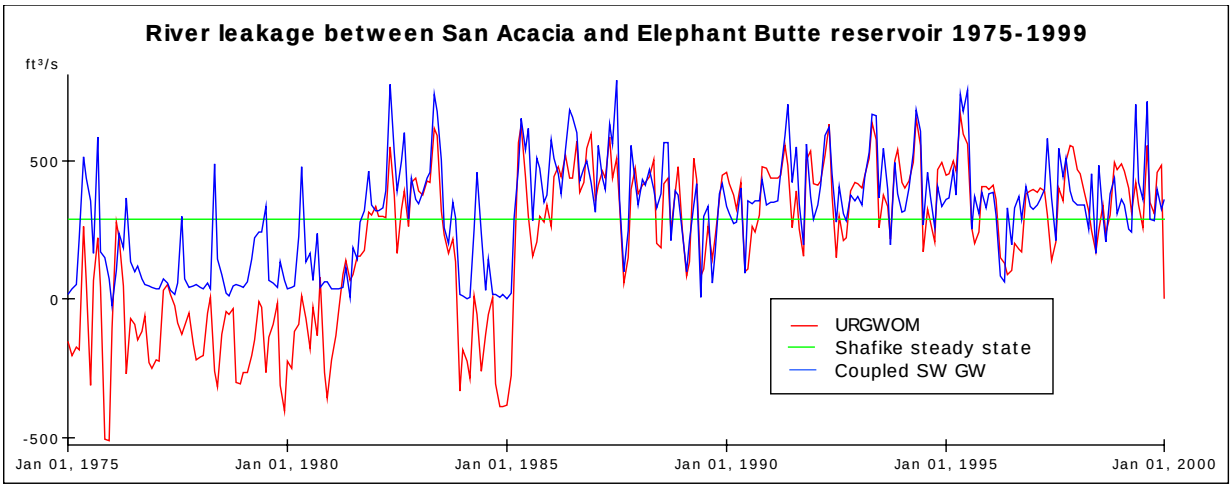

Figure 3-33. Rio Grande river leakage between San Acacia to Elephant Butte as modeled by the coupled monthly timestep model, the URGWOM surface water model, and steady state values reported by Shafike (2005).

Riparian ET values predicted by the different models are shown in Figure 3-34, and cumulatively in Figure A-11 in Appendix A. As discussed in Chapter 2, the seemingly overly large losses observed between San Acacia and San Marcial may be a result of gage errors, particularly between 1985 and 1988; however, analysis of systematic gage error is beyond the scope of this effort, and so gage error is assumed to be normally distributed about zero, and other methods are used to obtain mass balance at each gage between 1975 and 1999. In the case of the San Acacia to San Marcial reach, calibration of the coupled model was achieved by increasing riparian vegetation area in the reach by 33%. See Chapter 2 for further discussion. As a result of this calibration, the coupled values shown in Figure 3-34 are significantly higher than the URGWOM values. The surface water balance between San Acacia and San Marcial appears to be closed in URGWOM with large crop seepage rates as seen in Figure 3-35. In the coupled model, large seepage rates end up back in the drain system (LFCC), and so cannot be used to close the surface mass balance.

The last head-dependent flux of consideration for the historic period in the Socorro Basin groundwater system is canal leakage, which is modeled from San Acacia to San Marcial in the coupled model. It is not modeled explicitly in URGWOM, and not included in the steady state mass balance done by Shafike (2005). This is a relatively small flux in the coupled model, averaging a fairly steady 8 cfs, as shown in Figure A-12 in Appendix A.

The spatially aggregated and coupled surfacewater/groundwater model of Socorro Basin is able to capture many of the temporal signals of the surface water system modeled by URGWOM as seen in Figures 3-32 and 3-33, while maintaining a quasi-steady state groundwater mass balance as shown in Figure 3-31 and predicted by Shafike (2005). The combination of the surface and groundwater mass balance constraints suggest that either gage error led to significant overestimates of reach losses between 1985 and 1988 (see also Chapter 2), or the ET losses in that reach are larger than suggested by either URGWOM or Shafike's (2005) steady state analysis. These conclusions support the value of basin scale multi-decadal analysis of coupled surface water groundwater systems that is made rapid and accessible by the spatial aggregation techniques for groundwater modeling described in this chapter.

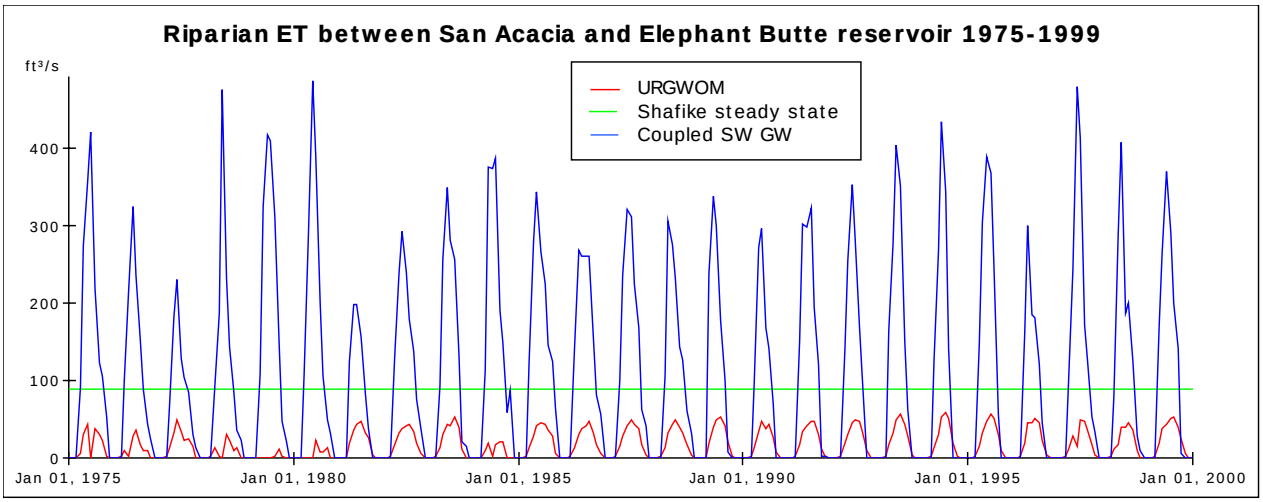

Figure 3-34. Riparian ET between San Acacia and Elephant Butte as modeled by the coupled monthly timestep model, the URGWOM surface water model, and steady state values reported by Shafike (2005).

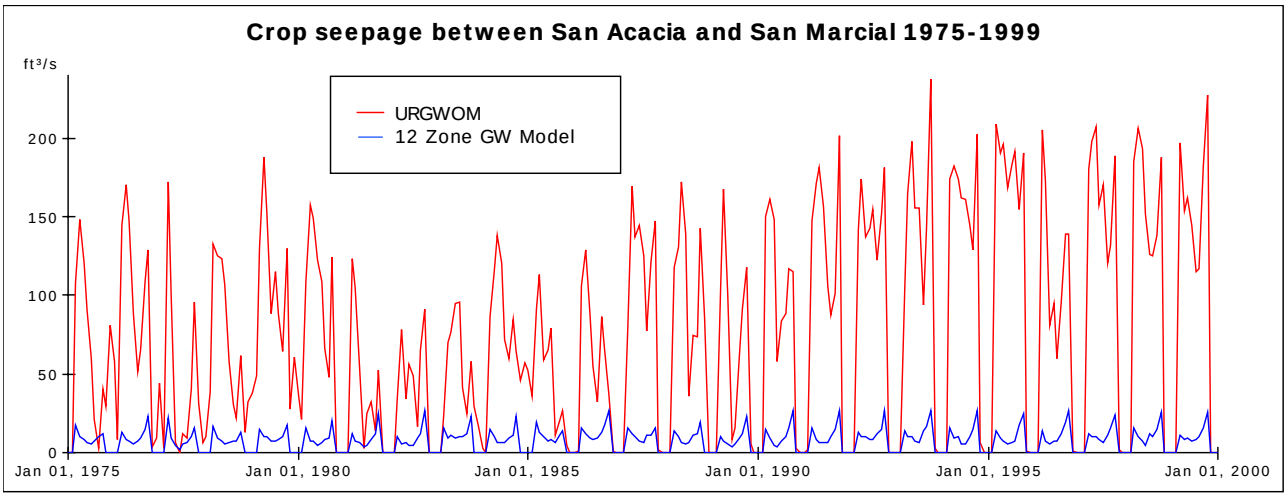

Figure 3-35. Crop seepage between San Acacia and Elephant Butte as modeled by the coupled monthly timestep model and the URGWOM surface water model.

3.5 Acknowledgments

The authors would like to express their gratitude to the many people who have helped in the development of this work, including our colleagues at the University of Arizona, SAHRA, and Sandia, as well as Doug McAda of the USGS, Peggy Barroll of the New Mexico Office of the State Engineer, and Nabile Shafike of the New Mexico Interstate Stream Commission, all of whom provided insight and clarification in response to repeated unsolicited questions!

4. LAND SURFACE PROCESS MODULES

Carlos A. Aragón, Sarah Gonzales, and Enrique R. Vivoni
New Mexico Institute of Mining and Technology

4.1 Introduction

Uninstrumented watersheds pose a problem to scientists around the world in that the degree to which they contribute to the water balance of a region cannot be directly measured. Often this unaccounted for water is simply lumped with other difficult to measure components of the water balance such as groundwater discharge or evapotranspiration. While this may produce a balanced model of the river system, it may also lead to erroneous estimates of surface water and groundwater flow rates. The problem of not being able to accurately measure discharge in ungaged basins affects the decision-making process. In order for water policy decisions to be made correctly, there should be a proper allocation of water resources from different sources (Ward et al. 2006).

A major problem with ungaged basins is of the lack of available data, both in the form of inputs that can be used to force a model and outputs that allow for testing to build confidence in the model. Physical rainfall-runoff models address this issue by describing the watershed with a series of analytical equations that convert rainfall to runoff (Beven 2000). While these processes are accurate at small scales, their validity at larger scales is not well known. Typically, physical equations valid at the point scale are applied over larger regions with reasonable practical success (Burnash et al. 1973; USACE 1994). Some models go as far as to apply rainfall runoff equations at the continent scale (Nijssen and Lettenmaier 1997).

Toward these needs we are developing a land surface model for simulating rainfall-runoff processes. The unique aspect of this work is a desire to balance model accuracy with computational time so as to allow near-real-time use in a decision-making setting with interested stakeholders (Ahmad et al. 2004; Nandalal et al. 2003). The set of modules described in this chapter complement the surface and groundwater modules described in the previous chapters. Specifically, land surface processes generate the tributary flows (both gaged and ungaged) to the river routing tools described in Chapter 2 and the infiltration/recharge volumes that supply the regional aquifer systems described in Chapter 3. In the following we describe the generic framework for the rainfall-runoff model. To test the accuracy of the model, application is made to the Río Salado watershed in central New Mexico. This basin has undergone the gaged-to-ungaged transition over the historical record with approximately 40 years of gaging record during the 20th century. Since 1984, the Río Salado gage has been inoperational, except for manual streamflow estimates made during large flooding events. This history presents an ideal situation for testing a semi-distributed model of an ungaged semi-arid basin.

4.2 Methods

4.2.1 Overview

Comprised of multiple components that account for the physical processes that take place in a watershed, the ungaged tributary model attempts to determine the amount of runoff produced by a watershed given a rainfall event. The primary driver of model simulations is rainfall. To

account for variable precipitation within a month, an event-based timing structure was implemented in the ungaged tributary model. Dividing the time series in this way improves the model's ability to produce accurate discharge volumes in semi-arid regions.

In order to produce a semi-distributed model that approximates point scale processes, watersheds are divided into hydrologic response units (HRUs). These are areas within a watershed that have a unique combination of soil and vegetation types. This allows grid cells of the same class to be lumped together as a single unit with distinct hydrological properties. The use of HRUs greatly reduces the number of calculations that must be performed while retaining the distinctive properties associated with each class. The HRUs in each watershed are created by overlaying soil and vegetation maps using ArcMap. Properties such as HRU area, root depth, and porosity are then entered in a table to be used later as parameters within the model. It is important that these properties be uniform over the HRU area because they can greatly affect runoff response (USACE 1994).

In order to accurately describe the hydrologic behavior of each HRU, water-balance processes such as precipitation, evapotranspiration (ET), infiltration, and runoff are simulated. Historical precipitation data are used to calibrate the model while stochastically generated time series are used when rain gage data are unavailable.

ET is calculated using the Hargreaves equation, a temperature-based method for estimating ET. The Variable Infiltration Capacity method created by Liang et al. (1994) is used to calculate the amount of infiltration as well as the amount of runoff produced within each HRU. This runoff is then routed to the outlet of each watershed based on the Manning equation, with a portion lost within the channel as the flow is transmitted.

For the model development described here, Powersim is the primary software package utilized. Powersim is dynamically linked to Microsoft EXCEL, in that it is able to transfer input and output directly to EXCEL. Parameter values necessary for the model were calculated using ESRI Geographical Information System (GIS) software packages, and then modified in EXCEL to be used by the Powersim model. After the model runs are completed, output is stored in EXCEL and used to create maps in GIS, such as the percentage of total runoff contributed by each portion of the watershed (Figure 4-1).

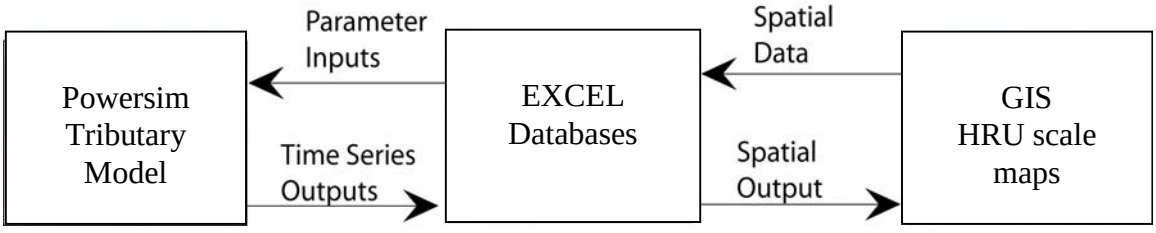

Figure 4-1. Flowchart describing how the software packages interact, with EXCEL acting as the link between GIS and the Powerism model.

4.2.2 Rainfall Processes

The ungaged tributary model attempts to determine the amount of runoff produced by a watershed given a rainfall event. The watershed is comprised of multiple components that account for the physical processes that take place in a watershed. Input of rainfall is first step in the water balance. Due to the scarcity of rainfall data, models often create synthetic rainfall time series to use as forcing. A stochastic rainfall model based on work by Eagleson (1978) is used in this work. It has been widely used in hydrology and geomorphology (e.g., Rodríguez-Iturbe and Eagleson 1987; Tucker and Bras 2000). The stochastic model samples the storm intensity (P), storm duration (D_S), and interstorm duration (D_{IS}) as follows:

$$f(P) = \frac{1}{P_{bar}} e^{(-\frac{P}{P_{bar}})} \tag{4-1}$$

$$f(D_S) = \frac{1}{D_{Sbar}} e^{(-\frac{D_s}{D_{sbar}})} \tag{4-2}$$

$$f(D_{IS}) = \frac{1}{D_{ISbar}} e^{(-\frac{D_{IS}}{D_{ISbar}})} \tag{4-3}$$

Equations 4-4 through 4-6 are the inverted forms of these probability density functions, which are used to calculate the actual values for each storm given a mean value for the month:

$$P = -P_{bar} \ln(P_{rand}) \tag{4-4}$$

$$D_S = - D_{Sbar} \ln(D_{Srand}) \tag{4-5}$$

$$D_{IS} = -D_{ISbar} \ln(D_{ISrand}) \tag{4-6}$$

where P, D_S, and D_{IS} are the calculated precipitation and temperature values for each event and P_{rand}, D_{Srand}, and D_{ISrand} are sampled from a uniform distribution.

Using the mean values for each month, the new value for each event is calculated for each variable. When the sum of the storm and interstorm durations adds up to 30 days (one month), the code terminates for that month. The output of the code will be a set of randomly selected storm events within a month, each with storm intensity, storm duration, and interstorm duration. The three variables for the sequence of all events can be combined to generate a single rainfall time series. The maximum and minimum temperatures for each storm event were calculated in the same manner. A method is also currently being developed by Sandia National Laboratories to produce HRU averaged daily estimates of precipitation and temperature. These estimates are derived from monthly datasets such as PRISM data (Daly 1994).

4.2.3 Rain and Snow Partitioning and Snow Melt

A temperature-based precipitation allocation method was used to partition a portion of the precipitation as snowfall (Federer 1995). When the temperature is below a threshold value, all of the precipitation falls in the form of snow. Similarly, if the upper temperature threshold is exceeded, rain is the exclusive form of precipitation. Equation 4-7 describes the rain-snow partition at temperatures within the threshold values.

$$S_f = \frac{T_b - T_{\min}}{T_{\max} - T_{\min}} \tag{4-7}$$

where S_f is the fraction of precipitation that falls as snow, T_b is the base temperature for snow-rain transition, and T_{min} and T_{max} are the average minimum and maximum temperature for the month. Melting of the snow is based on the degree-day method developed by Martinec et al. (1983).

$$M = M_f \left(T_i - T_b\right) \tag{4-8}$$

where M_f is an empirical melt factor (0.011 ρ_s), T_b is the base temperature, T_i is the index air temperature often set to the mean air temperature, and ρs is the snow density.

4.2.4 Interception

The next step in the water balance for a watershed is rainfall interception by the vegetation canopy in each HRU. The interception rate is the fraction of total rainfall intercepted by leafs in the canopy based on the leaf area index, or *LAI* (Federer 1995). In Equation 4-9, the vegetated area A_{veg} is calculated based on the fraction p_{veg}. Interception occurs only over the vegetated area. The interception capacity of the canopy is calculated in Equation 4-10, where *LAI* is the leaf area index and I_{CL} is the leaf interception capacity. Equation 4-11 describes the rate at which rainfall is intercepted, where F_{IntL} is the fraction of rainfall intercepted by leafs and *R* is the rainfall rate. Finally, the volume of water intercepted during a storm event is determined in Equation 4-12, where p_{Rain} is the percent of the total rainfall that falls over the vegetated area, and *D* is the duration of the event. The un-intercepted volume of water, V_{Unint}, which falls over nonvegetated areas and thus automatically reaches the ground, is the difference between the total precipitation volume and the intercepted volume, calculated in Equation 4-13.

$$A_{veg} = p_{veg} A \tag{4-9}$$

$$I_C = I_{CL} A_{veg} LAI \tag{4-10}$$

$$I_R = F_{IntL} R \cdot LAI \tag{4-11}$$

$$V_{Int} = I_R A_{veg} p_{Rain} D \tag{4-12}$$

$$V_{Un\,int} = V_P - V_{Int} \tag{4-13}$$

The volume of water that is intercepted during an event fills the remaining storage space in the canopy until the interception capacity of the canopy is reached. Once filled, any further input of water to the canopy is released to the ground as throughfall.

4.2.5 Infiltration and Soil Moisture Storage

Rain reaching the soil surface is allocated depending on the state of the hydrologic system. The water balance at the land surface is modeled after the Three-Layer Variable Infiltration Capacity (VIC-3) model of Liang et al. (1994) and Liang and Xie (2001). The VIC-3 model divides a watershed into land cover units based on vegetation type and calculates runoff based on a three-soil-layer infiltration model (see Figure 4-2). The land surface was classified into HRUs. Water that reaches an HRU infiltrates into the first 10-cm layer of the soil, which represents the topsoil. The VIC method partitions the water in the upper layers of the soil column so that the degree of saturation over the HRU area varies spatially. This produces a more realistic estimate of the amount of water produced by saturation excess runoff than would occur using an HRU averaged value of soil moisture. Water that is not lost to saturation excess runoff is then able to infiltrate into the lower layers. However, if the rate that this remaining water infiltrates is greater than the saturated hydraulic conductivity of the soil column, infiltration excess runoff will occur. It is necessary to utilize both mechanisms for runoff generation in order to more accurately depict the potential runoff processes involved.

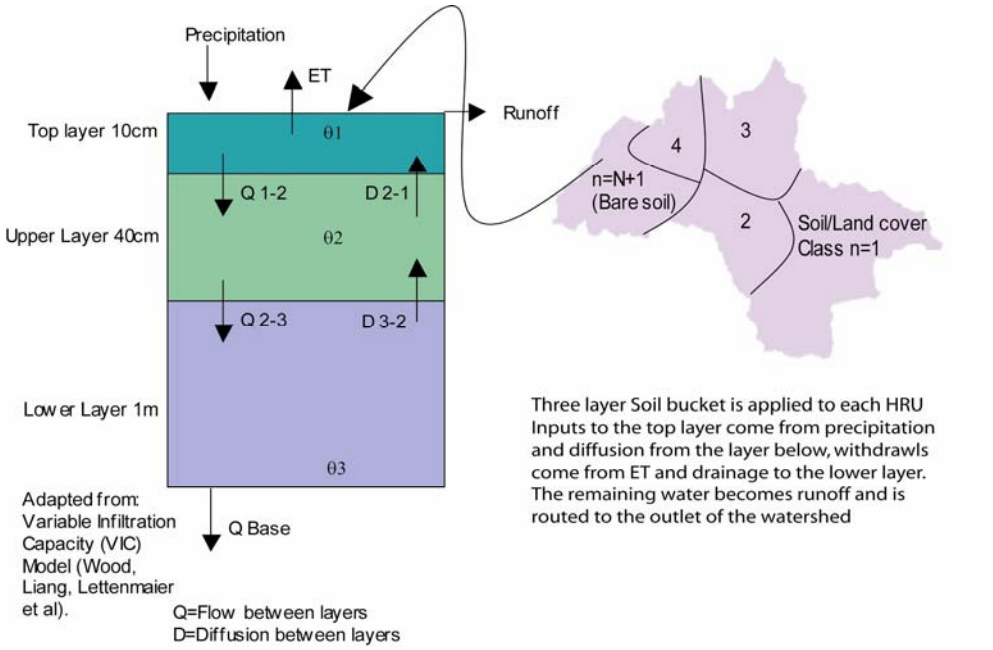

Figure 4-2. Schematic representing the three-soil-layer infiltration model as applied to each HRU in the Río Salado.

The soil column is divided into three layers following the method outlined in the VIC model (Liang and Xie 2001). The first 10 cm allow for a quick response to rainfall events, the second 40 cm act as storage for water to be transpired and moves water to the lower layer, and the final 1 m accounts for long term storage of water and provides drainage to the regional aquifer. Movement of water between layers is calculated using the Brooks Corey equation.

$$Q = AK_s\left(\frac{MLW}{MLW_{\max}}\right)^{\frac{2}{B_p}+3} \tag{4-14}$$

where Q is the flow rate between layers, A is the HRU area, K_s is the saturated hydraulic conductivity, MLW is the difference between the current soil moisture value and the residual soil moisture, $MLW_{\max}$ is the difference between the maximum soil moisture and the residual, and B_o is the pore size distribution index (Liang et al. 1994).

4.2.6 Evapotranspiration

As the soil layer fills, water can either drain to the lower layers, evaporate directly from the soil, or be transpired by vegetation. Evapotranspiration from the first layer is fashioned after the Hargreaves ET model (Hargreaves 1975; Hargreaves et al. 1985; Hargreaves et al. 2003). The maximum monthly potential ET is calculated based on the amount of incoming solar radiation and the monthly air temperature values (max, min, mean).

The potential ET rate is calculated each month in the model. A monthly time series of air temperature is needed as input. Equation 4-15 is an example of the Hargreaves equation, where T_{avg} is the average monthly air temperature. The difference between max and min monthly temperature is calculated in Equation 4-16. An example of an ET time series can be seen in Figure 4-3. The calculation of incoming solar radiation, Equation 4-17, is based on Bras (1990).

$$E_H = 0.0023\left(S_o\left(T_{avg}+17.8\right)\right)T_R^{\,0.50} \tag{4-15}$$

$$\mathrm{T_R} = \mathrm{T_{max}} - \mathrm{T_{min}} \tag{4-16}$$

$$S_o = 15.392r(W_s\sin(\phi)\sin(\theta)+\cos(\phi)\cos(\theta)\sin(W_s)) \tag{4-17}$$

$$r = 1+0.033\cos(\frac{2\pi JD}{365}) \tag{4-18}$$

$$W_s = a\cos(-\tan(\phi)\tan(\theta)) \tag{4-19}$$

$$\theta = 0.4093\sin(\frac{2\pi JD}{365}-1.405) \tag{4-20}$$

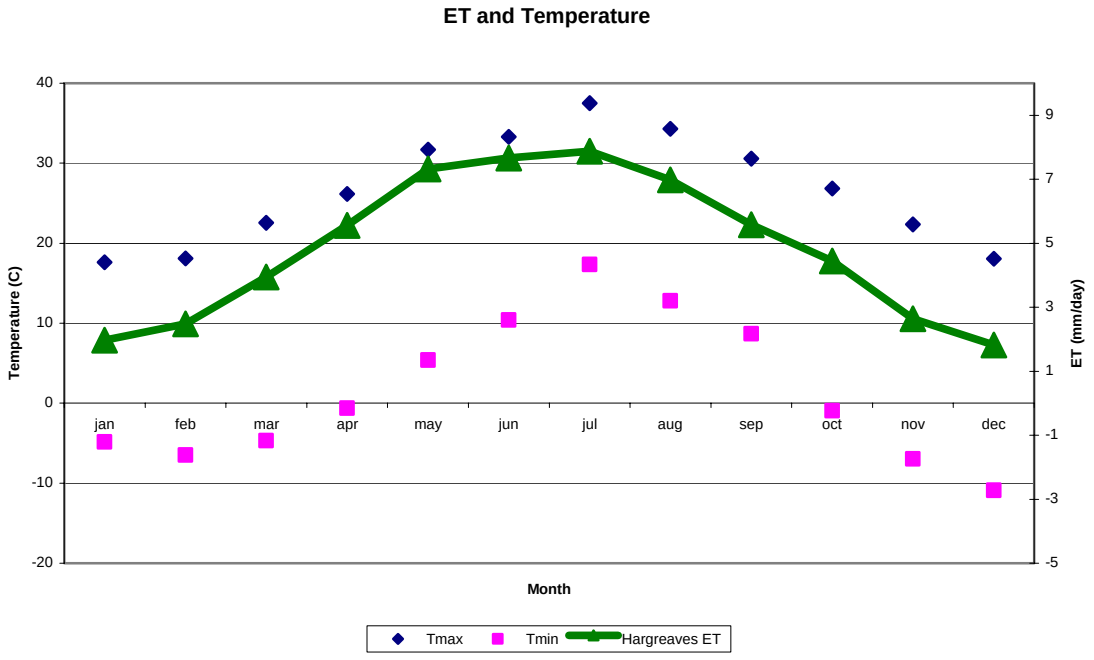

Figure 4-3. A single-year estimate of evapotranspiration based on monthly maximum and minimum air temperature measurements, using the Hargreaves method.

where r is the ratio of the actual Earth-Sun distance to the mean Earth-Sun distance, W_s is the sunset hour angle in radians, ϕ is the Latitude in radians, θ is the solar declination angle in radians, and JD is the Julian day.

4.2.7 Routing

The runoff produced by an HRU is routed directly to the outlet. The time required for a runoff pulse to reach the watershed outlet is determined based on the Manning equation and the travel distance to the outlet. First, the slope to the outlet is calculated for each HRU based on the average differences in elevation and length. A time lag (T_L) is introduced due to the roughness of the channel, as shown in the following equation:

$$T_L = \frac{L_{out}}{\frac{1}{n} d^{\frac{2}{3}} S^{\frac{1}{2}}} \tag{4-21}$$

where L_{out} is the average distance to the watershed outlet, n is Manning's roughness coefficient, d is the depth of water in the channel, and S is the slope of the channel. Variables required in this calculation such as the slope and the distance to the outlet are obtained from the GIS processing of the HRUs and topographic field.

4.2.8 Geographical Information Systems

In order to acquire input parameters for the Powersim model, preprocessing was performed using the ArcHydro toolbar in ArcMap, an ESRI GIS software package. The HRUs for the Río Salado were created in ArcMap presented in a graphical manner in Figure 4-4. Soil and vegetation classes are overlain to form the HRU distribution and then important parameter information is stored in an EXCEL spreadsheet. The original soils map was created from the NM STATSGO Soil Classes data, while the vegetation map was created from the National Land Cover Data for NM. Both datasets can be located on the University of New Mexico's RGIS database website.

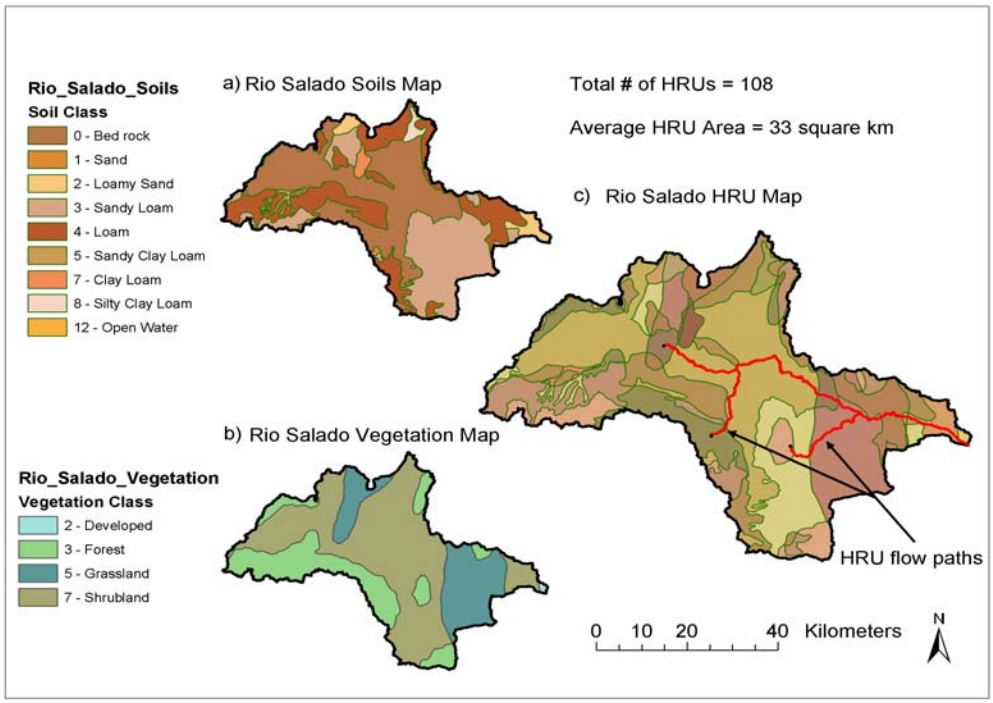

Figure 4-4. GIS processing to reclassify soil and vegetation maps, which combined produce an HRU map. Note in c) the flow paths to the basin outlet for three of the HRUs are shown.

4.3 Application and Results

This study focuses on the Río Salado, a semi-arid watershed located in central New Mexico. The basin covers 3,500 km^2 and has an average annual rainfall of about 400 mm (Simcox 1983; Vigerstøl 2003). The Río Salado was selected because of its location in the Middle Río Grande study area (Figure 4-5, upper left corner) and because of its semi-arid nature (Caylor et al. 2005). Although the Río Salado does not contribute much flow to the Río Grande, it does contribute a great deal of sediment (Simcox 1983). The ability to predict future flow rates in the Río Salado may aid in predicting sediment loading as well. It is also interesting because it provides an example of both a gaged and ungaged basin depending on the time period studied. A stream gage located near the outlet to the Río Grande recorded hourly measurements from 1947 to 1984. In addition, rain gages with records of varying lengths can also be found within the study area (Figure 4-5). The datasets from these gages will be used to calibrate the model and assess its performance.

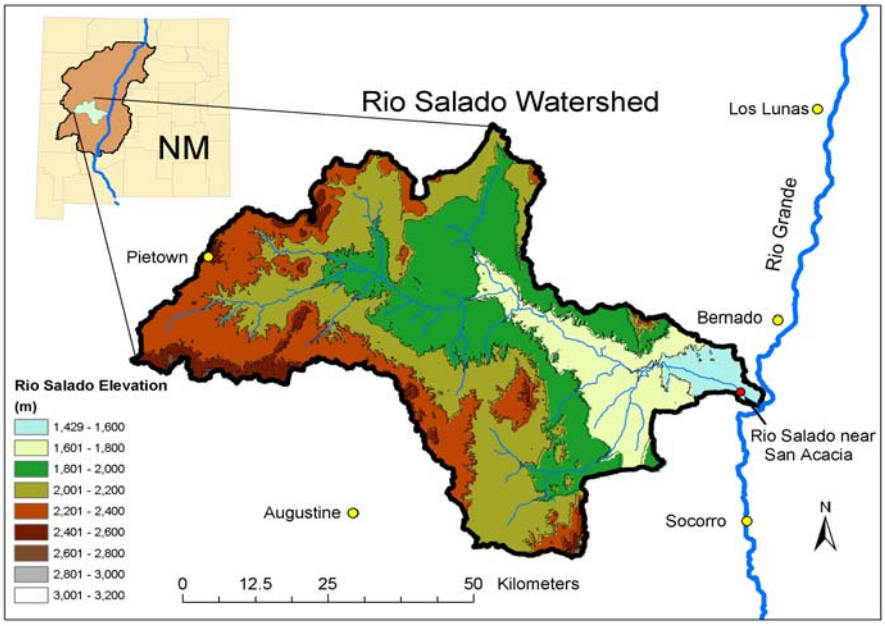

Figure 4-5. Río Salado watershed location in the state of New Mexico. The colors on the watershed are 200-m elevation contours. Rain gages are shown in yellow and the stream gage near the outlet to the Río Grande is shown in red.

Setting up the model for its initial run on the Río Salado required the collection of soil and vegetation parameters for each HRU and creation of a parameter database. Soil parameters in the model, such as hydraulic conductivity and porosity, were based on values from Clapp and Hornberger (1978). The necessary vegetation parameters were obtained from tables found in two sources: LAI values (Federer 1996) and other plant parameters such as interception capacity (Breuer et al. 2003). The mean monthly air temperature data, used to stochastically generate event temperatures, were derived from daily values collected at the Red Tank site for 2003. Red Tank is located within the Río Salado watershed just northwest of the outlet, in a juniper shrubland.

The model was set up to run for over the historical period of record for the Río Salado stream gage, 1947 to 1984. A comparison of the modeled runoff time series to the historical gage data can be seen in Figure 4-6. The total calculated runoff volume from the model data is approximately 4.7 million cubic meters of water, considerably greater than the 2.3 million cubic meters measured by the stream gage. It is possible that this is due to an overestimation of streamflow during winter months and the model's current inability to simulate extended drought periods such as those in the late 1940s and late 1970s. Application of rainfall uniformly over each HRU may also be contributing to the runoff overestimation. The use of PRISM rainfall data as model input should improve these results by restricting rainfall to areas with positive radar precipitation values.

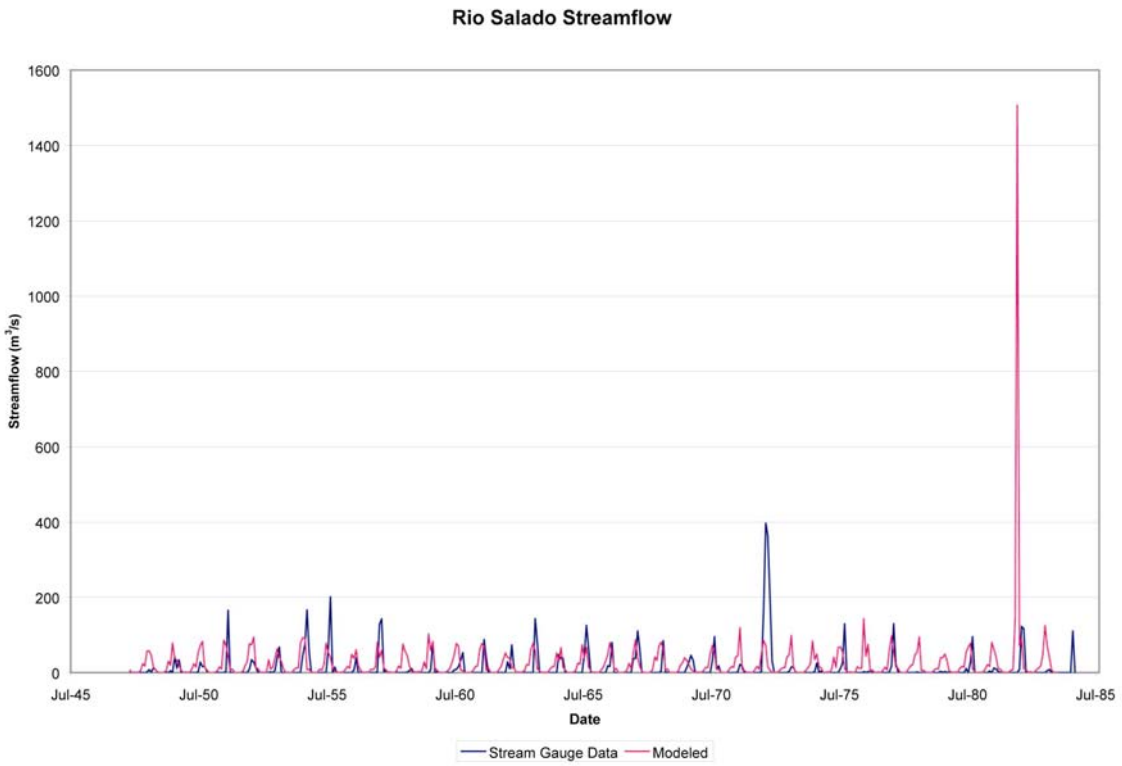

Figure 4-6. Monthly averaged historical streamflow on the Río Salado versus the semi-distributed model output of monthly runoff.

Figure 4-7 illustrates an example of spatial output from the model. It is important to note that the percentage of the total runoff contributed by each HRU shows that very few HRUs are responsible for the amount of runoff that reaches the river. In this simulation, three HRUs contribute over 65 percent of the total runoff. The average response time for storms in this simulation is 16 hours, because the HRUs that produce runoff are located a large distance (60–100 km) from the basin outlet.

4.4 Conclusions

The output from the model is very encouraging because the watershed seems to respond realistically to the synthetic rainfall that is applied, when examining the timing and magnitude of the runoff pulses. The results seem reasonable even though the model still requires further calibration. Improvements will include new parameter values that better represent the actual conditions in the Río Salado. Once the model has been shown to accurately simulate the Río Salado, it will be tested in another instrumented basin such as the Río Puerco to see which parameter values are transferable and which will need to be calibrated to each watershed. Finally, it will be applied to the remaining watersheds in the middle Río Grande Basin to estimate the ungaged additions to monthly flow in the river. The usefulness of this model for real-time decision-making will require pre-processing to set up the model before use with stakeholders.

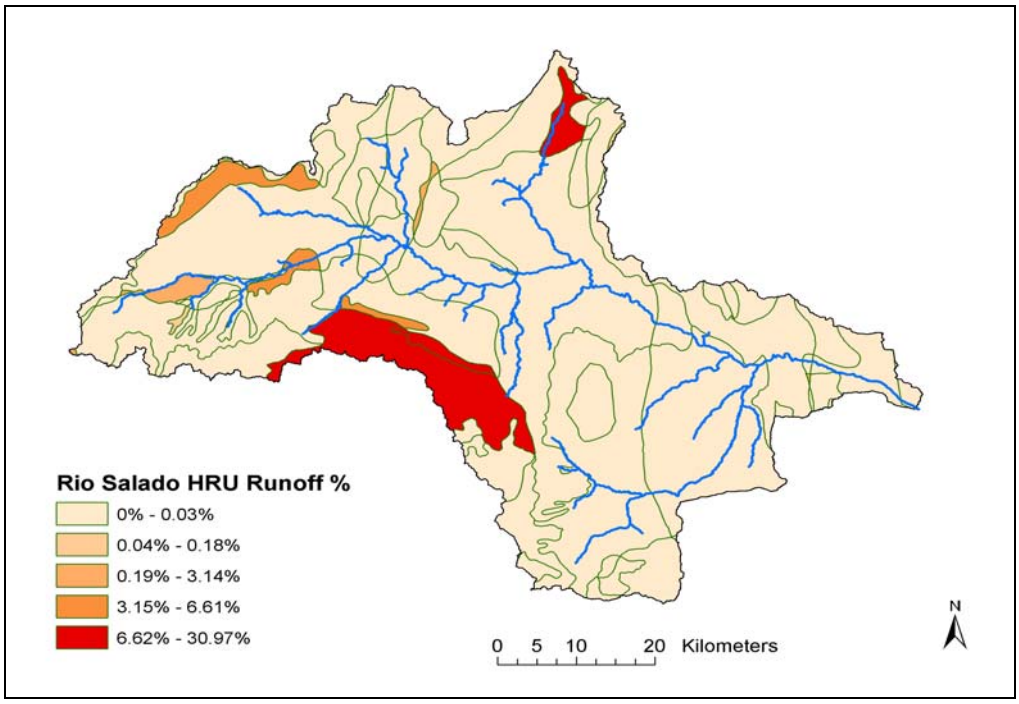

Figure 4-7. Spatial map of the percentage of the total runoff contributed by each HRU. Note that a majority of the runoff is produced by three HRUs, while the remainder of the watershed produces little to no runoff.

5. WATER QUALITY PROCESS MODULES

Heather F. Hallett, New Mexico Institute of Mining and Technology

5.1 Introduction

5.1.1 Background and Motivation

Salinization of rivers is a problem in the southwestern United States as well as in other semiarid and arid regions of the world (Postel 1999). Arid and semiarid rivers often exhibit increasing salinity with distance downstream, which is often attributed to irrigated agriculture (Lippincott 1939). Increased river salinity causes economic losses by reducing crop productivity, rendering the water unsuitable for many municipal and industrial uses, and corroding or plugging pipes (Postel 1999). Irrigated agriculture provides about 40% of the world's food crops, much of which are grown in water-stressed river basins such as the Indus, Nile, Rio Grande, Tigris-Euphrates, and Orange (Johnson 2001). Therefore, it is important to understand the causes of salinization in order to protect both agriculture and industry in arid and semiarid river basins.

Early Rio Grande studies agreed that salinity in the Rio Grande increases with distance downstream (Figure 5-1). Data from early studies consistently showed an increase in chloride concentration and chloride burden with distance in the river, on average increasing from less than 10 mg L^{-1} at the headwaters to several hundred mg L^{-1} at Ft. Quitman, TX. The consistency of the results from studies conducted over the last 100 years implies that a constant, ongoing process has been responsible for increasing salinity in the Rio Grande over the past century. Some of the earliest studies (Lippincott 1939) attributed the salinization of the Rio Grande to evaporative concentration due to irrigated agriculture and reservoir storage. Other early studies suggested flushing of soil salts by agricultural drains could be responsible for increasing salinity in the river (NRC 1938; Wilcox 1957; Trock et al. 1978). Recent studies have presented the theory that a significant portion of the salinization of the Rio Grande is geologically controlled and can be ascribed to localized deep brine fluxes controlled by geologic structures and geothermal activity (Phillips et al. 2003; Mills 2003).

5.1.2 Objectives

Rio Grande discharge and upstream chloride burden are highly transient, which renders calculation of chloride additions quite difficult. A model was therefore designed in the system dynamics software "Powersim Studio" to simulate the solute history of the Rio Grande over the past 30 years with the goal of quantifying the additions of chloride to the river from deep brine sources over this time period. This chapter will first describe a water-and-chloride mass-balance model built for Elephant Butte Reservoir, and then detail how the concepts used in this reservoir model were extended to model the rest of the river. Also included is a description of how the Rio Grande chloride model was extended to simulate bromide in the river.

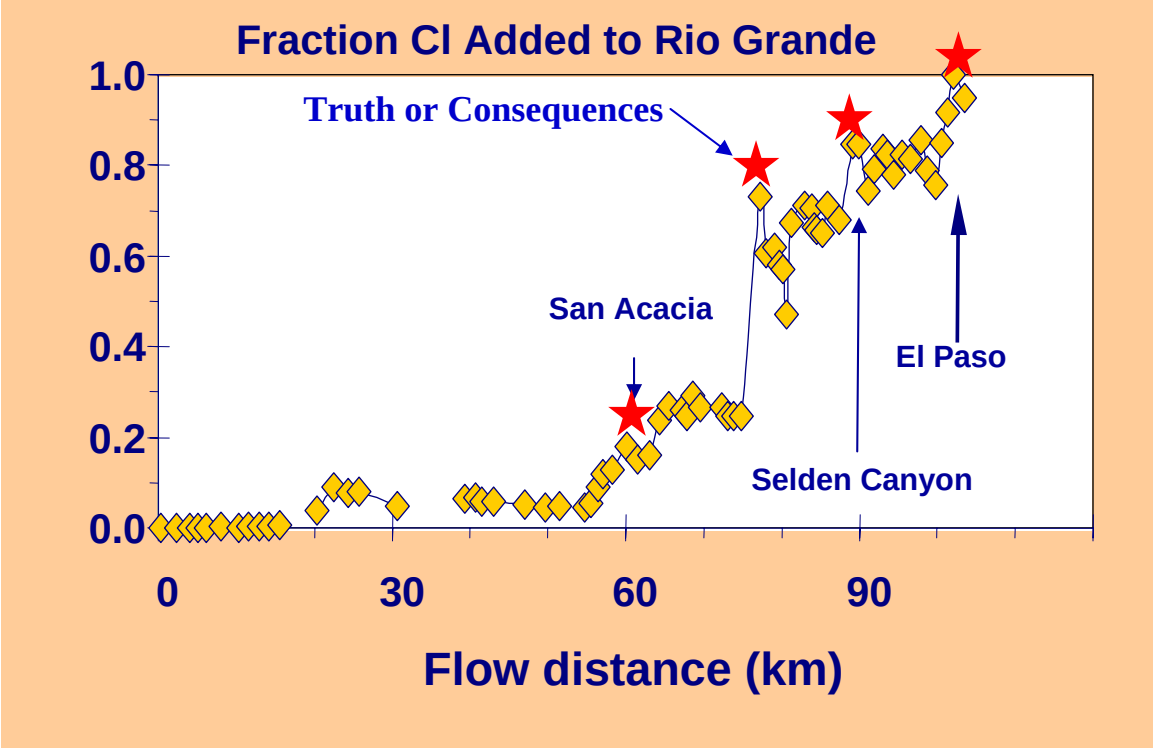

Figure 5-1. Fraction of total chloride added to the Rio Grande with distance downstream from the headwaters. Stars indicate locations of termini of sedimentary basins. From Mills (2003).

Although the salinity model described here is specific to the Rio Grande, it is structured in a generic fashion to allow application to most any river system. Additionally, the basic framework described is capable of modeling any conservative solute (such as bromide, which also is addressed in this chapter). Specifically, application to other river systems is possible through structuring the generic hydrology and geochemistry modules to represent the system of interest and then parameterizing the modules through calibration to available data. Multiple solute species can be modeled by simply representing module input/output as vectors dimensioned to the desired list of ions.

5.2 Modeling the Chloride Balance for Elephant Butte Reservoir

Chloride and water storage in Elephant Butte Reservoir was simulated by a model developed in Powersim in order to explore the effects of bank storage on the water and chloride mass balance. The system was modeled as two volumes, one to represent storage in the reservoir and another to represent bank storage, separated by a theoretical barrier of a given conductivity and width (Figure 5-2). When water is added to or withdrawn from the volume representing the reservoir, the model uses Darcy's Law to calculate the flow rate and direction between the reservoir storage and bank storage for each timestep. This calculation involves one term each for hydraulic conductivity of the aquifer material, the contact area between the reservoir and the bank storage volumes, the head difference between reservoir storage and the bank storage, and a length term that represents the width of a theoretical barrier between the reservoir storage and bank storage.

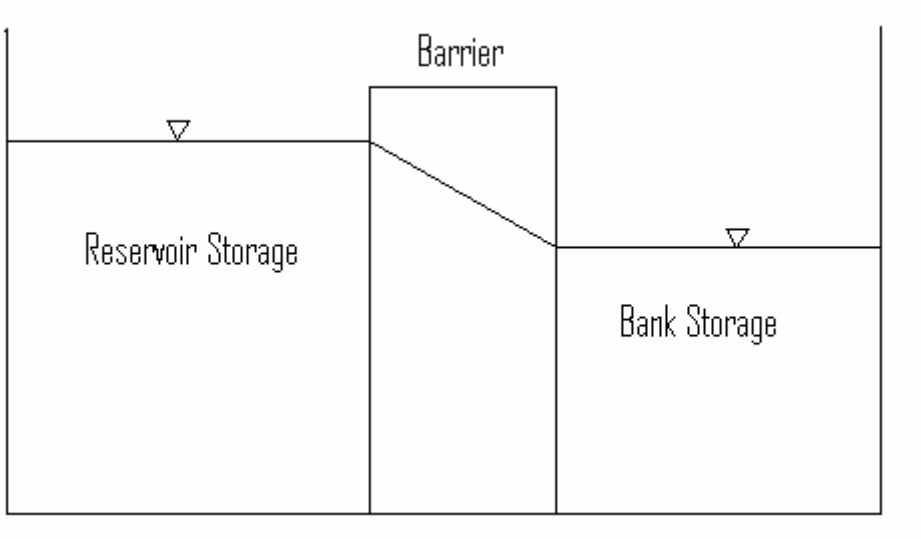

Figure 5-2. Schematic diagram illustrating how the bank storage model of Elephant Butte Reservoir works. The system was modeled as two volumes representing storage in the reservoir and bank storage, separated by a theoretical barrier of unknown conductivity and width. The figure shows a period of increasing reservoir level; therefore, some of the water being added to the reservoir will be lost temporarily to bank storage. Using Darcy's Law, the model calculates the flow rate and direction between the reservoir storage and bank storage for each timestep. Volume and chloride concentration of inflows and outflow are constrained as well as pan evaporation and precipitation. The model then uses the inputs and outputs to calculate the volume of water and mass of chloride in the reservoir for each timestep.

Other inflows and outflows include inflow to the reservoir from the river and from the Low Flow Conveyance Channel (LFCC), outflow from the dam, and evaporation from the surface of the reservoir (see Chapter 2). In order to simulate the chloride balance in the reservoir, the inflows and outflows are multiplied by a chloride concentration to obtain a mass flux of chloride (Figure 5-3). These mass fluxes of chloride into and out of the reservoir and bank storage are integrated by Powersim to calculate the mass of chloride in each of these volumes for each timestep.

5.2.1 Constrained Parameters

Discharge data were available for San Marcial (both the main stem Rio Grande and the LFCC) and below Elephant Butte Dam for 1950 to 2004 from the United States Geological Survey (USGS). Chloride concentration data were also available for the Rio Grande at San Marcial and below Elephant Butte Dam as well as for the LFCC for 1950 to 2004; however, chloride concentration data were missing for the station below Elephant Butte Dam between January 1964 and June 1975. Chloride data were estimated for the last 8 years of the record using semiannual field data collected as part of this project. Additionally, pan evaporation data were available for Elephant Butte Dam for 1950 to 2004 from the United States Bureau of Reclamation (BoR) and the length of the reservoir was estimated to be 39 km.

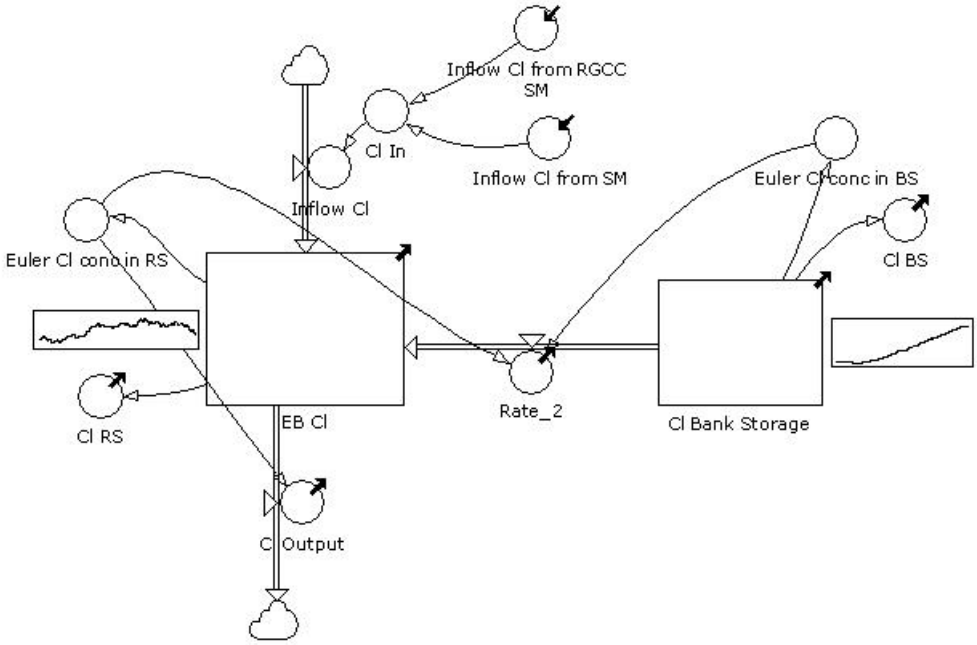

Figure 5-3. Chloride balance model of Elephant Butte Reservoir in Powersim.

5.2.2 Tuned Parameters

The hydraulic conductivity and width of the theoretical barrier between the reservoir volume and the bank storage volume were treated as unknowns in the model. For convenience, these two terms were combined in the constant named "coefficient for conductivity and thickness of barrier." The width of the bank storage volume was also a tuned parameter in the model. Finally, the pan coefficient used to calculate reservoir evaporation from pan evaporation was treated as an unknown, rather than using the pan coefficient of 0.7 used by the BoR, which is an average pan coefficient for the nation, but not specific to the region. Values for these parameters were estimated by model optimization.

5.2.3 Model Assumptions

The design of the model uses a few simplifying assumptions. The first of these assumptions is that the chloride concentration of the water in the reservoir is equal to that of the Rio Grande where it is sampled below the dam. In the chloride model, the chloride concentration of the reservoir (Cl RS) is used to calculate the chloride outflow (Cl Output). This assumes that the reservoir is well-mixed and that the Cl concentration of the water being released at the dam is representative of the well-mixed reservoir. Secondly, the model assumes that the only sources of chloride in the system are the river and conveyance channel inputs and interaction with bank storage. This ignores the possibility of chloride input from groundwater sources other than bank storage, such as hot springs or other geothermal groundwater sources, which could be present in the area. The validity of these assumptions is examined below.

5.2.4 Calibration of Tuned Parameters

An optimization study was performed to obtain estimates for the unknown parameters in the model including the conductivity of the aquifer medium, the width of the theoretical barrier, the horizontal width of the bank storage volume and also the pan coefficient used by the model to calculate evaporation from pan evaporation data. The calibration terms were varied over a reasonable range and optimized by minimizing the square of the errors in both reservoir volume and mass of chloride stored in the reservoir.

The conductivity of the aquifer medium and the width of the theoretical barrier were combined into one term ("coefficient for conductivity and thickness of barrier"). This term represents the conductivity of the aquifer medium divided by the thickness of the barrier, as in Darcy's Law:

$$Q = -K \times A \times dh/dl \qquad (5\text{-}1)$$

where here Q represents flow between bank storage and reservoir storage, K is the hydraulic conductivity of the theoretical barrier between reservoir and bank storage, dl is the width of this theoretical barrier, dh is the head gradient between reservoir and bank storage, and A is the head in bank storage multiplied by estimated length of the reservoir.

The "coefficient for conductivity and thickness of barrier" term was varied between 0, 1×10^{-10}, 1×10^{-9}, and 1×10^{-8} s^{-1}, with 0 simulating no flow between the reservoir and bank storage and 1×10^{-8} s^{-1} representing a hydraulic conductivity of 1×10^{-8} m s^{-1} divided by a thickness of 1 meter. Given that 1^{-8} m s^{-1} is a reasonable conductivity for the Santa Fe group and assuming that the thickness of the theoretical barrier is at least 1 m, 1×10^{-8} s^{-1} is the maximum assumed value for the coefficient term.

The horizontal width of the bank storage volume was varied between 0 and 10,000 m during the optimization study. A width of 0 represents no bank storage and a width of 10,000 m represents a bank storage volume that is more than 100 percent of the reservoir volume for any given surface elevation.

The pan evaporation coefficient was varied in the optimization study between 0.64 and 0.74, which is an average range for pan coefficients in the southwestern United States (Dingman 2001).

5.2.5 Results of Model Optimization

Each of these parameters was varied over the ranges specified while holding the other parameters constant. To analyze the success of the results, the volume of water and mass of chloride in the reservoir were compared to historical values and the squares of the errors were computed. Each parameter was varied systematically to test all combinations of values. The squares of the errors between model results and historical data (difference between modeled and historical squared) were then computed and averaged over the simulation period. An optimized set of values was chosen based on which simulation resulted in the lowest average square of the error.

Instead of comparing modeled reservoir chloride storage to historical storage the mass of chloride in reservoir storage was added to the mass of chloride in bank storage to get a total mass of chloride in the system. The initial total mass of chloride in the system for the simulation was subtracted from the total mass of chloride in the system for each month to obtain the chloride mass excess for each month:

$$E = (Cl_R+Cl_{BS})-(Cl_R+Cl_{BS})_I \quad (5\text{-}2)$$

where:

E = modeled mass excess of chloride for each month,
(Cl_R+Cl_{BR}) = mass of chloride in the reservoir + mass of chloride in bank storage for each month, and
$(Cl_R+Cl_{BR})_i$ = initial mass of chloride in the reservoir + mass of chloride in bank storage for each month at the beginning of the simulation.

The chloride mass excess was also calculated for the actual data by differencing the mass of chloride flowing into the reservoir (from the main-stem Rio Grande and the conveyance channel) and mass of chloride flowing out of the reservoir (at the gaging station below the dam) for each month and summing these imbalances to obtain the cumulative mass excess over the simulation period:

$$E = (Q_{SM} \times Cl_{SM}+Q_{LFCC} \times Cl_{LFCC})-(Q_{out} \times Cl_{out}) \quad (5\text{-}3)$$

where:

E = mass excess of chloride for each month of historical record,
Q_{SM} = discharge into the reservoir from the river at San Marcial gaging station,
Q_{LFCC} = discharge into the reservoir from LFCC gage at San Marcial,
Q_{out} = discharge from Elephant Butte Dam,
Cl_{SM} = chloride concentration of river at San Marcial,
Cl_{LFCC} = chloride concentration of LFCC, and
Cl_{out} = chloride concentration of river below Elephant Butte Dam.

Enough data were available for inputs and outputs to run the model from December 1951 to April 2004; however, chloride concentration data were not available for the station below Elephant Butte Dam from January 1964 to June 1975, so the model results could not be compared with the historical data for this time range. Therefore, the model was run separately for two time periods, one from 1951 to 1963 and the other from 1975 to 2004, and compared independently with the historical data from the corresponding time periods.

5.2.6 Conclusions from the Elephant Butte Reservoir Model

From the optimization study, the best fit to both the historical Cl data and the historical reservoir storage record was obtained using no bank storage and a pan coefficient of 0.64. Using bank storage, the best fit to the data was obtained using conductivity of 1^{-8} m s^{-1}, a bank storage width of 7,500 m, and a pan coefficient of 0.64; however, the fit to the data using no bank storage was better. The fit of the chloride model results to the first 13 years of data (1951–1963) (Figures 5-4 and 5-5) was not as good as the fit of the last 29 years (1975–2004) (Figure 5-6 and 5-7). The reservoir was at a much lower level on average from 1951 to 1979 than from 1979 to 2004. The reservoir system may have acted differently during the later time period due to different inputs and outputs of chloride or other differences in the hydrologic system when the reservoir level was higher. This may account for why the model results did not fit the data as well for the 1951–1963 time period.

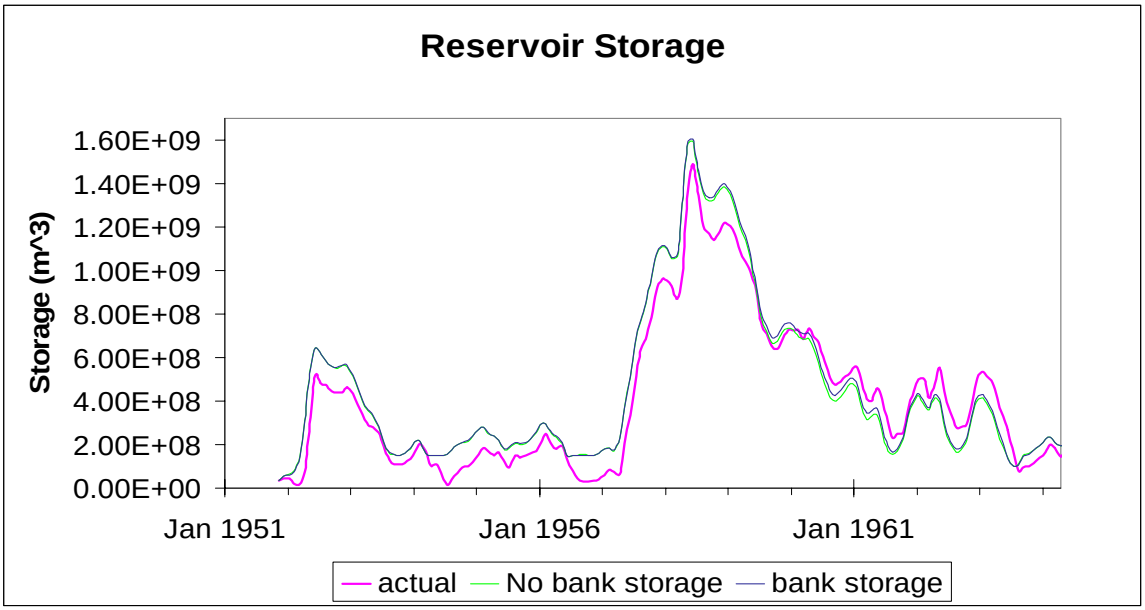

Figure 5-4. Modeled and historical Elephant Butte Reservoir storage for 1951 to 1964.

There is not much difference between the model results with bank storage and without for this time period. Bank storage simulation had pan evaporation coefficient of 0.6, width of barrier 7,500 m, and coefficient for conductivity and width of barrier of $1 \times 10^{-8} s^{-1}$. No bank storage had pan evaporation coefficient of 0.64. The simulation period was December 1951 to May 1964.

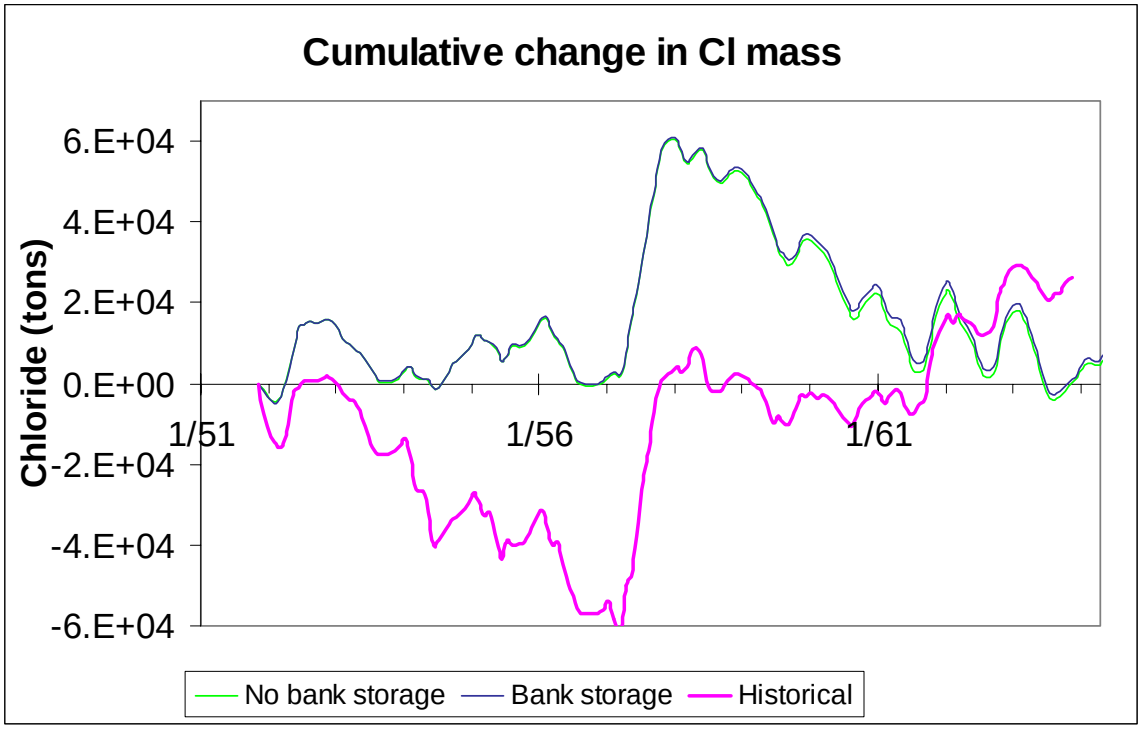

Figure 5-5. Modeled and historical mass excess of chloride for 1951 to 1964. The model is not successful at modeling chloride in Elephant Butte Reservoir for this period. Storage in the reservoir was low during this period and there may have been differences in the inputs and outputs of chloride for which the model is not accounting. The simulation with bank storage was run with a pan coefficient of 0.6, a width of 7,500 m, and a coefficient for conductivity and width of barrier of 1 $\times 10^{-8}$ s^{-1}. The simulation with no bank storage was run with a pan coefficient of 0.64. The simulation period was December 1951 to May 1964.

The model adequately simulated reservoir storage using no bank storage from 1979 up until about late 1993 when the model started to underestimate storage (Figure 5-7). The model results for the chloride mass excess from 1979 to 2004 also matched the data well up until late 1993, when the chloride mass excess from the data dropped below zero, meaning that more chloride was leaving the reservoir than had entered the reservoir during this time period (Figure 5-7). Since these errors begin at about the same time in the model simulation (Figure 5-8), this suggests that there is a source of saline water to the reservoir, which cannot be accounted for by bank storage, starting in about late 1993, that is not represented in the model. A possible explanation for these results could be inflow of saline groundwater to the reservoir. It is possible that saline groundwater is held back by high hydraulic head in the reservoir when the reservoir storage is high and then flows into the reservoir when the reservoir storage drops. This would explain the inflow of saline water during the 1993 to 2004 time period when the reservoir level was dropping. If this is the cause of the discrepancy, the saline water is probably of fairly high concentration. The fact that over most of the simulated reservoir history the historical data are best matched by a no-bank-storage simulation implies that the hydraulic conductivity and/or volume of any aquifer in connection with the lake must be low. Thus, to significantly influence the salt balance at the end of the period simulated, the concentration of water entering during that period must be high.

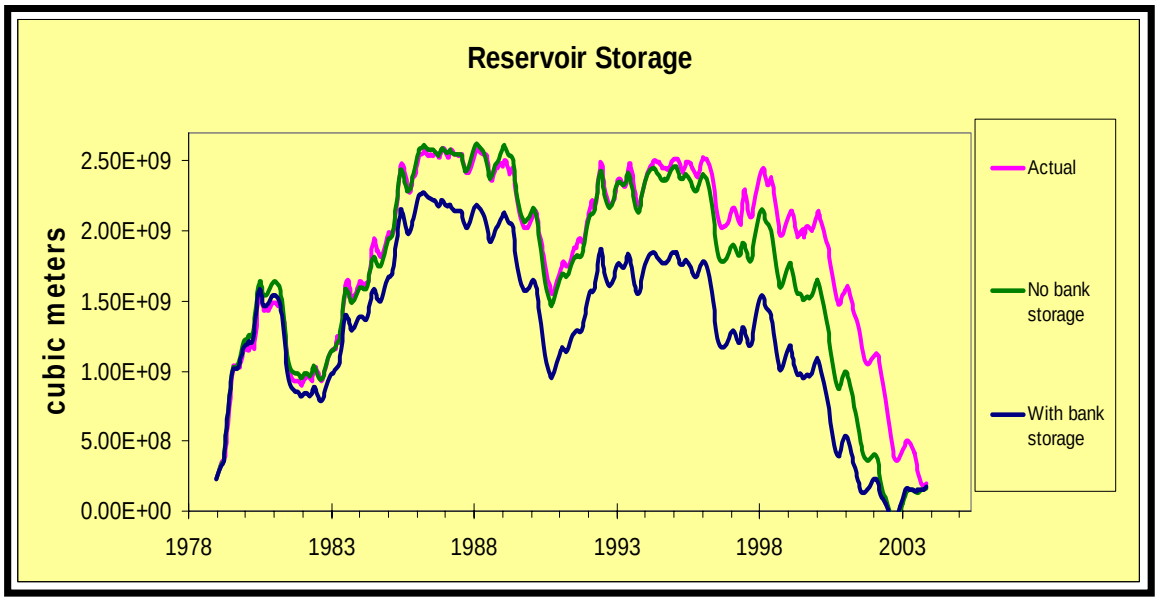

Figure 5-6. Modeled Elephant Butte Reservoir storage compared with historical data for model simulations with bank storage and without bank storage. Model run without bank storage gives a better match to historical data indicating that bank storage does not play a major role in the water balance of the reservoir. Simulation with bank storage was run with a pan evaporation coefficient of 0.64, a width of 10,000 m, and coefficient for conductivity and width of barrier of 1 $\times 10^{-7}$ s^{-1}. Simulation with no bank storage was run with a pan coefficient of 0.64. The simulation period was January 1979 to November 2003.

5.3 Modeling the Chloride Balance for the Rio Grande

Water quality modeling begins with a solid model of the hydrology. Description of the surface and groundwater model of the upper Rio Grande is given in Chapters 2 and 3. For purposes of this analysis, the aforementioned hydrology model was extended to the lower Rio Grande Basin (below Elephant Butte), as described below.

5.3.1 Lower Rio Grande Water-Balance Model

The lower Rio Grande model was divided into four reaches: Elephant Butte Dam to Caballo, Caballo to Leasburg (see Figure 5-9), Leasburg to Mesilla, and Mesilla to El Paso. The design of this model is very similar to that of the middle Rio Grande; however, the lower Rio Grande uses a much simplified groundwater model and a different method for calculating leakage from the river.

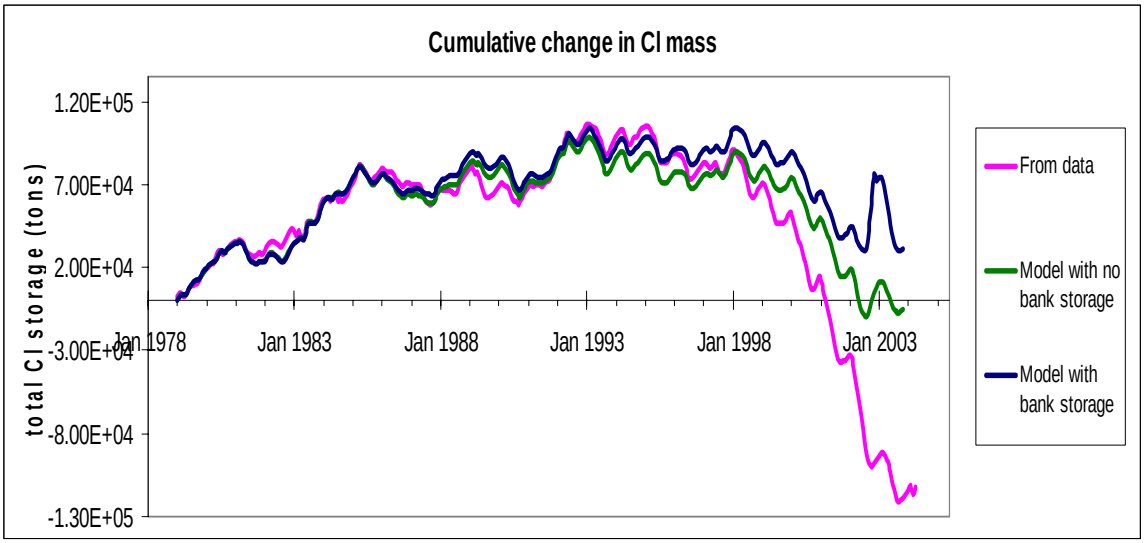

Figure 5-7. Cumulative change in mass of chloride in Elephant Butte Reservoir over the simulation period compared with historical cumulative change in chloride mass. Historical storage was estimated using chloride concentration at Elephant Butte Dam. The model simulation using no bank storage gives a better match to the estimated historical chloride storage, suggesting that bank storage does not play a major role in the chloride balance of Elephant Butte Reservoir. The drop in historical chloride storage after 2001 indicates that more chloride left the reservoir than entered the reservoir between 1979 and 2004; therefore there is a source of chloride in the reservoir. Simulation with bank storage was run with a pan evaporation coefficient of 0.64, a width of 10,000 m, and coefficient for conductivity and width of barrier of 1 $\times 10^{-7}$ s^{-1}. Simulation with no bank storage was run with a pan coefficient of 0.64. The simulation period was January 1979 to November 2003.

River leakage and evaporation from the surface of the river in the lower Rio Grande were used as calibration variables. Leakage from the river was set to be proportional to the diversions for each reach so that river leakage is highest when diversions are low (Table 5-1). These two variables were then tuned for each reach to give the best match to USGS historical river discharge at the end of the reach and also to ensure that the groundwater volume for each reach remained relatively constant over the calibration period, so that groundwater was neither a source nor a sink for water. This calibration was done in reach calibration mode, meaning that inflow at the top of each reach is equal to historical USGS discharge data. One variable at a time was then systematically varied for each reach to obtain the best match to the historical USGS discharge data at the bottom of the reach. The model results were more sensitive to the evaporation term than the leakage term. For example, in the reach between Caballo and Leasburg, increasing the evaporation term by 50% resulted in a 9% decrease in river discharge on average over the calibration period, whereas increasing leakage in this reach by 50% resulted in only a 3% average decrease in river discharge over the same time period. Figure 5-10 shows modeled discharge at El Paso compared with historical discharge before and after calibration. Model calibration resulted in a much better match of high and low flows to the historical record.

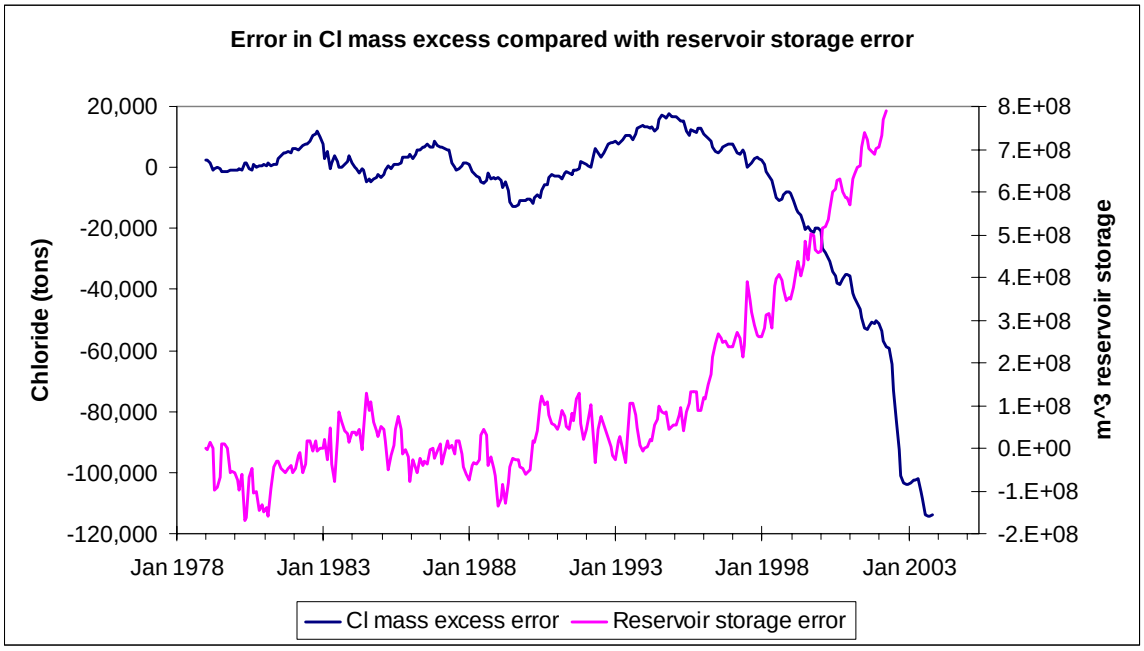

Figure 5-8. Error in mass excess of chloride and error in reservoir storage from Elephant Butte Reservoir model for 1979 to 2004. The mass excess of chloride starts to decrease in late 1993. At about the same time, the reservoir storage error starts to increase. This suggests that there is a source of saline water to the reservoir that appears in the record in late 1993 that is not represented in the model.

The groundwater model for the lower Rio Grande consists of a shallow aquifer model only, which was divided into three sections with a level to represent each section. There is no flow between the aquifer levels for different reaches, only flow between the aquifer and river and between the aquifer and the agricultural conveyance system. The first aquifer level represents the shallow aquifer between Elephant Butte Dam to Caballo Dam (RG12). It is assumed that Caballo Reservoir creates a natural barrier to groundwater flow and that no shallow aquifer water flows past it, so this portion of the shallow aquifer is assumed to be self-contained. The next aquifer level represents the shallow aquifer between Caballo Dam and Leasburg (RG13). This section of aquifer is also assumed to be self-contained, with the narrowing of the river channel at Selden Canyon acting as a natural barrier to groundwater flow. The final aquifer level represents the shallow aquifer between Leasburg and El Paso (RG14 and RG15). Narrowing of the river channel at the El Paso Narrows (just south of El Paso) is assumed to act as a natural barrier to groundwater flow here. Therefore, reaches RG14 and RG15 (Leasburg to Mesilla and Mesilla to El Paso) were lumped together in the groundwater model. Each aquifer level was started with a volume that was reasonable for the length of the reach compared with the starting volumes of the middle Rio Grande aquifer model.

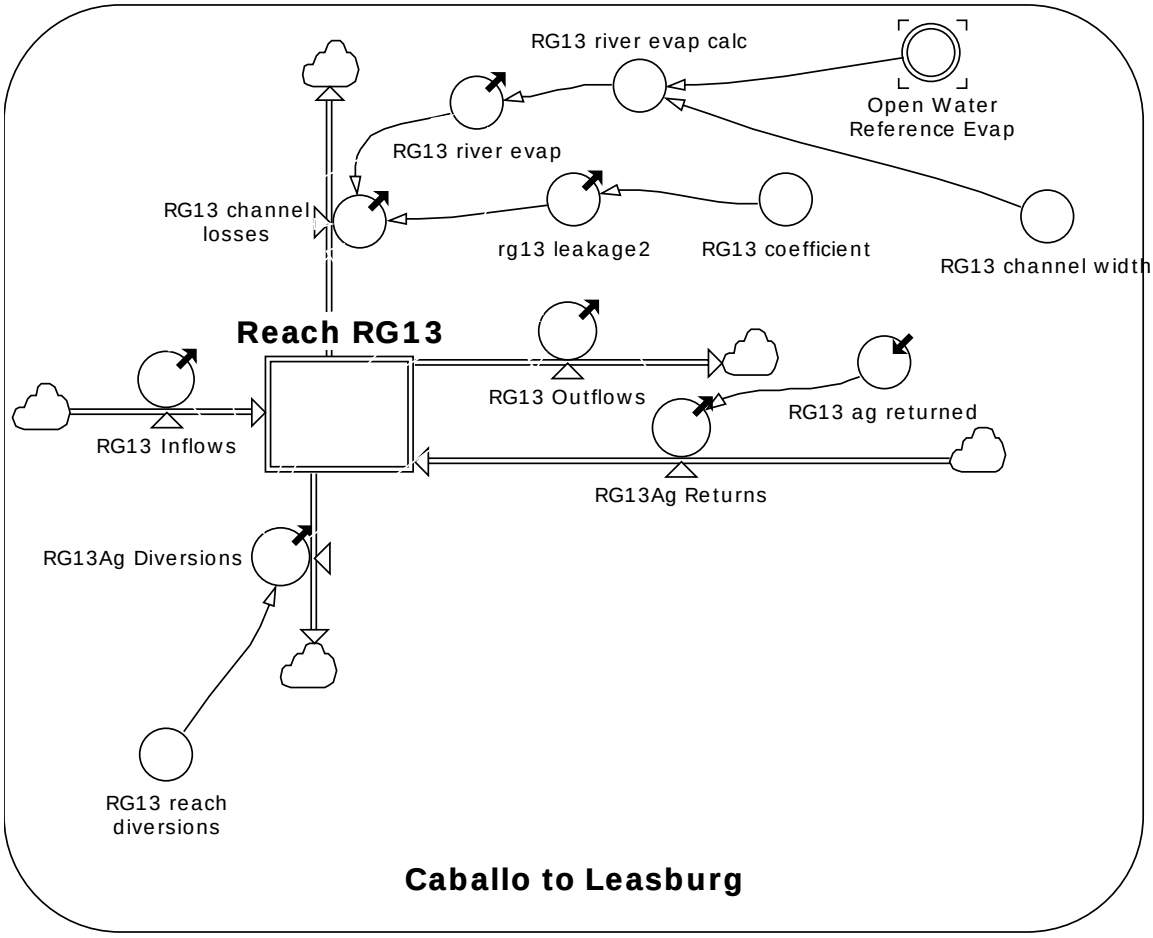

Figure 5-9. Water-balance model for one reach of the lower Rio Grande.

Diversion records were available from the Elephant Butte Irrigation District (EBID) for Percha Diversion Dam, Leasburg Diversion Dam, and Mesilla Diversion Dam as well as returns records between Percha Dam and El Paso. Unused water diverted at Percha Diversion Dam is all returned by drains to the river above Leasburg Diversion Dam (personal communication with James Narvaez, EBID Las Cruces October 2005), so the agricultural conveyance system for reach RG13 (Caballo Dam to Leasburg) in the model was considered to be a closed system. Some unused water diverted at Leasburg is returned by drains to the river above Mesilla Diversion Dam, but some of the water in the drains bypasses Mesilla Dam and is returned further downstream (personal communication with James Narvaez, EBID Las Cruces October 2005). Therefore, reaches RG14 and RG15 (Leasburg to Mesilla and Mesilla to El Paso) in the agricultural conveyance model were lumped together to create a closed section of the system. In the main-stem model, however, RG14 and RG15 are modeled separately and diversions and returns are constrained by EBID records.

Table 5-1. Model equations for the lower Rio Grande water-balance model.

Term	Definition
Evaporation	length of reach × channel width × open water reference evaporation
Leakage	coefficient × (agricultural diversions-average agricultural diversions for calibration period)
Outflows	inflows-evaporation-leakage-ag diversions+returns
GW-SW interaction rate	ag consumption+ag returns-ag diversions
Agricultural consumption	crop ET volume by reach × ag delivery factor
Agricultural delivery factor	amount of water diverted/potential crop consumption

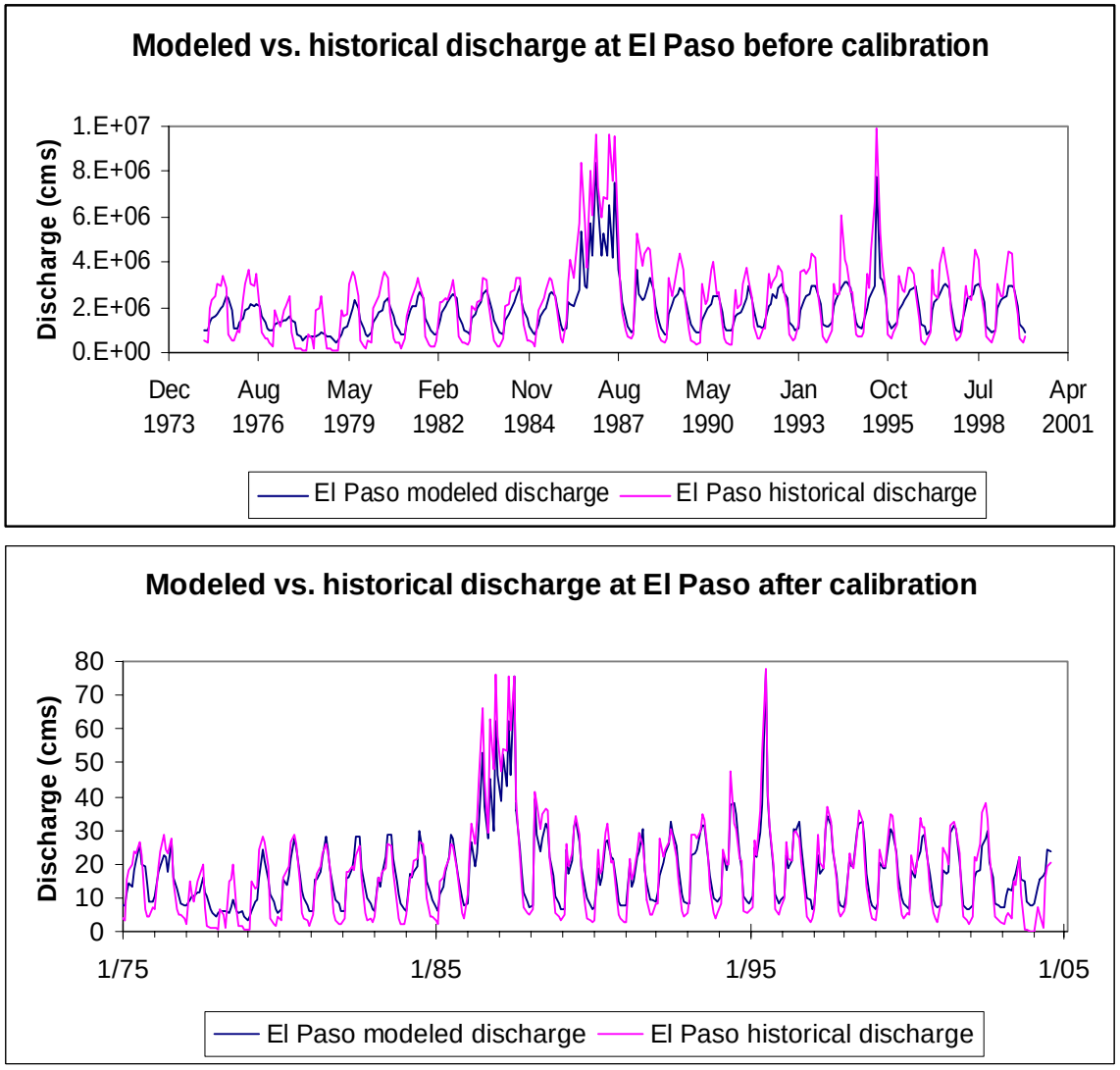

Figure 5-10. Modeled discharge at El Paso before and after calibration compared with historical discharge.

Detailed information on groundwater-surface water interactions was not available for the lower Rio Grande as in the middle Rio Grande, so the groundwater/surface water interaction term was used to close the mass balance in the agricultural model. Water is diverted from the river model into the agricultural model (Figure 5-11) based on historical diversion data. Some water is then lost to agricultural evaportranspiration (ET), which is calculated the same way as in the middle Rio Grande, and some water is returned to the river based on historical return records. The mass balance is then closed using the groundwater/surface water interaction term. The model was calibrated by varying the river leakage term such that the volume in the reservoir levels stayed relatively constant over the calibration period and did not gain or lose a significant amount of water over the simulation period.

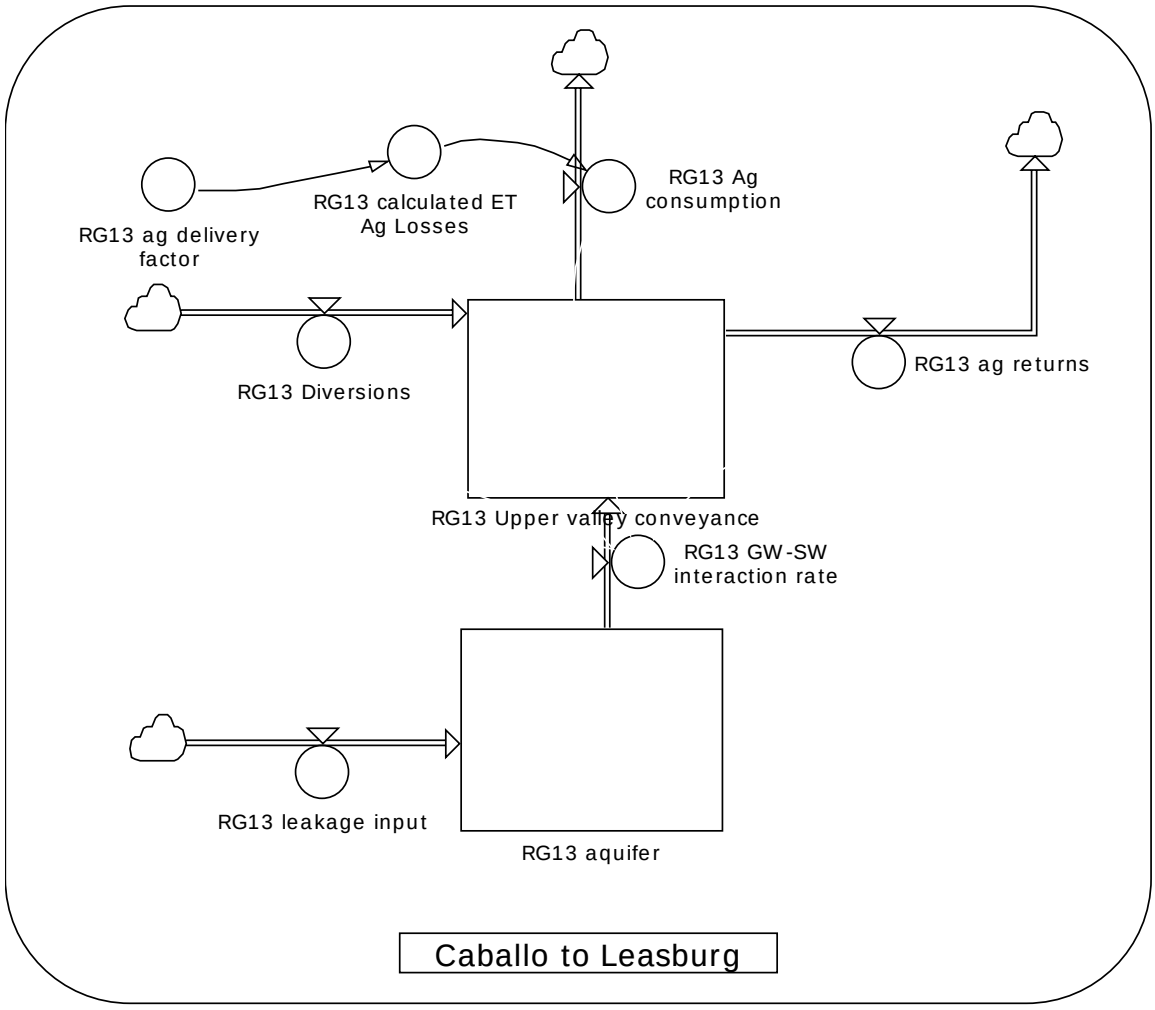

Figure 5-11. Water-balance model in Powersim for one reach of the agricultural conveyance system of the lower Rio Grande including the shallow aquifer model for this reach. Agricultural diversions from the river flow into the agricultural model ("RG13 Diversions"). Some of this water is consumed by agriculture ("RG13 Ag Consumption") and some is returned to the river ("RG13 ag returns"). The groundwater/surface water interaction term ("RG13 GW-SW interaction rate") closes the water balance for each time step. The term labeled "RG13 leakage input" is leakage from the river to the shallow aquifer.

5.3.2 Chloride-Balance Model of the Rio Grande

The chloride-balance model is developed as a co-flow to the surface water flow model. That is, the hydraulic model routes the volumetric flow of water down the river while the solute model tracts the mass transport of solute by the water. Combining the solute mass with the volumetric flow yields the concentration at key points in the system. Equations for the Rio Grande chloride model are given in Table 5-2. Note that the complexity of the chloride models corresponds to the complexity of the hydraulic model as constrained by the available data.

Table 5-2. Equations for the Rio Grande chloride model.

Cl model equations	
Inflow Cl	Inflow × Cl conc
Tributary Cl	Tributary flow × average tributary Cl concentration
Wastewater Cl	Wastewater inflow × average wastewater Cl concentration
Leakage Cl	If (leakage>0, leakage Cl out of river, leakage Cl into river)
Leakage Cl out of river	reach loss Cl concentration × leakage
Leakage Cl into river	aquifer Cl concentration × leakage
Reach loss Cl concentration	(inflow Cl-ag diversions Cl+tributary Cl+wastewater Cl)/(inflows-ag diversions+tributaries+wastewater)
Ag diversions Cl	ag diversions × reach inflow Cl conc
Ag returns Cl	ag outflow Cl concentration × ag returns
Ag outflow Cl conc	(diversions Cl inflow+Cl GW-SW interaction rate)/(diversions+GW-SW interaction rate-ag consumption)
Aquifer Cl conc	aquifer Cl storage/aquifer volume
Cl GW-SW interaction	If (GW-SW interaction rate>0, GW-SW interaction rate × aquifer Cl concentration, GW-SW interaction rate × reach inflow Cl concentration)

5.3.2.1 Upper Rio Grande Chloride-Balance Model

Inflow at Lobatos from the water-balance model is multiplied by the historical Rio Grande chloride concentration at Lobatos in the chloride-balance model for each month of the simulation (Table 5-3, Figure 5-12). Tributaries then enter the river and add an amount of chloride equal to the discharge of the tributary times the average chloride concentration of the tributary to the main stem of the river. All tributary chloride concentrations are a constant value and are equal to the average concentration of the samples available from the USGS from 1975 to 2004 for each tributary. A local-inflow chloride term is then added to the reach that accounts for ungaged surface-water addition as well as seepage of groundwater into the river. Chloride concentrations for local inflow were estimated from average tributary concentrations for each reach and are also a constant value. In reaches RG3 and RG4 (Taos Junction Bridge to Otowi) agricultural diversions and returns are modeled. In these reaches the agricultural conveyance system is not modeled explicitly; instead, the impact of agriculture on the chloride balance is accounted for simply by using the volume flux of agricultural ET to concentrate the chloride outflows from each reach.

Table 5-3. Chloride concentrations used as input to the Rio Grande chloride-balance model. All tributary chloride concentrations are from the USGS, and local-inflow chloride concentrations were estimated from tributary concentrations. Wastewater chloride concentrations for RG2–RG10 were estimated from three samples taken from Albuquerque wastewater treatment plant and wastewater concentrations from RG12–RG15 were assumed to be higher due to higher groundwater chloride concentration in the Mesilla Basin (see text). Starting chloride concentrations for Cochiti Reservoir (RG5) and Caballo Reservoir (RG12) are from the USGS. Starting chloride concentration for Elephant Butte Reservoir is from the BoR.

	Tributary Cl conc	**Other Tributary Cl conc**	**Local Inflow Cl conc**	**Wastewater Cl conc**
RG1	1.7	-	1.7	-
RG2	6	7.5 (Rio Pueblo de Taos)	6	-
RG3	5	-	5	-
RG4	5	-	5	-
RG5	5	-	5	95
RG6	37	-	-	-
RG7	2	75 (Jemez R)	-	95
RG8	10	-	-	95
RG9	112	-	-	-
RG10	-	-	-	95
RG11	-	-	-	-
RG12	-	-	-	200
RG13	-	-	-	-
RG14	-	-	-	200
RG15	-	-	-	200

	Starting Reservoir Cl conc	**Starting Aquifer Cl conc**
RG1	-	-
RG2	-	-
RG3	-	-
RG4	-	-
RG5	6	-
RG6	-	6
RG7	-	9
RG8	-	16
RG9	-	25
RG10	-	18
RG11	53	19
RG12	50	23
RG13	-	25
RG14	-	42
RG15	-	42

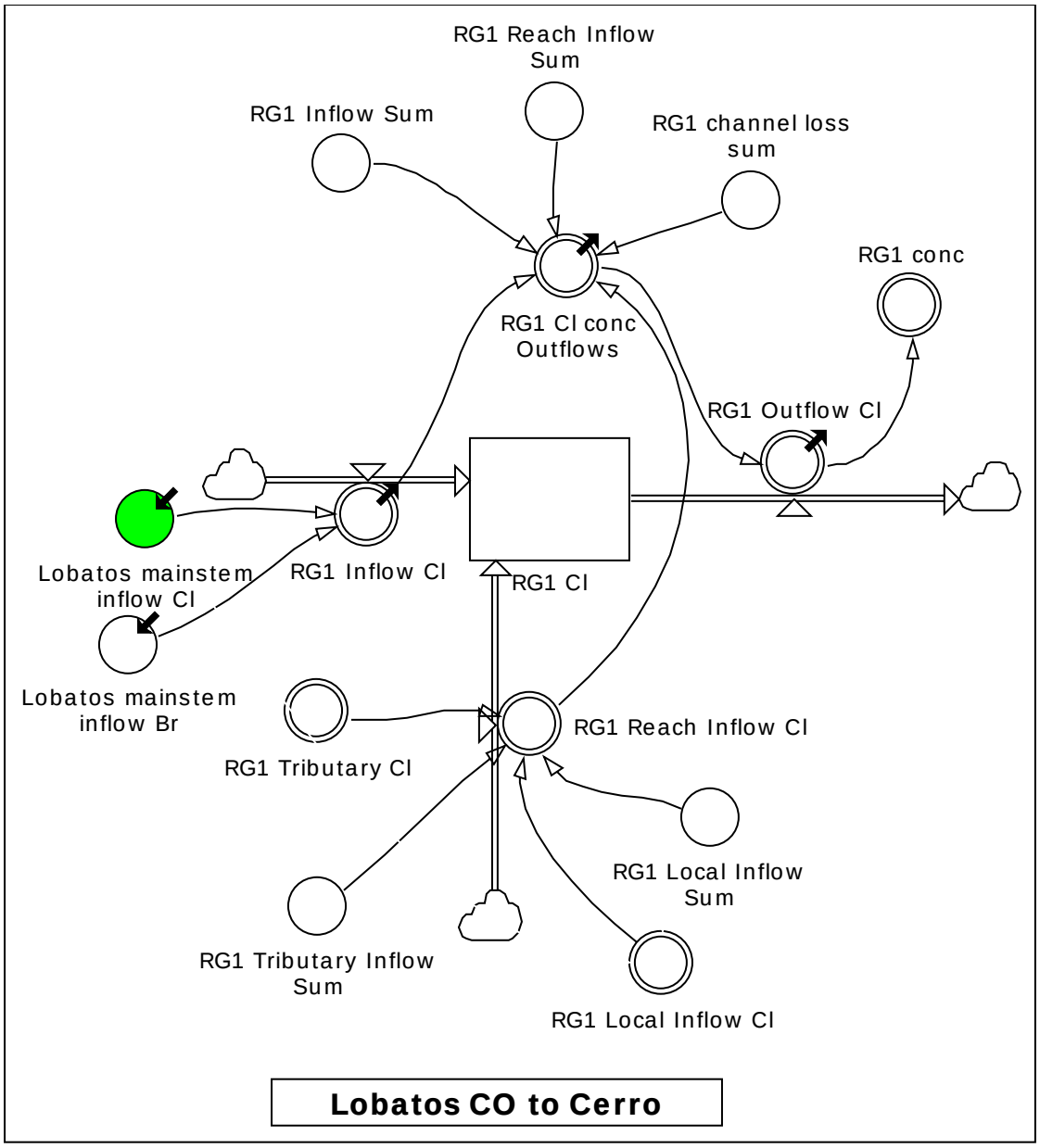

Figure 5-12. Chloride-balance model for one reach of the upper Rio Grande in Powersim. Flows from the water-balance model are multiplied by chloride concentrations to obtain a mass flux of chloride for each source. The outflow chloride flux is also concentrated by evaporative loss.

Wastewater effluent flows into reach RG4 (Embudo to Otowi) from the Española wastewater treatment plant. Chloride-concentration data for wastewater are not available from the Environmental Protection Agency (EPA). The chloride concentration of this wastewater was estimated from three samples taken from the Albuquerque wastewater treatment plant outfall in August 2004, January 2005, and August 2005. The chloride concentrations of these samples were very consistent and ranged between 92 and 95 mg L^{-1}. A chloride-concentration value of 95 mg L^{-1} was used for all wastewater inflows from Embudo to San Marcial.

At the end of each reach in the chloride model, the chloride inflows and outflows are summed up for each month to determine the outflow of chloride and an outflow chloride-concentration value is calculated.

Cochiti Reservoir was given a starting chloride-concentration value of 6 mg L^{-1} from historical USGS chloride data. Outflows from the reservoir are multiplied by the reservoir chloride concentration for each timestep. It is assumed that the reservoir is well-mixed and has a uniform chloride concentration throughout. This is probably reasonably accurate since Cochiti Reservoir is small. Precipitation entering the reservoir is assumed to have a negligible chloride concentration and, therefore, dilutes the chloride concentration of the reservoir. Bank storage is assumed to have a negligible effect on the mass balance of the reservoir.

5.3.2.2 Middle Rio Grande Chloride-Balance Model

As in the middle Rio Grande water-balance model, the agricultural conveyance system and groundwater are modeled explicitly in the middle Rio Grande chloride-balance model. The main-stem middle Rio Grande chloride-balance model includes tributary and wastewater inflows that are calculated in the same way as in the upper Rio Grande chloride model (Figure 5-13). Diversions, however, flow from the river model into the middle Rio Grande agricultural conveyance model (Figure 5-14). In the agricultural model, chloride is exchanged between groundwater and surface water according to the exchanges that take place in the water-balance model. When water flows from the conveyance system into the aquifer, the flow is multiplied by the chloride concentration of the flows going into that reach of the agricultural model. When water flows from the aquifer into the agricultural system, the flow is multiplied by the chloride concentration of the aquifer for that timestep. Groundwater/surface-water interaction between the river and shallow aquifer is also represented in the chloride model. When leakage is positive (leaking from the river into the shallow aquifer), the flow is multiplied by the concentration of the river after diversions, tributary and wastewater inflow, and evaporation have all taken place in that reach. When the flow is negative (seeping from the shallow aquifer into the river), it is multiplied by the aquifer concentration for that timestep. In reaches RG6 through RG9 (Cochiti to San Acacia), the groundwater model includes a term for "other recharge," which is a catchall term for recharge to the shallow aquifer from tributaries, septic tanks, and some mountain front recharge. The volume of water added by this term is small (less than 1% of river discharge) and it was multiplied by an estimated chloride-concentration value of 10 mg L^{-1}.

The aquifer starting concentrations were estimated in model calibration (Table 5-2). The starting aquifer concentrations are within the range of measured values for shallow groundwater in the middle Rio Grande basin from Plummer et al. (2004) of 10 to 47 mg L^{-1}. The model was calibrated so that the mass of chloride in each aquifer reach stays relatively constant over the simulation period. The shallow aquifer therefore acts neither as a source nor a sink of chloride in the model for long periods of simulation.

Elephant Butte Reservoir was assigned an initial a chloride concentration of 53 mg L^{-1} based on BoR data. The assumptions used for Cochiti Reservoir were also used for Elephant Butte Reservoir.

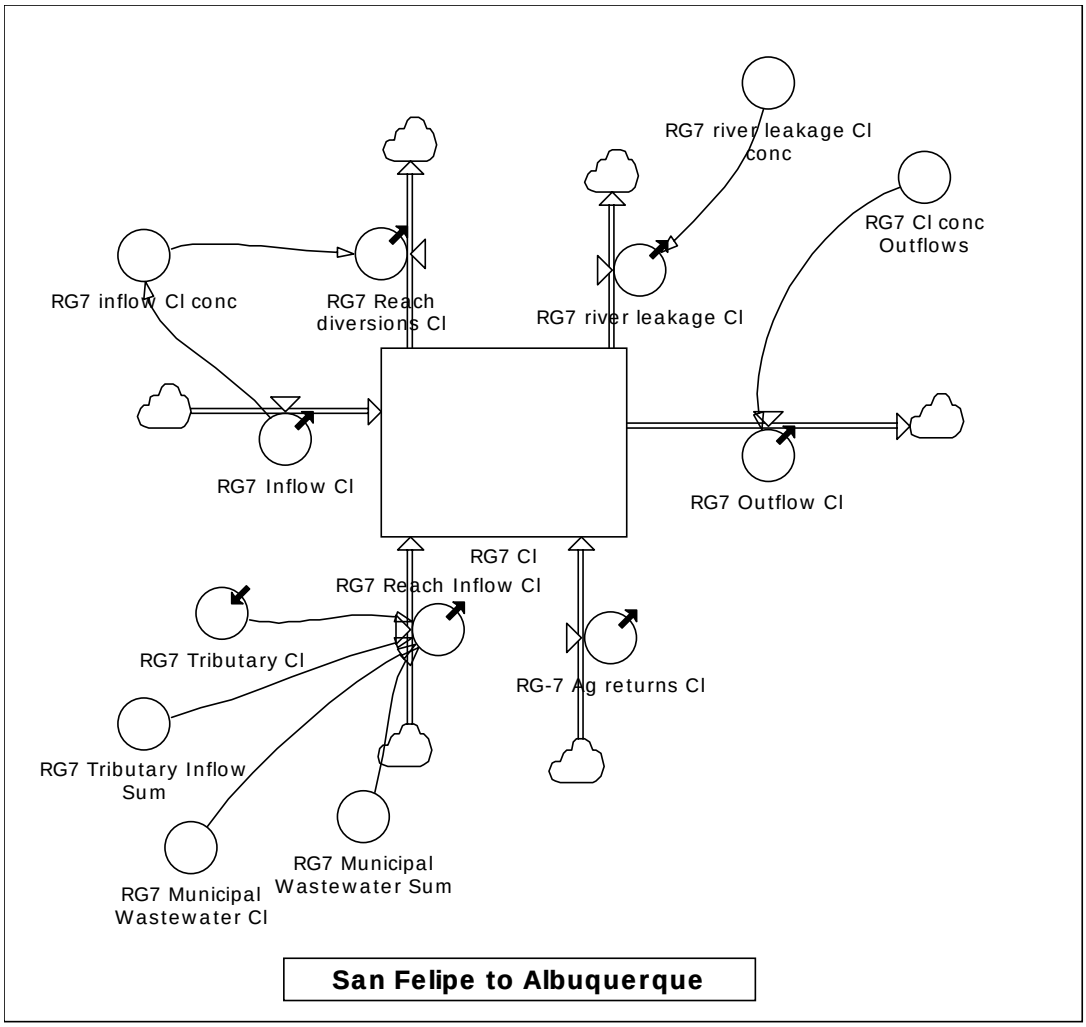

Figure 5-13. Chloride-balance model in Powersim for one reach of the main-stem Rio Grande.

5.3.2.3 Lower Rio Grande Chloride-Balance Model

The chloride-balance model for the lower Rio Grande uses the same design as the middle Rio Grande chloride model for the main stem, groundwater, and agricultural portions of the model (Figures 5-15 and 5-16). Caballo Reservoir was given a chloride concentration of 50 mg L^{-1} at the start of the simulation and employed the same assumptions used for the other reservoirs.

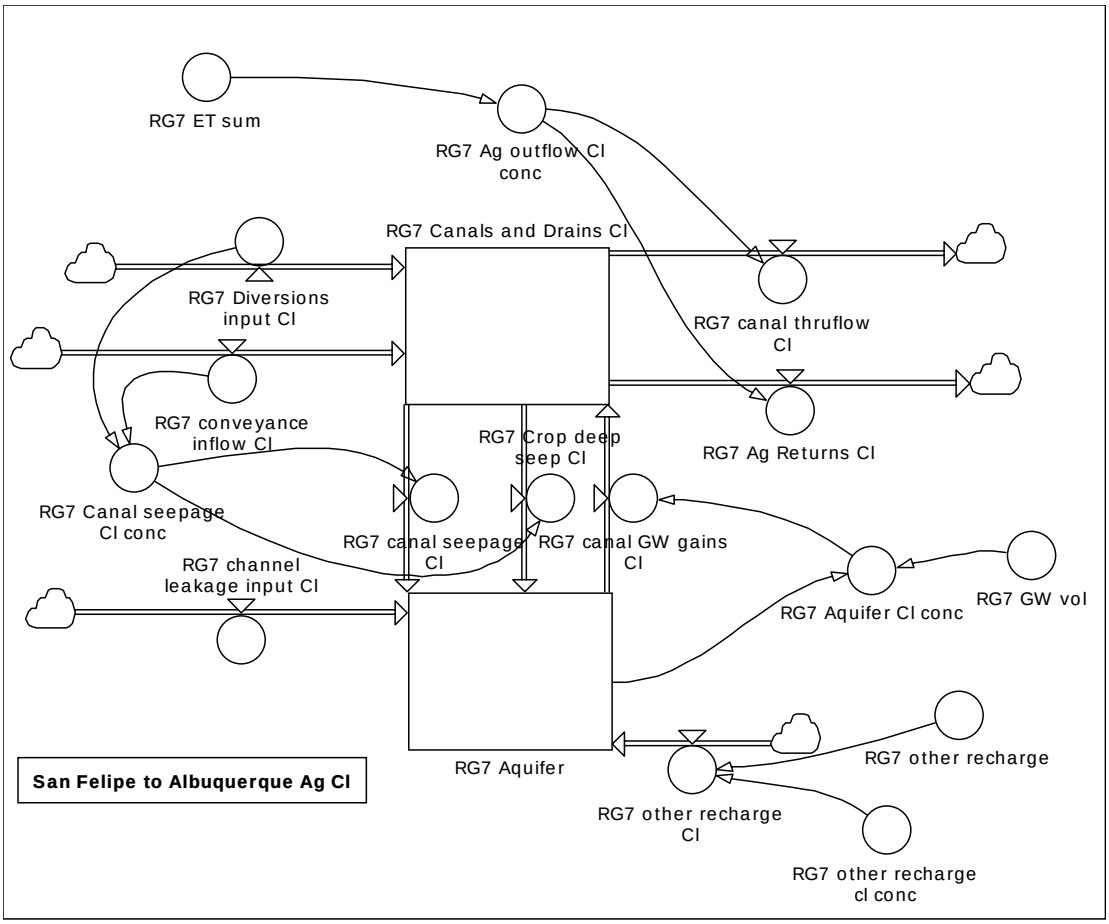

Figure 5-14. Chloride-balance model in Powersim for one reach of the agricultural conveyance system of the middle Rio Grande.

The starting chloride-concentration values for the shallow aquifer levels were also estimated in this reach by model optimization. The shallow aquifer levels did not have a significant gain or loss of chloride over the simulation period.

Wastewater inflows in the lower Rio Grande chloride model were given a higher chloride concentration than in the middle and upper Rio Grande. Chloride-concentration data were not available for the lower Rio Grande wastewater treatment plants (Truth or Consequences, NM, Las Cruces, NM, and El Paso, TX). Therefore, wastewater chloride concentration was estimated using an average well-water chloride-concentration value of 150 mg L^{-1} for the Mesilla Basin (Witcher 1995) and adding 50 mg L^{-1} to account for addition of chloride from human waste (Tchobanoglous et al. 2003). If the chloride concentration for wastewater in the reach between Mesilla and El Paso is decreased from 200 mg L^{-1} to 100 mg L^{-1} the average chloride burden over the calibration period at El Paso is reduced by 10%. If the wastewater chloride concentration is increased to 300 mg L^{-1} for this reach, the average chloride burden is increased by 10%.

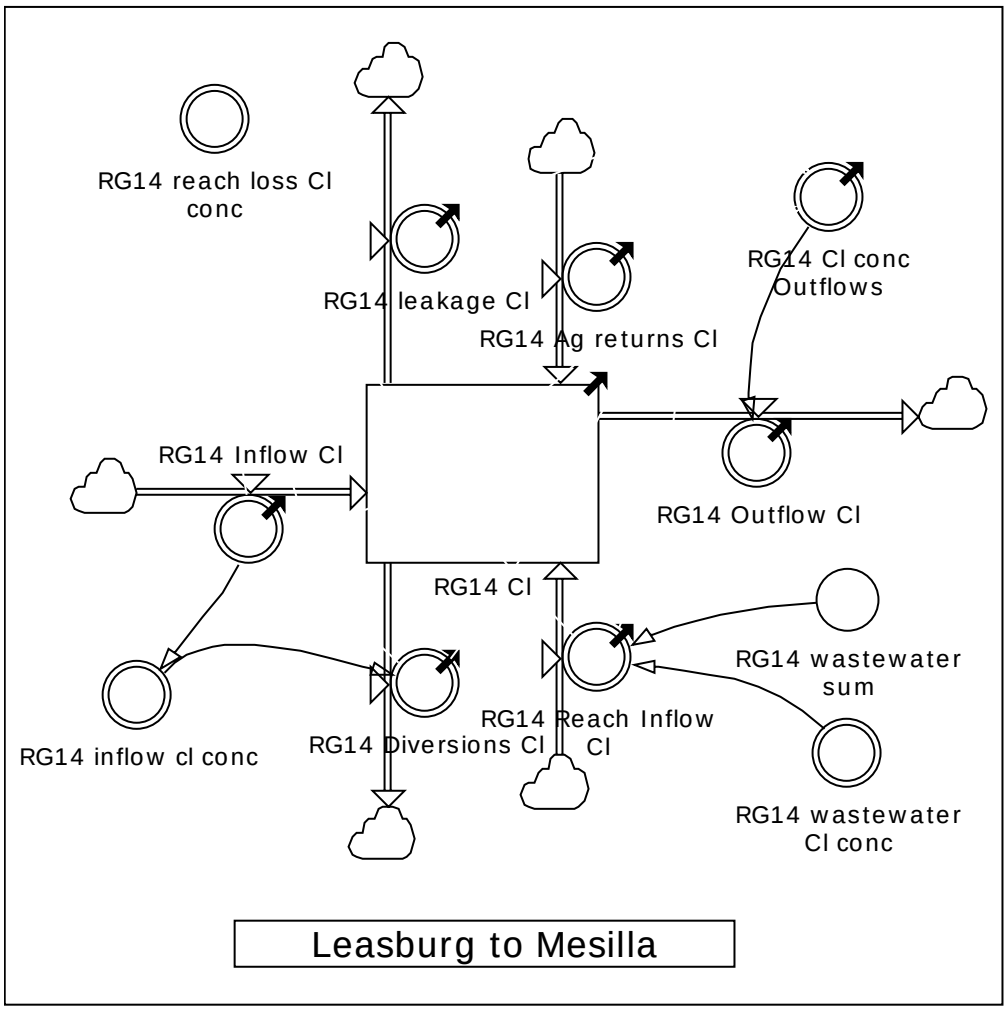

Figure 5-15. Chloride-balance model for one reach of the lower Rio Grande.

5.3.3 Results from the Rio Grande Chloride Mass-Balance Model

The model was first run under the assumption that there is no inflow of saline groundwater to the Rio Grande and that salinization is due to wastewater and tributary inflows and evaporative concentration. Using these assumptions, the model adequately simulated chloride burden and chloride concentration in the Upper Rio Grande, but began to underpredict chloride burden and chloride concentration starting near San Acacia and continuing to El Paso (Figures 5-17 through 5-20, Tables 5-4 and 5-5). Errors for the chloride model were computed using Equations 5-4, 5-5, and 5-6.

Percent error = absolute value(((historical discharge-modeled discharge)/historical discharge) × 100) (5-4)

Absolute error = absolute value (historical discharge-modeled discharge) (5-5)

Average absolute error percent of historical average discharge = average absolute error/average discharge over simulation period (5-6)

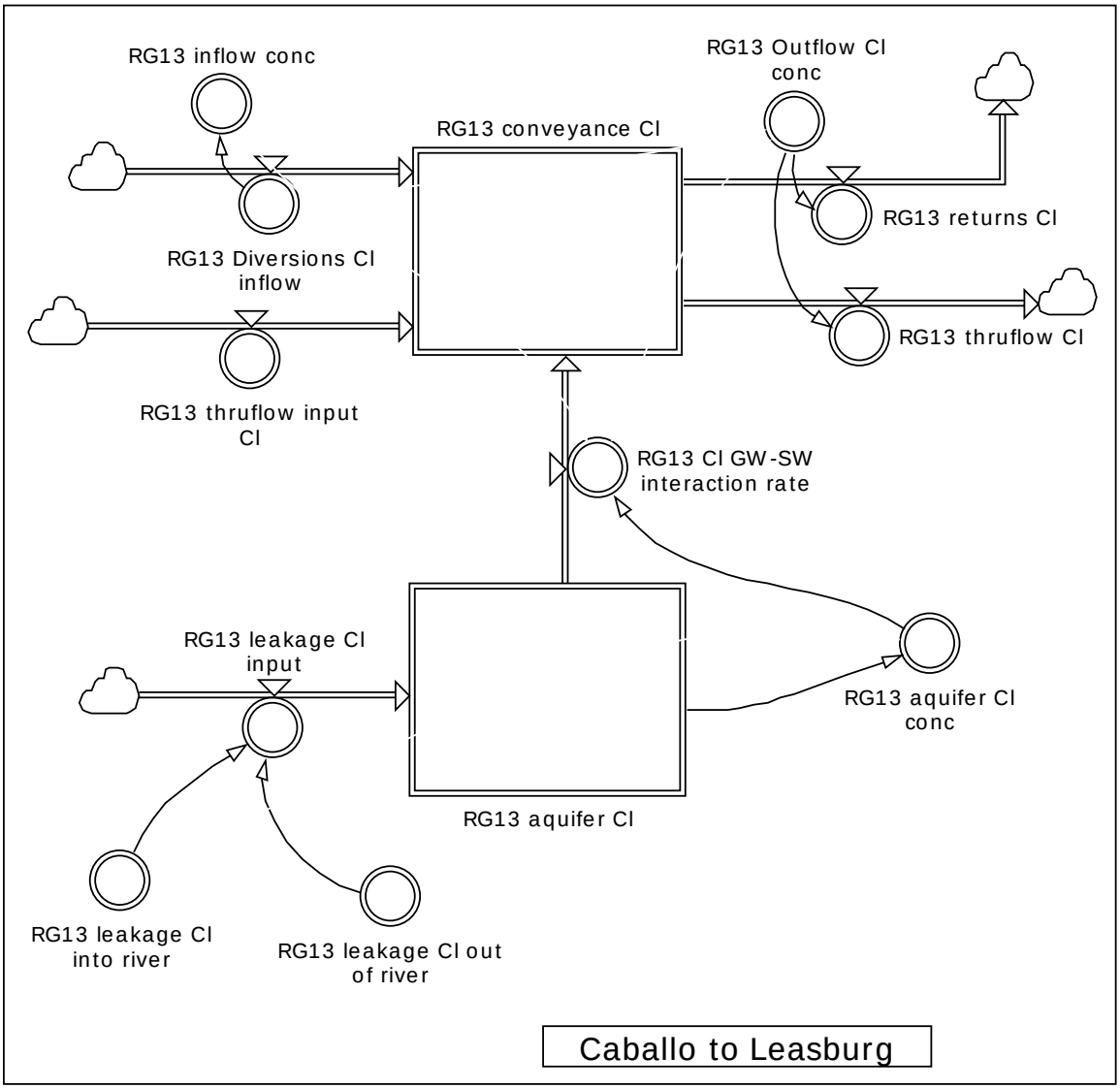

Figure 5-16. Chloride-balance model for one reach of the agricultural conveyance system in the Lower Rio Grande including the shallow aquifer.

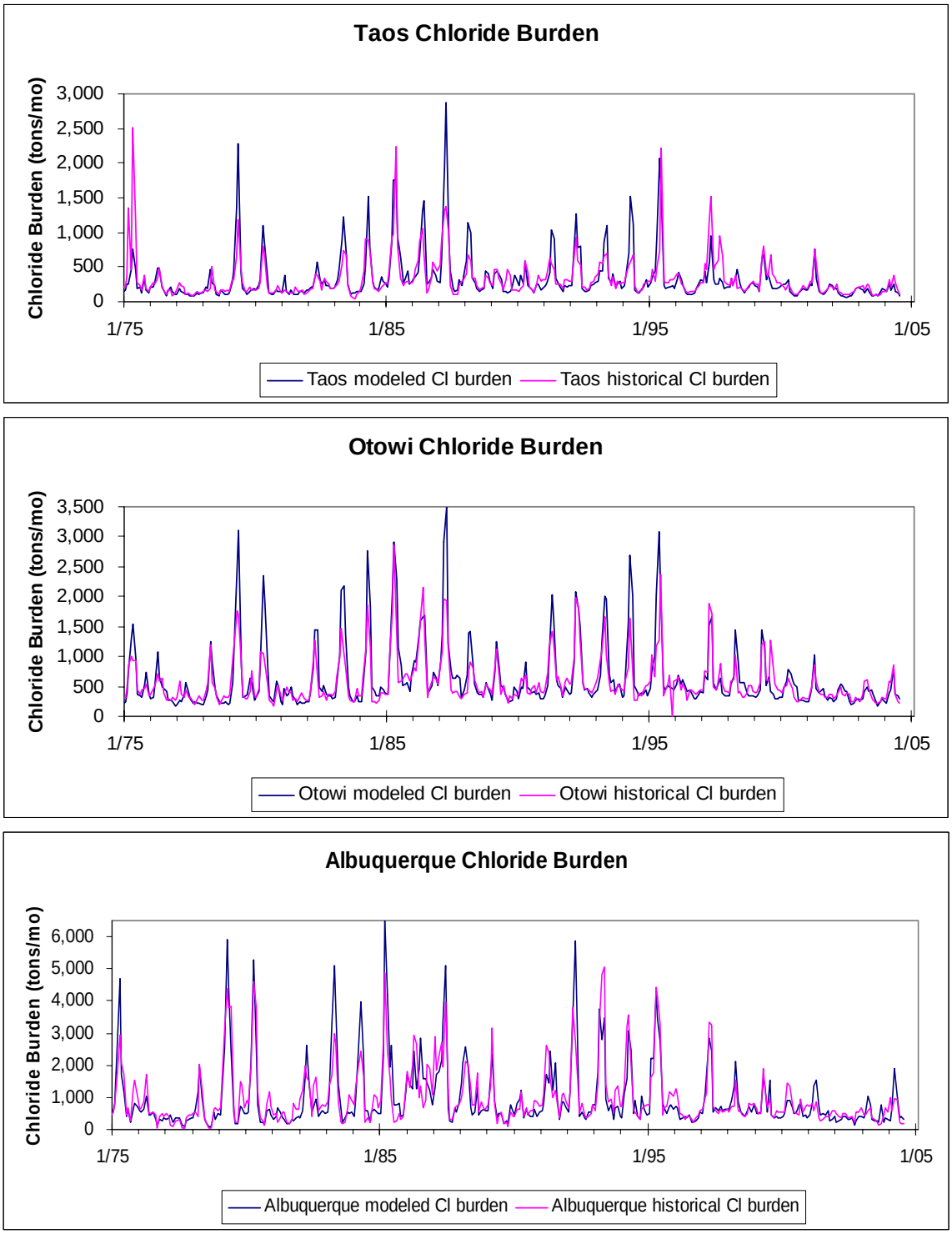

Figure 5-17. Modeled and historical chloride burden in kg mo^{-1} without addition of brine inflows for selected gaging stations on the main-stem Rio Grande including Taos Junction Bridge, Otowi, and Albuquerque. Historical chloride burden is shown in pink and modeled in blue.

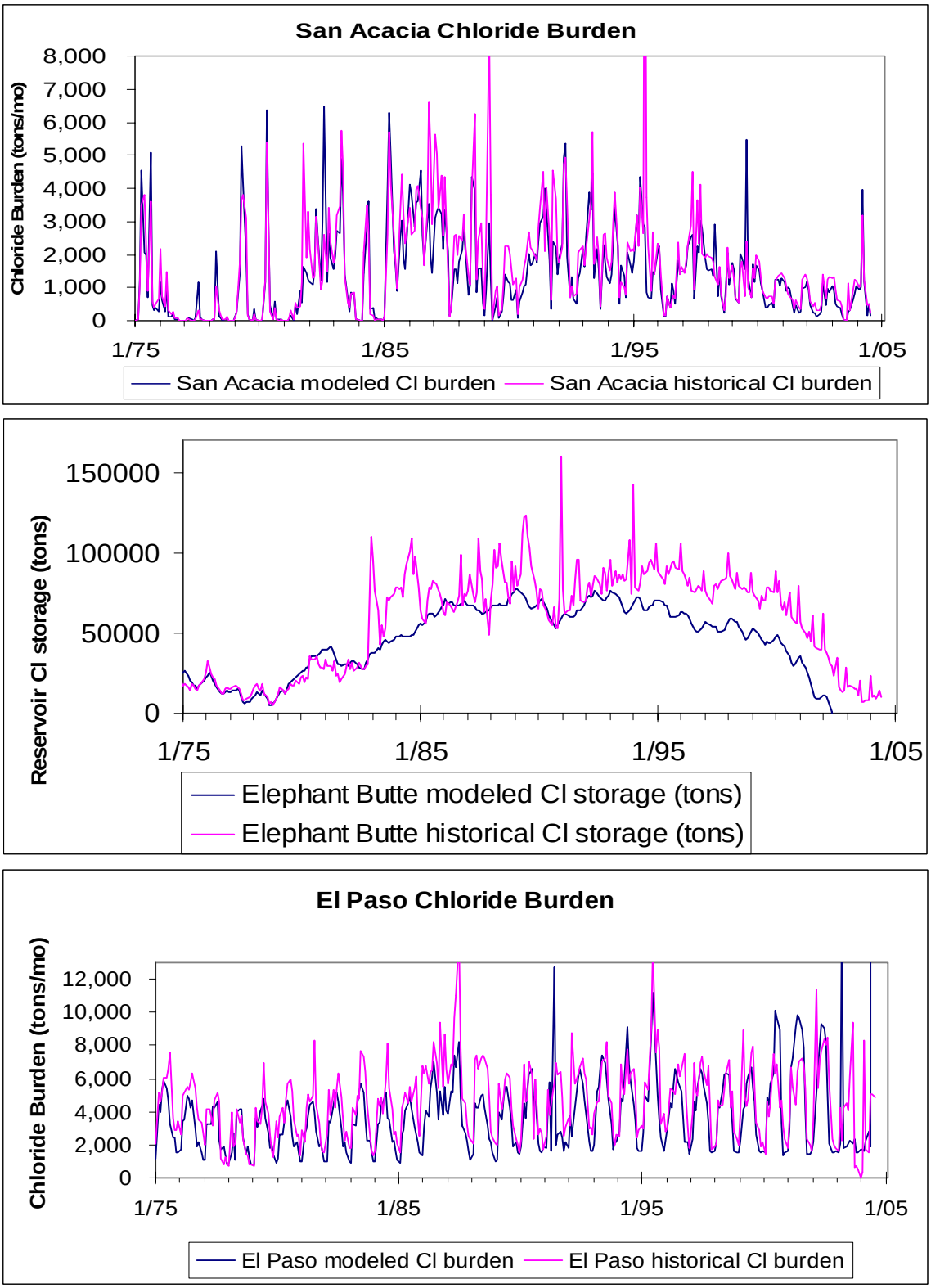

Figure 5-18. Modeled and historical chloride burden in kg mo^{-1} without addition of brine inflows for selected gaging stations on the main-stem Rio Grande including San Acacia, Elephant Butte Dam, and El Paso. Historical chloride burden is shown in pink and modeled in blue.

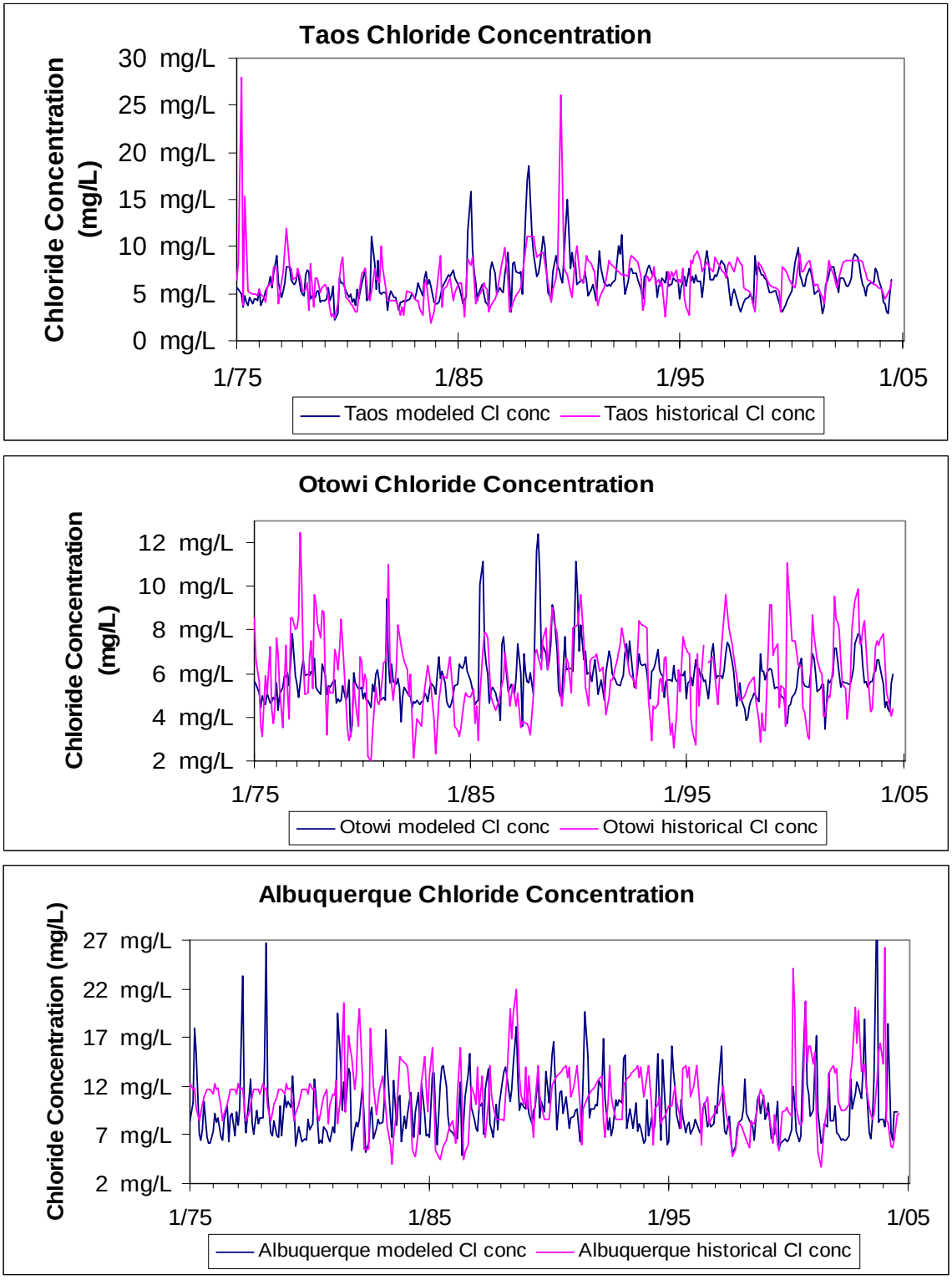

Figure 5-19. Modeled and historical chloride concentration in kg mo^{-1} without addition of brine inflows for selected gaging stations on the main-stem Rio Grande including Taos Junction Bridge, Otowi, and Albuquerque. Historical chloride burden is shown in pink and modeled in blue.

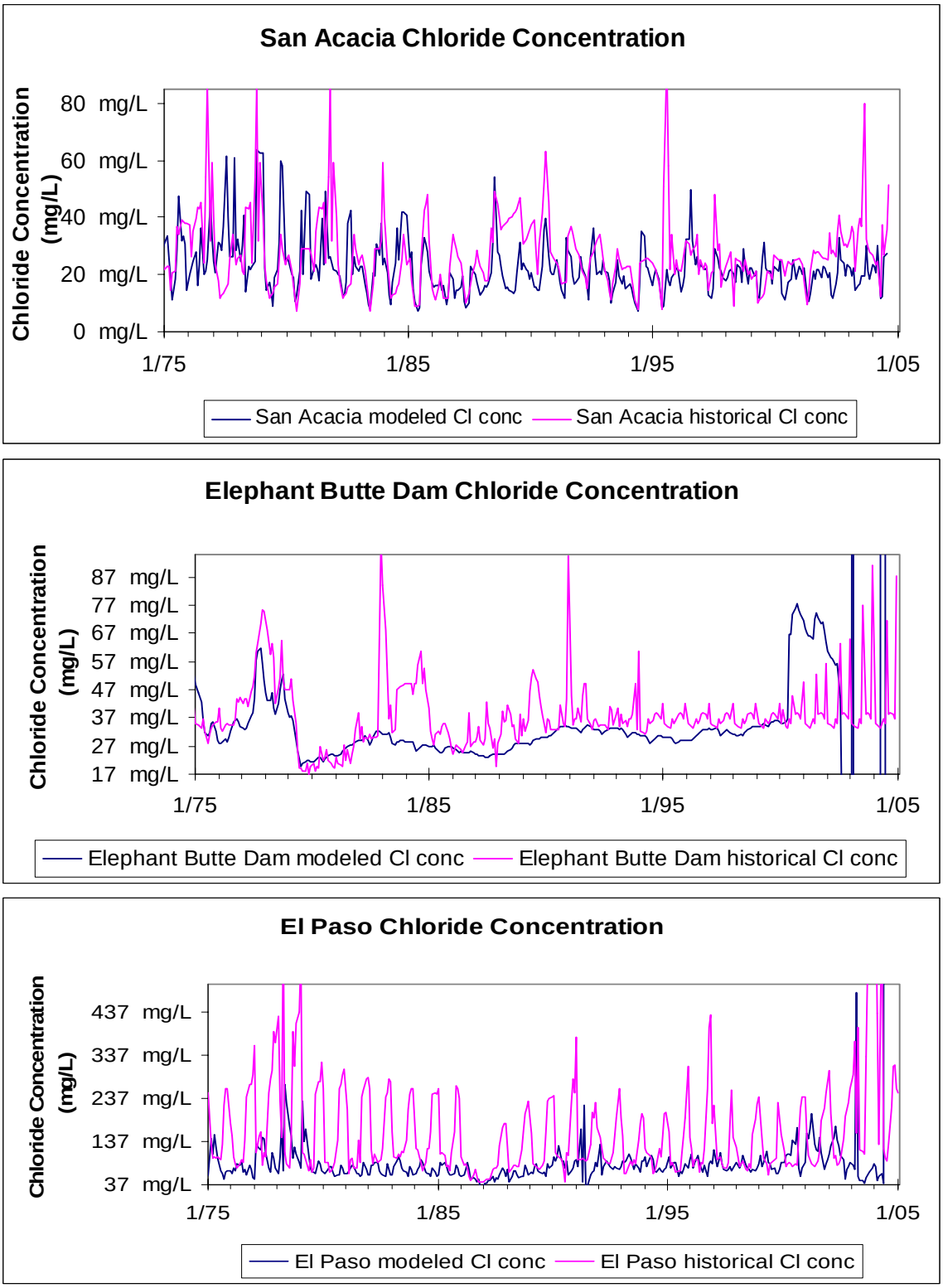

Figure 5-20. Modeled and historical chloride concentration in kg mo^{-1} without addition of brine inflows for selected gaging stations on the main-stem Rio Grande including San Acacia, Elephant Butte Dam, and El Paso. Historical chloride burden is shown in blue and modeled in red.

Table 5-4. Summary of errors between model and historical values for chloride burden (tons/mo) from the model simulation without brine inflows from 1975 to 2004. Errors were computed for all stations for which historical chloride-concentration data were available. Error calculations include percent error between historical and modeled, absolute value of error between historical and modeled, and the absolute value of the error expressed as a percent of the average historical value. All errors are averaged over the simulation period.

Station	Average Percent Error	Average Absolute Error (tons/mo)	Average Historical Chloride Burden (tons/mo)	Average Absolute Error Percent of Historical Average Discharge
Taos	28	115	333	35
Otowi	26	163	581	28
San Felipe	26	156	682	23
Albuquerque	37	335	1004	33
Bernardo	339	471	1301	36
San Acacia	33	492	1643	30
San Marcial	366	640	1630	39
Elephant Butte Dam	64	1642	2720	60
El Paso	46	2005	4583	44

Table 5-5. Summary of errors between model and historical values for chloride concentration (mg/L) from the model simulation without brine inflows from 1975 to 2004. Errors were computed for all stations for which historical chloride-concentration data were available. Error calculations include percent error between historical and modeled, absolute value of error between historical and modeled, and the absolute value of the error expressed as a percent of the average historical value. All errors are averaged over the simulation period.

Station	Average Percent Error	Average Absolute Error (mg/L)	Average Historical Chloride Concentration (mg/L)	Average Absolute Error Percent of Historical Average Discharge
Taos	27	2	7	26
Otowi	26	1	6	24
San Felipe	25	1	6	22
Albuquerque	32	3	11	31
Bernardo	30	5	18	26
San Acacia	33	10	27	35
San Marcial	135	40	33	122
Elephant Butte Dam	32	12	38	31
El Paso	47	85	161	53

It was assumed that upwelling of deep brine accounts for the chloride source not represented in the model. Brine inflows to the river were calculated for San Acacia, the LFCC, and El Paso by subtracting modeled chloride burden from historical chloride burden. These locations were chosen because they were the only points south of Bernardo where enough data were available to make a meaningful comparison with historical data. In order to make the comparison between modeled and historical chloride burden at these three locations, the model was run in three separate sections, Lobatos to San Acacia, San Acacia to Elephant Butte Dam, and Elephant Butte Dam to El Paso. Each of these sections used historical chloride burden as input at the top of the reach. Therefore, the difference between modeled and historical chloride burden at San Acacia represents chloride added to the river north of San Acacia; the difference between modeled and historical chloride burden in the LFCC at San Marcial represents chloride added only between San Acacia and Elephant Butte Dam; and the difference in chloride burden at El Paso represents only chloride added between Elephant Butte Dam and El Paso (Figure 5-21). It is assumed that these additions of chloride to the Rio Grande are due to upwelling of deep saline groundwater. Negative brine inflow values are assumed to be due to model error or in some cases error in historical data.

Brine inflows at San Acacia, the LFCC, and El Paso are more strongly correlated with discharge than the drought index (Figure 5-22), although the correlations with discharge are also weak (Table 5-6). Correlation coefficients between brine inflows and discharge were positive at all three locations. However, the correlation coefficients between the Palmer drought index and brine inflows were negative at San Acacia and El Paso and positive for the LFCC. The negative correlation between brine inflows and the drought index indicates that brine inflows are higher in drier times. Perhaps during dry times, the head in the shallow aquifer drops, allowing deeper saline brine to flow into the shallow aquifer. This saline water is then pumped onto fields for irrigation during periods of drought. However, the positive correlation between discharge and brine inflows indicates that brine inflows were higher during wetter periods in the record. This could actually be due to flushing of salts temporarily stored in agricultural soils during dry periods.

The brine inflows at San Acacia, the LFCC, and El Paso do not show much of a clear seasonal variation (Figure 5-23) except that brine inflows seem to rise at all three locations over the dry months of September and October.

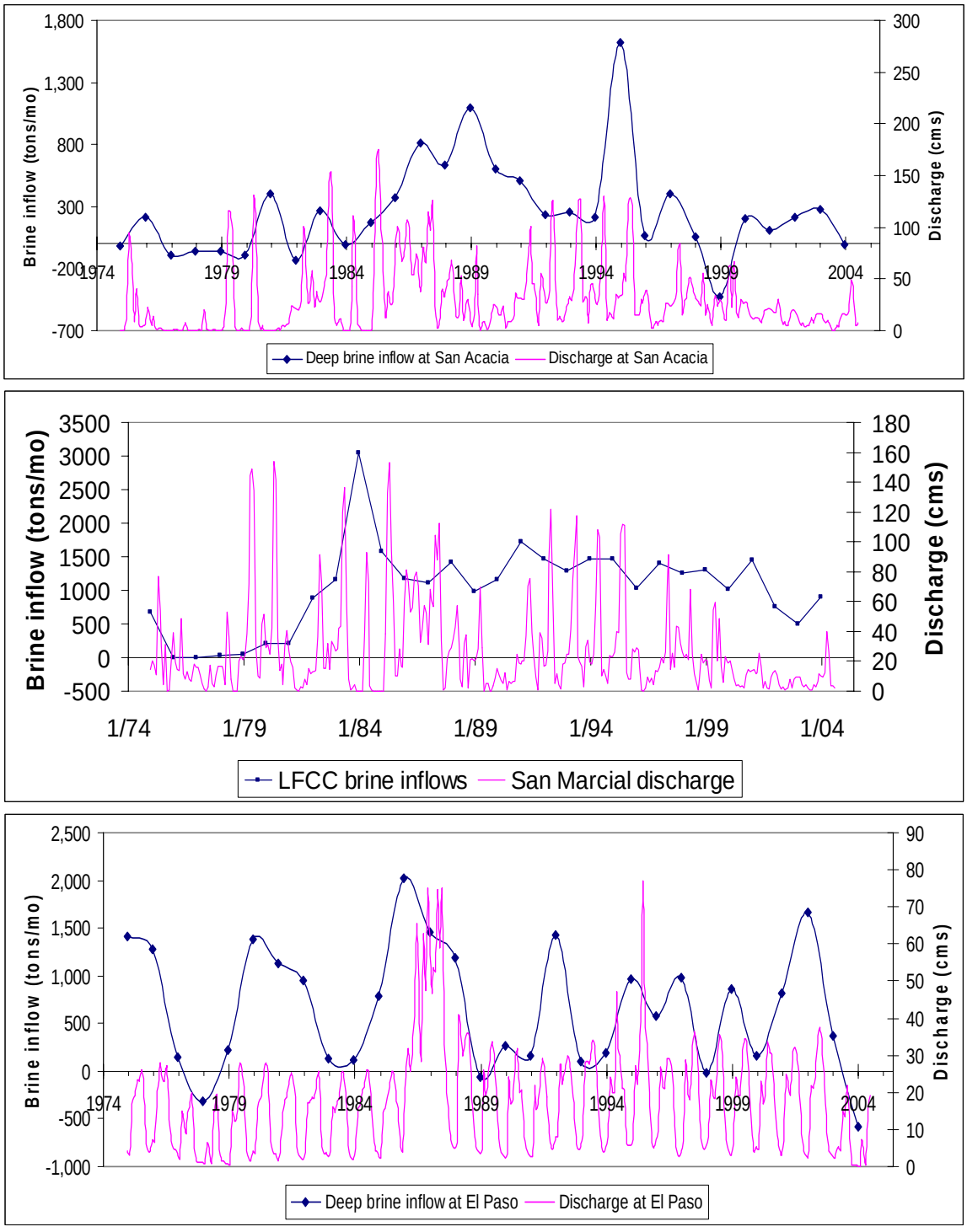

Figure 5-21. Brine inflow at San Acacia, Elephant Butte Dam, and El Paso calculated from the Rio Grande chloride model. Brine inflow at San Acacia represents brine added north of the San Acacia gage, Elephant Butte Dam brine inflow represents inflow between San Acacia and Elephant Butte Dam, and inflow at El Paso enters between Elephant Butte Dam and El Paso. The brine inflow at these locations is roughly correlated with discharge in the river.

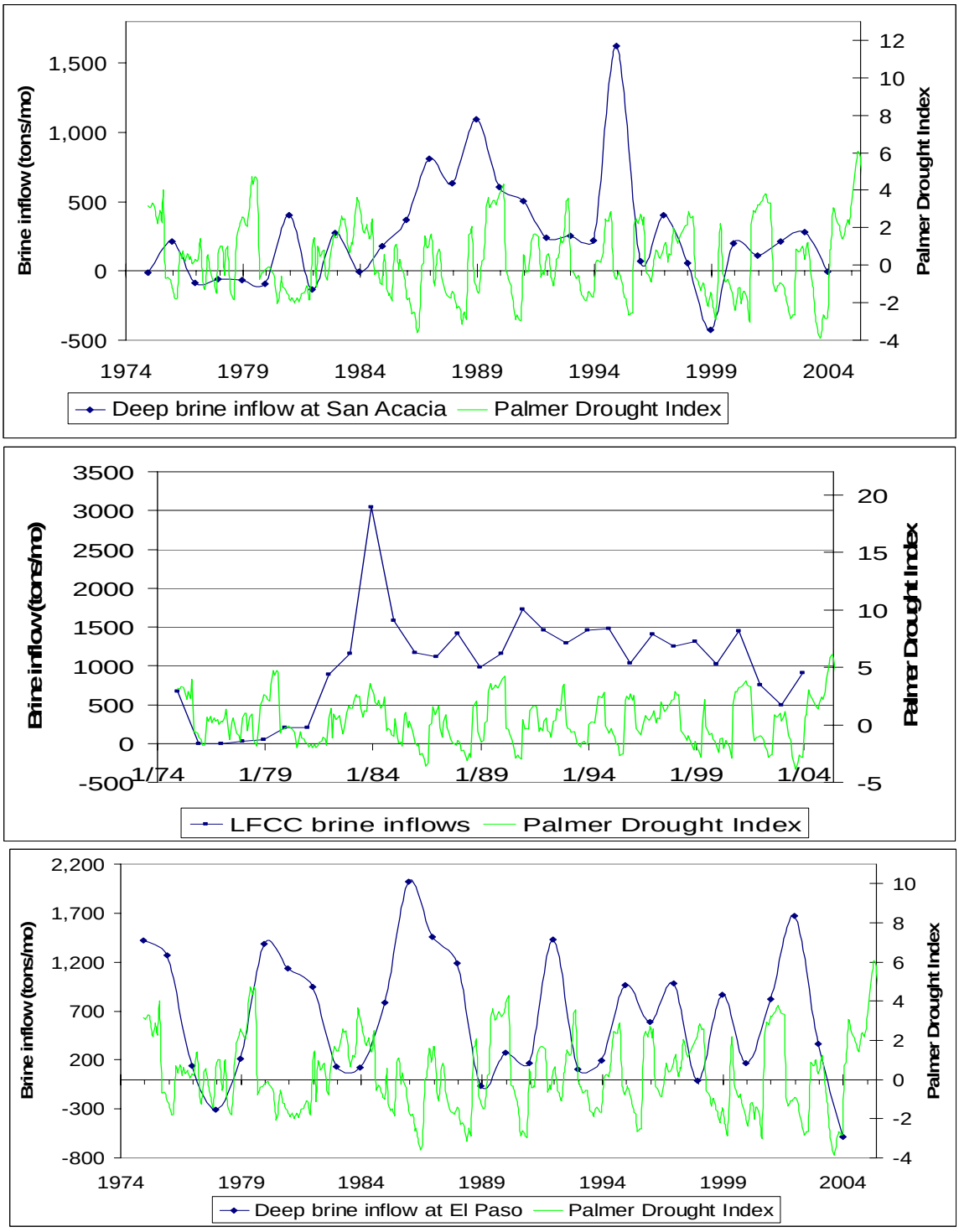

Figure 5-22. Brine inflow at San Acacia, Elephant Butte Dam, and El Paso calculated from the Rio Grande chloride model. The brine inflow at San Acacia and El Paso is weakly correlated with the drought index. This may be due to a change in head gradient as river discharge decreases and it may also be due to pumping of saline groundwater for irrigation during drought periods. Palmer drought index data is from the National Climatic Data Center (NCDC).

Table 5-6. Correlation coefficients between brine inflows and discharge and the drought index for San Acacia, the Low Flow Conveyance Channel, and El Paso. Correlations were computed using the correlation function in Excel, which calculates the correlation coefficient to determine the relationship between two properties. The river discharges at San Acacia and El Paso and the discharge of the LFCC at San Marcial were used in the calculation.

	Correlation Coefficient Between Brine Inflow and Discharge	Correlation Coefficient Between Brine Inflow and Palmer Drought Index
San Acacia	0.19	-0.11
Low Flow Conveyance Channel	0.39	0.16
El Paso	0.31	-0.20

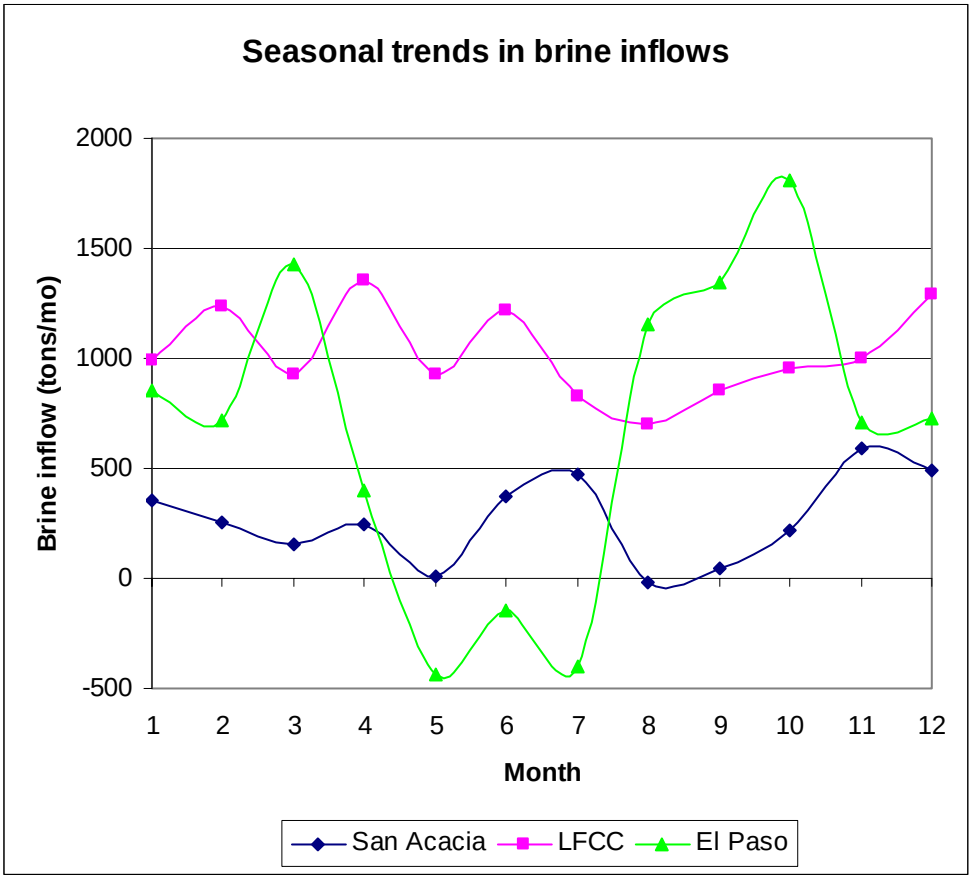

Figure 5-23. Seasonal variation in brine inflows at San Acacia, the Low Flow Conveyance Channel, and El Paso. The graph shows monthly average brine inflows for these three locations.

The model was run again using the calculated deep saline groundwater inflows. Saline groundwater was added to the river at the end of the Bernardo to San Acacia and Mesilla to El Paso reaches and also at Elephant Butte Reservoir. Negative calculated brine inflows were assumed to be in error and were not included in the model. The brine additions at San Acacia and El Paso were assumed to have a negligible volume, so no water was added to the water-balance model. However, additional water was added to Elephant Butte Reservoir from January 1996 to December 2002 to close the gap in the water balance (Figure 5-24, Table 5-7). When this additional water was added to Elephant Butte Reservoir and additional chloride was added to the LFCC to match the historical chloride burden record, the chloride storage in Elephant Butte Reservoir increased, causing the model to slightly overestimate chloride storage in the reservoir. Therefore, the model slightly overestimates chloride burden in the river south of Elephant Butte Reservoir. Using the calculated brine inflows, the chloride-balance model was able to adequately simulate the chloride burden of the river (Figures 5-25 and 5-26).

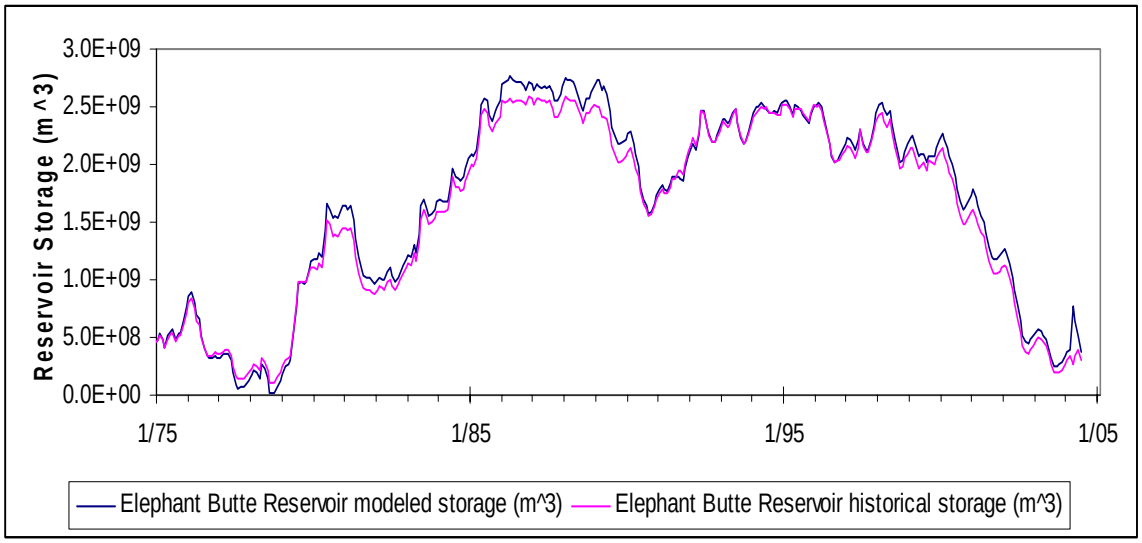

Figure 5-24. Modeled Elephant Butte Reservoir storage (m^3) after addition of extra water from January 1996 to December 2002 to account for an unknown source not represented in the model compared with historical reservoir storage.

Table 5-7. Summary of errors between model and historical values for discharge from the model simulation with brine inflows and added water at Elephant Butte Reservoir from 1975 to 2004. Error calculations include percent error between historical and modeled, absolute value of error between historical and modeled, and the absolute value of the error expressed as a percent of the average historical value. All errors are averaged over the simulation period. EB Dam stands for Elephant Butte Dam.

Station	Average Percent Error	Average Absolute Error (cms)	Average Historical Discharge (cms)	Average Absolute Error Percent of Historical Average Discharge
Lobatos	6	1	15	6
Taos	4	1	22	5
Embudo	4	1	25	4
Otowi	5	2	44	5
Cochiti	0	0	43	0
San Felipe	6	2	42	5
Albuquerque	15	3	38	7
Bernardo	105	6	26	22
San Acacia	1	0	30	1
San Marcial	94	4	21	19
EB Dam	1	0	29	1
Caballo	1	0	23	1
Leasburg	71	2	17	14
Mesilla	35	3	10	28
El Paso	100	4	17	23
Station	**Average Percent Error**	**Average Absolute Error (cms)**	**Average Historical Discharge (cms)**	**Average Absolute Error Percent of Historical Average Discharge**
Lobatos	6	1	15	6
Taos	4	1	22	5
Embudo	4	1	25	4
Otowi	5	2	44	5
Cochiti	0	0	43	0
San Felipe	6	2	42	5
Albuquerque	15	3	38	7
Bernardo	105	6	26	22
San Acacia	1	0	30	1
San Marcial	94	4	21	19
EB Dam	1	0	29	1
Caballo	1	0	23	1
Leasburg	71	2	17	14
Mesilla	35	3	10	28
El Paso	100	4	17	23

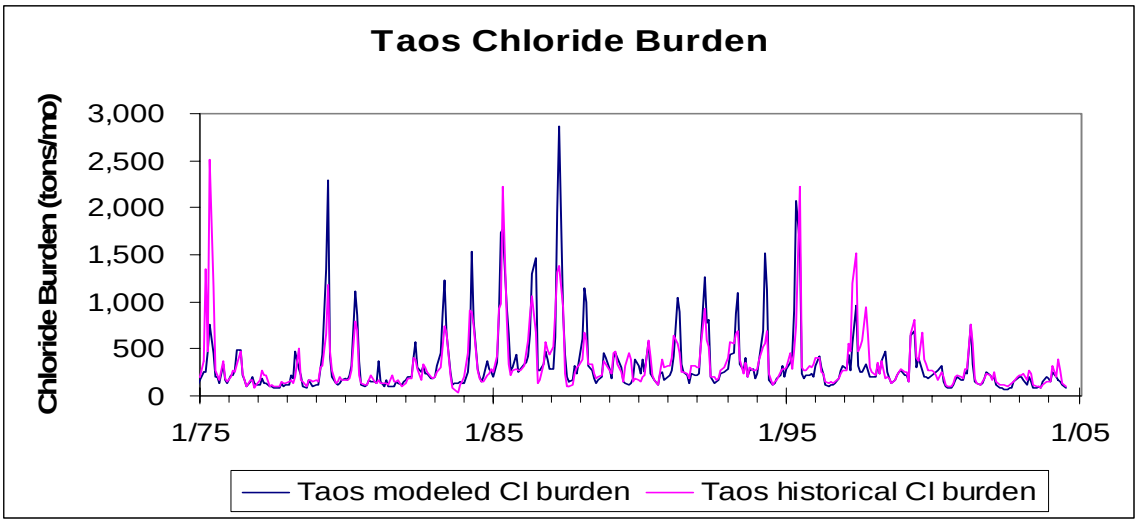

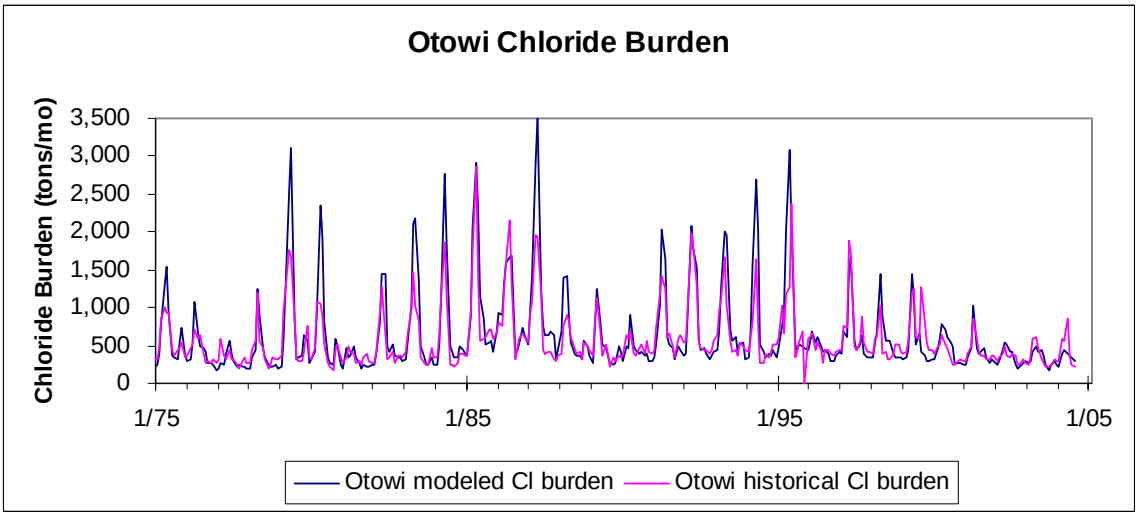

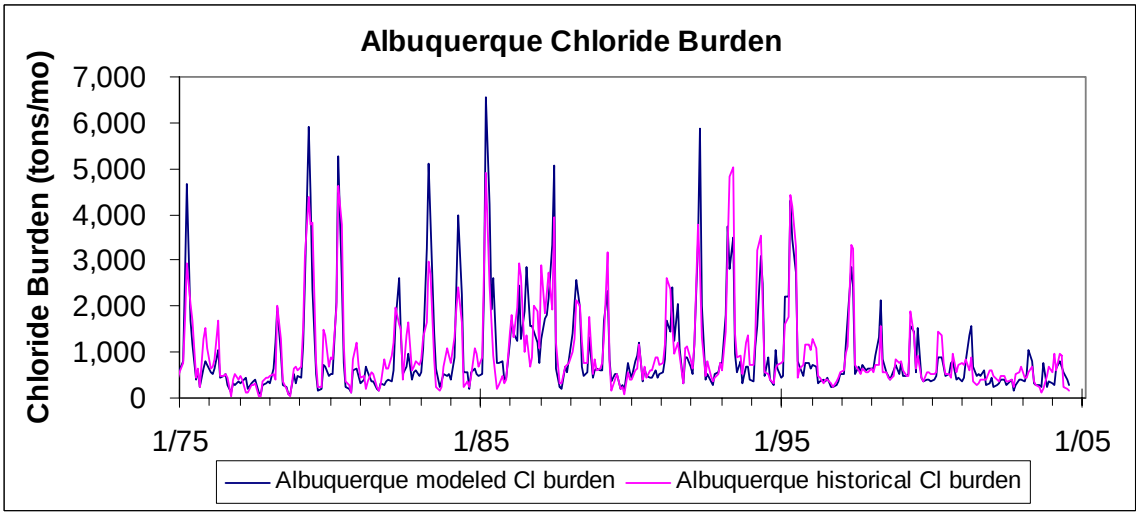

Figure 5-25. Modeled and historical chloride burden in kg mo^{-1} with added brine inflows for selected gaging stations on the main-stem Rio Grande including Taos Junction Bridge, Otowi, and Albuquerque. Historical chloride burden is shown in pink and modeled in blue, both in tons mo^{-1}.

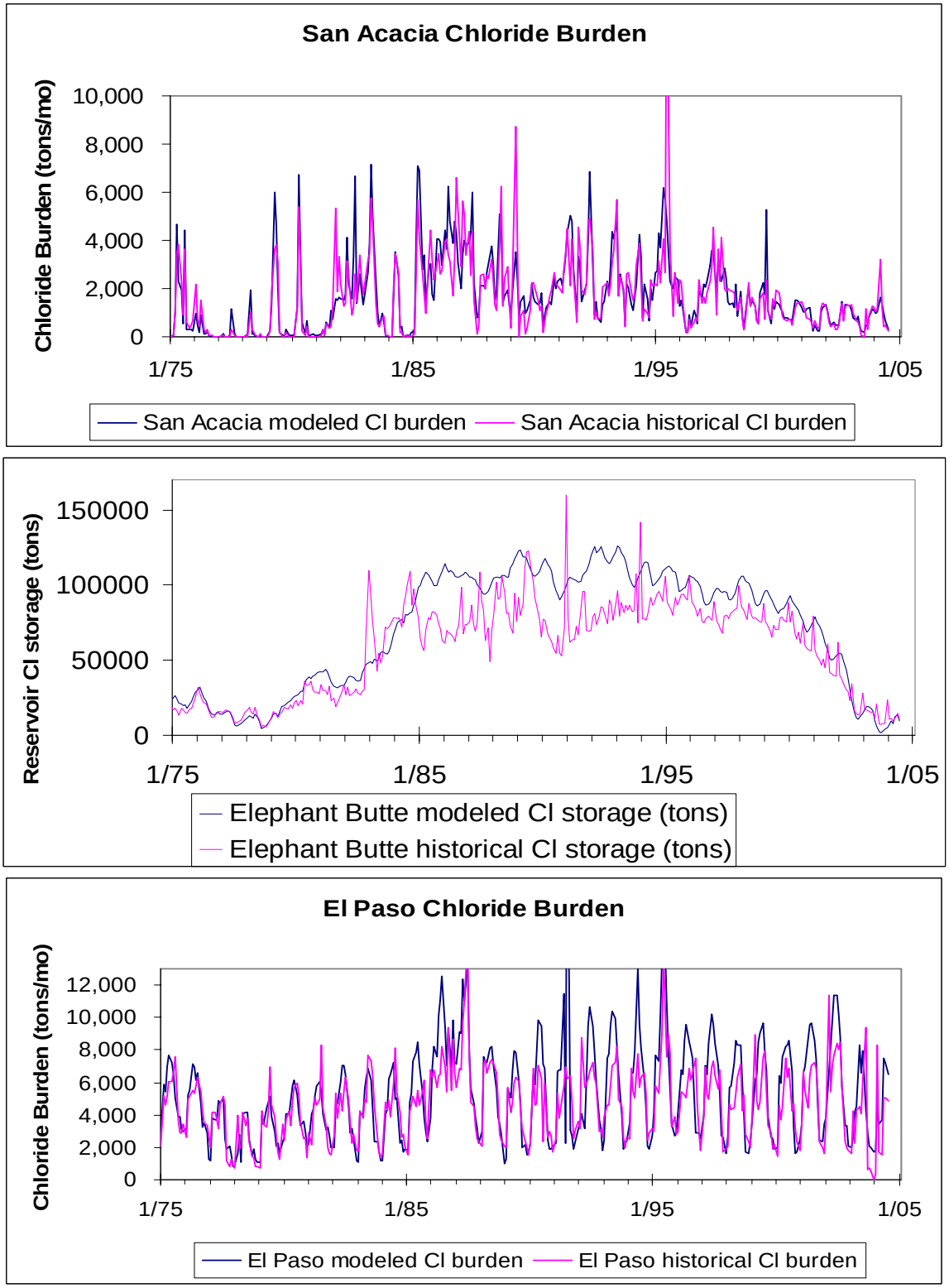

Figure 5-26. Modeled and historical chloride burden in tons mo^{-1} with added brine inflows for selected gaging stations on the main-stem Rio Grande including San Acacia, Elephant Butte Dam, and El Paso. Historical chloride burden is shown in pink and modeled in blue.

The model was not able to capture all of the variations in chloride concentration in the river (Figures 5-27 and 5-28). A major limiting characteristic of the model is in how chloride concentration is calculated. The model calculates chloride-burden outflow from each reach based on the inflows and outflows for that reach. It then divides the chloride burden by the discharge to get a chloride concentration for the outflows from the reach. The problem with this is that when discharge in the river approaches zero it causes the chloride concentration to spike, and when discharge equals zero the model fails to compute reasonable results. This may actually be representative of a limitation of the groundwater model in that it cannot adequately represent flow of salinity into the river from the subsurface during dry times. The other problem with simulating chloride concentration in this model is the availability of historical data. USGS chloride-concentration data availability is limited to one or two samples per month from each sampling location. For the purposes of this model, these samples were assumed to represent an average chloride concentration for the month at a given location. However, chloride concentration in the Rio Grande is highly variable (Mills 2003), so these isolated samples may not accurately represent the average for the month. Additionally, the model uses a constant, average chloride concentration for inputs such as tributaries and wastewater (due to lack of high temporal resolution data for these sources), so the outflow chloride concentration for each reach does not represent jumps in chloride concentration of such inputs, which may be reflected in the historical Rio Grande chloride-concentration data. Also, the chloride concentration of outflow from the reservoirs in the model is smoothed out in comparison with the historical data (Figure 5-26). This is because the model assumes that the reservoirs are well mixed, which may not be a valid assumption.

The most obvious discrepancy between modeled and historical chloride concentration is at El Paso (Figure 5-26). This discrepancy is due to frequent very low discharges in the river at El Paso, which make it difficult for the model to calculate chloride concentration. Since discharge at El Paso is very low in the winter, when water is not being released from Elephant Butte Reservoir, this reach of the model was calibrated to slightly overestimate discharge in the winter by slightly increasing seepage of groundwater into the river during winter. When chloride burdens are divided by these discharges it results in an underestimate in chloride concentration in the winter at El Paso.

A summary of model results compared with historical data is given in Tables 5-4 through 5-9. Equations similar to those in Equations 5-4 through 5-6 were used to compute errors. The percent error between modeled and historical discharge, chloride burden, and chloride concentration was computed for each reach at which enough historical data were available to make a meaningful comparison with model results. The percent-error calculation was somewhat misleading where historical values (especially discharge and chloride burden) were low. Low historical values caused high percent error values. Therefore, the absolute value of the difference between modeled and historical values was also computed. This value was compared with the average values for each reach to give an alternative evaluation of error.

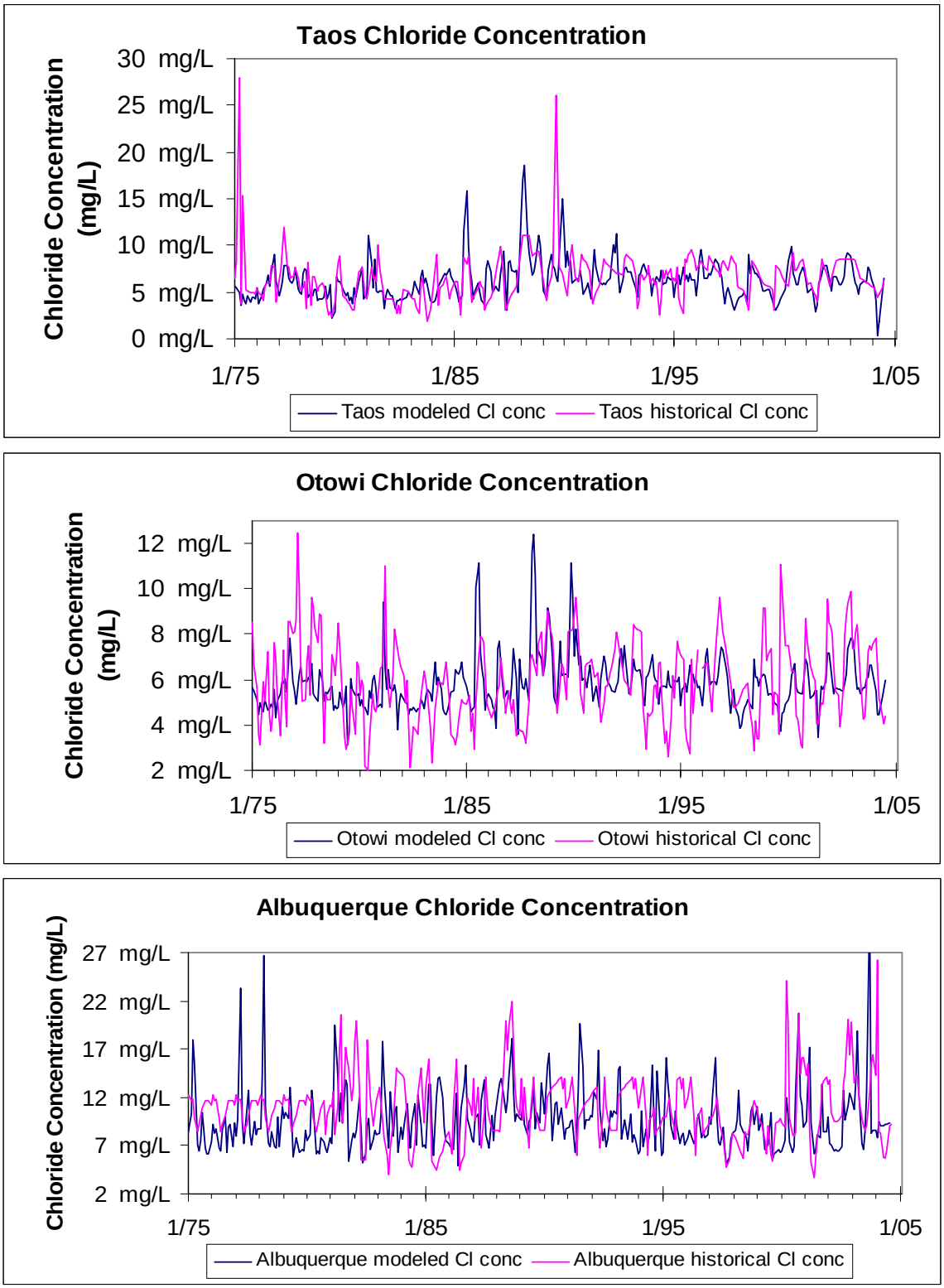

Figure 5-27. Modeled and historical chloride concentration in mg L^{-1} with added brine inflows for selected gaging stations on the main-stem Rio Grande including Taos Junction Bridge, Otowi, and Albuquerque. Historical chloride concentration is shown in pink and modeled in blue.

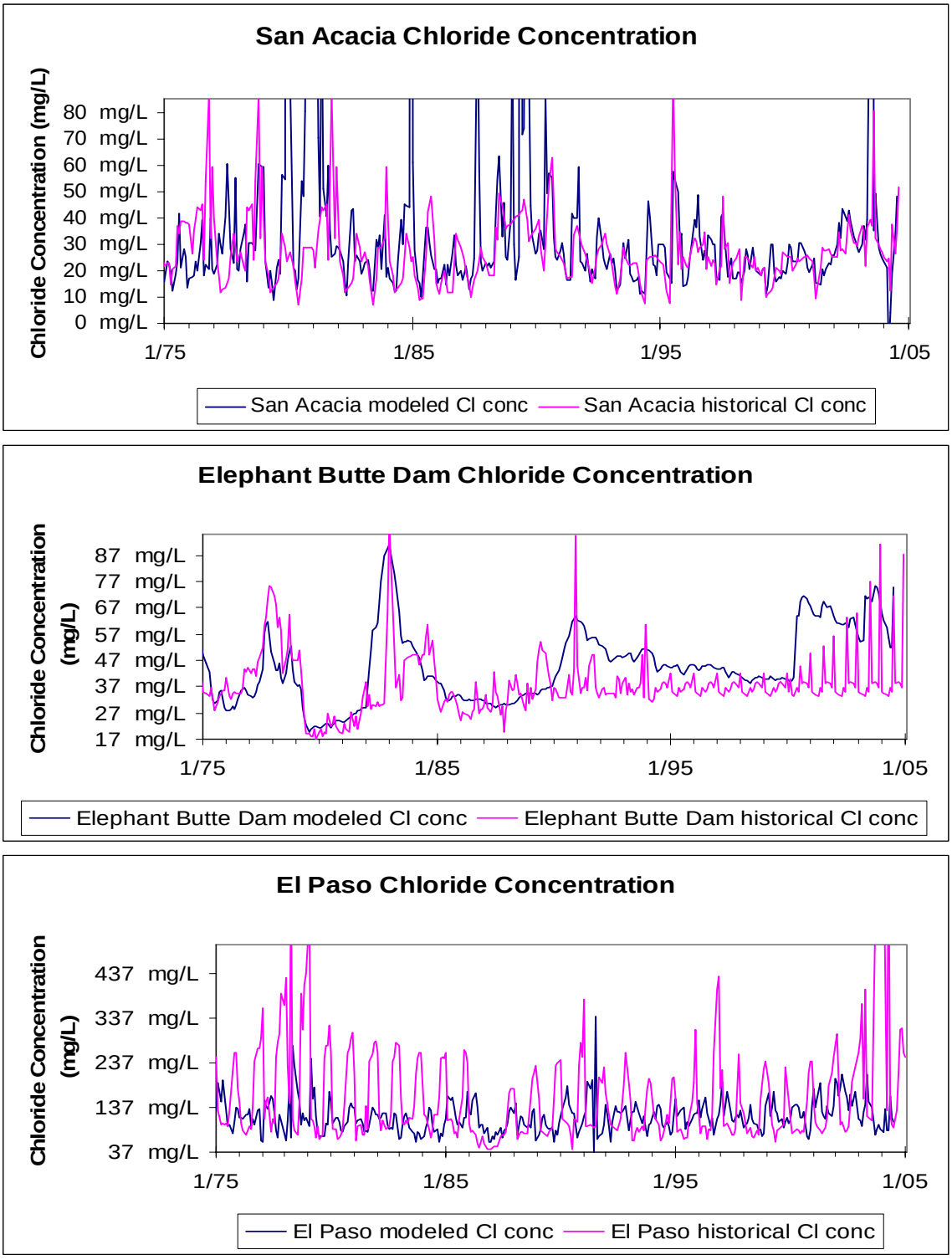

Figure 5-28. Modeled and historical chloride concentration in mg L^{-1} with added brine inflows for selected gaging stations on the main-stem Rio Grande including San Acacia, Elephant Butte Dam, and El Paso. Historical chloride concentration is shown in pink and modeled in blue.

Table 5-8. Summary of errors between model and historical values for chloride burden (tons/mo) from the model simulation with brine inflows from 1975 to 2004. Errors were computed for all stations for which historical chloride-concentration data were available. Error calculations include percent error between historical and modeled, absolute value of error between historical and modeled, and the absolute value of the error expressed as a percent of the average historical value. All errors are averaged over the simulation period.

Station	Average Percent Error	Average Absolute Error (tons/mo)	Average Historical Chloride Burden (tons/mo)	Average Absolute Error Percent of Historical Average Discharge
Taos	28	115	333	35
Otowi	26	165	581	28
San Felipe	26	158	682	23
Albuquerque	37	334	1004	33
Bernardo	349	476	1301	37
San Acacia	128	527	1643	32
San Marcial	382	755	1630	67
Elephant Butte Dam	32	889	2720	30
El Paso	34	1386	4583	30

The water-and-chloride-mass-balance model developed was successfully used as a tool to estimate brine inflows to the Rio Grande over time. The model also gave an indication that brine inflows to the river may be influenced by climate. However, as a mass-balance model, it does not fully represent the physical processes which control brine inflow to the river. The groundwater model in the middle Rio Grande does simulate heads in groundwater and surface water, but head gradients are not simulated in the rest of the river. Therefore, this model acts as a tool to understand the historical chloride record, but may not adequately predict future conditions in the chloride cycle of the Rio Grande.

Table 5-9. Summary of errors between model and historical values for chloride concentration (mg L^{-1}) from the model simulation with brine inflows from 1975 to 2004. Errors were computed for all stations for which historical chloride-concentration data were available. Error calculations include percent error between historical and modeled, absolute value of error between historical and modeled, and the absolute value of the error expressed as a percent of the average historical value. All errors are averaged over the simulation period.

Station	Average Percent Error	Average Absolute Error (mg/L)	Average Historical Chloride Concentration (mg/L)	Average Absolute Error Percent of Historical Average Discharge
Taos	27	2	7	26
Otowi	26	1	6	24
San Felipe	25	1	6	23
Albuquerque	32	3	11	31
Bernardo	30	5	18	27
San Acacia	129	35	27	129
San Marcial	135	40	33	122
Elephant Butte Dam	32	12	38	31
El Paso	47	85	161	53

5.4 Bromide-Balance Model of the Rio Grande

Bromide in the Rio Grande was modeled by adapting the Rio Grande chloride-balance model described in Section 5.3.2. Very little bromide data are available for the Rio Grande. The USGS does not collect bromide samples from gaging stations; therefore, the only Rio Grande and tributary bromide-concentration data used in the model were field sampling data collected from January 2000 to August 2004 as part of this study. The average Cl/Br ratio was computed for the Rio Grande at Lobatos as well as for tributaries and wastewater from all available field data (Table 5-10). The chloride inputs for tributaries and wastewater as well as starting chloride-concentration values for reservoirs and aquifers from the chloride-balance model were divided by the Cl/Br ratios in Table 5-10 to obtain bromide-concentration-input values for the bromide model (Table 5-11). Bromide concentration of inflow at Lobatos was estimated by dividing the historical chloride-concentration values at Lobatos by the average Cl/Br ratio from field data. As in the chloride-balance model, tributaries and wastewater were considered to have a constant concentration, whereas inflow at Lobatos varied according to the historical record.

Table 5-10. Cl/Br ratio values used to calculate bromide concentration inputs to the Rio Grande bromide-balance model. Cl/Br ratio values are averages of all field data available for each location. Cl/Br ratio values for wastewater are an average of field data collected for the Albuquerque wastewater treatment plant.

	Tributary Cl/Br	Other Tributary Cl/Br	Local Inflow Cl/Br	Wastewater Cl/Br
RG1	95.8		95.8	
RG2	146.5	146.5 (Rio Pueblo de Taos)	146.5	280
RG3	154		154	
RG4	292		218	
RG5	384		384	280
RG6	242.7			
RG7	150	384 (Jemez R)		280
RG8	150			280
RG9	575			
RG10				280
RG11	-	-	-	-
RG12				280
RG13				
RG14				280
RG15				280

	Starting Reservoir Cl/Br	Starting Aquifer Cl/Br	Headwaters Cl/Br	El Paso Cl/Br
RG1			138.84	501.34
RG2				
RG3				
RG4				
RG5	197			
RG6		231		
RG7		231		
RG8		231		
RG9		231		
RG10		231		
RG11	418	231		
RG12	470.2	231		
RG13		231		
RG14		231		
RG15		231		

Table 5-11. Bromide concentration values used as input to the Rio Grande chloride-balance model. Bromide values for were estimated from the chloride model inputs by dividing by the Cl/Br ratios from Table 5-7.

	Tributary Br conc	Other Tributary Br conc	Local Inflow Br conc	Wastewater Br conc
RG1	0.02		0.02	
RG2	0.04	0.05 (Rio Pueblo de Taos)	0.04	0.34
RG3	0.03		0.03	
RG4	0.02		0.02	
RG5	0.01		0.01	0.34
RG6	0.15			
RG7	0.01	0.20 (Jemez R)		0.34
RG8	0.07			0.34
RG9	0.19			
RG10				0.34
RG11				
RG12				0.71
RG13				
RG14				0.71
RG15				0.71

	Starting Reservoir Br conc	Starting Aquifer Br conc
RG1		
RG2		
RG3		
RG4		
RG5	0.03	
RG6		0.03
RG7		0.04
RG8		0.07
RG9		0.11
RG10		0.08
RG11	0.13	0.08
RG12	0.11	0.10
RG13		0.11
RG14		0.18
RG15		0.18

The model was run from 1975 through 1999 without addition of brine inflows in an attempt to estimate the Cl/Br ratio of the brine inflows to the Rio Grande, which would give more information about the origin of the brine. Historical bromide load for several locations along the river was estimated by dividing the historical chloride load by the average Cl/Br ratio from field data for the purpose of evaluating the model results. Even without the brine inflows, the model consistently overestimated bromide load at El Paso (Figure 5-29) as well as at other locations along the river. This overestimation of bromide load means that the model cannot be used to calculate the Cl/Br ratio of brine inflows, since they are not present in the bromide simulation. The overestimation is most likely due to poor bromide data availability. The results of this simulation could indicate a lack of sinks of solutes in the model, but it is difficult to determine if this is true since the bromide data are so sparse.

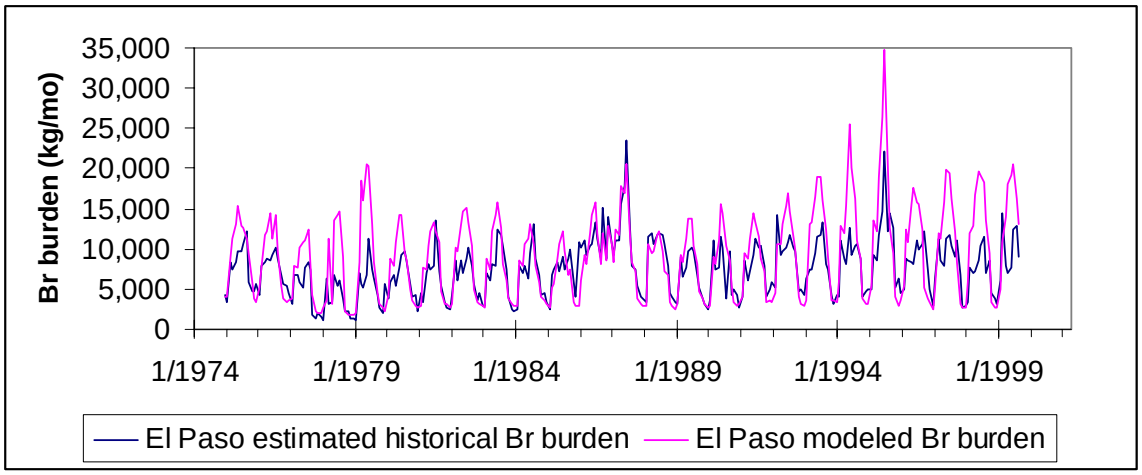

Figure 5-29. Modeled bromide burden plotted with estimated historical bromide burden at El Paso. El Paso bromide burden was estimated by dividing the historical chloride burden at El Paso by the average Cl/Br ratio from field samples.

5.5 Conclusions of Rio Grande Chloride and Bromide Modeling

Historical chloride concentration and discharge data were used in hydrologic modeling to simulate the solute history of the Rio Grande. Modeling of Elephant Butte Reservoir revealed a significant, unexplained source of chloride in the reservoir, which contributed 114,500 tons of chloride between 1979 and 2004, the majority of which flowed into the reservoir as the reservoir level was dropping. Modeling of the river from Lobatos, CO, to El Paso, TX, revealed sources of chloride at San Acacia, the LFCC, and between Elephant Butte Dam and El Paso, all of which contributed on average at least 16% of the total chloride load in each reach. The chloride additions at these locations were not constant over the historical record but varied over time, and these variations were weakly correlated with discharge. Brine inflows at San Acacia and El Paso showed a weak negative correlation with the drought index.

Figure 5-30 plots the cumulative contribution of chloride to the Rio Grande from different sources of salinity. The average chloride burden over the simulation period for each source was calculated and then summed up cumulatively over the length of the river. Modeled chloride burden from the LFCC was included in the agricultural returns, whereas brine inflow to the LFCC was included with brine inflows. The average chloride burden at Lobatos for the simulation period is plotted as a reference point. The most significant source of chloride cumulatively over the length of the river is wastewater. Wastewater contributes an average of 1,871 tons of chloride per month cumulatively to the Rio Grande. Additions of wastewater are localized and are most significant at Albuquerque, Mesilla, and El Paso. Brine inflows are the second most significant source of chloride to the portion of the Rio Grande studied. Brine inflows contribute an average of 1,716 tons of chloride per month to the Rio Grande cumulatively. It is estimated that brine is added to the river at San Acacia, the LFCC, and El Paso, the largest of these additions being at the LFCC. Tributaries are also a significant source of chloride to the Rio Grande, contributing an average of 1,078 tons of chloride per month to the river. Tributaries make the most impact on the upper and middle Rio Grande. The Ojo Caliente, Rio Puerco, and Rio Salado are some of the most significant tributaries to the Rio Grande in terms of chloride load. The Ojo Caliente, which enters the river between Embudo and Otowi, contributes on average 234 tons of chloride per month and the Rio Puerco and Rio Salado, which enter the river between Bernardo and San Acacia, jointly contribute on average 236 tons of chloride per month to the river. Agricultural return flows are not really considered to be a source of chloride to the river themselves, but then can transport stored salts and saline groundwater to the river. In Figure 5-30 the most significant increase in agricultural return chloride burden occurs between San Marcial and Elephant Butte Dam, where the LFCC enters the river. In the model, some chloride is picked up by the LFCC from groundwater before it enters the river, which may be due to error in the groundwater portion of the water-balance model for this section of the river.

Figure 5-31 shows what the chloride burden of the Rio Grande would be without each of the previously mentioned sources of chloride. The dotted line shows the average modeled chloride burden of the Rio Grande with all chloride sources included and the other lines show the cumulative average chloride burden of the Rio Grande without each source of chloride. It is evident from the graph that tributaries affect the chloride burden of the river most in the upper Rio Grande and have less relative impact on the chloride burden in the lower Rio Grande. In the lower Rio Grande, brine inflows and wastewater are of greater relative importance to the chloride burden.

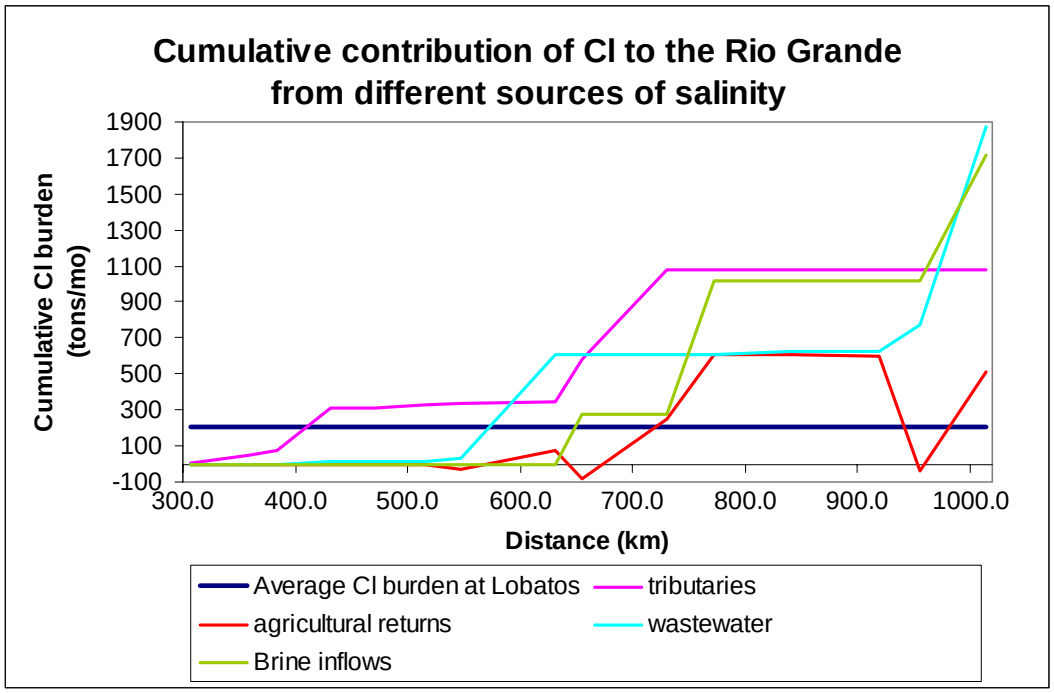

Figure 5-30. Cumulative contribution of chloride to the Rio Grande from different sources of salinity including agricultural returns, tributaries, wastewater, and brine inflows.

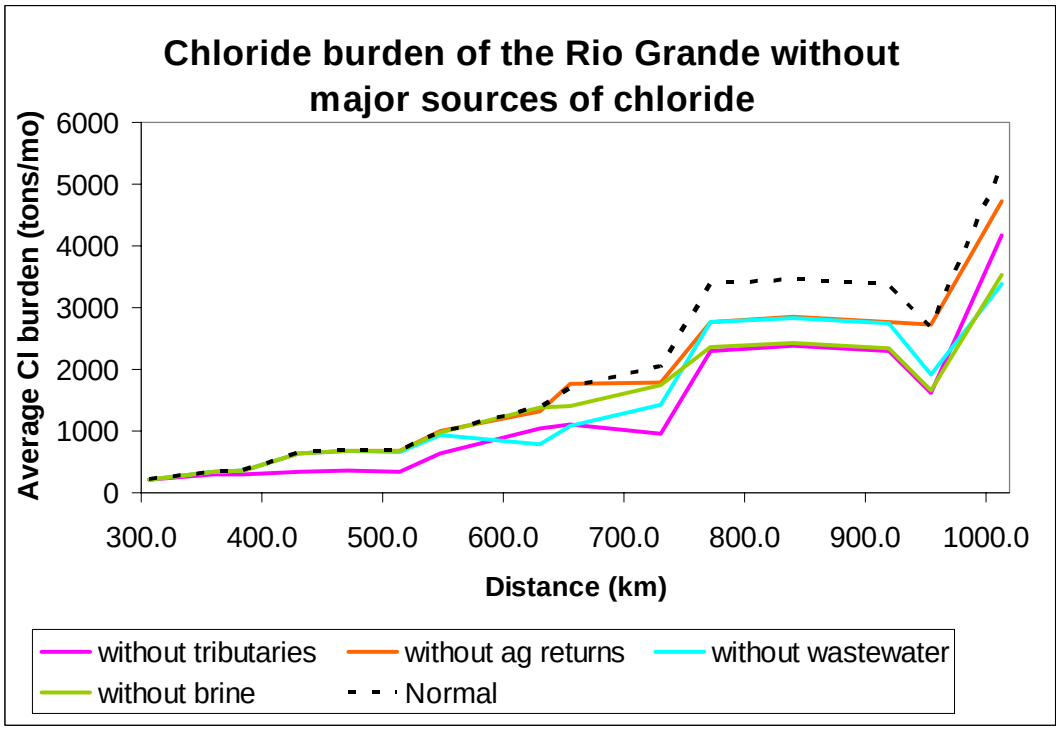

Figure 5-31. Chloride burden of the Rio Grande without major sources of chloride. Each line represents the modeled chloride burden of the Rio Grande without a major source of chloride. The dotted line represents the modeled chloride burden of the river including all of the chloride sources for reference.

The results of modeling the solute history of the Rio Grande suggest that salinization of the Rio Grande cannot be attributed entirely to the effects of irrigated agriculture, as earlier Rio Grande salinity studies suggested. Evapotranspiration from agriculture and reservoirs does play a role in salinization of the river, as does wastewater. However, analysis of field data and model results support the conclusions of Mills (2003), Moore and Anderholm (2002), and Phillips et al. (2003) that a significant portion of the salinization of the Rio Grande is geologically controlled and can be ascribed to localized deep brine fluxes controlled by geologic structures and possibly geothermal activity. Furthermore, model results suggest that brine has consistently been added to the river at the locations mentioned above, but that these additions have not been constant over time, but respond to changes in the system, in particular to drought conditions and river discharge.

Further modeling could be used to look at other constituents in water to determine if other solutes show the same or different trends in the river as chloride. Studying other constituents may give a clue as to how water is cycled through agricultural areas and how water chemistry is affected by agriculture. Also, adding more physical detail to the model, especially improving groundwater modeling, may provide a better understanding of physical processes that affect inflow of brine to the Rio Grande.

Rio Grande chloride data show that salinization of the Rio Grande is not a gradual process with distance downstream. Rather, the increase in salinity occurs in steps at certain points along the way. Modeling has identified the key processes controlling salinization to be natural tributaries, brine upwelling, wastewater, and agricultural returns. These first two processes are naturally occurring, the effects of which on salinization of the river can probably only be mitigated by increasing discharge in the river in order to dilute the concentration of salts. The latter two causes of salinization, agricultural ET and wastewater, are human-caused. Therefore, it may be possible to reduce their effects on river salinization. Understanding the processes affecting Rio Grande salinization is crucial to planning for the future water needs of the residents of the Rio Grande Basin.

6. ECOLOGIC PROCESS MODULES

Howard D. Passell, Will J. Peplinski, Len A. Malczynski, Marty L. Ennis
Sandia National Laboratories

6.1 Introduction

Managing endangered aquatic species populations is a complex task demanding the integration of knowledge from many areas of expertise, including biology, ecology, hydrology, and toxicology. The already complex interactions among all these disciplines are further complicated by spatial dynamics (i.e., varying land uses across a region), and temporal dynamics (i.e., precipitation and river discharge trends over time), as well as by impacts of human activities at multiple scales. Understanding the interactions among all these variables and the relative importance of each is crucial to managing natural resource systems and maintaining viable species populations. Computational tools are helpful for integrating data and knowledge, and for understanding interactions between those complex dynamic systems.

6.1.1 Objectives

This chapter describes an effort to model the population dynamics of the endemic Rio Grande silvery minnow (RGSM) (*Cyprinidae*: *Hybognathus amarus*), a federally listed endangered fish species in the Rio Grande of central New Mexico, USA. The modeling effort is placed in the context of complex water quality, hydrological, toxicological, and anthropogenic impacts. The model is intended to be a first-order tool for better understanding the interactions among systems associated with RGSM population dynamics, and for leading to better data collection and to more tightly targeted studies. This module also provides a generic framework which can be applied to other fish in other rivers, although some degree of system-specific parameterization and modification would be required to tailor this model to other cases.

6.1.2 Background

The silvery minnow is the last surviving endemic pelagic minnow of the family *Cyprinidae* in the main-stem of the Rio Grande (USFWS 1999). Four other cyprinids have been extirpated from the main-stem of the Rio Grande (Sublette et al. 1990). The current habitat of the silvery minnow in the middle Rio Grande represents about five percent of its historic range, which once included extensive parts of the Rio Grande, Rio Pecos, and Rio Conchos (USFWS 1999). Although long-term population data for the RGSM are not available, recent data show considerable variation in populations, including some trends of precipitous decline (Dudley and Platania 2002; USFWS 2003). Hydrological changes throughout the Rio Grande (dams, channelization, diversions, desiccation, etc.) are frequently blamed for the decline of silvery minnow populations. Biological factors such as predation, competition with non-native species, and changes to algal community structure and productivity also may have contributed to silvery minnow declines (USFWS 2003). Water quality also may have contributed to the precipitous decline, but the role that changes in water quality play in the decline of silvery minnow populations has been difficult to assess or quantify (USFWS 2003). Silvery minnow survival has

become highly politicized, and now has strong effects on regional water management, agriculture, urban growth, and politics.

6.2 Methods

The model is built in Powersim Studio 2005, and runs on a monthly timestep from 1975 through 2005. The model is arrayed over three dimensions; it includes six reaches (Cochiti to San Felipe, San Felipe to Central, Central to Bernardo, Bernardo to San Acacia, San Acacia to San Marcial, San Marcial to Elephant Butte) and two genders (male and female), distributed over either 48 or 24 monthly age cohorts. Array ranges are abbreviated (r,s,a) for reach, sex, and age. Ranges are explicit in the discussion below to show generalities within the model.

Initial model development and paramaterization were completed with data and information from numerous sources within the literature (Sublette et al. 1990; Bestgen and Platania 1991; Platania and Altenbach 1998; USFWS 1999, 2001, 2002a, 2002b, 2003; Buhl 2002; Dudley and Platania 2002; Passell et al. 2005; Passell et al. in review)

and with data and information from personal communications with various regional RGSM experts (David Cowley, Cliff Dahm, Rob Dudley, Mike Hatch, Joel Lusk, Steve Platania, Tom Turner; personal communication).

Fish population P follows the general equation

$$P(r,s,a)_{t+1} = P(r,s,a)_t + B(r,a)_t - D(r,s,a)_t - M(r,s,a)_t + M(r\pm1,s,a)_t$$

where:

B is number of eggs, or births	$B(r,a) = (P(r,a) / 2) \times$ Fertility (a)
D is number of deaths	$D(r,s,a) = P(r,s,a) \times$ DeathRate(r,a)
M is number of migrations	$M(r,s,a) = P(r,s,a) \times$ MigrationRate(r,a)

Many life history traits for the RGSM are uncertain, so the model is built to allow users to test the impact of some of those uncertainties. In the reference (or default) run, there are 48 monthly age cohorts representing fish that live four years; the user can also simulate 24 monthly cohorts for a fish that lives only two years. In the reference run, females between 12 and 48 months old breed each May/June and lay a varying number of eggs per female, with egg-laying capacity increasing as age and body size increase. The user can also vary these values.

For each reach of the river the death rate is calculated as

DeathRate(r,a) = background mortality(a) + discharge mortality(r) + ammonia mortality(r)

The model includes the capability to test user-defined "background mortality" by age and gender, as well as user-defined "discharge mortality" relationships and user-defined "ammonia mortality" relationships. Discharge mortality (Figure 6-1) refers to mortality associated with variations in discharge, and ammonia mortality (Figure 6-2) refers to mortality associated with aqueous ammonia concentrations calculated for each river reach in the model. For these model runs we maintained a uniform value of background mortality across gender.

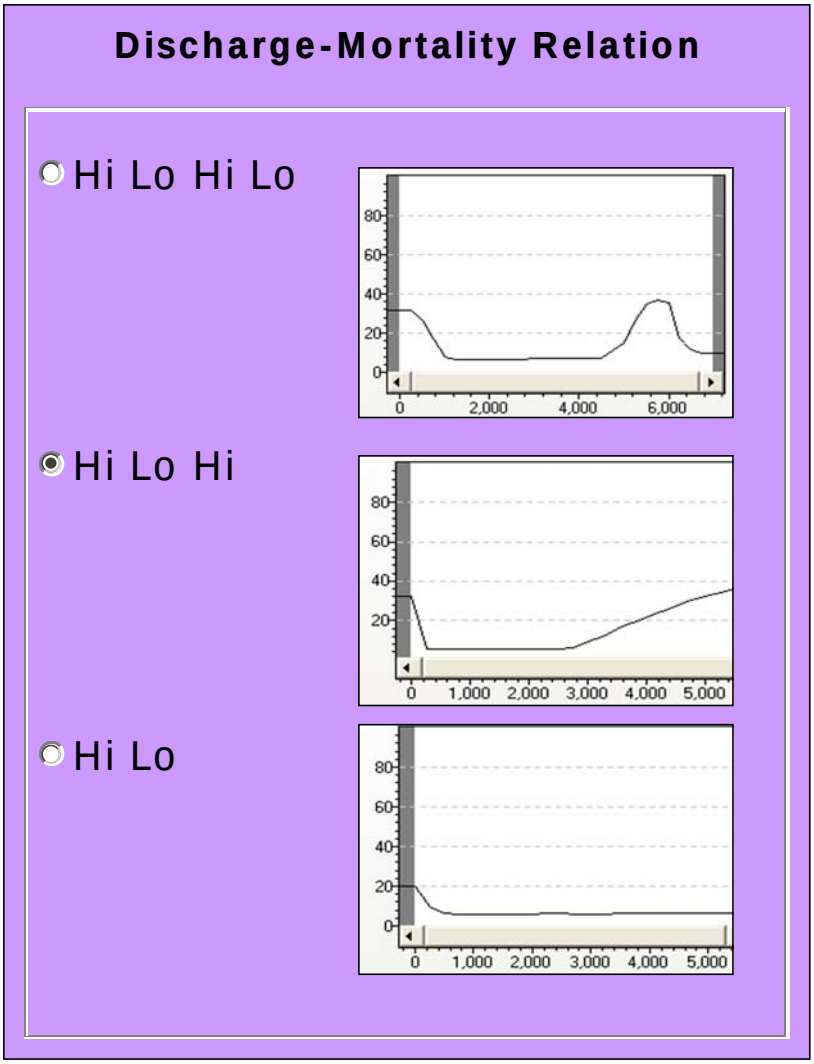

Figure 6-1. Discharge mortality relationship.
Y axis is percent mortality, X axis is river discharge in cubic feet per second.
These relationships are hypothetical. Sensitivity analyses were done for each of the different relationships. For each, the mortality rate was halved and doubled.

Discharge data come from historic values. Point source ammonia concentrations are calculated using historic population, ammonium and Albuquerque's South Side Water Reclamation Plant (SSWRP) discharge, extrapolations of historic data, estimated loss rates, and standard NH_4/NH_3 equilibrium calculations (Passell et al. in review). Biological and adsorptive losses of NH_4 are subtracted for each timestep and are user-controlled. Volatilization of NH_3 is treated as an exponential loss based on the length of the individual reaches. Non-point source ammonia concentrations are calculated using agricultural acreages per reach and estimated NH_4 runoff values per acre.

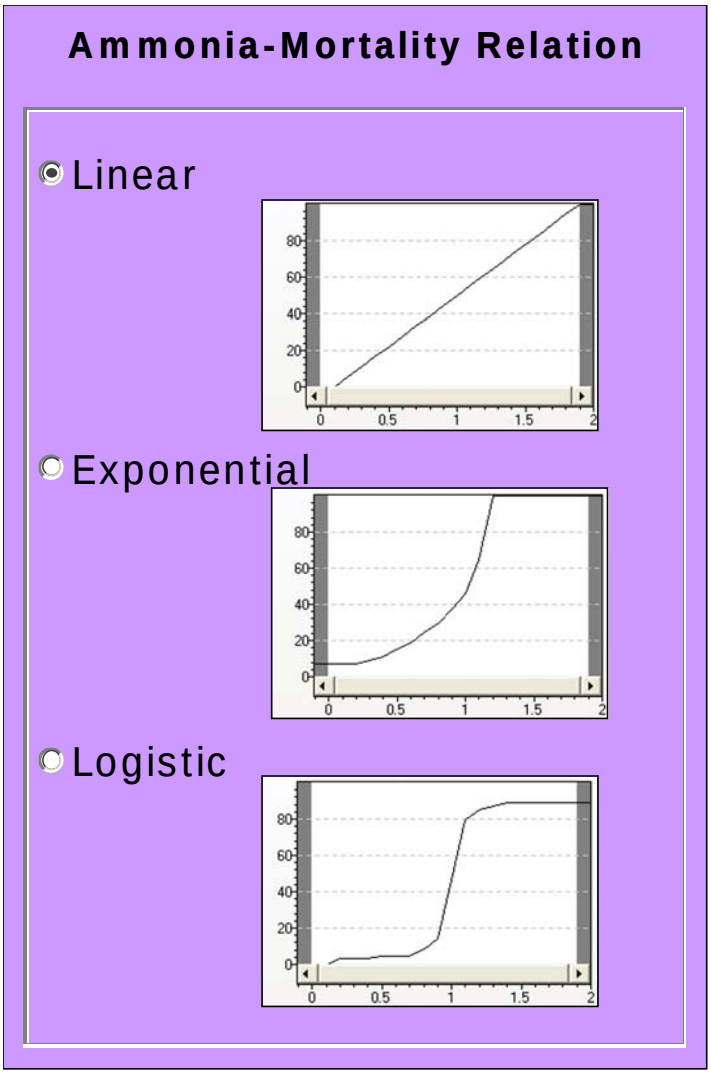

Figure 6-2. Ammonia mortality relationship. Y axis is percent mortality, X axis is ammonia concentration in the river in mg/L. Linear relationship was used in the reference run. All relationships are hypothetical. Since ammonia mortality played such a small role in overall minnow mortality, no sensitivity analyses were done using these variables.

The model allows for user-defined initial fish concentrations per mile for each reach, and allows for user-defined, upstream and downstream migration rates between reaches. Migration rates are age-dependent, as most eggs and larvae will float downstream while adult fish will likely remain in one location. This feature can be controlled with an on-off switch and can be used to simulate diversion dams blocking upstream migration. The model has a linear, density-dependent carrying capacity function that serves to limit population explosions. A carrying capacity is chosen by the user and as the population approaches that value mortality increases in the specific reach. This function was not used in the analyses reported upon in this paper because the authors felt that limiting dramatic population explosions with a density-dependence function could mask poor model structure or parameterization.

After initial model development was complete, we calibrated the model so that it returned population dynamics similar to those found for the RGSM in empirical field studies. Calibration was performed by manipulating the impact on population dynamics made by the combination of discharge and ammonia mortality. A "calibration" slider bar was constructed to facilitate the calibration process. A zero percent value on the calibration slider bar meant that ammonia and discharge mortality were completely ignored, and that model results reflected simple population cycling driven by seasonal births and deaths. A 100 percent value on the slider bar meant that discharge and ammonia mortality operated with full strength on population dynamics, using default values and calculations for both forms of mortality. A zero percent setting on the calibration slider bar returned regular cycling of the population, with little net average gain or loss in individuals over the 31 years (1975–2005). A 100 percent setting on the slider bar causes populations to crash dramatically in all reaches within a few years. A setting of 15 percent returns results that are biologically reasonable, i.e., populations become extinct in some reaches and persist in others, all at levels that are reasonable relative to actual historic dynamics in the middle Rio Grande, poorly understood as they are. Discharge and ammonia mortality for the RGSM were used as calibration parameters because the actual nature of those relationships is so poorly known.

Sensitivity analysis (SA) coefficients were calculated following Brugnach (2005), such that Sensitivity = $[(O\text{p} - O\text{b})/O\text{b}] / [(P\text{p} - P\text{b})/P\text{b}]$, where Pb is the baseline output from the process, Pp the output from process after perturbing it, Ob the baseline response variable that is subject to analysis, and Op the perturbed response variable that is subject to analysis (Brugnach 2005).

SAs were performed using the reference run of the model as a background against which changes to individual parameter values were tested (Tables 6-1 and 6-2). The reference run includes the calibration slider bar set at 15 percent. SAs were performed on all the important variables of the model, including the calibration slider bar. SAs were performed by starting with the model in the reference run, selecting one variable at a time, and then both doubling and halving the value for the selected variable and observing the response to the model output. Model output is measured in adult minnows per reach, with an adult defined as a minnow over 7 months old.

For calculating SA coefficients (SACs), minnow population data are aggregated in the following way. In the model, populations by reach are calculated on a monthly timestep. The monthly populations are averaged into an annual population, and then the annual populations are averaged over the 31 years of the model run time. These annual average populations by reach for the reference run and the SA runs are used in the SAC calculation.

Description of the variables in the model to which SAs were applied, along with the reference run values, are shown in Table 6-3. Captive release scenarios are shown in Table 6-4.

Table 6-1. Sensitivity analyses parameters, reference run parameters doubled and halved.

RR * 0.5	Reach 2[1]	Reach 3	Reach 4	Reach 5	Reach 6
Initial Population	1.00	1.00	1.00	1.00	1.00
Migration Rate	-0.37	-0.01	0.01	-0.06	0.01
Fertility	1.86	1.04	0.69	1.18	1.82
Background Mortality	-9718878.69	-178848.39	-38835.13	-293570.75	-2379558.18
NH_3 Mortality	0.00	-0.11	-0.14	-0.46	-0.07
NH_4 Runoff	0.00	0.00	0.00	0.00	0.00
NH_4 BioLoss	0.00	0.15	0.34	1.17	1.84
Discharge HLH mortality	-299.34	-8.28	-3.76	-66.90	-339.79
Rio Grande Discharge	-0.71	0.21	0.19	0.41	0.77
Human Growth Rate	0.00	0.00	0.00	-0.03	-0.02
RR * 2					
Initial Population	1.00	1.00	1.00	1.00	1.00
Migration Rate	-0.20	-0.01	0.02	-0.04	0.01
Fertility	34828544.25	529684.66	91329.50	225998.87	18335353.28
Background Mortality	-0.97	-0.84	-0.57	-0.77	-0.95
NH_3 Mortality	0.00	-0.03	-0.06	-0.27	-0.07
NH_4 Runoff	0.00	0.00	0.00	0.00	0.00
NH_4 BioLoss	0.00	0.93	1.25	1.37	0.18
Discharge HLH	-0.91	-0.38	-0.40	-0.58	-0.91
Rio Grande Discharge	-0.69	-0.27	-0.06	0.06	-0.59
Human Growth Rate	0.00	0.00	0.00	-0.03	-0.02

[1]Field research indicates that there may be no RGSM in Reach 1, so in the reference run the starting fish population is reduced to zero in that reach.

6.3 Results

Sensitivity coefficients ranged in value from smaller than 1 into both the positive and negative millions for a few variables. A positive coefficient indicates a positive relationship between a variable and the model output, and a negative coefficient indicates a negative relationship. Also, a large coefficient indicates a large impact of the variable on the output, and a small coefficient indicates a small impact.

One of the first noteworthy sets of results offers a good example. SACs for background mortality*2 are very large negative numbers (Table 6-1). These occur because as background mortality rates go down, then average populations per reach go up and produce a negative coefficient. Further, if the background mortality rates are cut in half the population explodes, toward numbers as high as 2×10^{12}, producing very large negative coefficients.

Table 6-2. Sensitivity analyses parameters, and other modifications to reference run.

	Reach 2[1]	Reach 3	Reach 4	Reach 5	Reach 6
Fish Lifespan 2 Years	-0.04	-0.03	-0.02	-0.02	-0.03
Variation in Discharge					
Mortality Graphs					
HLHL QM RR[2]	-48.00	-12.00	8.00	5.00	708.00
HLHL QM*.5	-347.12	-5.81	-2.91	-93.84	-196.82
HLHL QM*2	-0.87	-0.42	-0.38	-0.65	-0.98
HL QM RR[3]	247.00	-2.00	1.00	14.00	-34.00
HL QM*.5	-195.85	-13.63	-5.66	-86.18	-347.25
HL QM *2	-0.96	-0.44	-0.41	-0.65	-0.87
Captive Release Scenarios					
CR Sc2[4]	0.00	0.08	0.03	0.00	0.00
CR Sc3	0.00	0.03	0.01	0.11	0.04
CR Sc4	0.00	0.10	0.03	0.34	0.03
CR Sc5	0.00	0.05	0.02	0.22	0.07
CR Sc6	0.00	0.21	0.05	0.68	0.06
Migration Scenarios[5]					
Migration Off	42.00	1.00	-1.00	6.00	-1.00
Migration Split	0	-1.00	0.00	2.00	-6.00
Fish Passage	--	--	0.40	-0.10	--

[1]Field research indicates that there may be no RGSM in Reach 1, so in the reference run the starting fish population is reduced to zero in that reach.

[2,3,4]Numbers in these sections are not SACs, but describe the percentage change in population when using the HLHL curve, the HL curve, and the various captive release scenarios, respectively, in the reference run.

[5]All numbers describe percentage change from Reference Run. "Migration Off" allows no migration, "Migration Split" sends half of migrating fish upstream, half downstream; "Fish Passage" assumes upstream migration from Reach 5 to Reach 4, simulating a fish passage around a diversion dam.

The SACs for background mortality*2 are small negative numbers. These are negative because as background mortality increases, populations in many cases go extinct. However, in the reference run the average number of adult fish per reach range from the tens to the hundreds of thousands, and so the decline of those already small populations to zero does not produce a large SAC.

The SACs for fertility show a similar dynamic. After cutting fertility rates by half, all populations become extinct within 27 years in the simulation, but since populations are small to begin with the decreases return SACs of small positive numbers, from +0.69 to +1.86. Doubling the fertility rate, on the other hand, causes the population to explode to the order of 1×10^{14}, returning very large SACs.

Table 6-3. Description of variables to which sensitivity analyses were performed.

Initial Population	8,560 fish/km, based on studies done by U.S. Fish and Wildlife Service Albuquerque District Office.
Migration Rate	Rates are equal for males and females; they are 85, 40, 20, and 10%/month for fish aged 1,2,3, and 4 months, respectively. At five months and older 8%/month migrate. All migration goes downstream to next reach, except for last reach, from which there is no migration.
Fertility	Egg production first occurs in females at age of 12 months with 2,000 eggs, and increases throughout life span following an exponential curve ($y=1{,}511.9e^{0.0233x}$) to 4,412 eggs at 48 months.
Background Mortality	Monthly background mortality (not associated with discharge or ammonia) is 90, 80, 65, 50, 40, 30, and 20.8 percent for fish aged 1 to 7 months, respectively, and then is 20.8 percent for fish 8 months or older.
NH_3 Mortality	See Figure 6-2.
NH_4 Runoff	0.12 kg/acre/month is an approximation based on data presented in Woodside and Simerl (1995).
NH_4 BioLoss	NH_4 losses to biological uptake and adsorption before its conversion to NH_3 is set to 70%.
Discharge Mortality	See Figure 6-1.
Rio Grande Discharge	Actual historic data reported by the USGS.
Human Growth Rate	Actual historic data for Albuquerque.
Fish Lifespan	Reference run assumes fish live to 48 months. Sensitivity analysis assumes fish live to 24 months.

Table 6-4. Captive Release Scenarios (CRSs.)

CRS 1	Reference run (RR), as described in Table 6-3.
CRS 2	RR with 5 years of release, 1985–90, with two episodes of 50,000 fish released each November and April, for a total of 100,000 fish/yr released to Reach 3.
CRS 3	RR with 5 years of release, 1985–90, with two episodes of 16,000 fish released each November and April. 96,000 fish/yr released to reaches 3, 5, and 6.
CRS 4	RR with 20 years of release 1975–95, with two episodes of 16,000 fish released each November and April. 96,000 fish/yr released to reaches 3, 5, and 6.
CRS 5	RR with 5 years of release 1985–90, with two episodes of 32,000 fish released each November and April. 192,000 fish/yr released to reaches 3, 5, and 6.
CRS 6	RR with 20 years of release 1975–95, with two episodes of 32,000 fish released each November and April. 192,000 fish/yr released in reaches 3, 5, and 6.

Shifting the curve up and down along the Y-axis resulted in generally large but widely variable SACs for "discharge Hi-Low-H mortality" (Figure 6-1). "Hi-Low-Hi," or HLH, in Table 6-1 and Figure 6-1 refers to the pattern of the uppermost curve shown in Figure 6-1.

Reducing mortality relative to discharge increases population considerably in Reach 2 (SAC = -299.34) and Reach 6 (SAC = -339.79), but increases it much less in the other reaches

(ranging from approximately -4 to -67). Increasing mortality relative to discharge reduced the already small populations to extinction, resulting in relatively small SACs. Similarly, wide variation can be seen in testing of the HLHL and the HL discharge mortality relationships (Table 6-2 and Figure 6-1).

Testing "NH_4 BioLoss," using a linear ammonia mortality (middle curve in Figure 6-2), returns a very predictable set of dynamics in the SACs. Reducing the percentage of NH_4 lost to biological uptake and physical adsorption increases toxic ammonia concentrations and reduces the minnow population. Increasing the percentage lost decreases ammonia concentrations and increases the population. Similarly, increasing the percentage of NH_4 increases the population. The relatively small magnitude of the SACs (0.0 to 1.84) suggests that cutting ammonium loss terms by half in the river would in itself not have an extremely important impact on final populations. Since the impact of changing this term in the model is relatively small, and since ammonia mortality relationships are so poorly known — especially in the presence of other toxicants present in river water such as chlorine and copper (Buhl 2002) — no SAs were performed using the other ammonia mortality curves (Figure 6-2).

A surprising result of the SA is the very small impact of terrestrial NH_4 surface runoff rates on SACs, which appear as zeroes to two decimal places. Changes in fish lifespan, from 48 months in the reference run to 24 months in the test run, also result in very small SACs.

Three test scenarios were applied to migration variables. In the first, migration is turned off, so that no migration takes place at all. In the second, migration is split exactly in half between upstream and downstream migration, simulating a river with no impediments to upstream fish migration. In the third, downstream migration occurs at all the reaches but upstream migration only occurs from Reach 5. This scenario models the potential impact of fish passages that allow fish to swim upstream past diversion dams.

Different captive release scenarios and the changes associated with them are shown in Table 6-3.

6.4 Discussion

The model described here simulates population dynamics for a species for which many important life history characteristics are poorly known, and for which the relationships between population dynamics and environmental variables are poorly known. As such it cannot be expected to make robust predictions about future population dynamics in any absolute sense. This model's greatest value is its ability to begin to identify reasonable ranges of poorly known variables, to experiment with different strengths of interactions among those variables, and to identify and even help prioritize the most important data gaps.

A model like this returns two kinds of results, those that are completely predictable to researchers based upon the way the model was built, and those that create surprises for the researchers. The predictable results are reassuring to model developers and serve to verify or validate the model, since they show that the model behaves in a way that is consistent with researchers' understanding of the systems being modeled. The surprises that come from a model are the great prize associated with modeling exercises. The most valuable surprises are those

that illuminate some kind of property that emerges from the model's complex interactions, which without the help of the model would be too difficult for the researcher to see. However, great care must be taken in the assessment of the a model's surprises, since in most cases they are simply the logical result of the model structure and reflect not so much the emergent properties of interacting systems, but the intentions of the authors.

SAs were performed on the model to address all these issues. First, we wanted to test the model to find out if it behaved in a way that was consistent with our understanding of the systems being modeled. This was a kind of model validation or verification exercise, since unexpected results could point toward an error in model structure or data (Sterman 2000), as well as to an important insight into system dynamics. Also, we wanted to find out which parameters might have the greatest influence on population dynamics, and if the model could provide any special insights into those dynamics.

The variables tested in the SA represent most but not all the important variables in the model, and appear in Tables 6-1 and 6-2. Those described in the "Results" section, above, represent a subset of those variables. Variables in Tables 6-1 and 6-2 that appeared to have little important impact or pattern were omitted from Section 6.3.

The very strong response in the model to variations in mortality rates and fertility rates underlines the obvious importance of those variables in the study of a species' population dynamics. Similarly, the wide variation in SACs for all the different hypothetical discharge mortality relationships suggests that real minnow populations may be very sensitive to whatever the appropriate discharge mortality relationship might be. None of this is surprising, but it does help identify the importance of further field studies and data collection on those variables as some of the most important work that should be done in the interest of better understanding RGSM population dynamics.

The relatively unimportant impact of NH_4 BioLoss on minnow populations supports findings made by Passell et al. (in review), but this is no surprise since the modeling in the current project is styled after the modeling in the previous one. A surprising result does come from the SA of changes to NH_4 surface runoff rates, which showed very small SACs.

In general, non-point inputs, such as those that occur via land surface runoff and shallow groundwater seepage, are the major source of pollution to aquatic systems in the United States. Point sources of nutrient inputs also are significant sources for surface waters in urbanizing regions, and municipal wastewater — such as that produced by Albuquerque's wastewater treatment plant — is the primary point source of nitrogen in U.S. rivers (Carpenter et al. 1998; Mitsch et al. 2001; Passell et al. 2005). The very small impact of changes to NH_4 runoff rates in the model raises questions about the importance of land surface runoff to nitrogen levels in the Rio Grande, as well as about the structure and function of the model itself. Both questions require further work in the future.

The reference run included no releases of captively bred fish, although a captive breeding program has been adding fish to the Rio Grande for over five years. Captive Release Scenario 2 (Table 6-4) simulates the captive release program being implemented in Reach 3 twice annually.

Results show that the introduction increases the population in Reach 3 by 8 percent, and migration downstream increases the population in Reach 4 by 3 percent. These results suggest that the captive release program has a fairly small impact on fish populations in the Rio Grande, although results suggest that the program could be expected to prevent minnow populations from dipping into local extinction.

Captive release scenarios of increasing intensity increase fish populations throughout the reaches as expected. Captive Release Scenario 6 introduces 192,000 fish annually over 20 years in Reaches 3, 5 and 6, and populations in those reaches increase by 21, 67 and 6 percent, respectively. However, by the end of the 20-year period, graphs not included here show that even the 67 percent increase in Reach 6 is starting to decline, suggesting that the artificially increased populations are not sustainable.

6.5 Acknowledgments

We are especially grateful to David Cowley of the Department of Fisheries and Wildlife Sciences at New Mexico State University, Cliff Dahm and Tom Turner of the Department of Biology at the University of New Mexico, Rob Dudley and Steve Platania of American Southwest Ichthyological Research Foundation, and Mike Hatch and Joel Lusk of the U.S. Fish and Wildlife Service Albuquerque District Office for their generous help and advice on this project.

7. ECONOMIC AND DEMOGRAPHIC PROCESS MODULES

Janie Chermak, Jennifer Thacher, Kristine Grimsrud,
David Brookshire, and Jason Hanson, University of New Mexico

Len Malczynski, Sandia National Laboratories

7.1 Introduction

The impact of human behavior on a physical system is through the use of the resources in that system. In the case of the System Dynamics Toolbox, this includes the impact of the use of surface and ground water in the middle Rio Grande (MRG) valley. Water use provides market-based benefits to the population through direct consumption for survival, as an input to the production of other goods; for example, agricultural products, industrial and commercial products, or green lawns. Water also provides public values through nonmarket benefits; for example, shoreline value or birding values. The feasible set of human choices is obviously constrained by the physical system itself; for example, the quantity of water available in a river system. Thus a model of the human behavior/economic, physical system requires models that account for the simultaneous interaction between the components. This chapter focuses on the behavioral and economic components of the system.

The brief description above provides a snapshot of micro-level activities; that is, activities that are specific to a single water-use component such as urban residential demand, agricultural demand, or recreational demand.[5] Each of these competing uses is a micro-level use, which in turn can impact the macro-level economy of a region.[6] While the micro-level impacts can be measured through profits, or social welfare, the macro-level activity is measured in economic growth. Economic growth in turn impacts the micro-components through changes in population and/or through changes in per capita product. Thus, the economic components have to consider, at a minimum:

- the disaggregated, micro components of the system,
- the macro components of the system,
- the interactions between the micro and the macro system,
- the exogenous impacts to the system,
- temporal and spatial changes in the system, and
- the interaction between the physical and the behavioral components.

Figure 7-1 presents a schematic of the interactions. The arrows indicate potential interactions. Note that in most cases, the interaction can be in either direction. In the center of the figure are "Activities." These are the micro components of the model. Each of these may or may not

[5] It could be argued that each of these uses could be disaggregated to more micro levels, the most disaggregated considering behavior of a single agent within the composite activity. That level of disaggregation does not lend itself easily to dynamic simulation.

[6] The macro economy of a region is also impacted by exogenous factors such as the growth of the national economy.

interact with the other micro components. Each also can interact with the physical system through their use of water and through the impact on the physical system of the use and timing of use of the water. The micro components of the model are also tied to the macro economy. That is, each micro activity contributes the macro economy with the primary activity, as well as through secondary effects. The macro economy is also influenced through exogenous factors. The macro economy of the region, i.e., economic growth, impacts the population. Changes in population levels, due to economic growth or contraction, in turn impact the level of economic activity at the microeconomic level, which in turn impacts (and is impacted by) the physical system. Thus, policies, structural shifts, or shocks to any part of the overall system can have impacts throughout the system.

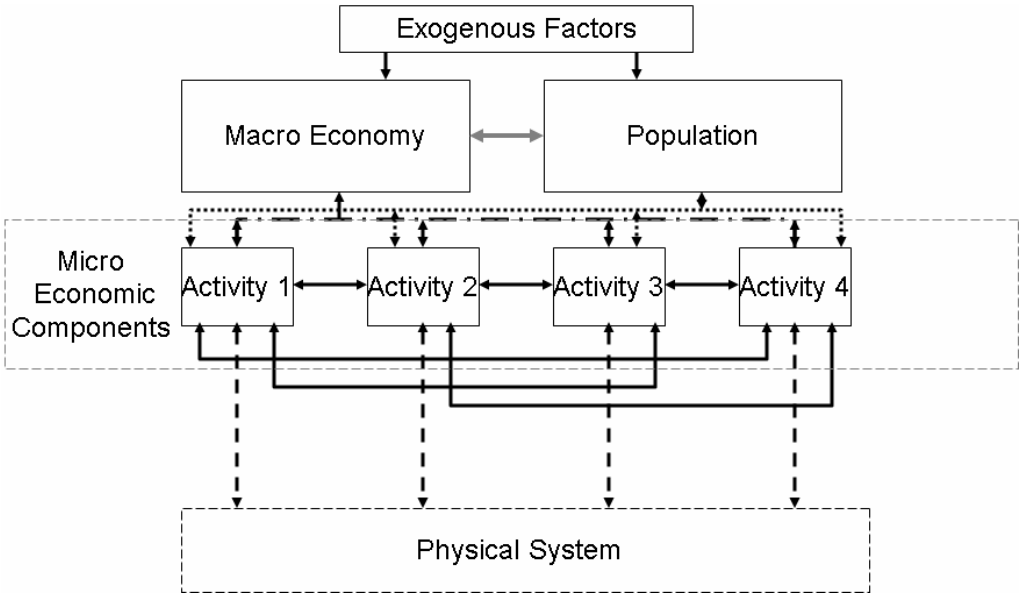

Figure 7-1. Interactions.

This chapter first presents a discussion of modeling components and their interactions followed by a description of each individual behavioral component. We begin with a presentation of the economic model of behavior, on which we base our components.

7.2 Economic Models

There are two levels of economic models that are included in the model: micro-level components and the overall, regional macro economy.

7.2.1 Microeconomic Models

From the economic perspective, an agent's actions are modeled based on the objective of maximizing net benefits, subject to constraints imposed and the incentives offered. Those benefits may be in the form, for example, of profits of the firm or consumer surplus. Constraints

may be budget constraints for the consumer or production requirements for the producer. Incentives can come in many forms, including prices and/or regulatory mechanisms. An agent's basic problem can be described by

$$\max_{\mathbf{x}} NB(\mathbf{x}) \quad s.t. f(\mathbf{x}) \leq h \tag{7-1}$$

where the agent's objective is described by the *NB* to be maximized, **x** is a vector of choice variables, and $f(\mathbf{x}) \leq h$ is the constraint on the system. The optimal choice conforms to $NB_{x_i} = \lambda f_{x_i}$, which implies the optimal choice for the consumption of input x_i is the point where the marginal benefit (NB_{x_i}) is equal to the marginal value of the constraint (λf_{x_i}) where λ is the impact on the value of the marginal impact of the constraint on the objective.[7] The interpretation of the result is that the agent will choose to undertake an activity to the point where the marginal value (benefit) is equal to the marginal cost of the activity. In the case of many possible activities, the optimal solution is found when the ratio NB_{x_i} / f_{x_i} is equal across all activities.[8]

Within an economic system, there are many agents, each trying to maximize his or her objective, which results in competition across different agents or types of agents. This is especially problematic in cases where there are very limited resources that may be depletable, as is the case of water in the arid southwest.

Within the area, we consider the following economic behavior in the following sectors:

- Urban residential,
- Agricultural,
- Commercial,
- Industrial,
- Institutional,
- Shoreline use,
- Birding, and
- Non-use values (instream use).

The first five components are market-based, while the last three are environmental components. The economic component of the initial System Dynamics Toolbox is not an optimization tool. This reduces the complexity because it allows us to construct the model with sequential interaction rather than simultaneous interaction. The components, as modeled, will provide the trade-offs between allocation choices in a common valuation frame, dollars per unit of water moved. This, coupled with the results from the physical model, provides a decision-maker with a more complete package of information that provides feedback not only on the physical consequences, but also on the economic consequences of proposed policy.

---

[7] This is analogous to the utility maximization problem of the consumer or the cost minimization problem of the producer (which is the dual of the producer's unconstrained profit maximization problem).

[8] Since $\lambda = NB_{x_i} / f_{x_i}$ and there is only one value for λ this has to hold.

7.2.2 Macroeconomic Model

Market microeconomic components impact the regional or macro economy through their impact on productivity and employment. The regional economy is the composite activity of primary and secondary (indirect and induced) impacts. We model the regional economy via an input-output analysis, which provides a predictive model of activity and employment by sector based on the assumption that the economy is driven by final use and that industries sell goods and services to final demand or other inter-related industry activities that are then sold to final demand.

$$\mathbf{X} = (\mathbf{I} - \mathbf{A})^{-1}\mathbf{Y}, \tag{7-2}$$

where

$\mathbf{X}$ = the output vector,
$(\mathbf{I} - \mathbf{A})^{-1}$ = multipliers (where $\mathbf{A}$ is the coefficient matrix), and
$\mathbf{Y}$ = final demand vector.

The output and final demand vectors designate sectors of the economy, such as agriculture, which in turn could be broken into more micro-level components. The input-output model in Equation 7-2 is based on a linear production technology assumption, no supply constraints, and no labor constraints. The input-output analysis provides an estimate of the value of economic activity by sector under the provided economic scenario and the labor requirements for each sector. These estimates provide information to the System Dynamics Toolbox concerning the labor requirements, which can impact the demographic and labor force models.

7.3 Demographics and Labor Force

In the upper right corner of Figure 7-1 there is a box labeled "Population." This includes the population, demographics, and labor force models. Figure 7-2 provides a schematic of the interactions between the labor force, the regional economy, population, and water demand. If the available labor force is not large enough to supply labor to the regional economy, there is net migration into the system. Birth and death rates as well as aging the population contribute to the makeup of the population model. The population is divided into 19 age cohorts. From the population model, the working class is developed. The labor force is characterized by both the number of individuals in the working class and the skill level of those workers. Labor force participation rates are used to estimate the size of the working class while education levels are used to determine skill levels. Each of the sectors demands labor relative to the skill level distribution of each sector. Estimating the skill level distribution of each sector is discussed. Last, migration is jointly determined by either an excess or shortage of labor supply given labor demand in the sectors. If the labor force is too large, there is a net migration out of the system. In either case, there is an impact on water use, not only through the economic activity, but also because of a change in the demand for residential water.

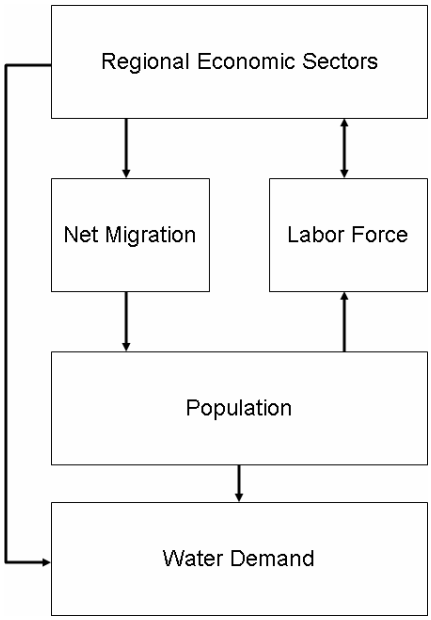

Figure 7-2. Demographic Model.

7.4 Agricultural Sector

Agriculture is one of the largest water users in the MRG, accounting for approximately 76% of the surface water use.[9] Water is an input into the production of alfalfa, pasture grass, corn, grains, vegetables, and chile peppers.

7.4.1 Background

The MRG agricultural model focuses on Sandoval, Bernalillo, and Valencia counties, with agriculture being present in five of the eight river reaches.[10] The cropping patterns are fairly consistent along these reaches of the river. Table 7-1 presents the cropping patterns. As can be seen from the table, alfalfa is the major crop grown in the area, followed by pasture grasses. These two crops account for almost 90% of the planted acreage. Grains, vegetables, and chilies account for the remaining acreage.

[9] New Mexico Office of the State Engineer from http://www.ose.state.nm.us/faq_intex.html (last accessed 10/24/06).

[10] Agricultural production is found in the following five reaches: Cochiti Dam–San Felipe (2087.8 acres), San Felipe–Albuquerque, Albuquerque–Bernardo (33669.7 acres), Bernardo–San Acacia (1595.3 acres) and San Acacia–San Marcial.

Table 7-1. Average cropping patterns.

Crop	Percentage of Total Acres Planted
Alfalfa	53%
Pasture Grass	35%
Corn	4%
Grain	4%
Miscellaneous Vegetables[11]	3%
Chile Peppers	1%

In order to model agricultural activity, we need to model the agent's choice of how much water to use as an input into the production of his or her crops. That is, we need to estimate agricultural water demand or the benefits derived from agricultural water use. The most common approach to estimate agricultural water demand is to use mathematical programming (multiple activity analysis) (see e.g., Bernardo et al. 1987). Other methods appropriate for estimating agricultural water demand are hedonic valuation (see e.g., Faux and Perry 1999) and the production function approach (e.g., Scheierling et al. 2004). Often data limitations determine which approach is used (Griffin 2006).

We employ the production function approach. Because of data limitations, we model net benefits from the economic value of water in agriculture rather than water demand.

7.4.2 Model

Water demand for agriculture is determined by net benefits, as determined in a perfectly competitive market, weighted by the cropping pattern. Gross benefits per acre (equal to total revenues, *TR*) are per unit price (*p*) times yield, where yield is a function of evapotranspiration (*ET*), which is equal to the water consumed. That is;

$$TR=pf(ET)$$

The agriculturalists objective is to maximize the difference between benefits and costs to produce. We employ a net benefits model (no fixed costs are included) for the each of the crops:

$$\max_{\alpha_i} NB_i = A\sum_{i=1}^{N}\alpha_i\left[p_i f_i(ET_i) - c_i\right] \quad \text{subject to} \quad \sum_{i=1}^{N}\frac{a_i}{A}\le 1 \qquad (7\text{-}3)$$

[11] Includes miscellaneous vegetables (1.9%), grapes (0.1%), melons (0.1%), miscellaneous fruit (0.5%), nursery stock (0.45%), and tree fruit (0.02%).

where

A	=	the total acreage in each reach,
N	=	total number of crops ($i = 1,\ldots,N$),
α_i	=	the proportion of total acreage allocated to each crop in each reach,
p_i	=	the price received by farmer for crop i,
$f_i(ET_i)$	=	the water production function for crop i, and
c_i	=	the per acre cost of production for crop i.

The choice is the amount of acreage that will be planted in each crop. That is, we assume the farmer uses the optimal amount of water on each crop and chooses the optimal number of acres over which to apply the available water. The constraint is the total number of acres available for planting.

The net benefits functions use water production functions to relate consumptive use[12] of water and crop yield. Water production functions account for the actual losses of water, evapotranspiration (*ET*), to agricultural production.

The water production functions are of the form $y = f(ET)$ where y denotes yield and ET denotes evapotranspiration that approximately equals water consumption (some water is also stored in the plant material). The specific water production functions used in the System Dynamics Toolbox are adopted from the New Mexico Climate Center (NMCC). Water production functions are available for most of the major crops. If the water production function was not derived, the water production function for a "similar" crop was used. For example, a water production function is available for barley but not for any of the other grains. The barley water production function is therefore used as an approximation for the water production function for "grains."

The agricultural water demand model within the System Dynamics Toolbox uses an annual timestep. This is because producers' crop-choice decisions are made annually. The economic decision units in the model are each of the five reaches. Ideally, the decision unit would be each individual farmer; however, that level of micro-level data is unavailable. This model assumes that each crop-producing reach in MRG maximizes net benefits and that each of these five river reaches represent the model's agricultural decision units.

Economic decision variables are crop choices and acreages each season if ignoring decisions related to technological improvements. Technology investments in one crop production do not cheaply transfer for use in a different crop production. As a result, the model as is does not include the possibility of substitutions between crops with different degrees of water demands in the light of water scarcity. The relevant decision variable is the number of acres dedicated to each crop, keeping crop proportions constant. This limitation of the model may be of minor

[12] Typically three measures of water use exist: water withdrawals, deliveries, and consumptive use. Water withdrawal minus conveyance losses equals delivery. Consumptive uses include evaporation and transpiration (evapotranspiration, ET) as well as water stored in plant material (Scheierling et al. 2004).

importance since 88% of acres in usage are dedicated to hay and forage production, which are similar productions.

The agricultural model is not optimization based—that is, producers will not change their production in response to external changes in production-relevant parameters. Instead, the System Dynamics Toolbox compares the net benefits of using water for agriculture with the net benefits of water in alternative uses. Assuming that each decision unit has already optimally chosen the crops grown and acreage in production for a given set of market prices (assuming perfect competition), the net benefit function gives an estimate of the profits for each reach. The total benefits of agricultural production in each reach are the dollar value of each crop grown weighted by acreage and the total costs of production in each reach are estimated as the sum of the costs of each crop grown weighted by acreage.

The model in Equation 7-3 requires data to parameterize it. The data are discussed in the following section.

7.4.3 Agricultural Water Model Data

Inputs needed are crop prices (price received by the producer), crop production costs, other fixed costs related to production, discount rates, and water production functions for each crop. We incorporate an economic crop budget driven by the ET factors for each of the 20 crops in the model. Using an estimate of ET by month for a particular crop, the model sums the annual water consumption. This water consumption amount is used in a linear regression equation that estimates crop yield. These equations are provided from agricultural experiment station results and require that total annual water consumption be used as the independent variable. The model accumulates monthly water consumption per crop and resets the value to zero each January. The total water consumption is then used to calculate crop yield. Crop revenues are then determined from a historical and projected price series. Cropping costs on a per acre basis are then used to determine crop net benefit. Finally, with estimates of the irrigated acreage per reach per crop over time, the model can estimate the total net benefit from agricultural crops.

7.4.3.1 Crop Prices (p_i)

Prices and costs are also approximately the same for each decision unit because of similar production and geographical nearness; the marginal value of production will be approximately the same for each reach.

Data for crop prices were gathered from the National Agricultural Statistics Service (NASS). The following discusses some of the data limitations for each crop category:

- Alfalfa: crop prices were available for 1989–2003. For the time interval from 1975 to 1988, the discounted 1989 price was used.
- Chile peppers (green and red): crop prices were available for 2000–2003. For the time interval from 1975 to 1999, the discounted 2000 price was used.

- Corn: no prices were available from NASS for New Mexico (on their website). Therefore, the Texas price of corn for grain was used. A complete time-series from 1975 to 2003 was available. These are not the prices of corn for silage.
- Miscellaneous vegetables: the price of onion was used as a proxy for the price of miscellaneous vegetables. Prices were available from 1998 to 2002. For the time interval from 1975 to 1997, the discounted 1998 price was used. The 2003 price was calculated using the 2002 price and a discount rate of 4 percent.
- Grains: for the grains barley, oats, sorghum and wheat, the price of wheat was used. Wheat price represented a middle ground of price for this group of grains. Prices were available from 1975 to 2003.
- Pasture grass: the price of hay was used. Prices were available for 1989–2003. For the time interval from 1975 to 1988, the discounted 1989 price was used.

An estimate of the real discount rate (rate of return of AAA bonds minus inflation rate) was used to calculate discounted prices. Future prices were calculated using an inflation rate of 4 percent, which is the average of the real interest rates for the time period 1975–2003. Table B-1 in Appendix B provides price paths.

7.4.3.2 Production Costs (c_i)

New Mexico State University Cooperative Extension Service provides cost estimates for different types of example farms. Two farms (a 30-acre, part-time, flood-irrigated farm in Valencia/Southern Bernalillo County that is growing alfalfa, oat hay, sorghum hay, green chile, and jalapenos and a 200-acre farm in Socorro that grows alfalfa, pasture grass, wheat, corm and chilies) were used to estimate costs. The costs for these operations and the parameters used in the model are included in Table 7-2. The costs in the table include the cost of pumping ground water. In addition to the costs in the table, farmers in the Middle Rio Grande Conservancy District pay $28 per acre foot of water per year for access to the water.

The costs in Table 7-2 are for 2004. The discounted costs over time are included in Table B-2 in Appendix B.

Table 7-2. Per acre crop costs.

Crop	Valencia Farm ($ per acre)	Socorro Farm ($ per acre)	Model Parameter ($ per acre)	Comments
Alfalfa	$413.60	$541.25	$477	Average of Valencia and Socorro
Pasture Grass	—	$238.45		From Socorro
Corn	—	$514.20		From Socorro
Grain		$424.60	$425	From Socorro
Chiles	$2209.90	$1906.72	$2058	Average of Valencia and Socorro
Miscellaneous Vegetables			$2058	No budgets north of Elephant Butte. Chile costs are used.

7.4.3.3 Water Production Functions ($y = f(ET)$)

Water production functions were adopted from the NMCC. Table 7-3 provides the water production functions developed for the System Dynamics Toolbox. NMCC provides a water crop production function for the main crop grown in the MRG, alfalfa. For chile peppers NMCC provides two water production functions, one for red and one for green chile. We only have information on chile acreage in general and create a water crop production function parameterized using the average slope and intercept for red and green chile. For the crop category grains we use NMCC's water crop production function for barley. For miscellaneous vegetables we use NMCC's water crop production function for onion. For pasture grass we use the average of the water-crop production function for crown orchard grass and fawn tall fescue. In middle altitudes and intermediate climates (4,500–6,000 feet) tall fescue and orchard grass are the suggested use for irrigated pastures in New Mexico (Glover, Foster, and Baker 1998, NMSU Cooperative Extension Service).

Table 7-3. Water production functions.[13]

Crop	Water Production Function	Units of Measurement
Alfalfa	y = 0.15 + 0.13 × ET	y[metric tons/ha] ET[cm]
Pasture Grass	y = -2206 + 289 × x	x = water applied [inches] y = dry matter (lbs/acre)
Corn	Y = -7309 + 238.9 × ET	y[kg/ha] ET[cm]
Grains[14]	y = -2323 + 157 × ET	y[metric tons/ha] ET[cm]
Miscellaneous Vegetables[15]	y = -38.9 + 135 × ET	Ungraded yield y (metric tons/ha) ET[cm]
Chile Peppers[16]	y = -7.54 + 0.3327 × x	y [ton/ha], x = water applied [cm]

7.4.4 Considerations

We calculate the net benefits of using water for agriculture in each of the five reaches of the MRG. Net benefits are calculated using water production function approach, crop prices from the NASS, and cost estimates from the Cooperative Extension Service at New Mexico State University.

There are, however, many questions, or extensions that could be undertaken to improve the model. The water production functions are linear and future research may look into whether nonlinear production functions are more appropriate. Data that could differentiate the economic

[13] kc*Eto = ET, Eto = reference ET or potential Et referenced to grass, kc = crop coefficient, which is a function of growing degree days (GDD).

[14] The production function for barley.

[15] The production function for onions.

[16] The average of the production function of green chile (y = -12.1 + 0.5168 * water applied [cm]) and red chile (y = -2.98 + 0.149 * water applied [cm]).

value of production in each of the reaches would be valuable. As discussed, several simplifications were made along the road in obtaining the net benefits functions. Furthermore, at some point, optimization across this and other components would provide another policy evaluation avenue. Optimization-based demand functions, however, require data of producer-level consumptive use with associated water price variability as well as micro-level production information. Currently such data do not exist. Future research would include how to gather data, for instance via surveys or experiments, in order to more accurately estimate agricultural water demand.

7.5 Residential Water Demand

The New Mexico Office of the State Engineer estimates public supplies and domestic use of water account for approximately 9% of water use in New Mexico. Domestic, or residential, use is the largest of these. In Albuquerque, this accounts for over 55% of total urban use where water is used year-round for indoor uses and more intensely during the summer for outdoor uses.[17]

7.5.1 Background

Residential water demand along the MRG is in the form of pumping from wells as well as consuming water provided by a water system. In the case of wells, there are no economic data as to economic incentives and so we assume that residential water use from wells is a constant portion of the maximum legal amount that can be consumed. In terms of water systems, there are several small towns and villages along the reaches. The two largest urban areas are Albuquerque and Santa Fe. The towns and cities are listed in Table 7-4. Given the overwhelming impact of the Albuquerque metropolitan area, we focus on residential water demand for Albuquerque.

[17] Gutzler and Nims (2003).

Table 7-4. Urban areas.

Reach	City/Town	Population	Total Population
Otowi–Cochiti			**62,203**
	Santa Fe	62,203	
Cochiti–San Felipe			
	None		
San Felipe–Albuquerque			**393,306**
	Cochiti Pueblo	507	
	Pena Blanca	661	
	Santa Domingo Pueblo	2,550	
	San Felipe Pueblo	2,080	
	Rio Rancho	51,765	
	Albuquerque (75% of 448,607)	336,456	
Albuquerque–Bernardo			**147,166**
	Albuquerque (25% of 448,607)	112,152	
	Pajarito	1,500	
	Los Padillas	2,500	
	Bosque Farms	3,931	
	Peralta	3,750	
	Los Lunas	10,034	
	Tome	600	
	Los Chavez	5,033	
	Belen	6,901	
	Casa Colorado	500	
Bernardo–San Acacia			**280**
	Contreras	40	
	La Joya	120	
	Alamillo	120	
San Acacia–San Marcial			**10,377**
	Polvadera	250	
	Lemitar	450	
	Florida	150	
	Socorro	8,877	
	Luis Lopez	200	
	San Antonio	450	
San Marcial–Elephant Butte			
	None		
TOTAL			**613,332**

There is a large literature that focuses on estimating empirical demand functions for residential water. The literature varies across the level of aggregation, the location and time frame of the study, as well as the factors included in the estimation (e.g., household characteristics). Included in the aggregate studies are Howe and Lineaweaver (1967), Gibbs (1978), Foster and Beattie (1981), Howe (1982), Shefter and David (1986), and Renwick and Green (2000). Empirical studies at the household level include Danielson (1979), Jones and Morris (1984), Nieswiadomy and Molina (1989), Lyman (1992), Martin and Wilder (1992), Hewitt and Hanemann (1995), Dandy et al. (1997), and Renwick and Archibald (1998). A large portion of these studies find that consumers are fairly unresponsive to changes in price. However, as Brookshire et al. (2002)

find, the lack of response may be due to the narrow historical range of prices that are found in the literature.

Studies that include observable characteristics include Gibbs (1978), Danielson (1979), Nieswiadomy (1992), Lyman (1992), and Renwick and Archibald (1998), and Renwick and Green (2000) consider the effects of climatic or seasonal conditions. Furthermore, some studies have found that demand is correlated with other observable factors such as income, lot size, or household size (e.g., Gibbs (1978), Foster and Beattie (1981), Jones and Morris (1984), Nieswiadomy and Molina (1989), Rizaiza (1991), Lyman (1992), Martin and Wilder (1992), Renwick and Archibald (1998), Renwick and Green (2000)).

7.5.2 Modeling

We model residential water demand at the level of the household. Beginning with a representative consumer household objective of maximizing utility (benefits from consumption of the good), where the consumer's problem is

$$\begin{aligned} &\max_{q,\mathbf{X}} u(q,\mathbf{X}) \\ &\text{subject to: } Pq + \mathbf{mX} \le B. \end{aligned} \tag{7-4}$$

where

q = household consumption of units of water,
P = the average cost per unit of water,
X = vector of other goods
m = price vector for other goods, and
B = household budget.

From Equation 7-4 we can derive the optimality condition for maximizing utility from which we derive the household demand function for water

$$q = f(P, \mathbf{m}, t). \tag{7-5}$$

That is, demand is a function of the price of water, the price of other goods, budget, and time.

Employing a five-year, monthly dataset for 37 representative households in Albuquerque that includes water usage in units (where 1 unit = 748 gallons) and cost per unit, we econometrically estimate a linear, monthly demand function for the representative consumer. That is;

$$q = \alpha_o + \sum_{i=1}^{11} \alpha_i D_i + \alpha_1 P + \sum_{j=2}^{11} \alpha_j D_j P + \varepsilon \tag{7-6}$$

where α_0 is the constant term associated with the base month (January) and α_i is the parameter estimate associated with the binary dummy, D_i, for month (February through December). Combining these first two terms gives the intercept for the demand function that can vary by

month. α_1 is the parameter estimate on the price variable, $\sum_{j=2}^{11} \alpha_j D_j P$ represents the cross terms that allow for slope variations between months, and ε_t is the error term, which is normally distributed with zero mean. Table 7-5 presents the results. As one might expect, the intercept terms for the winter months (mostly indoor use) are lower than for the summer. In addition, the results presented in Table 7-5 are for a representative consumer. In order to estimate demand for the entire city we multiply the representative consumer's demand by the total number of households in the city. That is

$$Q = Nq = Nf(P, \mathbf{m}, t) \tag{7-7}$$

where Q is total monthly demand and N is the total number of households in Albuquerque. Forecasting the number of households is discussed in a subsequent section.

Table 7-5. Consumer demand.

Month	Demand Function
January, February, March	$q = 16.9 - 8.8P$
April	$q = 16.9 - 3.4P$
May	$q = 19.9 - 3.4P$
June	$q = 25.6 - 3.4P$
July	$q = 26.3 - 3.4P$
August	$q = 22.8 - 3.4P$
September	$q = 20.6 - 3.4P$
October	$q = 16.9 - 3.4P$
November, December	$q = 16.9 - 8.8P$

7.5.3 Considerations

The demand functions presented in the previous section are functions based on average costs. They do not allow for variation across households, nor do they capture behavior outside a narrow range of prices. The demand functions could be refined by dissagregation and by larger ranges of price. The difficulty with dissagregation is that it is difficult to obtain the micro-level data necessary. However, there are some observable characteristics that could be considered future studies, for example, spatial variation. The difficulty with larger price ranges is that the Albuquerque has not, historically, had a large range of prices. Price experiments could fill in some data gaps.

7.6 Commercial, Industrial, and Institutional

Ideally, the demand for water in each of these sectors should be based on the production function for the final good or service, where water is an input into that product, which would provide us with a indirect demand for water. However, while there are some studies that have defined

production functions and water use for certain industries, there are no existing study results that we can transfer into the System Dynamics Toolbox that would be representative of the Albuquerque region. Primary collection of data and estimation of such demand functions was not feasible in the project, given that we employ a measure where water used in different sectors is based on the number of employees in that sector. This allows a proxy measure for water use in these sectors, which is a logical proxy. Labor (employees) is an input into the production of goods or services and so represents a production input. When there are no significant technological changes (which would alter the production function), labor should increase and decrease with production levels. Water consumption should also fluctuate with consumption levels. A caveat to this is that the water usage will be an average measure, rather than the marginal usage. If there are fluctuations over the production scale, the estimates we employ will not capture the changes at the margin.

Table 7-6 presents daily water use per employee for sectors. The sectors are those employed in the Input-Output model of the regional economy. Table 7-7 shows the daily per employee water use estimates used in the model.

Table 7-6. Daily per employee water use estimates.

Sector	Gallons per Employee per Day	Data Source
Ag & forestry services	NA	
Construction	70	Cook et al. (2001)
Textile products	300-1650	Gleick et al. (2003)
Paper manufacturing	155	Cook et al. (2001)
Printing & related	NA	
Nonmetal mineral products	1300	Cook et al. (2001)
Primary metal manufacturing	1300	Gleick et al. (2003)
Fabricated metal products	215	Gleick et al. (2003)
Machinery manufacturing	40	Cook et al. (2001)
Computer & other electronics	88	Gleick et al. (2003)
Electrical equipment & appliances	88	Gleick et al. (2003)
Transportation equipment	65	Cook et al. (2001)
Furniture & related products	45	Cook et al. (2001)
Miscellaneous manufacturing	25	Cook et al. (2001)
Wholesale trade	20	Cook et al. (2001)
Air transportation	65	Cook et al. (2001)
Rail transportation	NA	
Truck transportation	35	Cook et al. (2001)
Transit & ground pass	45	Cook et al. (2001)
Pipeline transportation	NA	
Sightseeing transportation	45	Cook et al. (2001)
Postal service	50	Cook et al. (2001)
Couriers & messengers	45	Cook et al. (2001)
Warehousing & storage	NA	
Motor vehicle & parts dealers	85	Cook et al. (2001)
Furniture & home furniture	25	Cook et al. (2001)
Electronics & appliances	260	Cook et al. (2001)
Bldg materials & garden supplies	90	Gleick et al. (2003)
Food & beverage stores	170	Gleick et al. (2003)

Table 7-6. Daily per employee water use estimates (continued).

Sector	Gallons per Employee per Day	Data Source
Health & personal care	155	Gleick et al. (2003)
Gasoline stations	85	Cook et al. (2001)
Clothing & accessories	135	Cook et al. (2001)
Sports/hobby/book	100	Gleick et al. (2003)
General merchandise stores	70	Cook et al. (2001)
Miscellaneous retailers	30	Cook et al. (2001)
Non-store retailers	100	Gleick et al. (2003)
Publishing industries	60	Cook et al. (2001)
Motion pictures & sound	55	Cook et al. (2001)
Broadcasting	100	Gleick et al. (2003)
Internet & data processing	100	Gleick et al. (2003)
Credit intermediation	100	Gleick et al. (2003)
Securities & other financial	176	Gleick et al. (2003)
Insurance carriers	149	Gleick et al. (2003)
Funds/trusts & other	176	Gleick et al. (2003)
Monetary authorities	100	Gleick et al. (2003)
Real estate	315	Cook et al. (2001)
Rental & leasing services	100	Gleick et al. (2003)
Lessor of nonfinance services	100	Gleick et al. (2003)
Professional/scientific	100	Gleick et al. (2003)
Management of companies	55	Cook et al. (2001)
Admin support services	100	Gleick et al. (2003)
Waste management & remediation	NA	
Educational services	140	Cook et al. (2001)
Ambulatory health care	100	Gleick et al. (2003)
Hospitals	124	Gleick et al. (2003)
Nursing & residential care	NA	
Social assistance	170	Cook et al. (2001)
Performing arts	NA	
Museums and similar	340	Gleick et al. (2003)
Amusement/gambling	105	Cook et al. (2001)
Accommodations	240	Gleick et al. (2003)
Food services & drinking establishments	265	Gleick et al. (2003)
Repair & maintenance	NA	
Personal & laundry services	980	Gleick et al. (2003)
Religious/grant making	100	Gleick et al. (2003)
Private households	NA	
Government & non-NAICS	136	Gleick et al. (2003)

Table 7-7. Daily per employee water use estimates used in model.

11 Ag, Forestry, Fish & Hunting	115
21 Mining	0
22 Utilities	0
23 Construction	70
31-33 Manufacturing	88
42 Wholesale Trade	42
48-49 Transportation & Warehousing	50
44-45 Retail trade	110
51 Information	100
52 Finance & insurance	150
53 Real estate & rental	100
54 Professional/scientific & tech services	100
55 Management of companies	100
56 Administrative & waste services	55
61 Educational services	100
62 Health & social services	124
71 Arts/entertainment & recreation	100
72 Accommodation & food services	250
81 Other services	500
92 Government & non-NAICS	136

7.7 Environmental Goods and Services

Environmental goods and services often have nonmarket values; these are values that society places on a good that are not captured through market transactions. Nonmarket values include use values and passive-use values. Use values are values that individuals have for the MRG because of activities in which they engage. Examples include birdwatching, jogging along the river, and picnicking. Individuals may also value flows in the river even if they never visit the area. Passive-use values include the value that people hold because they intend to visit it in the future (option value), because they value knowing it exists (existence value), or because they value knowing that it exists for future generations (bequest value). Finally, people may value an area because of the ecosystem services it provides. For example, water flow in the MRG affects native fish habitat, for which people may have an existence value. In addition, water flow affects vegetation along the river, thus impacting ecosystem services such as cleaning of sediments and pollution and maintaining water quality.

Not accounting for use values can severely underestimate the value of an environmental good. One would be particularly concerned about obtaining a value for instream flows solely from water transactions, given the high rate of subsidization of water. Loomis (1987, 1998) presents literature reviews of several studies that attempted to estimate the effect on recreation use and value of fluctuating instream flows. In general, he concludes that recreation and preservation values for instream flows can significantly exceed traditional consumptive use values.

7.7.1 Background

The task was to illustrate an approach for incorporating nonmarket values for instream flow into the System Dynamics Toolbox. The appropriate measure of these nonmarket values is the economic benefit of instream flow to individuals and society. This measure, known as consumer surplus, is the amount that individuals are willing to pay in excess of what they actually pay.

Economists have developed a number of tools to quantify nonmarket values, including stated preference surveys, travel cost models, and hedonic models. A binding constraint in this study was a lack of funding to conduct a primary study incorporating these tools to obtain nonmarket values. We were thus restricted to using the benefit-transfer method, discussed in more detail later.

In essence, the benefit-transfer method refers to the transfer of the monetary value of an environmental good calculated at a study site and transferred to another site (in this case, the MRG). Such a transfer is considered valid when site characteristics are reasonably similar and adjustments are made for socioeconomic characteristics. Benefit transfers have been applied in many natural resource management contexts, including forest management, water quality, waste management, and health risks associated with environmental degradation (Brouwer 2000).

There were two significant constraints that guided our approach to obtaining values for MRG instream flows. First, the focus of the study was on examining the effect of transferring water across reaches. Thus, we had to incorporate values that varied across reaches. A second important constraint is that values are often not additive. For example, because the silvery minnow is an indicator species of river and riparian health, values that residents might have for the silvery minnow could also include values for ecosystem services and riparian health. Thus we decided that it was inappropriate to identify all possible activities along the river, transfer values for these activities from other studies, and simply add them up. With these two constraints in mind, we decided to focus on three possible types of public value for instream flow: non-use values, shoreline recreation values, and birding values.

We elected to value birding as a distinct activity because of the presence of the Bosque Del Apache (BDA). The BDA refuge is a 57,191 acre (12,900 riparian acres) refuge located along the Rio Grande. The refuge has senior irrigation rights and irrigation is managed to maintain the wetland environment. Three hundred and forty-nine species of birds are known to occur at BDA, which is the highest number of species of all NM sites with official bird lists. The site has a large number of rare species of birds and over 100 species of breeding birds. Peak visitation occurs during winter months. During the spring and fall, visitors see warblers, flycatchers, and shorebirds. During summer months, visitors see songbirds, waders, shorebirds, and ducks. Annual visitation is estimated at 150,000 visitors/year.

As noted earlier, it was important to capture values that varied with instream flow, along the reaches. While there have been a number of studies valuing instream flows, most of these studies have focused on activities that do not occur along the MRG. Shoreline recreation was the primary exception to this.

The population of interest in conducting this benefit transfer was New Mexican households and visitors to the BDA. A survey by the UNM Institute for Public Policy (1996) found that 30% of a sample of state residents had spent time at the middle Rio Grande during the past year.

The first step in this study was conducting a thorough review of the literature. Below we summarize the general literature on birding values, shoreline recreation values, and non-use instream flow values. We also discuss in more detail the studies that were selected for the purposes of the benefit-transfer.

7.7.1.1 Birding

Appendix B-3 provides summary information on a number of studies examined for the purpose of this benefit transfer. Study areas included California, Texas, Nebraska, Montana, New Mexico, Arizona, Canada, and the United States.

First consider national and regional estimates for wildlife viewing; these numbers are relevant as 84% of away-from-home wildlife viewing is for birdwatching. For the United States, the mean annual national consumer surplus per wildlife watching day for instate residents was $35 (2001$); for out-of-state residents, it was significantly higher at $134 (2001$) (US FWS 2001). For 39 studies in the Intermountain West, the mean consumer surplus was $36.10 (1996$) per wildlife viewing day (Rosenberger and Loomis 2001).[18]

Looking at some example studies, Kaval and Loomis (2003) find a mean consumer value per day of birding of $24.67 (1996$), based on four studies conducted in NE and SE. Cooper and Loomis (1991) estimate consumer surplus per bird-watching trip of $37.33 under current conditions (28 birds seen) for the San Joaquin Valley, CA; values increase to $45.00/birdwatching trip for seeing 42 birds.

The literature review revealed that there were not many applicable studies dealing with riparian bird values. While the US Fish and Wildlife Service (2003) estimated a mean consumer surplus per wildlife viewing visit of $42 (2001$) for a New Mexico state resident, the sample size was not large enough to derive an estimate for out-of-state visitors. A specific study of the economic impact of birding and ecotourism at the BDA estimated that visitors spent between $167 and $278/day on a trip to the BDA (Kerlinger 1994).[19] While these estimates are directly connected to the BDA, a response rate for the survey is not reported, the estimate provided is not consumer surplus, and the estimate is not connected to instream flow.

We selected Crandall et al. (1992) as the most appropriate study for the benefit transfer for a number of reasons. Crandall et al. (1992) was the only study in which birding values were connected to riparian water levels. In addition, the study location shared similarities with the policy site both physically and in its sociodemographics. The study site was the Hassayampa River Preserve in Arizona, a riparian preserve located near Phoenix that is popular with birders. The authors conducted both a travel cost and contingent valuation survey. They estimated that

[18] The Intermountain West states include Montana, Idaho, Wyoming, Colorado, Arizona, New Mexico, Nevada, and Utah.

[19] Calculated based on the reported average of $300 to $500 per trip and an average trip length of 1.8 days.

visitors were willing to pay $65 (1992$) to change flow from intermittent to perennial and $97 (1992$) to maintain prime conditions at the preserve. The response rate was quite high (80%) although the sample size was relatively low (n = 118).

7.7.1.2 Shoreline Recreation

The MRG provides a number of shoreline recreation opportunities such as jogging, hiking, bicycling, paddling, walking, picnicking, and wildlife viewing that are enhanced by streamflow. Streamflow affects the aesthetic quality of these activities.

Looking at some specific activities, mean consumer surplus for the Intermountain West is estimated at $22.95 (1996$) per picnicking day (4 studies), $24.62 (1996$) per swimming day (1 study), and $31.85 (1996$) per hiking day (5 studies) (Rosenberger and Loomis 2001). Most studies on instream flow have focused on fishing/angling or rafting/boating and have primarily dealt with different geographic regions (e.g., Boyle et al. 1993; Douglas and Taylor 1999; Duffield et al. 1992; Duffield et al. 1990; Hansen and Hallam 1990). Very few studies have focused on shoreline use.

A review of contingent valuation model (CVM) and travel cost method (TCM) studies finds that recreationists were willing to pay anywhere from $1 to $25 for an additional acre foot of water during periods of recreation use to augment low instream flows (Brown 2004). Most studies showed the total value of flow reaching a peak at a relatively low flow and then decreasing with higher flow levels.

Duffield et al. (1992) estimated valuation equations for the Bitterroot and Big Hole Rivers in Montana as a function of instream flows. They used a dichotomous choice contingent valuation survey. The Bitterroot river visitors include anglers, but the majority of the use comes from floaters and shoreline recreation. Marginal values per acre foot ranged from $10.31 at 100 cubic feet per second (cfs) to - $0.48 at 2,000 cfs for the Bitterroot river.

Daubert and Young (1981) estimate values for shoreline use/streamline recreation, which is defined as picnicking, camping, and hiking. The study site is the Cache La Poudre river in northwestern Colorado. The authors collected the data using a contingent valuation survey that included both an entrance fee and a sales tax question. The authors calculated marginal WTP estimates for 50 cfs interval increases in stream flow. Individual willingness to pay (WTP) per day for each subsequent increase in streamflow declined and became negative at 700 cfs for shoreline activities. Value per day increased from $.10 to $.02 per cfs.

In the end, we selected Daubert and Young (1981) as having potential for a benefit-transfer to the MRG. A strength of the paper is that it provides equations for calculating marginal values for instream flow associated with shoreline use. Although more like the MRG than other sites, the study site is different in some key ways, including length of river study site, flow speed, and use statistics. We elected to use the results from the entrance fee question, which were slightly more conservative than the sales tax question. Duffield et al. (1992) was not selected because the estimates presented in the paper could not be disentangled from visitation assumptions.

7.7.1.3 Non-use Values

As discussed earlier, we anticipate that much of the value held by New Mexicans for flow in the MRG is value for the habitat provided, ecosystem services, etc. Previous valuation work has been done on a closely related topic in the MRG (Berrens et al. 1996; Berrens et al. 1998; Berrens et al. 2000).

We elected to use the results from Berrens et al. (2000), as it updates a previous paper (Berrens et al. 1996). The data for the study came from a telephone survey of New Mexico households conducted in February 1995 and 1996. The respective response rates were 64% and 65%. Respondents were asked "Would your household contribute $A dollars each year for five years to a special trust fund used to buy or lease water from willing parties in order to maintain minimum instream flows for the silvery minnow in the middle Rio Grande?" The estimated median WTP in New Mexico to provide minimum instream flows capable of supporting the silvery minnow was $25 (1996$) per household.[20]

7.7.2 Methodology

In applying the benefit-transfer method to this study, we followed a several-step process. We first identified which values/activities on the MRG made the most sense to value and which potentially varied between reaches. As noted earlier, the three selected were birding values, shoreline recreation values, and non-use values. We next identified existing valuation studies that could be used.

We then evaluated these studies to determine which seemed most reasonable for transfer. The evaluation criteria included a comparison of the environmental good/service, the physical attributes of the sites, and sociodemographic characteristics of the sites. Given these criteria, an emphasis was put on finding studies dealing with the Southwest. When this was not possible, Western studies were examined. An additional criterion was the quality of the studies.

In the case of the non-use values, the physical and sociodemographic characteristics of the study and policy site were exactly the same. The definition of the good varied somewhat between the study site and policy site. For example, it is not completely clear from the Berrens et al. (2000) study whether the values should be interpreted as just being the value for minimum instream flows to maintain the silvery minnow or whether they can be more broadly interpreted as capturing all non-use values that are complementary to maintaining minimum instream flow. For the purpose of this project, we assume that the estimate captures all values associated with maintaining a minimum level of instream flow. This is a conservative estimate.

In the case of the birding values, there were both similarities and differences between the study and policy sites. Differences between the two sites include hydrology, management, and proximity to a major urban center. Similarities include the sociodemographics of each area and the fact that both are riparian birding areas in the desert Southwest.

[20] Median WTP was selected as it was more stable than mean WTP across a variety of distributional assumptions.

Similarity of site, good, and sociodemographics is most problematic for the shoreline recreation value. Instream flows tend to be highly site-specific (Brown 1991; Frederick et al. 1996). As Brown (2004) warns, an instream flow value from one national forest may not even transfer to another stretch of the river, much less another location. The strongest reasons for its applicability is that the study site was in the West and focused on shoreline recreation. By the same token, there are many differences between Colorado and New Mexico and the Cache La Poudre is certainly a very different river than the MRG. In the end, however, shoreline recreation is the only value that gives us varying values by reach and Daubert and Young (1981) was the only applicable study that gave retrievable shoreline recreation values that varied with instream flow.

7.7.3 Data

In this section, we present the data used in the benefit transfer.

7.7.3.1 Birding Values

Crandall et al. (1992) provides an estimate of $65 (1992$) to change flow from intermittent to perennial. Converting this into 2003 dollars, this means that visitors are willing to pay an additional $85 (2003$) each to change flow from intermittent to perennial. Call this estimate BirdHi. Crandall et al. (1992) found that visitors were willing to pay $97 (1992$) to maintain prime conditions at the preserve. Differencing $97 (1992$) and $64 (1992$) and converting 2003 dollars gives an average of $42 per visitor (2003$) during periods of low flows. Call this estimate BirdLow. Monthly visitation data from 1999 through 2003 were obtained from Bosque del Apache. We used average monthly visitation for this period to calculate our values. Table 7-8 shows the birding values for BDA visitors for low flows and changes to perennial flows.

7.7.3.2 Non-use Values

For all reaches we use the Berrens et al. (2000) result, converted into 2003 dollars, that the median WTP in New Mexico to provide minimum instream flows capable of supporting the silvery minnow is $29 (2003$) per household. Given that New Mexico has 677,971 households this translates into a value of $19,870,193 to maintain minimum instream flows.[21] Denote this benefit-transfer value as MinFlow.

7.7.3.3 Shoreline Recreation Values

Daubert and Young (1981) provides a valuation equation for the marginal shoreline value for changes in water flow as a function of a number of demographic variables. We do not have demographic data for MRG users. Thus we assumed that other control variables such as experience, activity days, income, age, etc., would take on the same mean value as in the original study. Denote the benefit-transfer estimates from this study as Shore.

[21] Household estimates are for 2000 and from the U.S. Census Bureau (2004).

Table 7-8. Birding values for BDA visitors.[22]

Inflation adjustment factor (for 2003$)	0.763		
Low flow value/visitor (1992$)	$32		
Marginal value/visitor to increase levels from intermittent to perennial (1992$)	$65		
	Average monthly visits (1999-2003)	**Low Flow value (2003$)**	**Marginal Value: Intermittent to perennial (2003$)**
January	19998	$838,694	$1,703,596
February	19546	$819,737	$1,665,090
March	11110	$465,950	$946,461
April	8878	$372,324	$756,283
May	6065	$254,381	$516,712
June	4074	$170,846	$347,030
July	3838	$160,981	$326,993
August	3663	$153,634	$312,068
September	4829	$202,527	$411,383
October	9972	$418,206	$849,481
November	30890	$1,295,501	$2,631,486
December	15390	$645,444	$1,311,058

Calculating the WTP measures required participation estimates. We used approximations based on the UNM Institute for Public Policy survey of attitudes towards the MRG (1996). The survey found that of New Mexicans, 10% had gone to the MRG 1-2 times, 9% had gone 3-5 times, and 11% had gone more than 5 times in the past year (UNM Institute for Public Policy 1996). We used the lower endpoints on each range in conjunction with current population estimates to approximate average daily participation in recreation on the MRG. We also updated all estimates to 2003 dollars. From these calculations we are able to generate estimates of WTP/acre foot/day. Estimates range from $525 per acre foot per day at 100 cfs to <$1,194> per acre foot per day at 2,000 cfs and are shown in Table 7-9.

[22] Data based on Crandall et al. (1992) and visitation data from Bosque del Apache.

Table 7-9. Shoreline recreation values.[23]

MV equation from entrance fee game: MV = 0.029-.426e-4*Flow				
Inflation adjustment factor (for 2003$)				
Converted to acre feet (AF) per day using relation: cfs*1.9835 = AF/day				
Assumed # of visitors per day (approximation from IPP): 5,290				
Inflation adjustment factor: 0.494				
CFS	**MV/cfs/visit (1981$)**	**MV/visit/AF/day (1981$)**	**MV/AF/day (1981$)**	**MV/AF/day (2003$)**
100	0.02	$0	$260	**$525**
200	0.02	$0	$215	**$435**
300	0.02	$0	$170	**$345**
400	0.01	$0	$125	**$254**
500	0.01	$0	$81	**$164**
600	0.00	$0	$36	**$73**
700	0.00	$(0)	$(9)	**$(17)**
800	-0.01	$(0)	$(53)	**$(108)**
900	-0.01	$(0)	$(98)	**$(198)**
1000	-0.01	$(0)	$(143)	**$(289)**
1200	-0.02	$(0)	$(232)	**$(470)**
1400	-0.03	$(0)	$(321)	**$(651)**
1600	-0.04	$(0)	$(411)	**$(832)**
1800	-0.05	$(0)	$(500)	**$(1,013)**
2000	-0.06	$(0)	$(590)	**$(1,194)**

7.7.4 Model

The table below shows the general rules for estimating riparian values:

As shown in Table 7-10, there are three possible cases:

- Current flow levels are below minimum instream requirement and flow is increased so as to attain minimum levels in all reaches
- Current flow levels are below minimum instream requirement and flow is increased to the minimum level in some but not all reaches
- Current flow levels are at or above minimum instream requirements and flow is increased further in some reaches

In the first case, the MinFlow value is appropriate for all reaches. We assume that Shore values are captured by MinFlow. In the BDA reach, the MinFlow value must be adjusted to exclude BDA visitors. BDA visitor values for low water levels are then added in to the adjusted MinFlow value.

[23] Based on Daubert and Young (1981).

Table 7-10. Riparian rules.

Reach	If flows are less than minimum level, marginal value of attaining minimum levels in all reaches	If minimum level will not be achieved in all reaches, marginal value of increased flow	If flows are >= minimum level in all reaches, marginal value of increased flow
1	MinFlows	Shore	Shore
2	MinFlows	Shore	Shore
3	MinFlows	Shore	Shore
4	MinFlows	Shore	Shore
5	MinFlows	Shore	Shore
6	MinFlows	Shore	Shore
Bosque del Apache Reach	Population Adjusted MinFlow + BirdLow	Shore + BirdLow (if < min in BDA) +BirdHi (if >= min in BDA)	Shore +BirdHi

In the second case, the MinFlow value is not used as it requires that all reaches attain minimum instream requirements. In this case, we use Shore values to estimate the value of additional water flow in each reach. The Shore values will vary with the amount of flow. In addition, the BDA reach also has a birding value. Whether BirdHi or BirdLow is used will depend on the amount of flow in that reach.

The third case examines values for additional water flow, once minimum instream requirements have been met. Therefore, MinFlow values have already been incorporated into the total values for water levels. We are just interested in the marginal value of additional flow. Therefore, the applicable values are Shore for all reaches and Shore and BirdHi for the BDA reach.

Monthly variation in estimates will only occur for the Bosque del Apache, as this is the only region for which we currently have monthly data. Annual variation will occur through estimated population changes.

7.7.5 Considerations

This work illustrates a method for incorporating non-use values for instream flow into the System Dynamics Toolbox. In a first-best world, these values would be directly obtained through a primary study. Given a limited budget, however, we have used the benefit transfer method to illustrate this approach.

Of the three values examined, birding, non-use, and shoreline recreation, the shoreline recreation values are the least robust. As discussed, instream flow values can vary significantly between sites. The Shore values are significantly higher than results from the original Daubert and Young (1981) study site and from a similar study conducted in Montana by Duffield et al. (1992). This occurs because of the much higher participation rates, and may be a cause for concern. In

addition, the fact that we have assumed a constant participation rate implies that the marginal general use values will be overstated at both high and low flows.

We assume that the marginal non-use values of additional instream flow beyond the minimum levels are zero. This may underestimate non-use values. In addition, there is disagreement on exactly what the minimum required instream flow levels are. Therefore, it would be appropriate to vary the definition of "minimum instream flows" in the simulation.[24]

7.8 Demographics, Population, and Workforce

This section describes the "demographic model" (DM) used in conjunction with the larger system dynamic model. The purpose of the DM is to be able to, given a change in a specified NAICS (North American Industry Classification System) sector, analyze population changes and consequently changes in water demand. Intricate relationships exist between NAICS sectors, an available working class, and the current population. We present working relationships between these three components along with calculations and assumptions necessary in deriving the needed relationship coefficients.

Demographics have an impact on water consumption. The age distribution of the population, the makeup of families, and the distribution of the population by employment categories all impact water consumption. We attempted to develop a disaggregated human population dynamics model to account for the variety. Ideally a disaggregated demographic model would have individuals disaggregated to age cohort, gender, role in the workforce, and sector of employment.

In general, the incorporation of human demographics into the model is a difficult undertaking. First, the geographic boundaries of river reaches do not coincide with the boundaries used to estimate human population. Second, a complete demographic model should take into account fertility, mortality, and migration. Obtaining data for these factors on a political and river reach boundary system is nearly impossible. Third, published reports of population growth are typically provided for a political boundary with net growth rates but the underlying models themselves are not readily available.

We examined two disaggregated approaches, proportional aggregated age cohorts or 5-year cohorts. We chose to use 5-year cohorts starting with 0–4 year olds to 85–89 year olds and one final category of 90+ year olds. Age-specific fertility and mortality figures were provided for each cohort. Initial data for Bernalillo Country, NM, from the U.S. Census Bureau (2000) was used.

Each NAICS sector demands labor while the working class constitutes the labor supply. Labor supply is determined by population size and labor force participation rates. The working class distribution consists of 19 age cohorts where each cohort is described by four skill levels. Skill level ranges from "unskilled" to "professional" labor. The DM is set up such that population and

[24] Ward and Booker (2003) assume year-round minimum instream flows of 50 cfs in the San Acacia reach. According to testimony regarding the silvery minnow, the definition of required minimum flows has varied from a value of 300 cfs at the San Isleta dam to100 cfs.

labor force participation rates determine working class, working class provides workers with specific skill levels to each sector, and then working class and sectors jointly determine if migration, either in or out, will occur. Population is then adjusted by migration. Population in each period determines aggregate water demand.

The DM connects with the other modules in two places. First, the IMPLANS model specifies the quantity of labor demanded for each NAICS sector. The DM finds labor demand for each sector and supplies labor according to availability of both workers and workers with particular skill levels from the working class. The second connection is after the DM determines the population in time *t*. From population, total number of households is estimated, which is then used to estimate residential water demand. This water use then becomes a factor in the physical model.

7.8.1 Population

The DM models tracks population through time. Population is modeled in the DM with no disaggregating between men and women. Modeling population necessitates incorporation of fertility and mortality rates, breaking down the population by age into cohorts, aging the cohorts, and migrating persons both in and out of the population. Each component of the population in the DM requires assumptions, methods of derivation, and analysis of coefficients used in the DM. Each is presented in turn.

7.8.1.1 Age Cohorts

The population model is disaggregated by population age such that there are 19 age cohorts. These cohorts are as follows: person's age {*0-4, 5-9, 10-14, 15-19, 20-24, 25-44, 45-64, 65-69, 70-74, 75-79, 80-84, 85-89, 90+*}. In order for the DM to model population efficiently, it needs to allow for variation among groups through time. This is due to the assumption that age cohorts are not homogeneous in their characteristics. For example, the model assumes that individuals in cohort *65-69* do not experience the same fertility/mortality or labor force participation rates as individuals in, say, cohort *15-19*. The purpose of the cohorts as presented is that variance in cohort characteristics is allowed. Incorporating age cohorts as illustrated allows for the model to capture this variance and incorporate it through different stages of the model.

The DM is built such that for a given population, age cohorts are populated. Populating the cohorts is done using coefficients multiplied by the total population. Each cohort has a coefficient that is the ratio of cohort population to the total population. Coefficients are computed using data obtained for Bernalillo County from the U.S. Census Bureau.

Cohort coefficient computation methods are presented. Let the population of cohort *k* in time *t* be modeled as γ_{kt} where $k = \{1, 2, 3, 4, 5\}$ for cohorts {*0-4, 5-9, 10-14, 15-19, 20-24, 25-44, 45-64, 65-69, 70-74, 75-79, 80-84, 85-89, 90+*} and *t* = year {2000, 2001, 2002, 2003, 2004}. Let τ_t be the total population in year *t*. For use in the DM, the coefficient π_k is needed where this is the ratio of population in cohort *k* to total population. We find this by

$$\pi_{kt} = \frac{\gamma_{kt}}{\tau_t} \tag{7-8}$$

Equation 7-8 provides a ratio of cohort population to total population for years {2000 . . . 2004}. The DM requires the ratio π_k as described previously. Removing the dimension of time and finding π_k is done by taking a moving average of the ratios generated by Equation 7-8. The result of this procedure is a vector of ratios as presented in Table 7-11.

Table 7-11. Ratio of cohort population to total population.

Age Cohort (*k*)	Population	π_k
0-4	38688	0.0693
5-9	39139	0.0701
10-14	39550	0.0708
15-19	40857	0.0732
20-24	40956	0.0733
25-29	39935	0.0715
30-34	39739	0.0712
35-39	45058	0.0807
40-44	44841	0.0803
45-49	41855	0.0750
50-54	36567	0.0655
55-59	26394	0.0473
60-64	20499	0.0367
65-69	17909	0.0321
70-74	16102	0.0288
75-79	13875	0.0248
80-84	9006	0.0161
85-89	5025	0.0090
90+	2442	0.0044

Use of π_k in the DM is such that for each period of simulation, a population of cohort *k* can be found by multiplying total population by π_k (the vector of ratios used in the DM to find cohort population at each point in time).

7.8.1.2 Fertility and Mortality Rates

The data for fertility and mortality rate calculations are available from the *New Mexico Information for Community Assessment*[25] (NMICA). NMICA records statistics regarding births and deaths for all New Mexico counties. Birth statistics are available for the years 1997 through 2000 while death statistics are provided for 1997 through 1999. In an effort to maintain data consistency for the two rate calculations, data from 1999 are used. Given that needed data are not available specific to Albuquerque, this analysis relies on the assumption that fertility and mortality rates calculated for the county of Bernalillo, wherein Albuquerque is located, are

[25] *New Mexico Information for Community Assessment* is available at http://mica.health.state.nm.us/nmindex.html, last accessed September 4, 2006. Fertility and mortality data are for Bernalillo County 1999 specified by age of the mother, all births for fertility, and specified as all causes of death by age for mortality.

applicable to Albuquerque. As described previously, population is modeled across five age cohorts. This requires that fertility/mortality rate calculations be in terms of the five age cohorts. Data conversion methods are described in the following.

Rate calculations for fertility and mortality are calculated in an analogous fashion; namely, a ratio is calculated for each of the cohorts. Similar to Equation 7-8, fertility and mortality rates are calculated as follows: let α_k be total births by age of the mother in cohort *k*, ω_k be total deaths in cohort *k*. Fertility and mortality rates by cohort *k* are approximated then by A_k and Ω_k respectively where τ_0 is the total population of Bernalillo County in 1999.

$$\mathrm{A}_k = \frac{\alpha_k}{\tau_0} \tag{7-9}$$

$$\Omega_k = \frac{\omega_k}{\tau_0} \tag{7-10}$$

Equations 7-9 and 7-10 are the fertility and mortality rates for cohort *k* respectively. Assumptions and data conversion methods necessary in obtaining each are discussed.

Fertility rates are provided from NMICA formatted such that total births by age of the mother are available. Age of the mother categories are as follows: *15-19, 20-24, 25-29, 30-34, 35-39, 40-44*. In so doing, the assumption is made that those individuals of age greater than 44 years no longer give birth.

Death statistic data are provided such that age cohorts in NMICA match the age cohorts in the DM.

Interpretation of Table 7-12 is such that fertility rates A_k and mortality rates Ω_k multiplied by a total population will illustrate either births occurring to mothers in cohort *k* or death of individuals in cohort *k*. The vectors of alpha and omega in Table 7-12 are those used for fertility and mortality rates in the DM.

7.8.1.3 Working Class

Labor, in the DM, is demanded by NAICS sectors according to the System Dynamics Toolbox, and is supplied by the working class. As discussed in previously, the NAICS sectors demand labor with specific skill-level characteristics. This requirement necessitates the working class to supply labor with skill-level characteristics demanded by NAICS sectors. This section presents two fundamental aspects of the working class, namely the method of describing the working class by skill level and the procedure used to determine the numerical size of the working class at each point in time. Skill level of the working class is based on obtained education levels while size of the working class is determined using labor force participation rates. Each is discussed below.

Table 7-12. Fertility and mortality rates by cohort.

Cohort *k*	A_k	Ω_k
0-4	0.00000	0.00005
5-9	0.00000	0.00005
10-14	0.00000	0.00005
15-19	0.06800	0.00011
20-24	0.11447	0.00011
25-29	0.11346	0.00009
30-34	0.07313	0.00009
35-39	0.03182	0.00009
40-44	0.00498	0.00009
45-49	0.00000	0.00026
50-54	0.00000	0.00026
55-59	0.00000	0.00026
60-64	0.00000	0.00026
65-69	0.00000	0.00146
70-74	0.00000	0.00146
75-79	0.00000	0.00146
80-84	0.00000	0.00146
85-89	0.00000	0.00146
90+	0.00000	1.00000

7.8.1.3.1 Skill Level

The working class is described by four levels of skill: unskilled, blue collar, white collar, and professional. Skill-level classification is based on education levels. The assumption is made that unskilled workers have education less than a high school diploma. Blue collar workers have education greater than or equal to a high school diploma up to an associate's degree or equivalent. Blue collar definition is extended to include post-secondary training less than four years. White collar workers have education equal to a bachelor's degree or post-secondary training greater than or equal to four years. Professional skill-level category is taken to be individuals who have earned a master's, professional, or doctorate degree.

Post-secondary training includes training such as on-the-job training or that which is obtained outside of a formal college setting. Post-secondary training is added to the classification for the purpose of relating NAICS sector education requirements. By including this type of training, a clarifying assumption is made that if an individual obtains post-secondary training the individual first would have earned a high school diploma.

Estimating education levels is done using data from *American Community Survey* (ACS).[26] From ACS, we extract education levels by cohort. The data are of the form such that cohorts can be extracted from ACS for each age cohort. The DM requires that one of the cohorts be *15-19*. We account for the missing 15-, 16- and 17-year-olds by making the assumption that these

[26] See footnote 5.

individuals would not have yet obtained a high school diploma. This stems from the fact that if a student makes "normal" progress while in high school then their diploma is awarded to them during their eighteenth year, i.e., if they are not 18 when the diploma is issued then they will shortly become 18 years old. This assumption allows us to simply find the population of 15-, 16- and 17-year-olds from ACS.

We are interested in the ratio cohort population with a specific education level to cohort population. Let σ_{kjt} be education level j of cohort k in year t where j = education {less than high school diploma = 1, high school diploma through associate's degree = 2, bachelor's degree = 3, professional degree = 4}. We make the assumption that individuals in cohort *0-14* are not part of the work force. As such we let cohort = k for k {4 . . . 19}. We are interested in the ratio λ_{kjt} where λ is the ratio of education level by cohort to cohort population in time t. Formally we seek

$$\lambda_{kjt} = \frac{\sigma_{kjt}}{\gamma_{kt}} \tag{7-11}$$

From Equation 7-11 we find in each period of time and by each of the specified age cohort the ratio of the cohort holding less than a high school diploma, a high school diploma, and an associate's degree, bachelor's degree, or a professional degree to the population of cohort k. Cohorts are now described by education levels. For use in the DM, education levels need to be converted to skill level. The conversion is simply such that less than a high school diploma are unskilled workers, high school diploma through associate's degree are blue collar workers, individuals with bachelor's degrees are white collar, and those with a master's, professional, or doctorate degree are professional workers. In Equation 7-11 λ is three-dimensional in that time is a dimension. For use in the DM, it needs to be two-dimensional: age cohort and skill level. A moving average is taken on λ_{kjt} to reduce it to λ_{kj}. Table 7-13 is a table of the numerical values for λ_{kj}.

Table 7-13. Age cohort by skill level (λ_k).

Age Cohort	Unskilled	Blue Collar	White Collar	Professional
15-19	0.3208	0.5714	0.0539	0.0539
20-24	0.3208	0.5714	0.0539	0.0539
25-29	0.1101	0.5541	0.2102	0.1256
30-34	0.1101	0.5541	0.2102	0.1256
35-39	0.1101	0.5541	0.2102	0.1256
40-44	0.1101	0.5541	0.2102	0.1256
45-49	0.1075	0.5105	0.1937	0.1883
50-54	0.1075	0.5105	0.1937	0.1883
55-59	0.1075	0.5105	0.1937	0.1883
60-64	0.1075	0.5105	0.1937	0.1883
65-69	0.1793	0.5849	0.1251	0.1107
70-74	0.1793	0.5849	0.1251	0.1107
75-79	0.1793	0.5849	0.1251	0.1107
80-84	0.1793	0.5849	0.1251	0.1107
85-89	0.1793	0.5849	0.1251	0.1107
90+	0.1793	0.5849	0.1251	0.1107

The coefficients presented in Table 7-13 are used in the DM such that for a given population of cohort *k*, the coefficients multiplied by the cohort population will give the distribution of skill level of the cohort. The DM requires labor from the working class. The working class is now, with the coefficients in Table 7-13 described by skill level. Determining the size of the working class is done via labor force participation rates.

7.8.1.3.2 Labor Force Participation

Estimating the size of the working class in each time period of the model is done using labor force participation rates. Data for this estimation come from ACS. In the DM, labor force is defined to consist of individuals employed and those unemployed who are seeking employment. Workers who are unemployed but not actively seeking employment are considered discouraged workers and not captured by the labor force.

Data in the ACS regarding labor force can be extracted such that a perfect match exists between cohorts of the DM and the manner in which data can be retrieved from ACS. We extract by cohort individuals employed and unemployed. Let *k* be the index for age cohorts and *t* be the year index. Population of the k^{th} cohort in time *t* is specified as γ_{kt}. Let μ_{kt} be the labor force of cohort *k* in time *t*. We seek a coefficient expressing the ratio of labor force of cohort *k* in *t* to population of cohort *k* in *t*. Specifically we find η_{kt}.

$$\eta_{kt} = \frac{\mu_{kt}}{\gamma_{kt}} \tag{7-12}$$

Equation 7-12 expresses the coefficient η as a function of both the labor force of cohort *k* and population of cohort *k*. η_{kt} is then the labor force participation rate of cohort *k* in time *t*. For use in the DM, we are interested in a coefficient that can be used over many time periods and of dimension age cohort. From Equation 7-12, we take a moving average of η_{kt} until we are left with η_k. η_k can be used in the DM such that for any population of cohort *k* a labor force estimate of cohort *k* can be found by multiplying η_k by the population of cohort *k* in any time *t*. Table 7-14 presents the estimates of η_k used in the DM.

In Table 7-14, η_k is the labor force participation rate in cohort *k*. As defined previously, labor force consists of individuals both employed and seeking employment. Lacking in η_k is a natural rate of unemployment. In the DM, a natural rate of 3% unemployment is assumed. This implies that as η_k is used to determine the size of the working class for cohort *k*, the natural rate of unemployment subtracts 3% of the individuals in cohort *k* from those included in the working class.

Table 7-14. Labor force participation rates.

Age Cohort	$\eta_{k * 100}$
15-19	71.22879
20-24	71.22879
25-29	83.80008
30-34	83.80008
35-39	83.80008
40-44	83.80008
45-49	72.81655
50-54	72.81655
55-59	72.81655
60-64	72.81655
65-69	14.68680
70-74	14.68680
75-79	14.68680
80-84	14.68680
85-89	14.68680
90+	14.68680

IMPLAN output provides the number of actual jobs per NAICS sector whereas the demographic model provides the number of employees. This leads to a discrepancy since the number of full-time equivalent employees per sector is not known. This calculation requires an estimate of hours worked by NAICS code. This figure can be divided by a standard year of 2,080 hours and the result can be used to recalculate employment. The U.S. Census Bureau also provides, through the Quarterly Workforce Indicators, the total number of workers who were employed by the same employer in both the current and previous quarter. Unfortunately, these three measures do not correlate for Bernalillo County.

Each NAICS sector has a distribution of labor specified by skill level. Skill level of NAICS sectors is discussed in Section 7.8.1.3.1.

7.8.2 NAICS Sectors

NAICS sectors used in the DM are the broad category of industry classification by the Census. There are 20 sectors; these are presented in Table 7-15.

Table 7-15. NAICS sectors.

20 NAICS Sectors
1. Ag, Forestry, Fishing, Hunting
2. Mining
3. Utilities
4. Construction
5. Manufacturing
6. Wholesale Trade
7. Retail Trade
8. Transportation and Warehousing
9. Information
10. Finance and Insurance
11. Real Estate
12. Professional and Technical Services
13. Management of Companies
14. Administration and Waste Services
15. Education
16. Health and Social Services
17. Arts, Entertainment and Recreational Services
18. Accommodations and Food Services
19. Other Services
20. Government/Public Administration, and non-NAICS

The number of individuals needed to carry out jobs in each sector in Table 7-15 is estimated. The working class in the DM supplies labor, i.e., workers to fill jobs and labor demanded by each of the NAICS sectors. In each of the NAICS sectors there exists a distribution of jobs classified by types of work performed in each sector. From *Bureau of Labor Statistics*[27] we find the job type distribution associated with each NAICS sector. This distribution is presented in Appendix B, Tables B-4, B-5, and B-6. Job types are classified by the Bureau of Labor Statistics (BLS) as SOC where SOC is *Standard Occupations Classification System.* There are 22 SOC job types; these are listed in Table 7-16. These are the job types for which job types in each NAICS sector are distributed as presented in Appendix B, Tables B-7, B-8, and B-9.

[27] Data for NAICS and Standard Occupational Classification System job classification comes from the Bureau of Labor Statistics (BLS). Reports published by the BLS and used here are *Occupations Outlook Handbook* and *National Industry-Specific Occupational Employment and Wage Estimates.* Both are available at www.bls.gov/oco/home.htm and www.bls.gov/oes/current/oessrci.htm respectively, last accessed July 13, 2006.

Table 7-16. SOC job categories.

1. Management Occupations
2. Business and Financial Operations Occupations
3. Computer and Mathematical Occupations
4. Architecture and Engineering Occupations
5. Life, Physical, and Social Science Occupations
6. Community and Social Services Occupations
7. Legal Occupations
8. Education, Training, and Library Occupations
9. Arts, Design, Entertainment, Sports, and Media Occupations
10. Healthcare Practitioners and Technical Occupations
11. Healthcare Support Occupations
12. Protective Service Occupations
13. Food Preparation and Serving Related Occupations
14. Building and Grounds Cleaning and Maintenance Occupations
15. Personal Care and Service Occupations
16. Sales and Related Occupations
17. Office and Administrative Support Occupations
18. Farming, Fishing, and Forestry Occupations
19. Construction and Extraction Occupations
20. Installation, Maintenance, and Repair Occupations
21. Production Occupations
22. Transportation and Material Moving Occupations

From BLS at the national level, the 22 SOC job types can be disaggregated such that specific jobs can be found within each SOC job type. Associated with a specific job within an SOC job type is a specified level of education or training required to perform the specific job. We find for each SOC job type a distribution of education or training required. We find this distribution by finding in each SOC type the ratio of individuals with specific jobs in SOC job type to total individual jobs in SOC job type. We then sum the percentages by education type. Doing so allows us to produce Appendix B, Table B-7, which illustrates skill-level distribution for each of the SOC job types.

Our task is to define each of the NAICS sectors by required skill level for jobs performed in each NAICS sector. We do so by the following.

Table 7-17 is produced using the following method. Appendix B, Tables B-4, B-5, and B-6 provide weights. The weights indicate the share of the occupation types belonging to each NAICS sector. Appendix B, Table B-7 is a table of weighted skill level in each of the SOC job types. To find NAICS sectors described by skill level as presented in Table 7-17, we multiply the weights for each NAICS sector from Appendix B, Tables B-4, B-5, and B-6 (the rows) by the weights of skill level in each SOC category in Appendix B, Table B-7 (the columns). This operation gives by NAICS sector the distribution of skill level in each NAICS sector as presented in Table 7-15.

We test for accuracy of the procedure by summing the rows in Appendix B, Tables B-4, B-5, and B-6 then comparing this result to the summed rows of Table B-7. Appendix B, Table B-8 shows the result. Summed SOC weights from Appendix B, Tables B-4, B-5, and B-6 are weights obtained from BLS data. A result equal to unity indicates no error while variation from unity indicates the degree of error. Since test results in column two of Appendix B, Table B-8 are from actual BLS data, it is assumed that the data in column 1, test results of data transformation to obtain NAICS sectors by skill level, can only be as accurate as the data given in column 2. Comparison columns one and two indicate the data transformation performed to obtain Table 7-15 was done such that minimum error was introduced. Error can be interpreted from Appendix B, Table B-8 as the degree to which column one varies from column 2. Considering we feel Table 7-15 to be an accurate estimate of the skill-level distribution associated with each NAICS sector, Table 7-17 numbers are the coefficients used in the DM.

Table 7-17. NAICS sectors with required skill level distribution.

20 NAICS Sectors	Un-Skilled	Blue Collar	White Collar	Professional
Ag, forestry, fishing, hunting	0.05172	0.91930	0.02439	0.00464
Mining	0.06197	0.79434	0.11467	0.02842
Utilities	0.07764	0.73256	0.16573	0.02430
Construction	0.04236	0.90116	0.06309	0.00844
Manufacturing	0.08783	0.78443	0.11240	0.01556
Wholesale trade	0.05681	0.81018	0.12094	0.01369
Retail trade	0.05111	0.87069	0.07338	0.00874
Transportation and warehousing	0.03978	0.89999	0.05450	0.00597
Information	0.07222	0.59672	0.30867	0.02335
Finance and insurance	0.08590	0.62741	0.25096	0.03664
Real estate	0.05494	0.80518	0.12280	0.01890
Professional and technical services	0.09806	0.44153	0.35907	0.10146
Management of companies	0.08911	0.50716	0.34538	0.05870
Administration and waste services	0.05278	0.84710	0.08489	0.01565
Education	0.08971	0.29378	0.40752	0.20886
Health and social services	0.06250	0.60885	0.21661	0.11187
Arts, entertainment and recreational services	0.05110	0.82702	0.10955	0.01313
Accommodations and food services	0.01945	0.95133	0.02551	0.00345
Other services	0.06365	0.79511	0.10571	0.03577
Government/public administration, and non-NAICS	0.08265	0.64846	0.17788	0.09106

7.8.3 Migration

Migration in the DM is determined by the working class and NAICS sectors. In each period of simulation a total of the number of individuals in working class and NAICS sectors is known. Given that working class is labor supply and a NAICS sector is labor demand, then either an excess or shortage of labor supply can be calculated. If there exists an excess of labor supply, then migration out occurs. If there is a shortage of labor, then migration in occurs.

A migration factor is calculated. In Albuquerque, the location for which the majority of data in the model is used, average household size is 2.4 persons. The migration factor is calculated to be such that a difference between labor supply and demand is found. Based on average household size, this difference is then multiplied by 2.4, the average household size. Doing so assumes that if an individual migrates in or out, she or he will do so taking with them 1.4 more individuals. If the labor condition is excess supply, then the migration factor reduces the population. If the condition is shortage, then the migration factor increases the population. For cases when labor market is in equilibrium, the migration factor is zero.

For use in the DM, an assumption is made regarding the cohort of individuals who move. The DM assumes that individuals in cohorts *0-4 . . . 40-44* are those who move. The migrating factor produces a number of individuals to migrate. Based on the stated assumption, those migrating in or out equally change the population in age cohorts *0-4 . . . 40-44*. The assumption assumes workers in cohorts *15-19 . . . 40-44* are mobile in terms of looking for work. Also, by the assumption workers are assumed to have 0.4 children coming from cohorts *0-14*.

7.8.4 Aggregate Water Demand (N= Households)

Water demand is based on the number of residences in Albuquerque. These include both owned and rented units. Aggregate water demand is determined by the number of households in Albuquerque times the demand for the representative consumer, per Equation 7-7. The DM provides the number of households. That is the number of occupied owned and rented dwelling units at each point in time. Using dwelling unit estimates, we estimate aggregate water demand at each point in time.

In the DM, Equations 7-13 and 7-14 are used to estimate dwelling unit numbers. Equation 7-13 estimates owner occupied dwelling units while Equation 7-14 estimates rental unit dwellings.

$$U_{Owned} = (0.68 * Pop) / 2.61 \qquad (7\text{-}13)$$

$$U_{Rented} = (0.32 * Pop) / 2.22 \qquad (7\text{-}14)$$

In Albuquerque, 68% of residents are found to live in owner-occupied dwellings while 32% are found to live in rental units. Average household size for owner-occupied units is 2.61 individuals and for rented units is found to be 2.22 individuals. A complete description of percentage derivation for owned versus rented as well as household size can be found in Appendix B, Tables B-9 to B-12.

The DM supplies to Equations 7-13 and 7-14 total population data in each period of simulation. From there, Equations 7-13 and 7-14 estimate the number of owner-occupied and rented dwellings. These data are used to estimate aggregate water demand.

7.8.5 Considerations

The population and demographic models are based on characteristics in the population as they have been. Changes in the population, the characteristics of the population, or even quality of life characteristics could be changed by adjusting the relationships presented.

7.9 Modeling the Regional Economy Using IMPLAN Input/Output Relationships

We began by using the Bernalillo County IMPLAN (MIG, Inc. 2000) file for the year 2002. Although the MRG is composed of many municipalities and several counties, Bernalillo is the largest in population and it contains the largest city in the state, Albuquerque.

Using the IMPLAN software, we attempted to duplicate the modeling framework established in (Malczynski 2003). This framework permitted the manipulation of the appropriate input/output (I/O) matrices from within our simulation tool, Powersim Studio, using Studio's built-in linear algebra functions. Since Bernalillo County does not have industries in all the IMPLAN NAICS-based sectors, it was decided to move to a high level of economic aggregation with 20 sectors (Table 7-18). This has repercussions for further work, i.e., testing the impact of industries not currently represented in Bernalillo County poses special problems (Cox 1996). We extracted the precursors of the standard I/O matrices (Miller and Blair 1985) from the IMPLAN software and manipulated them in Microsoft Excel to produce the standard I/O matrices (Erickson 2005; Nowosielski 2002). These matrices are then manipulated in the simulation model. Due to several data inconsistencies, most likely due to rounding errors, we fell back to using multiplier, employment, and other data directly from the IMPLAN output sets. All-value added multipliers were obtained (labor income [proprietor and employee], other property type income, and indirect business taxes). Output multipliers were also obtained (Miller and Blair 1985). We did, however, include the A matrix and the Leontief Inverse obtained from the IMPLAN software and manipulated in EXCEL in the model.

The employment multipliers from IMPLAN were combined with the water per employee per day per sector to permit the calculation of water consumption. The user interface permits an increase in investment or a redistribution of investment in the 20 aggregated economic sectors in Bernalillo County. Using the water per employee data we can calculate the water consumption impact of different economic scenarios. Increases in employment also drive increases in residential water consumption as new employees purchase or rent a residence. Using persons per household for owned and rented housing and price response functions per month and type of housing we estimate water consumption changes. Thus, these portions of the complete model estimate increases in water consumption by establishing a demographic or economic driver. Linking the demographic and economic driven components of water consumption has yet to be completed. The demographic approach is described in the next section.

Table 7-18. IMPLAN aggregated economic sectors.

NAICS sector	Total Employment	Jobs	
	QWI	IMPLAN	% Jobs IMPLAN
Agriculture, forestry, fishing, hunting	207	642	0.16
Mining	160	372	0.09
Utilities	1141	497	0.12
Construction	21815	29,160	7.05
Manufacturing	20756	19,705	4.77
Wholesale trade	13932	15,790	3.82
Retail trade	42302	12,613	3.05
Transportation and warehousing	9961	45,991	11.12
Information	12162	10,618	2.57
Finance and insurance	12661	16,263	3.93
Real estate	4733	14,370	3.48
Professional and technical services	29756	41,985	10.15
Management of companies	3988	4,250	1.03
Administration and waste services	24455	29,403	7.11
Education	26944	5,196	1.26
Health and social services	37893	38,349	9.27
Arts, entertainment and recreational services	4457	5,414	1.31
Accommodations and food services	26249	32,360	7.83
Other services	8478	22,210	5.37
Government/public administration, and non-NAICS	8758	68,288	16.52
TOTAL	310808	413,474	100.00

8. WATER MARKETING PROCESS MODULES

David S. Brookshire and Craig D. Broadbent, University of New Mexico
Don Coursey, University of Chicago
Vincent Tidwell, Sandia National Laboratory

8.1 Introduction

The focus of this chapter is the development of decision support tools for the exploration and design of water markets. While water markets fall within the broad context of our economic process modules theme we chose to treat this subject separately. The reason is because of the unique human behavioral element inherent to this task. As there is insufficient information and data to model participant behavior in a water market, we have created an environment to allow potential water traders to explore and even design their desired market. Here we describe the decision support framework and test the framework through a set of experiments involving stakeholders and the public.

8.1.1 Background

Since 1950, the demand for water has more than doubled in the United States. Historically, growing demands have been met by increasing reservoir capacity and groundwater mining, often at the expense of environmental and cultural concerns. The future is expected to hold much of the same. Demand for water will continue to increase, particularly in response to the expanding urban sector, while growing concerns about the environment are prompting interest in allocating more water for in-stream uses, and cultural issues will remain at the fore. So where will this water come from? Virtually all water supplies are allocated. Providing for new users requires a reduction in the amount of water dedicated to existing users and a mechanism for transferring water between users.

Markets typically are formed to facilitate the efficient allocation of goods and services. Under simple conditions buyers and sellers pursuing their own self-interest willingly agree upon a single price that fully compensates sellers and provides the commodity to those who value it highest.[28] The general concepts of water rights marketing (here taken to mean a permanent transfer of a water right) and water leasing (a temporary transfer) have been used as a volunteer, market-mediated system for transferring water between competing uses. Water market rights transfers are also often slow, and do not necessarily increase the flexibility of water users to trade quickly in response to near-term shortages and thus they do not directly address the need for a trading mechanism that can rapidly respond to climatic-induced needs.

A sampling of investigations into water marketing where the focus is upon the formal trading of rights (as against leasing) can be found in Howe (1986), Burness and Quirk (1980), Simpson (1994), Saliba (1987), Easter et al. (1999), Colby (1993), Colby (2000), Howe and Goemans (2003) and Brookshire et al. (2005). Often water marketing is viewed as movement from agricultural use to urban uses, which are typically viewed as permanent. Rosen and Sexton (1993) state that farmers are price takers in the market for crops and in order to achieve equilibrium they must face decreasing marginal products for variable inputs and increasing

[28] It cannot be emphasized enough that any transfer of water within a market-based system is a voluntary transfer.

marginal costs in the short run. Tradable water rights in a district allow for farmers to negotiate a sale on a variable input. Hamilton et al. (1989) studied a water market in Idaho where water was transferred from agricultural to power generation in times of drought. Instituting a water market allowed for power generation to be higher than current generation in a low-flow year. This also increased economic profit as water has its lowest marginal value product in agricultural in this region. Colby (2000) studied three different water markets: (1) SO_2 allowances, (2) fishery quotas, and (3) water rights. The finding was that as economic gains became compellingly large, resistance to transactions receded and an active market eventually developed. There are also questions surrounding how to develop a market (i.e., what are the third-party effects, transaction costs, well-defined property right, and the length of a transfer). Griffin and Hsu (1993) found that the transfer of diversion rights do not have third-party effects where the transfer of consumptive rights do. Here collaborative market participation by in-stream users is necessary to have a successful market, with price differences representing in-stream values of the affected third parties.

Water-leasing approaches have been set forth as one possibility for addressing the increasing needs and the possibility of reallocation within and across current uses, in a timely fashion. *Water 2025: Preventing Crises and Conflict in the West* (U.S. Department of Interior 2005) calls for consideration of market-based principles in the context of existing institutional structures.[29] The New Mexico State Water plan also calls for an efficient water transfer plan (Office of the State Engineer 2003). The New Mexico plan specifically supports water transfers as a strategic management tool for efficient water transfers inclusive of water banks.[30] Specifically, the State Engineer is responsible for implementation and encourages the creation of water banks in areas that are experiencing shortages.

Illustrations of water leasing include Carey and Sunding (2002), who studied the Colorado Big Thompson project and the Central Valley Project in California and found that consolidation within a district can lead to a decrease in the transaction costs. Similarly, Weinberg et al. (1993) found that a water market price represents the opportunity costs of using water but only in crop production. This means that water markets create an incentive to reduce water use while policies such as effluent or input taxes motivate conservation of only the quantity of water applied in excess of crop needs.

A recent report details the limited nature of water leasing in the western United States (West Water Research 2004). The report provides an analysis of water-leasing legislation policies and programs in 12 western states. There are 23 active water banks of which seven are market-based pricing, meaning that the price is negotiated between the buyer and the seller, with one bank

---

[29] The 2025 report sets forth some guiding principles for water transfers. These include in part, that recognition and respect must be made for state, tribal, and federal water rights, contracts, and interstate compacts or decrees of the United States Supreme Court that allocate the right to use water, that methods should include efforts to enhance water conservation, use efficiency, and resource monitoring to allow existing water supplies to be used more effectively, and that collaborative approaches go hand in hand with market-based transfers in order to minimize conflicts.

[30] The New Mexico plan states: "Consider water rights transfer policies that balance the need to protect the customs, culture, environment and economics health and stability of the state's diverse communities while providing for timely and efficient transfers of water between uses to meet both short-term shortages and long-term economic development needs."

having online negotiations. The other 16 banks are fixed-pricing or administrative-pricing schemes that are set annually. Length of transaction varies and the number of transactions is limited annually.

8.1.2 Objectives

In this chapter we develop a framework for exploring and designing water markets. In particular, we develop a stylized template for temporary voluntary transfers amongst competing uses (agriculture, Native American farming, environmental interests, urban interests) on the middle Rio Grande. There are many issues (engineering, physical, legal, and institutional) to be addressed in allowing for water transfers within a basin. In our initial framework, we represent one physical component by tracking evaporation associated with trades up and down the river. Our stylized template allows for future exploration of different physical, hydrological, engineering, spatial resolutions, market systems, legal institutions and priority frameworks, option trading through time, various representations of uncertainty, and different frameworks for third-party effects. The model design allows behavioral experiments to be conducted with subjects from key water use sectors to test how a voluntary water-leasing exchange process might operate. Central to our effort is linking of a hydrological/engineering/institutional model that allows for water transfers to be evaluated within the various frameworks.

8.2 Water Rights

In developing a leasing market structure it is important to understand the structure of water rights found in the region to ensure that the market functions within the existing legal framework. Along the middle Rio Grande there are various types of water rights, prior appropriations, and Native American and Spanish acequias.

The Bureau of Land Management (2006) recognizes prior appropriation doctrine as “first in time – first in right,” where those with the earliest priority dates have the right to the use of that amount of water over other users with later priority dates. There are four essential elements of prior appropriations doctrine: intent, diversion, beneficial use, and priority. Historically, intent has been determined by acts such as land clearing, preparation of diversion points, and/or posting of notice. Today intent is generally indicated by the application for a permit to divert. A permit is necessary for a diversion of water. Beneficial use definitions are used to determine whether a certain use of water will be recognized and protected by law against later appropriations. The last feature of prior appropriations is the priority of a water right. The first appropriator on a water source has the right to use the water in the system necessary to fulfill their water right; a junior appropriator cannot use water to satisfy their water right if it will injure the senior appropriator.

From the New Mexico State Engineer (2006), an acequia is defined in a physical, political and legal context. In a physical sense an acequia is a community ditch that is typically a man-made, open, unlined channel that conveys water to individual tracts of land, with the right being held in common. In a political sense an acequia is a public entity that functions to allocate and distribute irrigation water to landowners that are the members. In a legal sense an acequia is a ditch that is

not private or incorporated under the laws of the state and is owned by three or more persons as tenants. The area that defines an acequia represents a cultural boundary or a physical boundary.

8.3 Model Structure

The water markets model (Figure 8-1) integrates physical/engineering modules (e.g., climate, surface water, groundwater, and riparian habitat) with a behavioral/economic module (e.g., lease trading system, water demand). The physical/engineering modules used are a simplified version of that described in Chapter 2. The most notable simplification is that the model operates on an annual timestep. Application of the water markets model is limited to the middle Rio Grande Basin, bounded by Cochiti Reservoir to the north and Elephant Butte Reservoir to the south. As described in Chapter 2, the middle Rio Grande region is divided into six reaches (as defined by the river gages), which are designated Reaches 1 through 6 in this chapter. The model allows a series of players representing agricultural/Native American farming, municipalities, and environmental interests to trade water under high, average, and low water supply years.

For each timestep, two model runs are performed. During the first run the model calculates river flows, conveyance losses, and available irrigation water. This information is supplied to the leasing/behavioral model. When a trading period ends, the water balance is recalculated with the physical/engineering model. The second run of the model then calculates impacts of the trades on the hydraulic system.

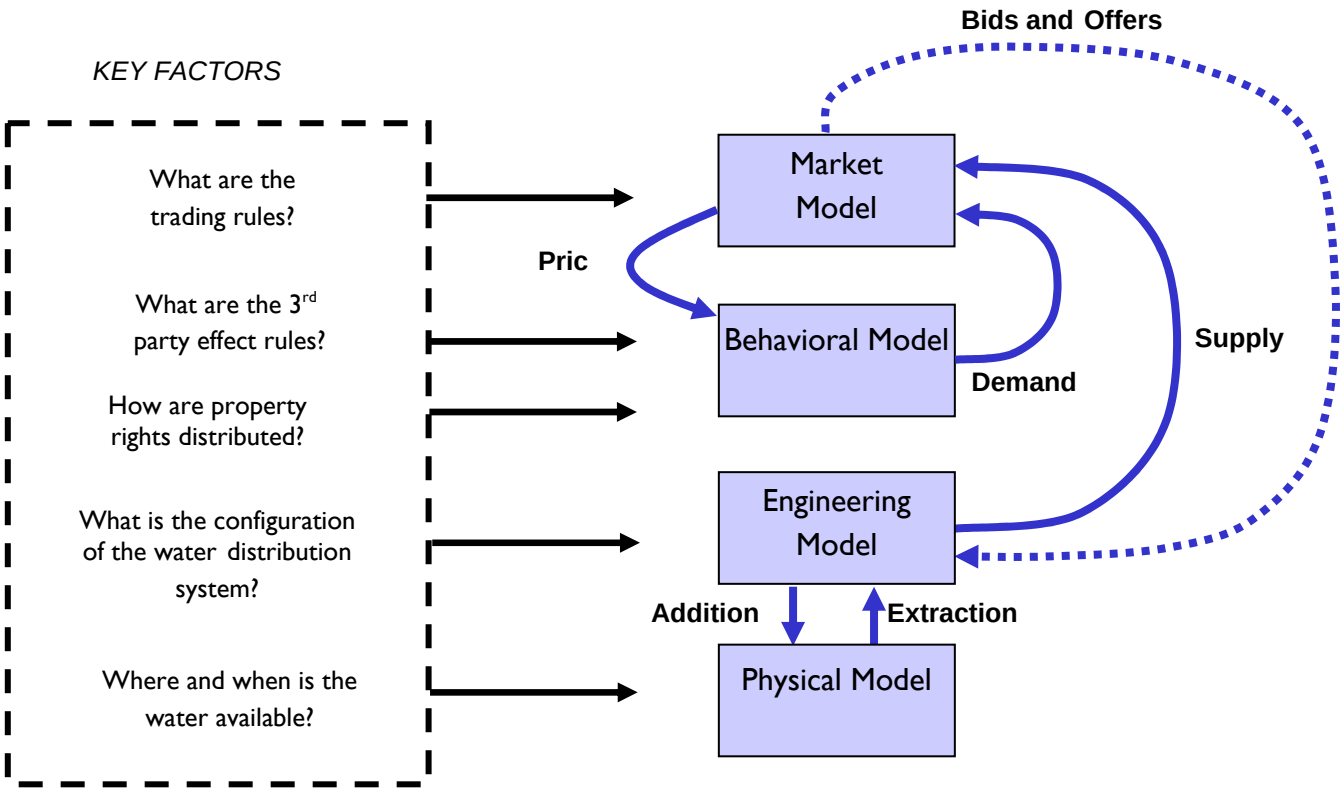

Figure 8-1. Schematic of integrated model architecture and feedback structure.

8.4 Market/Behavioral Model: Water Leasing Exchange Design

We utilize an open market trading system similar to the system used to trade other commodities such as wheat, corn, pork bellies, and metals. Specifically, we employ a system known as a double oral auction. Buyers and sellers declare their bids and offers to the market. Contracts are established when a buyer and a seller agree on a standing price. The market is open for a fixed amount of time. Time in the experiment consists of a series of years, during which the market for water occurs during the six months of the growing season. There are four classes of participants in a leasing experiment. The participants (subjects in the experiments) represent the interests of specific users, including agricultural, Native Americans, urban interests, and environmental interests. Each agent represents the interests of one of these four user groups in a single reach of the model. Trades are allowed between reaches and within reaches. Subjects are motivated by monetary reward in the experiments and are paid based on profits earned through the leasing of water or by obtaining their yearly payoff based on their water use. We are not conducting simulations; rather we are assuming the participants in the experiments maximize profits based on their underlying payoff functions. The experiment is based on the engineering model with a stylized river. The river flows from Reach 1 to Reach 6 (Figure 8-2). Using Powers Studio 2003 water reduction factors are calculated for the four different classes of experiments.

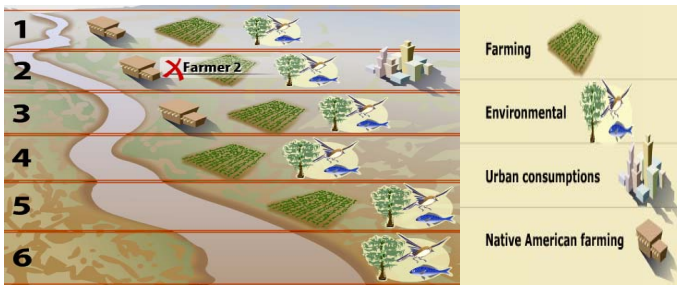

Figure 8-2. Depiction of stylized river.

Each water user group is motivated by a utility function unique to their needs. Agricultural/Native American users require three acre feet (AF) of water during the growing season for their crops. Failure to obtain this minimum amount of water results in complete failure of their crop for the season. Excess amounts do not increase the crop payoffs but can be leased out for monetary gain. Players have the option of leasing their water instead of growing a crop. The urban region within the model represents Albuquerque. For the urban user, it is assumed that water produces value in ever-increasing amounts but is subject to the law of diminishing marginal utility. For this reason, we model the urban payoff to water using a quadratic specification. Environmental uses of water are assumed to be for minnow protection and riparian restoration. These demands are modeled by a set of preferences that depend upon maintaining a minimum of two AF of water in the river. Below this minimum, environmental losses occur. Above the minimum, positive environmental outcomes are forthcoming.

Figure 8-3 shows the demand functions for the three user groups. The demand functions for agricultural/Native American farming and environmental interests are a step demand function

while the urban user has a downward sloping demand curve. Agricultural/Native American users seeking to maximize monetary payout will be willing to pay up to (b/a) to obtain (a) units of water. The environmental user's demand function is also a step function. The environmental user is willing to pay up to (c/b) to obtain (b) units of water. However, the environmental user receives a negative payoff if they allow water in the river to drop below a threshold of (b) units. This effectively models environmental concerns such as silvery minnow protection in the middle Rio Grande. The urban user faces a downward sloping demand curve to model the idea of diminishing marginal returns.

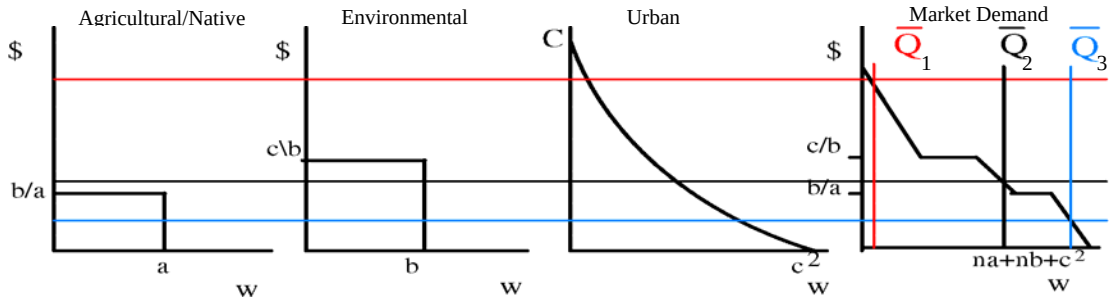

Figure 8-3. The three different water user groups are summed to create a market demand in order to develop the efficiency price. Q_1 represents a dry water scenario, Q_2 a normal water scenario, and Q_2 a wet water scenario.

Multiplying the agricultural/Native American demand function by the number of players (n), environmental by the number of players (n), and the urban by the number of players (n), then summing creates a market demand curve, the diagram on the far right of Figure 8-3. Using the experimentally set market supply and the market demand that comes from the aggregation of the three demand functions, an equilibrium or efficiency price can be calculated as the intersection of the market supply and the market demand. This allows the observed experimental prices to be compared to the efficiency price in order to determine if the market is efficient.

Three different climatic scenarios are also represented in Figure 8-3 with red (Q_1) representing a dry climatic scenario, black (Q_2) representing a normal climatic scenario, and blue (Q_3) representing a wet climatic scenario. The different climatic scenarios are the market supply of water, with the intersection of the aggregate demand curve being the efficiency price for the market.

8.5 Experiments and Results

The market experiments are conducted through a series of bidding sessions. In these sessions information from the physical/engineering model is passed to participants via a web interface. Water users may enter bid quantities and prices to sell or buy a unit of water, or they may accept specific offers at one-unit increments. The web interface checks to make sure both the buyer and seller each have sufficient amounts of money and water, and then determines if the transfer is possible using loss estimates from the physical/engineering model. Other potential constraints on a trade include water availability, Rio Grande Compact compliance, and/or minimum river

flow requirements. When a trade is made, the accepted bid or offer disappears from the bid/offer sheet. Buyers and sellers are free to update their bids and offers throughout the duration of the trading year. At the end of the year, the compact balance is checked and the hydrological model is recalibrated based upon the contract's impact on water flows. Bidding is concluded when all bidders have bought or sold as needed, some set number of transfers have been refused, or a fixed time limit is exceeded. All trades are voluntary. As with Smith (1982) these are not simulations; rather participants received real dollars for participating.

Fourteen experiments were conducted over the summer of 2005: three decreasing scenarios, three increasing scenarios, three dry scenarios, three normal scenarios, one above-normal scenario and one below-normal scenario. Scenarios were developed by coupling the physical (hydrological) model with the engineering model. The water reduction factors for the experiments are shown in Figure 8-4. For example, in the decreasing water scenario the agricultural/Native American user begins trading year 1 with 3.75 AF of water, which is above the 3 AF required to grow a crop for the trading year. Over the course of the trading years, water becomes scarce. In year 10 the user begins the trading year with 1.45 AF of water. The water reduction factor was used to calculate the allocation for each user. Results show that the weighted average price obtained in the experiment is above the efficiency price calculated from the demand functions (Figure 8-5). The model also proved to be robust, as all users engaged in multiple trades during each trading year.

Trading of water was observed both between reaches and within reaches. The current model only has one representative per user type on a reach (i.e., only one environmental user per reach). Even with a single representative, the results have shown that trading occurs amongst the user groups and within the user groups. Figure 8-6 shows how water was traded for the agricultural/Native American user during one decreasing water scenario (experiment 1). As can be seen, most of the trading occurs between the user group itself, with very few trades occurring with the urban user. As water became scarce, the number of trades engaged in by the agricultural/Native American group declined. Figure 8-7 shows that although the number of trades declined for this user group the amount of water traded increased as water became scarce. Results show that agricultural/Native American users leased water in dry years to obtain monetary benefits rather than grow a crop. The initial allocation of water for this user group is the point zero in Figure 8-7. The negative percentage means that farmers are net sellers of water.

Environmental users benefited the most in a decreasing water scenario, as they became net purchasers of water. The market system is able to meet environmental concerns such as protecting the silvery minnow and farmers were able to make a positive monetary reward by selling water to these users. The model is also able to track water movement between reaches and user groups. A priori expectations are that water would be traded upstream due to the effect of evaporation. Thus, water that would have been lost to evaporation can be saved through the trading of water from the lower reaches to the upper reaches. Results from the experiments have shown this to be true.

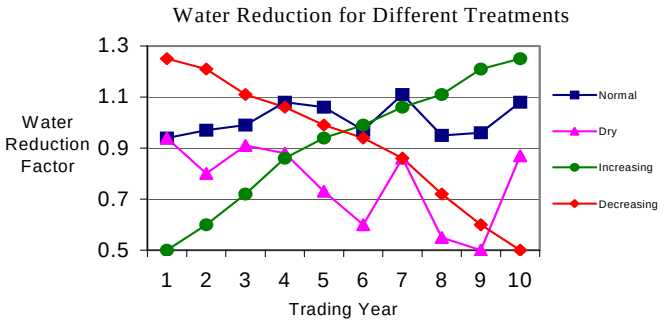

Figure 8-4. Four different climatic scenarios.

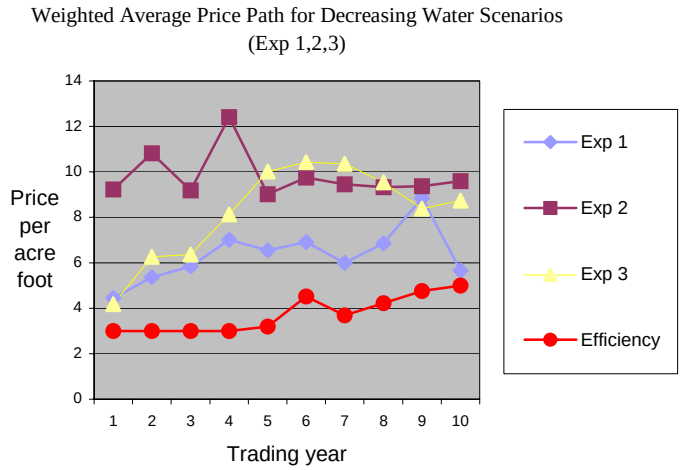

Figure 8-5. Weighted average price in relation to efficiency price.

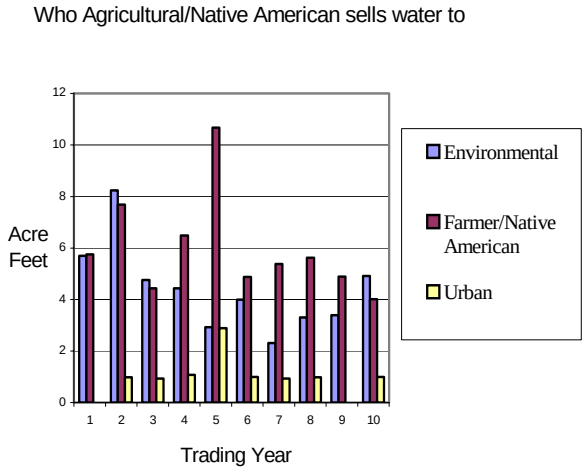

Figure 8-6. Agricultural/Native American trading of water.

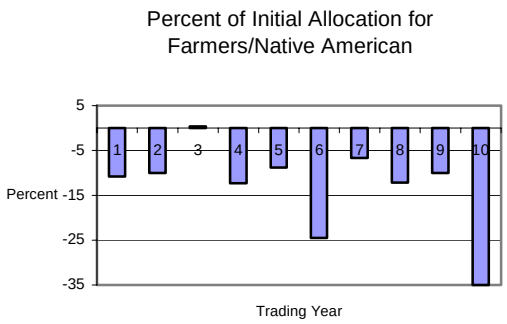

Figure 8-7. Agricultural/Native American percentage of initial allocation.

Figure 8-8 is a representation of the stylized river before a trading year (left side) and after a trading year (right side). The result shows the 7th round of a decreasing water scenario. To determine water movement by reach it was necessary to aggregate total water in each reach. Summing each user's water allotment by each reach did this. Since the environmental user's initial water allotment is below the minimum flow requirement needed to protect riparian interest and the silvery minnow, they purchase water since they are facing a monetary punishment if they allow the river to fall below this threshold. This explains why the results show a positive gain in the lower reaches of the river in Figure 8-8, as there are only an agricultural and an environmental user in Reaches 4 and 5 with only an environmental user in Reach 6. The environmental users in the lower reaches are purchasers of water because of the demand functions they face as shown in Figure 8-6.

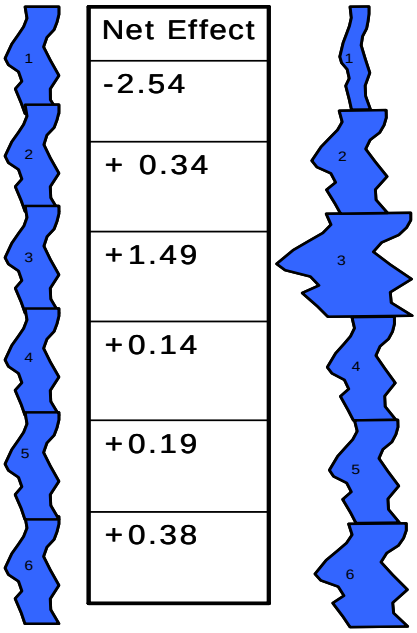

Figure 8-8. Representation of the stylized river before and after trading with the net effect for each reach.

Not only were these outcomes realized from the experiment, it was also observed that participants are able to handle the cognitive complexity of trading in a complex water market subject to exogenous hydrological forces. Multiple trading was observed in each experiment run showing that participants comprehend the cognitive complexity of the model and that the model is robust.

8.6 Extensions

This model is merely a starting point, where any possibly climatic scenario and its effect upon behavior can be modeled. Further research to be conducted will have real farmers play the role of the agricultural agent, along with Native Americans, environmentalists, and urban consumers playing their respective roles. This will allow for water and its role in the culture of acequias to be more accurately modeled and included in later experiments. Currently third-party effects are not included in the model; including such effects will introduce solution concepts for these situations. The current economic model is a double oral auction; other models will be examined as a way of conducting trades. Examination of intertemporal trading—both within years and between years—will be incorporated into the model. Including transaction costs, modeling laterals, and using a central planner in the model will also be explored as extensions or variations to the current economic model.

8.7 Acknowledgments

Some aspects of this project were funded through the National Science Foundation's Science and Technology Center, Sustainability of Semi-Arid Hydrology and Riparian Areas (www.sahra.arizona.edu). The authors also want to recognize Kyle Carpenter and Ramon Vazquez for their help in model interface design and implementation.

9. COLLABORATIVE MODELING PROCESS

Kristan Cockerill, Cockerill Consulting
Vincent Tidwell, Howard Passell, Len Malczynski, Sandia National Laboratories

9.1 Introduction

The previous chapters have dealt exclusively with the conceptualization, formulation, and testing of physical and social process modules. The purpose is to populate a system dynamics toolbox from which analysts can construct watershed models to support resource planning. These generic physical and social process modules can be structured so as to capture the unique qualities of a specific watershed and thus provide a venue for the professional and layman alike to perform what-if analysis and explore alternative futures. However, for such a model to reach its full potential requires attention to the technical modeling aspects as well as the process by which it is created and used. Specifically, transparency in the model development process is required if broad consensus is to be achieved. One approach toward this end is the implementation of an open "collaborative modelling" process, which is the subject of this chapter.

While collaborative modeling has been used for decades, its current popularity may be partially due to advances in computer technology. The software available for constructing system dynamic models makes it relatively simple for modelers to build a model and extremely simple for novices to run an existing model. Additionally, improvements in computer interface functions make model output more accessible to non-technical users.

The literature reflects that collaborative modeling has been employed on diverse environmental subjects including assessing the effects of sheep grazing on sage grouse populations (van den Belt 2004), energy use in iron and steel production (Costanza and Ruth 1998), air quality issues (Stave 2002), and numerous projects related to water management (Moxey and White 1998; van Eeten et al. 2002; Cockerill et al. 2006 [in press]).

Collaborative modeling team composition can vary in terms of disciplines represented (e.g., biology, hydrology, anthropology) and functional roles (e.g., professional researchers, members of the public). Some team members need to be modelers who write the necessary code for the model designed. Some teams employ a facilitator and a note-taker. The process for collaborative modeling is flexible to allow a team to meet the needs of their specific project. Some projects may be completed in a single meeting while others are multiyear endeavors. Traditionally, the team will meet face to face, but technology is now making it possible to conduct "virtual" meetings that still allow all team members to contribute to constructing the computer model.

There are numerous rationales posited to support using a collaborative modeling approach. Vennix (1999) documents that because human brains are not very efficient information processors and do not readily think in terms of causal relationships or feedback loops, collaborative modeling can be particularly helpful in dealing with "messy problems" that have complex system characteristics. Building a model allows participants to begin to appreciate the

complexity, and the team therefore develops a common understanding of the issue, which improves the odds that results from the collaborative effort will be implemented (Palmer et al. 1993; Vennix 1996; Rouwette et al. 2002; van den Belt 2004). By constructing a model together, participants can better appreciate the difficulties in capturing the relevant variables and securing accurate data so that participants come to be vested in the tool and hence support its output. Case studies of collaborative modeling for a variety of subjects show that the technique increases knowledge levels about the particular topic, and there is evidence that creating a model together is more successful in helping to resolve an issue than simply having participants use an existing model (Rouwette et al. 2002). The case studies available reveal that collaborative modeling often leads to increased consensus about a problem and mitigating approaches (Costanza and Ruth 1998; Rouwette et al. 2002; van den Belt 2004). Developing consensus is important as collaborative modeling can allow improved understanding not just among diverse disciplines, but can help span the divide between science and policy (Costanza and Ruth 1998; Cockerill et al. 2006 [in press]).

It is important to note, however, as Rouwette et al. (2002) do, that the literature does not well reflect efforts that failed to reach their goals or suffered from poor group dynamics or miscommunication. Therefore it is difficult to ascertain how widespread attempts at collaborative modeling have been. This paper contributes to the knowledge base by describing several collaborative modeling projects that provided the authors with a diverse array of experiences and lessons learned. The experiences reported here have provided insight into how to "do" collaborative modeling. Some of the lessons learned are not necessarily insightful to anyone who has attempted projects like those described here, but because the approach is relatively new, everyone is still on a steep learning curve and all lessons are valuable. Additionally, because these efforts are multidisciplinary, the existing literature is less than cohesive, as ecologists publish their experiences in the ecology journals, modelers publish in the modeling literature, and economists write for the economic publications. Further, the existing literature has paid less attention to the group dynamics of the collaborative modeling process than to the resultant models, their output and use (notable exceptions are Nicolson et al. 2002 and Moxey and White 1998). Our "lessons learned" suggest that a project's objective and focus as well as group composition and geographic dispersion of the team members affect group dynamics and hence the collaborative modeling process.

9.2 Collaborative Modeling Projects

Since 2002 the authors have worked together on several projects utilizing a system dynamics platform to collaboratively develop computer models related to water management issues. The methodology employed has been to establish a team that agrees to meet frequently (usually once or twice a month) over the course of the project, which can be one to three years. This paper describes four of these projects as a way to demonstrate various experiences with the collaborative modeling concept.

The projects reported here are multidisciplinary and reflect two broad categories: those that are directly tied to a policy process and those that are only indirectly linked to policy. The latter are technical efforts designed to explore ways to advance the system dynamics approach and the collaborative modeling method. For these more technical projects, the teams are professionals

("experts") from diverse disciplines. The projects with a direct policy focus are concerned with making decisions about resource management. The authors have participated in one project driven by members of the public and in another effort featuring a group of individuals representing professionals, the public, and policy-makers.

The following sections cover in more detail the unique aspects and lessons learned from these various efforts. Table 9-1 provides an overview of the characteristics of these four projects.

Table 9-1. Characteristics of the four collaborative modeling projects described.

	Type of Project	
	Policy Direct (Natural Resource Management)	**Policy Indirect (Technical Development)**
Team Characteristics		
Composition	Professionals and public	Professionals only
Size	6-15	25
Duration	2.5 years	3 years
Geographic dispersion	Low	High
Project Characteristics		
Topic	Narrow	Broad
Focus	Static	Several revisions
Geographic focus	Static	Several revisions
Team Characteristics		
Composition	Professionals, public, policy-makers	Professionals only
Size	20	12
Duration	1 year	1 year
Geographic dispersion	High	Low
Project Characteristics		
Topic	Narrow	Narrow
Focus	Static	One revision
Geographic	Static	Static

9.2.1 Professional-Only Teams

In 2003 the authors began work on a professional-only project focused on developing discrete system dynamics "process modules" that are "swappable," thereby enabling others to more rapidly build a model to address their specific water management needs. A team of more than 25 individuals from federal agencies, state universities, and consulting firms representing ecology, economics, law, geography, policy, hydrology, and chemistry are contributing to the model. Team members are geographically dispersed over a two-state area. There is not a facilitator for this project. The principal investigator runs the infrequent full-group meetings.

Since inception, this project has changed its geographic scope and has changed focus more than once by revising the specific system to be modeled as a test for the module concept. This team is not cohesive, owing in part to its size, the diversity of organizations and departments represented, and the infrequent group interaction. Additionally, there was some tension surrounding the foci changes, as decisions were not made within the team as a whole, but between the principal investigator and a subgroup. The whole team meets only about twice a

year, so the various disciplines do not interact with each other on a regular basis. Discipline-specific subgroups meet more often and are developing modules that the modelers are then integrating.

Because of this segregated approach the group has not developed cross-disciplinary communication skills and there have been issues with finding common language. For example, in trying to determine if data were available to demonstrate relationships among particular variables, the principal investigator reached an impasse with the economists who contended that it was not possible to show "trade-offs" among the variables being considered. After several discussions about options, one of the economists asked the principal investigator to define trade-off. From the principal investigator's perspective, a trade-off was simply showing a difference between one alternative and another. To the economists, a trade-off was a very specific term to reflect marginal value. With the broader definition in place, they were able to agree that the existing data were sufficient to show trade-offs.

Other communication problems have developed because some team members have not invested the time to thoroughly understand the modeling technique being used and the infrequent interaction has meant limited exposure to the technique. Reflecting this, the project was into its second year when some team members realized that they were not appropriately interpreting causal loop diagrams, a fundamental component of building a system dynamics model. This lack of understanding had contributed to long discussions in meetings where it is now apparent that individuals were "speaking past each other" because they were employing different interpretations.

Another professional-only team convened in 2004 including about 12 individuals with expertise in ecology, economics, anthropology, policy, law, agriculture, and hydrology. Participants were all from one geographic area and represented a federal agency, a state university, and private consultants who worked together for one year, meeting about once a month. This team did not include any formal facilitation, although when necessary the principal investigator took on that role. Although there were some early struggles in trying to understand research methodologies emanating from the diverse disciplines, the team became quite cohesive and effectively moved between small discipline-based or topic-based subgroups back into the unified group to integrate data and ideas. The team quickly developed a rapport that enabled cross-disciplinary communication. Team members were familiar with each other's terminology and avoided miscommunication due to multiple definitions of key words or concepts as we experienced in the first professional-only team. One contributing reason for this was that the project was fairly narrowly designed from the outset. The geographic area was defined, and the key question was established. Also contributing to the team's success was that early in the project team members prepared narratives to explain the systems relevant to the project, and these were used to draw preliminary diagrams showing causal relationships among variables. This further established the bounds of the project, and highlighted how the various disciplines might contribute to the effort.

About halfway through the year, the project team revised the focus question, as it became clear that key data were unreliable. Additionally, interviews with stakeholders revealed that some of the team's assumptions were erroneous while others were accurate at a macro scale, but incomplete at a more micro level. This highlighted the need for integration of team members

with first-hand process knowledge with specific disciplinary experts. Because of the lack of data and the late change in focus, the model developed is not terribly robust. The process, however, uncovered very interesting findings regarding the status of data and behavior in the region as well as provided lessons about applying methodologies from various disciplines. The team considered this effort a success because it did highlight issues in collaborating across disciplinary cultures and provided insight into integrating more social data into a system dynamics project. For example, the social scientists on the team encouraged stakeholder interviews earlier in the process, and if that had occurred the key question may have been revised earlier and changed the overall effort. Additionally, with a longer project timeframe alternative data for the revised focus may have been gathered and used to strengthen the model.

9.2.2 Professional and Public Team

In 2002 a volunteer group that was spearheading a regional water planning effort approached the authors and proposed that they collaboratively develop a model that would show the relationships among various water management and conservation strategies for the region. The team began its work with about 15 members, which dwindled to about six over the two and half years of the project. Team members were volunteers from the region who had expertise in geohydrology, ecology, agriculture, economic development, and law. For the first year the team met twice a month and then reduced this to about once a month. This group had a dedicated facilitator who also took notes during meetings. The project's topical focus and its geographic range were well established at the outset and remained constant throughout the effort.

The initial group lost cohesiveness, in part due to public participation pitfalls including a loss of trust, concerns with data, and concerns with political agendas, as well as the long duration of the project. Although it was largely successful, the project suffered from lack of attention to basic public participation guidelines and difficulties in communicating across the "expert" to "layman" disciplinary boundary. One issue was in differing perceptions about how to decide what data to include and what is "significant" in terms of affecting model output. For example, one team member repeatedly cited a data point but never supplied an actual source for the data, and hence it was not included in the model; this was perceived by some to be a bias. In other cases, team members or members of the broader public would suggest adding variables or particular data to the model that the modelers concluded would not have affected model output and hence was an inefficient use of time/resources. This, however, may have been interpreted as bias even when rationale for non-use was explained. The modelers also made some communication mistakes by holding meetings with officials not involved in the model development project. Several team members interpreted this as capitulating to political pressures regarding model content and output. For a more detailed description of this effort, see Cockerill et al. (2006, in press).

Despite these negatives, the smaller group that participated throughout the entire process did develop cross-disciplinary communication skills and the result was a very robust model. This model allows users to compare various water-management alternatives and has been demonstrated in diverse venues (e.g., public meetings, school groups, professional meetings). While the model was a key tool in facilitating the planning process, actual numbers from model output are not the basis for the plan's recommendations. One reason for this is the continued lack of consensus among the modeling team, the broad planning group, and policy-making

institutions as to the neutrality of the model, the validity of its assumptions, and the accuracy of various data sources. In post-project interviews, however, team members agreed that developing the regional water plan would have been more difficult without the model.

Modeling team members have touted the benefits of collaborative modeling to help the public see complex issues. The success of this effort has attracted attention to this technique that the authors have leveraged to develop other collaborative modeling efforts throughout the world.

9.2.3 Professional, Public, and Policy-maker Team

A 2004 legislated water settlement prompted the authors to become engaged in a collaborative process that involves professionals, the public, and policy-makers. This effort brings together a diverse group of individuals to explore the complexity and the trade-offs inherent in this policy decision.

The team includes representatives from several federal agencies, state agencies, county government, municipal government, county soil and water conservation districts, environmental interest groups, and the mining industry. Expertise includes hydrology, economics, ecology, policy, agriculture, ranching, and development. This team is employing a facilitator and a note-taker.

The team first met in September 2005 and agreed to meet twice a month for one year. One unique characteristic of this project is that the majority of the meetings are conducted via Webex, internet technology that allows numerous computers to be linked so that everyone participating sees and can use the same computer screen. During the meetings the team speaks via a conference call. While there have been a few technical glitches, the system has worked quite well and allows this geographically dispersed team to meet frequently. Although the project is its infancy, the team has been quite cohesive and is approaching some level of cross-disciplinary communication. Contributing to this early success is the fact that many of the modeling team members are also members of a regional water planning group, which has been meeting regularly for several years. Previous interaction has enabled them to become familiar with each other and to recognize common definitions of terms and concepts.

One of the lessons being learned in this effort is that individuals have not immediately understood that the team will make decisions about what to include in the model, what data to use, and what alternatives to explore. There has been a perception that the modelers have a model in mind that they are simply revealing to the team for comment. Precisely to better understand group dynamics like this, the lead author conducted individual interviews with each team member. These interviews revealed that individual team members are making some false assumptions about what outcomes other team members desire for the settlement. So, despite the previous relationships among various team members, there is still some level of misunderstanding about motivation and desires in addressing this particular water-management issue.

The policy relevance for this effort is clear, as the state agency representatives have explicitly told the team that this model will be one of several tools used in making decisions about how to

respond to the settlement. A new and unexpected challenge in this project has been to encourage the policy-makers to interject into the process to identify politically sensitive issues or data concerns. There have been several instances where a policy-maker remained silent or seemed to agree with a process-oriented decision during a meeting and then privately told the authors that what was agreed to was not possible. For example, the team approved a draft communication plan designed to disseminate information about the project to a broader public audience. Following the meeting, the team facilitator received an e-mail that the communication plan was unacceptable for the state agencies and needed to be revised.

9.3 Discussion

The authors have gleaned much from these experiences concerning group dynamics and multidisciplinary communication in collaborative modeling projects**.** Perhaps the primary lesson is that each group and each project is unique and it is difficult to tease out exactly what contributed to the specific experiences of that group. We do believe, however, that there are generalized lessons available from our experiences related to how closely linked the project is to a "real" policy decision, the group composition (e.g., professionals, public), and group interaction that is influenced by size and geographic dispersion.

This emphasis on group dynamics and the process is key because projects like this can provide significant insight into model development and potentially into policy questions without relying on model output. As noted in the second professional-only description, the team discovered important data gaps and personal motivation factors related to the topic, independent of the model created. They also successfully explored how to integrate social data into a system dynamics model. In the public-driven project, team members reported that the process of developing the model was tremendously helpful in getting the planning team in a position to write a plan. The model's numeric output, however, was not the primary source for the plan's final recommendations. This is not unexpected in system dynamics work, and in collaborative modeling the process is as important as the product. As Sterman (2000) describes, a typical attempt to model a problem using the system dynamics approach starts with listing variables of interest, creating reference modes or time graphs, building causal loop diagrams, developing dynamic hypotheses, and then, *if required*, building a computer model.

Key to establishing a productive process is learning to communicate among the diverse disciplines and interests that are represented on a collaborative modeling team. In any multidisciplinary team, communicating across disciplinary lines is a challenge. Each discipline comes to the table with its own vocabulary, theories, methodologies, and tools. A key element in collaborative modeling is to transcend disciplinary bounds and to find a place where all of the disciplines can mix into something new and truly interdisciplinary (see Klein 1990). The communication challenges are exacerbated in collaborative modeling as not only must individuals learn new vocabulary and concepts from other disciplines, but everyone must also learn about general principles of system dynamics modeling. Without this base level of understanding, team members from the various disciplines will have trouble deciphering how their skills and expertise may fit in. Additionally, collaborative modeling is intended to cross the science–policy divide, and hence the teams encounter the communication issues relevant to accomplishing this.

Process and communication lessons have been present in all of these projects, but there have also been discreet lessons to be learned from the different project objectives and composition. In the professional-only projects with their technical objective, the lessons echo findings that Moxey and White (1998) and Nicolson et al. (2002) document. Nicolson et al. (2002) present "heuristics" while Moxey and White (1998) discuss "reflections" related to collaborative modeling efforts. They use these terms rather than "rules" or "guidelines" to emphasize the fluid nature of this method. Each modeling project is unique and the dynamics generated cannot possibly be predicted at the outset; therefore they require flexibility rather than rigid rules. We agree with the previously published work that identifying what skills are necessary for the team, dedicating time to problem definition, allowing the project to change focus as it evolves, providing for face-to-face meetings, and trying to avoid generating "shelfware" are key to collaborative modeling projects with professionals.

One benefit to working with a professional-only team is that while research methods and standards differ among disciplines, participants are familiar with general research principles and have likely employed models of one kind or another. Another benefit is that professionals can more readily commit the time and energy required for a collaborative effort. There is no guarantee, however, that team members will offer this commitment, as the authors learned in the longer-term professional-only project.

Unique among documented collaborative modeling efforts, the professional-only projects described here were done "in-house," meaning there was not a client who requested the work and they were not directly tied to a policy process or specific decision-making goals. Therefore, the teams could experiment and had the freedom to try diverse approaches. This is beneficial when trying to truly understand a complex system and to identify new approaches to modeling those systems. As conditions change and knowledge grows, the team can respond without violating an obligation or agreement with a client. This provided excellent learning opportunities as both of the professional-only projects did change direction as the teams learned more about their topics.

While these professional-only projects were not intended to contribute directly to a policy process, the indirect and eventual point of improving the collaborative modeling approach is to assist the public and policy-makers in making better decisions. Therefore, a negative aspect of not having a client is that there is a strong likelihood that the work will never be used in any policy arena and will simply remain "shelfware." One reason for this is simple ignorance. If policy makers do not know that a model or modeling method exists, they are not going to employ it. However, such professional-only projects can be invaluable in developing the experiential and technological infrastructure for future policy-driven projects.

Like the professional-only projects, the authors' experience with the public participation reflected lessons from previous work as well as some additional lessons (see Palmer et al. 1993; Stave 2002). Involving the public in collaborative modeling increases the communication challenges, but the benefits are numerous. If members of the public who represent key interests are at the table when the model is developed and have a say in establishing parameters, delineating assumptions, and determining what data to use, they then have a vested interest in the model's output and are less likely to criticize the results. Additionally, public-driven efforts are potentially more likely to be used in making decisions.

The caveat to this is intentional ignorance on the part of policy-makers. Where the modeling project addressed complex and controversial public policy issues the authors at times have encountered an attitude among decision-makers that it is better for them to not know about the project's lessons and/or the model's output so that they do not need to address the issue or can maintain the status quo. In policy there can be a tendency to emphasize those variables that have been counted and quantified (Stone 2002). This principle may well hold with model output. With its numeric output, a computer model can promote a perspective of certainty to a policy process. There is also the possibility of "duelling models." If policy-makers already have a tool and the collaborative team's model disagrees with the policy-maker's model, this can create conflict, and policy-makers are likely to support the model with which they feel the most ownership.

A key drawback to public projects is that they are time- and resource-intensive. Because team members are likely volunteers, it can be difficult to obtain the level of commitment required to generate a sound model. Additionally, the public participants may come to the process with little or no experience in conducting research, with little or no background in the issue to be addressed, and with numerous misconceptions about the issue. Some members may want to participate simply to pursue their personal agenda rather than truly investing the time to create an interdisciplinary tool.

When projects are expanded to include the public, many of the heuristics applicable to professional-only projects remain valid, but there are additional issues to consider. For public projects, clearly defining the project should include communicating what system dynamics models are well designed to do and what they are not capable of doing, as well as discussing how data should be gathered, interpreted, and used in the effort. Experience with the public project described here revealed that it is important to establish ground rules for how the team will make decisions and how the team will interact. For example, how will decisions be made (e.g., simple majority vote, unanimity) and what roles will team members play? What level of commitment can the team give? Teams should explicitly discuss how to balance team control with efficiency in completing the project. For example, will the team members be responsible for identifying and gathering data to give to the modelers? Or will the modelers find the data and generate draft models for team comment? Is it permissible for the modelers to meet independently with potential sources and agencies not involved in the project? These kinds of questions should be addressed at the outset to avoid miscommunication in a public-focused effort.

The success of the public-driven model has also been instrumental in showcasing the possibilities for improved decision-making using collaborative modeling and was a key factor in why the professional, public, and decision-maker team was convened. This more complicated team makeup has presented a new set of communication challenges. Presumably if decision-makers are on the team, they too become vested in the process and the product and will employ the results from the process and the model in actual decisions. Ideally, this more holistic approach can also alleviate the "duelling model" problem, as the decision-makers are familiar with the collaboratively generated model and can well assess its relationship to other models in making a policy decision. When policy-makers are involved, it is appropriate for them to delineate how they see the model development process and/or the model itself being used in making a particular decision. Policy-makers can contribute to the discussion by explicating

political barriers and/or identifying data sources that are not available. It is important to recognize Sterman's (2000) ideas, however, that teams should not limit themselves with assumptions about what is politically palatable. It is more interesting and potentially more effective to pursue all possible options and see what the causal loops and model reveal.

In the two projects with direct policy relevance, there is an overlying concern (not necessarily directly stated) about the project's results and a sense of the "realness" of the stakes in developing a tool to be used in a decision-making process. Conversely, in the more technical efforts, there was less concern with what the model might reveal because the projects were more "academic" than "real." This, coupled with the greater diversity of interest affected how the team members interacted with each other. In the technical projects there was a greater sense of freedom to propose any and all ideas without fear of being perceived as pushing an agenda. Additionally, the ability to change foci is perhaps more appropriate in the technically focused efforts, whereas in public projects shifting foci may lead to greater controversy if the shifts are not well explained or are perceived to be the result of some bias.

Team size and its geographic dispersal contributed to the group dynamics in each of these efforts. Meeting is important in encouraging cross-disciplinary communication and developing a solid rapport among team members. For the long-term professional-only project, meeting frequently as a whole group was not feasible because of the group's large size and dispersed nature. This has resulted in minimal group communication and responsibility for integrating across disciplines has fallen on the principal investigator. The impact on the actual model, however, may be minimal because its objective is not directed toward a specific policy.

The two project teams that were not geographically dispersed were also relatively small. Convening meetings was still a challenge due to busy schedules, but the principal investigators emphasized the need to meet regularly early in the project, and hence the team members got to know each other and cemented their commitment to the project. Because of this cohesion, the teams continued to meet regularly to see their projects through to conclusion. In both cases, despite the differences in the robustness of the final model produced, the team members declared their project successful.

The lessons about frequent, in-person meetings were taken to heart in framing the latest project involving professionals, the public, and policy-makers. The team is fairly large and is geographically dispersed. Most of the non-government team members, however, know each other from previous work. This coupled with the internet technology that allows the team to meet "virtually" every two weeks seems to be enabling the cross-disciplinary cohesiveness that the smaller, less geographically dispersed groups experienced. The computer-linking software that the authors are using reflects yet another advance in technology that can contribute to collaborative modeling being used more extensively.

9.4 Conclusion

As previous authors have indicated, collaborative modeling does offer significant advantages for improving environmental decision-making. The experiences described here offer insight into some of the advantages and disadvantages of various types of collaborative efforts and highlights that each experience is unique. While previous lessons are helpful, they do not protect a collaborative team from making mistakes and do not ensure a successful venture. Because this is still a relatively new approach, teams should be encouraged to report their lessons, both positive and negative, so that others might continue to learn how to best employ collaborative modeling as an environmental management tool.

10. CONCLUSIONS

It is not appropriate to speak of conclusions at this time as the project is far from complete. Given the breath and complexity of issues related to water management it is inconceivable to ever complete a full compendium of physical and social process modules. It is also inappropriate to think that work on these modules will cease with the end of this project. Rather, modules are constantly being added to the toolbox as unique resource challenges are encountered with each new project. In fact, efforts are currently in process to develop modules for nutrient cycling, transport of reactive aqueous solutes, the energy-water nexus, temperature dynamics in rivers and lakes, and non-market valuation of riparian areas.

Although work on the modules may not be complete, the basic goals set forth in the original proposal were achieved. Specifically, a broad decision framework encompassing surface/groundwater hydrology, water quality, land surface processes, ecology, economics, policy, and law has been established. Additionally, the framework has been formulated within a structured architecture that allows modules to be easily networked to model complex watershed dynamics. The modules have also been applied and calibrated to a real-world problem, namely the Rio Grande. This application has demonstrated both the utility of the toolbox and its ability to model complex multidisciplinary problems.

An additional goal of this project was to establish Sandia National Laboratories as a leader in system dynamics decision support modeling for water resource planning. Although quantifying progress toward this goal is very difficult, there are a couple of accomplishments that suggest we are moving in the right direction. First, a collaboration has been forged with the U.S. Army Corps of Engineers' Institute of Water Resources to develop a Center for Computer Aided Dispute Resolution (CADRe). In addition, negotiations are ongoing with other federal agencies and universities to join this Center. This is a unique program aimed at supporting federal, state, and local water management agencies through technology and process development, education, and project support. Second, a number of new decision support projects have been established, each of which are making use of the toolbox. Projects include the Rio Grande, Gila River of southwest New Mexico, a model to assist in the design of water markets for the Mimbres Basin (also in southwestern New Mexico), Willamette River in Oregon, and the Barton Springs Aquifer in Texas.

REFERENCES

Adar, E. M., and S. P. Neuman, 1986, The use of environmental tracers (isotopes and hydrochemistry) for quantification of natural recharge and flow components in arid basins, *Proceedings of the 5th International Symposium on Underground Tracing*, Athens, Greece: 235-253.

Adar, E., and S. Sorek, 1989, Multi-compartmental modeling for aquifer parameter estimation using natural tracers in non-steady flow, *Advances in Water Resources* Vol. 12: 84-89.

Adar, E. M., S. P. Neuman, and D. A. Woolhiser, 1988, Estimation of spatial recharge distribution using environmental isotopes and hydrochemical data. 1. Mathematical model and application to synthetic data, *Journal of Hydrology* Vol. 97: 251-277.

Ahmad, S., and S. P. Simonovic, 2004, Spatial system dynamics: New approach for simulation of water resources systems, *Journal of Computing in Civil Engineering* 18(4): 331-340.

Arnold, J. G., and N. Fohrer, 2005, SWAT2000: Current capabilities and research opportunities in applied watershed modeling, *Hydrological Processes* 19(3): 563-572.

Barroll, P., and P. Burck, 2005, *Documentation of the OSE Taos Area Calibrated Groundwater Flow Model T17.0. Review Draft 11/08/2005*. New Mexico Office of the State Engineer, Water Resource Allocation Program, Technical Services Division, Hydrology Bureau Report, Santa Fe, New Mexico.

Bear, J., and A. Verruijt, 1987, *Modeling Groundwater Flow and Pollution*. Theory and Applications of Transport in Porous Media book series, J. Bear, ed. D. Reidel Publishing Company, Dordrecht, Holland.

Bernardo, D. J., N. K. Whittlesey, K. E. Saxton and D. L. Bassett, 1987, "An Irrigation Model for Management of Limited Water Supplies 12 (December): 149-157.

Berrens, R., P. Ganderton, and C. Silva, 1996, Valuing the protection of minimum instream flows in New Mexico. *Journal of Agricultural and Resource Economics* 21(2): 90-104.

Berrens, R., A. Bohara, H. Jenkins-Smith, C. Silva, P. Ganderton, and D. Brookshire, 1998, A joint investigation of public support and public values: Case of instream flows in New Mexico, *Ecological Economics* 27(2): 189-203.

Berrens, R., A. Bohara, C. Silva, M. McKee, and D. Brookshire, 2000, Contingent valuation of instream flows in New Mexico: With tests of scope, group-size reminder and temporal reliability, *Journal of Environmental Management* 58(1): 73-90.

Bestgen, K. R., and S. P. Platania, 1991, Status and conservation of the Rio Grande silvery minnow, *Hybognathus amarus, Southwestern Naturalist* 26(2): 225:232.

Beven, K. J., 2000, *Rainfall-Runoff Modelling, A Primer*. John Wiley, Hoboken, NJ, 360 pp.

Blackburn G., and S. McLeod, 1983, Salinity of atmospheric precipitation in the Murray-Darling drainage division, Australia, *Australian Journal of Soil Research* 21: 411-434.

Boyle, K., M. Welsh, and R. Bishop, 1993, The role of question order and response experience in contingent-valuation studies, *Journal of Environmental Economics and Management* 25: S-80 – S-99.

Bras, R. L., 1990, *Hydrology: An introduction to hydrologic science*. Addison-Wesley, Reading, MA, 643 pp.

Breuer, L., K. Eckhardt, and H. G. Frede, 2003, Plant parameter values for models in temperate climates, *Ecological Modeling* 169(2-3): 237-293.

Brookshire, D., S. Burness, J. Chermak, and K. Krause, 2002, Western Urban Water Demand, *Natural Resource Journal* 42(4): 1-26.

Brookshire, D. S., B. Colby, M. Ewers, and P. Ganderton, 2005, Market Prices for Water in the Semi Arid West, *Water Resources Research* 40(9).

Brouwer, R., 2000, Environmental Value Transfer: State of the Art and Future Prospects, *Ecological Economics* 32(1): 137-152.

Brower, A., 2004, *ET Toolbox, Evapotranspiration Toolbox for the Middle Rio Grande. A Water Resources Decision Support Tool*, Water Resources Division Technical Service Center, Denver, Colorado, Bureau of Reclamation, United States Department of the Interior. http://www.usbr.gov/pmts/rivers/awards/ettoolbox.pdf

Brown, T. C., 1991, Water for wilderness areas: Instream flow needs, protection, and economic value, *Rivers* 2(4): 311-325.

Brown, T. C., 2004, *The marginal economic value of streamflow from national forests*. USDA Forest Service Discussion Paper DP-04-1, Rocky Mountain Research Station.

Buhl, K. J., 2002, *The relative toxicity of waterborne inorganic contaminants to the Rio Grande silvery minnow (Hybognathus amarus) and fathead minnow (Pimephales promelas) in a water quality simulating that in the Rio Grande, New Mexico*. Final Report to the U.S. Fish and Wildlife Service, Study Number 2F33-9620003. U.S. Geological Survey, Columbia Environmental Research Center, Yankton, SD.

Bureau of Land Management, 2006, *Western States Water Laws*, accessed July 17, 2006, at http://www.blm.gov/nstc/WaterLaws/appsystems.html.

Burnash, R. J. C., R. L. Ferral, and R. A. McGuire, 1973, *A generalized streamflow simulation system: Conceptual modeling for digital computers*. Technical Report, National Weather Service, Sacramento, CA, 204 pp.

Burness, H. S., and J. P. Quirk, 1980, Economic Aspects of Appropriative Water Rights, *Journal of Environmental Economics and Management* 7(4): 372-388.

Campana, M. E., and E. S. Simpson, 1984, Groundwater residence times and recharge rates using a dicrete state compartmental model and C-14 data, *Journal of Hydrology* Vol.72: 171-185.

Campana, M. E., G. A. Harrington, and L. Tezcan, 2001, Environmental Isotopes in the Hydrological Cycle: Principles and Applications, W. Mook, ed. UNESCO/IAEA, Vol. VI, pp. 37-73. http://www.iaea.org/programmes/ripc/ih/volumes/volumes.htm

Carey, J. M., and D. L. Sunding, 2002, Emerging Markets in Water: A Comparative Institutional Analysis of the Central Valley and Colorado-Big Thompson Projects, *Natural Resources Journal* 41(2): 283-328.

Carpenter, S. R., N. F. Caraco, D. L. Correll, R. W. Howarth, A. N. Sharpley, and V. H. Smith, 1998, Nonpoint pollution of surface waters with phosphorus and nitrogen, *Ecological Applications* 8(3): 559-568.

Caylor, K. K., S. Manfreda, and I. Rodriguez-Iturbe, 2005, On the coupled geomorphological and ecohydrological organization of river basins, *Advances in Water Resources* 28(1): 69-86.

Clapp, R. B., and G. M. Hornberger, 1978, Empirical equations for some soil hydraulic-properties, *Water Resources Research* 14(4): 601-604.

Clark, I. D., and P. Fritz, 1997, *Environmental Isotopes in Hydrogeology*. CRC Press, Boca Raton, Florida, 328 pp.

Claussen, E., 2001, Making Collaboration a Matter of Course: A New Approach to Environmental Policy Making, *Environmental Practice* 3: 202-205.

Cockerill, K., H. Passell, and V. Tidwell, 2006, Cooperative Modeling: Building Bridges Between Science and the Public, *Journal of the American Water Resources Association*, in press.

Colby, B. G., 1993, Applying Fair Market Value Concepts to Water Rights, *Real Estate Issues*, Spring/Summer 1993: 8-14.

Colby, B. G., 2000, Cap and trade policy challenges: A tale of three markets, *Land Economics* 76(4): 638-58.

Connick, S., and J. E. Innes, 2003, Outcomes of Collaborative Water Policy Making: Applying Complexity Thinking to Evaluation, *Journal of Environmental Planning and Management* 46: 177-197.

Cook, Z., S. Urban, M. Maupin, R. Pratt, and J. Church, 2001, *Domestic, Commercial, and Industrial Water Demand Assessment and Forecast in Ada and Canyon Counties, Idaho*, Idaho Water Resources Report, at http://www.idwr.state.id.us/waterboard/planning/Documents/dcmi%20final%20report.pdf (last accessed 10/06/06).

Cooper, J., and J. Loomis, 1991, Economic value of wildlife resources in the San Joaquin valley: Hunting and viewing values, in A. Dinar and D. Zilberman (eds.), *Economics and management of water and drainage in agriculture*. Kluwer Academic Publishers.

Costanza, R., and M. Ruth, 1998, Using Dynamic Modeling to Scope Environmental Problems and Build Consensus, *Environmental Management* 22: 183-195.

Cox, A. M., 1996, Proactive Industrial Targeting: An Application of the Analytical Hierarchy Process, Master's Thesis, Virginia Polytechnic Institute and State University, July 1996.

Crandall, K., B. Colby, and K. Rait, 1992, Valuing riparian areas: A southwestern case study, *Rivers* 3(2): 88-98.

Daly, C., 1994, A statistical topographic model for mapping climatological precipitation over mountainous terrain. *Journal of Applied Meteorology* 33: 140-158.

Dandy, G., C. Davies, and T. Nyugen, 1997, Estimating Residential Water Demand in the Presence of Free Allowances, *Land Economics* 73: 125-39.

Danielson, L. E., 1979, An Analysis of Residential Demand for Water Using Micro Time-Series Data, *Water Resources Research* 15: 763-67.

Daubert, J., and R. Young, 1981, Recreational demands for maintaining instream flows: A contingent valuation approach, *American Journal of Agricultural Economics* 63(4): 666-676.

Davis, S. N., D. O. Whittemore, and J. Fabryka-Martin, 1998, Uses of chloride/bromide ratios in studies of potable water, *Ground Water* 36: 338-350.

Dingman, S. L., 2001, *Physical Hydrology*, 2nd Ed. Prentice Hall, Princeton, New Jersey, 600 pp.

Douglas, A., and J. Taylor, 1999, Economic value of Trinity River water, *International Journal of Water Resources Development* 15(3): 309-322.

Dudley, R. K., and S. P. Platania, 2002, *Summary of population monitoring of Rio Grande silvery minnow (1994–2002)*. Report to the N.M. Ecological Services Field Office, U.S. Fish and Wildlife Service, Albuquerque, N.M. Also known as USFWS Supplement 469, September 10, 2002.

Duffield, J. W., C. Neher, D. Patterson, and S. Allen, 1990, *Instream Flows in the Missouri River Basin: A Recreational Survey and Economic Study*. Missoula, MT: Montana Department of Natural Resources and Conservation.

Duffield, J., C. Neher, and T. Brown, 1992, Recreation benefits of instream flow: Application to montana's big hole and bitterroot rivers, *Water Resource Research* 28(9): 2169-81.

Eagleson, P. S., 1978, *Climate, soil, and vegetation—1. Introduction to water balance dynamics*, Water Resources Research 14(5): 749-764.

Easter, W. R., W. Mark, and A. Dinar, 1999, Formal and informal markets for water: Institutions, Performance, and Constraints, *World Bank Observer* 14(1): 99-116.

Erickson, J., 2005, Personal communication, Exporting matrices from IMPLAN, December 26, 2005.

Faux, J., and G. Perry, 1999, Estimating Irrigation Water Value Using Hedonic Price Analysis: A Case Study in Malheur County, Oregon, *Land Economics* 75(3): 440-452.

Federer, C. A., 1995, BROOK90: A simulation model for evaporation, soil water, and streamflow, version 3.1. Computer freeware and documentation. Durham, NH, U.S Forest Service.

Federer, C. A., 1996, Intercomparison of methods for calculating potential evaporation in regional and global water balance models, *Water Resources Research* 32(7): 2315-2321.

Feth, J. H., 1981, Chloride in natural continental water, *U.S. Geological Survey Water Supply Paper 2167*, 36 pp.

Fetter, C. W., Jr., 1980, *Applied Hydrogeology*. Charles E. Merrill Publishing Co., Columbus, Ohio.

Flury, M., and A. Papritz, 1993, Bromide in the natural environment: occurrence and toxicity, *Journal of Environmental Quality* 22: 747-758.

Forrester, J. W., 1990, *Principles of Systems*. Productivity Press, Portland, Oregon.

Foster, H. S., Jr. and B. R. Beattie, 1981, On the Specification of Price in the Study of Domestic Water Demand, Unpublished Paper. Department of Economics, University of Illinois at Urbana-Champaign.

Frederick, K. D., T. VandenBerg, and J. Hanson, 1996, *Economic values of freshwater in the United States*. Discussion Paper 97-03, Washington, D. C.

Frenzel, P. F., 1995, *Geohydrology and Simulation of Groundwater Flow near Los Alamos, North-Central New Mexico*. United States Geological Survey Water Resources Investigations Report 95-4091, Albuquerque, New Mexico.

Gelhar, L. W., and J. L. Wilson, 1974, Ground-Water Quality Modeling, *Ground Water*, Vol. 12, no. 6, pp. 399-408.

Gibbs, K. C., 1978, Price Variable in Residential Water Demand Models, *Water Resources Research* 14: 15-18.

Gleick, P. H., D. Haasz, C. Henges-Jeck, V. Srinivasan, G. Wolff, K. Kao Cushing, and A. Mann, 2003, *Waste Not, Want Not: The Potential for Urban Water Conservation in California*, a Pacific Institute for the Studies in Development, Environment, and Security report, at http://www.pacinst.org/reports/urban_usage/ (last accessed 10/05/06).

Glover, C. R., C. L. Foster, and R. D. Baker, 1997, *Irrigated Pastures for New Mexico*, Circular 494 New Mexico State Extension Service, at http://cahe.nmsu.edu/pubs/_circulars/circ494.pdf (last accessed 11/29/06).

Grant, D. M., and B. D. Dawson, 1997, *Isco Open Channel Flow Measurement Handbook, Fifth Edition*. Isco Inc., Lincoln, Nebraska.

Griffen, R. C., and S. H. Hsu, 1993, The Potential for Water Market Efficiency When Instream Flows Have Value, *American Journal of Agricultural Economics* 75(2): 292-303.

Griffin, R., 2006, *Water Resource Economics*. MIT press, Cambridge, Massachusetts.

Gutzler, D. S., and J. S. Nimms, 2003, "Climatic Modulation of Water Demand in the City of Albuquerque, New Mexico USA," powerpoint presentation at the 2003 NOAA Climate Diagnostics Workshop, at http://www.cpc.noaa.gov/products/outreach/proceedings/cdw28_proceedings/dgutzler_2003.ppt#256,1, Climatic modulation of water demand in the City of Albuquerque, New Mexico USA (last accessed 11/29/06).

Hamilton, J. R., N. K. Whittlesey, and P. Halverson, 1989, Interruptible Water Markets in the Pacific Northwest, *American Journal of Agricultural Economics* 71(1): 63-75.

Hansen, L., and A. Hallam, 1990, Single-stage and two-stage decision modeling of the recreational demand for water, *Journal of Agricultural Economic Resources* 42(1): 16-26.

Harbaugh, A. W., 1990, *A Computer Program for Calculating Subregional Water Budgets Using Results from the U.S. Geological Survey Modular Three-dimensional Finite-difference Ground-water Flow Model*. U.S. Geological Survey Open-File Report 90-392.

Hargreaves, G. H., 1975, Moisture availability and crop production, *Trans. ASAE* 18(5): 980-984.

Hargreaves, G. H., and R. G. Allen, 2003, History and evaluation of Hargreaves evapotranspiration equation, *Journal of Irrigation and Drainage Engineering-ASCE* 129.1: 53-63.

Hargreaves, G. L., G. H. Hargreaves, and J. P. Riley, 1985, Irrigation Water Requirements for Senegal River Basin, *Journal of Irrigation and Drainage Engineering-ASCE* 111(3): 265-275.

Hearne, G. A., and J. D. Dewey, 1988, *Hydrologic Analysis of the Rio Grande Basin North of Embudo, New Mexico, Colorado and New Mexico*. United States Geological Survey Water Resources Investigations Report 86-4113, Denver, Colorado.

Hendrickx, J. M. H., 1998, *Water quality protection for El Paso County Water Improvement District No. 1*, Draft report to the El Paso County Water Improvement District No. 1, 32 pp. plus appendices.

Hewitt, J. A., and W. M. Hanemann, 1995, A Discrete/Continuous Choice Approach to Residential Water Demand Under Block Rate Pricing, *Land Economics* 71: 173-92.

Howe, C. W., 1982, The Impact of Price on Residential Water Demand: Some New Insights, *Water Resources Research* 18: 713-16.

Howe, C. W, 1986, Innovative Approaches to Water Allocation: The Potential for Water Markets, *Water Resources Research* 22(4): 439-445.

Howe, C. W., and C. Goemans, 2003, *Economic Efficiency and Equity Considerations in Regional Water Transfers: A Comparative Analysis of Two Basins in Colorado*, accessed July 17, 2006, at http://www2.soc.hawaii.edu/econ/seminars/2003/01-17.htm.

Howe, C. W., and F. P. Linaweaver, Jr., 1967, The Impact of Price on Residential Water Demand and Its Relation to System Design and Price Structure, *Water Resources Research* 31: 13-32.

Jemez y Sangre Water Planning Council, 2003, *Jemez y Sangre Regional Water Plan*. Prepared by Daniel B. Stephens and Associates, Albuquerque, New Mexico, in association with Amy C. Lewis, Santa Fe, New Mexico. Available October 2006 at http://www.ose.state.nm.us/water-info/NMWaterPlanning/regions/jemezysangre/jys_sec1-5.pdf

Jensen, M. E., 1998, *Coefficients for Vegetative Evapotranspiration and Open Water Evaporation for the Lower Colorado River Accounting System*. Report prepared for the U.S. Bureau of Reclamation, Boulder City, Nevada.

Johnson, L. E., 1990, Computer-Aided Planning for Multiple-Purpose Reservoir Operating Policies. A*WRA Water Resources Bulletin* 26: 299-311.

Johnson, N., 2001, Managing Water for People and Nature, *Science* 292: 1071-1072.

Johnson, P. S., and J. W. Shomaker, 2002, *New Mexico's water: perceptions, reality, and imperatives, background report for the 28th New Mexico First Town Hall*, New Mexico First, Albuquerque, New Mexico, 76 pp.

Jones, C. V., and J. R. Morris, 1984, Instrumental Price Estimates and Residential Water Demand, *Water Resources Research* 20: 197-202.

Jordão, L., P. Antones, R. Santos, N. Videira, and S. Martinho, 1997, Pages 463-466 in Barlas, Yaman, Dker, Vedat, Polat, Seckin (eds.), *15th International System Dynamics Conference: Systems Approach to Learning and Education into the 21st Century*. Istanbul, Turkey, Bogazici University Printing Office.

Jury, W. A., and H. Vaux, 2005, The role of science in solving the world's emerging water problems, *Proceedings of the National Academy of Sciences*, Vol. 102, no. 44, 15715-15720. http://www.pnas.org/cgi/doi/10.1073/pnas.0506467102

Kaval, P., and J. Loomis, 2003, *Updated outdoor recreation use values with emphasis on national park recreation, final report* (Tech. Rep.). Fort Collins, CO: National Park Service.

Kerlinger, P., 1994, *The economic impact of birding and ecotourism on the Bosque del Apache National Wildlife Refuge Area, New Mexico: 1993-1994* (Tech. Rep.). New Jersey Audubon Society.

Klein, J., 1990, *Interdisciplinarity: History, theory and practice*. Wayne State University Press.

Konikow, L. F., and J. D. Bredehoeft, 1992, Ground-water models cannot be validated, *Advances in Water Resources*, Vol. 15, no. 1, pp. 75-83.

Lenzen, M., and B. Foran, 2001, An input-output analysis of Australian water usage, *Water Policy* 3(2001): 321-340.

Levings, G. W., D. F. Healy, S. F. Richey, and L. F. Carter, 1998, Water quality in the Rio Grande valley, Colorado, New Mexico and Texas, 1992-95, *U.S. Geological Survey Circular 1162*, 39 pp.

Liang, X., and Z. H. Xie, 2001, A new surface runoff parameterization with subgrid-scale soil heterogeneity for land surface models, *Advances in Water Resources* 24(9-10): 1173–1193.

Liang, X., D. P. Lettenmaier, E. F. Wood, and S. J. Burges, 1994, A simple hydrologically based model of land surface water and energy fluxes for general circulation models, *Journal of Geophysical Research* 99(D7): 14415–14428.

Libecap, G. D., 2005, *The Problem of Water*. Working paper. Department of Economics, University of Arizona, November 2005.

Lippincott, J. B., 1939, Southwest border water problems, *Journal of the American Water Works Association* 31: 1-28.

Loomis, J., 1987, The economic value of instream flow: Methodology and benefit estimates for optimum flows, *Journal of Environmental Management* 24(1): 169-179.

Loomis, J., 1998, Estimating the public values for instream flow: Economic techniques and dollar values, *Journal of the American Water Resources Association* 34(5): 1007-1114.

Lyman, R. A., 1992, Peak and Off-Peak Residential Water Demand, *Water Resources Research* 28: 2159-67.

Malczynski, L., O. Paananen, D. Harris, A. Baker, and J. Erickson, 2003, *Dynamics Simulation Model of the National Security Consequences from Energy Supply Disruptions*, SAND2002-3738. Sandia National Laboratories, Albuquerque, New Mexico.

Martin, R., and R. Wilder, 1992, Residential Demand for Water and the Pricing of Municipal Water Services, *Public Finance Quarterly* 20: 93-102.

Martinec, J., A. Rango, and E. Major, 1983, T*he Snowmelt-Runoff Model (SRM) User's Manual*. NASA Reference Publ. 1100, Washington, D.C., USA.

McAda, D. P., and M. Wasiolek, 1988, *Simulation of the Regional Geohydrology of the Tesuque Aquifer System near Santa Fe, New Mexico*. U.S. Geological Survey Water-Resources Investigations Report 87-4056, Albuquerque, New Mexico.

McAda, D. P., and P. Barroll, 2002, *Simulation of Ground-Water Flow in the Middle Rio Grande Basin Between Cochiti and San Acacia, New Mexico*. U.S. Geological Survey Water-Resources Investigations Report 02-4200, Albuquerque, New Mexico.

McDonald, M. G., and A. W. Harbaugh, 1988, *A modular three-dimensional finite-difference ground-water flow model: U.S. Geological Survey Techniques of Water Resources Investigations*, Book 6, Chapter A1, 14 ch.

MIG, Inc., 2000, IMPLAN Professional Version 2.0. User's Guide, Analysis Guide, Data Guide. June 2000.

Miller, R., and P. D. Blair, 1985, *Input-Output Analysis*, Prentice Hall.

Mills, S. K., 2003, *Quantifying Salinization of the Rio Grande Using Environmental Tracers*, M. S. thesis, New Mexico Institute of Mining and Technology, Socorro, New Mexico.

Mitsch, W. J., J. W. Day, and J. Gilliam, Jr., 2001, Reducing nitrogen loading to the Gulf of Mexico from the Mississippi River Basin: Strategies to Counter a Persistent Ecological Problem. *BioScience* 51(5): 373-388.

Moore, S. J., and S. K. Anderholm, 2002, Spatial and temporal variations in streamflow, dissolved solids, nutrients, and suspended sediment in the Rio Grande valley study unit, Colorado, New Mexico, and Texas, 1993-95, *Water Resources Investigations Report* 02-4224, 52 pp.

Moxey, A., and B. White, 1998, NELUP: Some Reflections on Undertaking and Reporting Interdisciplinary River Catchment Modelling, *Journal of Environmental Planning and Management* 41(3): 397-402.

Nandalal, K. D. W., and S. P. Simonovic, 2003, Resolving conflicts in water sharing: A systemic approach, *Water Resources Research* 39(12): 1362.

National Agricultural Statistics Service (NASS). New Mexico Agricultural Statistics, http://www.nass.usda.gov/nm/nmbulletin/bulletin02.htm, last accessed 07/27/2006.

Neuman, S. P., and P. J. Wierenga, 2003, *A Comprehensive Strategy of Hydrogeologic Modeling and Uncertainty Analysis for Nuclear Facilities and Sites*. Prepared for Division of Systems Analysis and Regulatory Effectiveness, Office of Nuclear Regulatory Research, U.S.

Nuclear Regulatory Commission, Washington D.C. 20555-0001. NRC Job Code W6790. NUREG/CR-6805.

New Mexico Climate Center, http://weather.nmsu.edu/nmcrops/, last accessed 07/27/2006.

New Mexico State University Cooperative Extension Service, http://costsandreturns.nmsu.edu/, last accessed 07/27/2006.

Nicolson, C. R., A. M. Starfield, G. P. Kofinas, and J. A. Kruse, 2002, Ten Heuristics for Interdisciplinary Modeling Projects, *Ecosystems* 5 (4): 376-384.

Nieswiadomy, M. L., 1992, Estimating Urban Residential Water Demand: Effects of Price Structure, Conservation, and Education, *Water Resources Research* 28: 609-15.

Nieswiadomy, M. L., and D. J. Molina, 1989, Comparing Residential Water Demand Estimates under Decreasing and Increasing Block Rates Using Household Data, *Land Economics* 65: 280-89.

Nijssen, B., and D. P. Lettenmaier, 1997, Streamflow simulation for continental-scale river basins, *Water Resources Research* 33(4): 711– 724.

Nowosielski, A., 2002, Geo-Referenced Social Accounting with Application to Integrated Watershed Planning in the Hudson River Valley. PhD dissertation, Rensselaer Polytechnic Institute, August 2002.

NRC, 1938, *Regional Planning Report part VI, Rio Grande joint investigation in the upper Rio Grande basin in Colorado, New Mexico, and Texas, 1936-1937*. National Resources Committee, U. S. Government Printing Office, Washington, D.C., 566 pp.

Office of the State Engineer and the Interstate Stream Commission, 2006, *Fact Sheet*, accessed July 17, 2006, at http://www.ose.state.nm.us/water-info/NMWaterPlanning/fact-sheets/acequia.pdf.

Office of the State Engineer, 2003, *New Mexico State Water Plan*, adopted by the New Mexico Interstate Stream Commission, December 17, 2003.

Palmer, R. N., A. M. Keyes, and S. Fisher, 1993, Empowering Stakeholders Through Simulation in Water Resources Planning, in K. Hon (ed.), *Water Management in the 90's: A Time for Innovation*. Proceedings of the 20th Anniversary Conference, American Society for Civil Engineering, pp. 451-454.

Papadopulos, S. S., and I. Associates, 2000, *Middle Rio Grande Water Supply Study*, Unpublished report prepared for the U. S. Army Corps of Engineers Albuquerque District.

Passell, H. D., C. N. Dahm, and E. J. Bedrick, 2005, Nutrient and organic carbon patterns and trends in the Upper Rio Grande, 1975–1999, *Science for the Total Environment* 345: 239-260.

Passell, H. D., C. N. Dahm, and E. J. Bedrick, in review. Ammonia modeling for assessing potential toxicity to fish species in the Rio Grande, 1989–2002, *Ecological Applications*.

Phillips, F. M., 2000, Chlorine-36, in *Environmental Tracers in Subsurface Hydrology*, P. Cook and A. L. Herczeg, eds. Kluwer Academic, Dordrecht, pp. 248-299.

Phillips, F. M., and M. C. Castro, 2003, Groundwater dating and residence time measurements, in *Treatise on Geochemistry*, H. D. Holland and K. K. Turekian; eds., Vol. 5, in *Surface and Ground Water, Weathering, and Soils*, J. I. Drever, ed., Oxford University Press, Oxford, pp. 451-497.

Phillips, F. M., J. F. Hogan, S. K. Mills, and J. M. H. Hendrickx, 2003, Environmental tracers applied to quantifying causes of salinity in arid-region rivers: preliminary results from the Rio Grande, southwestern USA, in *Water Resources Perspectives: Evaluation, Management and Policy*, A. S. Alsharhan and W. W. Wood, eds., Elsevier, Amsterdam.

Platania, S. P., and C. S. Altenbach, 1998, Reproductive strategies and egg types of seven Rio Grande basin cyprinids, *Copeia* 1998: 559-569.

Plummer, L. N., L. M. Bexfield, S. K. Anderholm, W. E. Sanford, and E. Busenberg, 2004, *Geochemical Characteristics of Ground-Water Flow in the Santa Fe Group Aquifer System, Middle Rio Grande Basin, New Mexico.* U. S. Geological Survey Water Resources Investigations Report 03-4131.

Postel, S., 1999, *Pillar of sand: can the irrigation miracle last?* W. W. Norton and Company, London, 313 pp.

Potapchuk, W. R., 1991, New Approaches to Citizen Participation: Building Consent, *National Civic Review*, Spring: 158-168.

Powersim, 2006, Powersim Software – The Business Simulation Company. http://www.powersim.com/.

Renwick, M. E., and S. O. Archibald, 1998, Demand Side Management Policies for Residential Water Use: Who Bears the Conservation Burden? *Land Economics* 74: 343-59.

Renwick, M., and R. Green, 2000, Do Residential Water Demand Side Management Policies Measure Up? An Analysis of Eight California Water Agencies, *Journal of Environmental Economics and Management* 40: 37-55.

Rio Grande Compact Commission, 2000, *Report of the Rio Grande Compact Commission 1999 to the Governors of Colorado, New Mexico, and Texas*.

Rizaiza, A., 1991, Residential Water Use: A Case Study of the Major Cities of the Western Region of Saudi Arabia, *Water Resources Research* 27(5): 667-671.

Rodriguez-Iturbe, I. and P. S. Eagleson, 1987, Mathematical-Models of rainstorm events in space and time, *Water Resources Research* 23(1): 181-190.

Rosen, M. D., and R. Sexton, Irrigation Districts and Water Markets: An Application of Cooperative Decision-Making Theory, *Land Economics* 69(1): 39-53.

Rosenberger, R., and J. Loomis, 2001, *Benefit transfer of outdoor recreation use values: A technical document supporting the forest service strategic plan (2000 revision)* (Tech. Rep. No. RMRS-GTR-72). Fort Collins, CO: U.S. Department of Agriculture, Forest Service, Rocky Mountain Research Station.

Rouwette, E. A., J. A. M. Vennix, and T. van Mullekom, 2002, Group Model Building Effectiveness: A Review of Assessment Studies, *System Dynamics Review* 18(1): 5-45.

Roybal, F. E., 1991, *Groundwater Resources of Socorro County, New Mexico*. U.S. Geological Survey Water Resources Investigation Report 89-4083, Albuquerque, New Mexico.

Saliba, B. C., 1987, Do Water Markets Work?, *Water Resources Research* 23(7): 1113-1122.

Schefter, J. E., and E. L. David, 1986, Estimating Residential Water Demand Under Multi-Part Tariffs Using Aggregate Data, *Land Economics* 61: 272-80.

Scheierling, S. M., G. E. Cardon, and R. A. Young, 2004, Impact of Irrigation Timing on Simulated Water-Crop Production Functions, *Irrigation Science*, 18(1): 23-31.

Scurlock, D., 1998, *From the rio to the sierra: an environmental history of the middle Rio Grande basin*, General Technical Report 5 (RMRS-GTR-5), U.S. Department of Agriculture, Forest Service, Rocky Mountain Research Station, 440 pp.

Serageldin, I., 1995, Water Resources Management: A New Policy for a Sustainable Future. *Water International* 20: 15-21.

Shafike, N. G., 2005, *Linked Surface Water and Groundwater Model for Socorro and San Marcial Basins between San Acacia and Elephant Butte Reservoir. Appendix J in Upper Rio Grande Water Operations Review DEIS*, pp. J-59 to J-94. http://www.spa.usace.army.mil/urgwops/deis/URGWOPS%20DEIS%20Volume%202/URGWOPS%20Appendix%20J.pdf

Simcox, A. C., 1983, The Río Salado at flood, New Mexico Geological Society Guidebook, 34th field conference, Socorro Region II.

Simonovic, S. P., and H. Fahmy, 1999, A new modeling approach for water resources policy analysis, Water Resources Research 35(1): 295-304.

Simpson, L. D., 1994, Are Water Markets a Viable Option?, *Finance and Development* 31(2): 30-32.

Smith, G. A., 2001, *The Volcanic Foundation of Cochiti Dam, Sandoval County, New Mexico. New Mexico Decision-Makers Field Guide No. 1: Water, Watersheds, and Land Use in New Mexico. Impacts of Population Growth on Natural Resources. Santa Fe Region,*

P. S. Johnson (ed.). New Mexico Bureau of Mines and Mineral Resources. http://geoinfo.nmt.edu/publications/decisionmakers/2001/dmfg2001_complete.pdf

Smith, V., 1982, Microeconomics Systems as an Experimental Science, *American Economic Review* 72(5): 923-955.

Spash, C. L., 2001, Broadening Democracy in Environmental Policy Processes, *Environment and Planning C: Government and Policy* 19: 475-481.

Stabler, H., 1911, Some stream waters of the western United States, *U. S. Geological Survey Water Supply Paper 274*, 188 pp.

Stave, K. A., 2002, Using system dynamics to improve public participation in environmental decisions, *System Dynamics Review* 18(2): 139-167.

Sterman, J. D., 2000, *Business Dynamics, Systems Thinking and Modeling for a Complex World*. McGraw-Hill, Boston, 982 pp.

Stone, D., 2002 (1988), *Policy Paradox*. New York: WW Norton & Company.

Sublette, J. E., M. D. Hatch, and M. Sublette, 1990, *The fishes of New Mexico*. University of New Mexico Press, Albuquerque, NM.

Susskind, L. E., R. K. Jain, and A. O. Martyniuk, 2001, *Better Environmental Policy Studies: How to Design and Conduct More Effective Analyses*. Washington: Island Press.

Tchobanoglous, G., F. L. Burton, H. D. Stensel/Metcalf and Eddy, Inc., 2003, *Wastewater Engineering: Treatment and Reuse.* McGraw-Hill, New York, NY, 1848 pp.

Tetratech Inc., 2003, *Rio Grande Seepage Study Report, Taos Box Canyon*. Final Report for United States Bureau of Reclamation. Tetra Tech ISG Project No. P06000-0023-01, April 2003.

Tidwell, V.C., H. D. Passell, S. H. Conrad, and R. P. Thomas, 2004, System Dynamics Modeling for Community-Based Water Planning: An Application to the Middle Rio Grande. *Journal of Aquatic Sciences* (in press).

Trock, W. L., P. C. Huszar, G. E. Radosevich, G. V. Skogerboe, and E. C. Vlachos, 1978, *Socio-economic and institutional factors in irrigation return flow quality control volume III: middle Rio Grande valley case study*. Report EPA-600/2-78-174c, Environmental Protection Agency.

Tucker, G. E., and R. L. Bras, 2000. *A stochastic approach to modeling the role of rainfall variability in drainage basin evolution*, Water Resources Research 36(7): 1953–1964.

U. S. Bureau of Reclamation Alamosa Field Division, 2006, *San Luis Valley Project, Closed Basin Division, Colorado*, June 4, 2006. http://www.nps.gov/grsa/resources/docs/Trp2026.pdf

U.S. Census Bureau, 2004, *State and county quick facts* (Tech. Rep.).

U.S. Department of Interior, Bureau of Reclamation, 2005, *Water 2025 Preventing Crises and Conflict in the West*, accessed July 17, 2006, at http://www.doi.gov/water2025.

U.S. Fish and Wildlife Service, 2001, Birding in the United States: A demographic and economic analysis: Addendum to the 2001 national survey of fishing, hunting and wildlife-associated recreation (Tech. Rep. No. 2001-1).

U.S. Fish and Wildlife Service, 2003, Net economic values for wildlife-related recreation in 2001: Addendum to the 2001 national survey of fishing, hunting, and wildlife-associated recreation (Tech. Rep. No. 2001-3).

United States Army Corps of Engineers (USACE), United States Geological Survey (USGS), United States Bureau of Reclamation (BoR), United States Fish and Wildlife Service (USFWS), United States Bureau of Indian Affairs (BIA), and the International Boundary and Water Commission (IBWC), 2002, *Upper Rio Grande Water Operations Model*, Model Documentation, Draft by the Technical Review Committee. http://www.spa.usace.army.mil/urgwom/docintro.asp

United States Census Bureau, 2005, County population estimate for Socorro County, New Mexico, 2005. http://www.census.gov

United States Department of the Interior (USDoI), Bureau of Reclamation (BoR), 2006, *Environmental Assessment: San Juan-Chama Water Contract Amendments with City of Santa Fe, County of Santa Fe, County of Los Alamos, Town of Taos, Village of Taos Ski Valley, Village of Los Lunas, and City of Espanola*. Prepared by Aspen Environmental Group for BoR Albuquerque Area Office, May 19, 2006. http://www.usbr.gov/uc/albuq/envdocs/ea/sanjuanchama/finalEA.pdf

United States Fish and Wildlife Service (USFWS), 1999, *Rio Grande silvery minnow Recovery plan*. Region 2, U.S. Fish and Wildlife Service, Albuquerque, NM.

United States Fish and Wildlife Service (USFWS), 2001, *Programmatic biological opinion on the effects of actions associated with the U.S. Bureau of Reclamation's, U.S. Army Corps of Engineers', and Non-Federal Entities Discretionary Actions Related to Water Management on the Middle Rio Grande, New Mexico*. U.S. Fish and Wildlife Service, Albuquerque, NM.

United States Fish and Wildlife Service (USFWS), 2002a, *Designation of critical habitat for the Rio Grande silvery minnow*, Draft Environmental Impact Statement. U.S. Fish and Wildlife Service, Albuquerque, NM.

United States Fish and Wildlife Service (USFWS), 2002b, *Biological opinion and conference report on U.S. Bureau of Reclamation's amended water management operation on the middle Rio Grande through December 31, 2002*. U.S. Fish and Wildlife Service, Albuquerque, NM.

United States Fish and Wildlife Service (USFWS), 2003, *Biological and conference opinions on the effects of actions associated with the programmatic biological assessment of the Bureau of Reclamation's Water and River Maintenance Operations, Army Corps of Engineers' Flood Control Operation, and Related Non-Federal Actions on the Middle Rio Grande, New Mexico*. U.S. Fish and Wildlife Service, Albuquerque, NM.

UNM Institute for Public Policy, 1996, Quarterly profile of New Mexico citizens (Vol. 8; No. 4).

USACE, 1994, *Multi-sub-basin modeling*. Report EM 1110-2-1417: 10.1-10.5.

USBR, 2006, *Dataweb, Dams and Reservoirs.* http://www.usbr.gov/dataweb/dams/index.html

USGS, 2003a, *NWISWeb data for the nation*, United States Geological Survey. http://waterdata.usgs.gov/nwis

USGS, 2003b, *Historical Rio Grande flow conditions*. International Boundary and Water Commission. http://www.ibwc.state.gov/wad/histflo1.htm

van den Belt, M., 1998, *Mediated Modeling Project: An Integrated Scoping Model of the Upper Fox River Basin*. University of Wisconsin, Green Bay.

van den Belt, M., 2004, *Mediated Modeling: A System Dynamics Approach to Environmental Consensus Building*. ISBN1559639601, Island Press, 296 pp.

van Eeten, M. J. G., D. P. Loucks, and E. Roe, 2002, Bringing Actors Together Around Large-Scale Water Systems: Participatory Modeling and Other Innovations, *Knowledge, Technology & Policy* 14(4): 94-108.

Vennix, J., 1996, *Group Model Building: Facilitating Team Learning Using System Dynamics*. ISBN 047195355, New York: Wiley, 312 pp.

Vennix, Jac A. M., 1999, Group model-building: tackling messy problems, *System Dynamics Review* 15 (4): 379-401.

Vigerstøl, K., 2003, Drought management in Mexico's Río Bravo Basin. Master's thesis, University of Washington.

Wallace, S. D. and F. Sancar, 1988, Pages 448-459 in J.B. Homer and A. Ford (eds.), *Proceedings of the 1988 International Conference of the Systems Dynamics Society*. La Jolla, California.

Ward, F. A., and J. F. Booker, 2003, Economic Costs and Benefits of Instream Flow Protection for Endangered Species in an International Basin, *Journal of the American Water Resources Association* 39(2): 427-440.

Ward, F. A., B. H. Hurd, T. Rahmani, and N. Gollehon, 2006, Economic impacts of federal policy responses to drought in the Río Grande Basin, *Water Resources Research* 42.

Weinberg, M., C. L. Kling, and J. E. Wilen, 1993, Water Markets and Water Quality, *American Journal of Agricultural Economics* 75(2): 278-291.

Wells, S. M., 2002, *Watermaster's Report Rio Chama Mainstream 2002*. State of New Mexico, Office of the State Engineer, Santa Fe, New Mexico.

West Water Research, Washington State Department of Ecology, 2004, *Analysis of Water Banking in the Western States*, Publication No. 04-11-011.

Wilcox, L. V., 1957, Analysis of salt balance and salt-burden data on the Rio Grande, in *Problems of the Upper Rio Grande: an Arid Zone River, Publication No. 1*, P. C. Duisberg, ed. U. S. Commission for Arid Resource Improvement and Development, Socorro, New Mexico, pp. 39-44.

Wilkins, D. W., 1986, *Geohydrology of the Southwest Alluvial Basins Regional Aquifer-Systems Analysis, parts of Colorado, New Mexico, and Texas*. United States Geological Survey Water Resources Investigations Report 84-4224, Albuquerque, New Mexico.

Wilkins, D. W., 1998, *Summary of the southwest alluvial basins regional aquifer-system analysis in parts of Colorado, New Mexico, and Texas*. U. S. Geological Survey Professional Paper 1407A, 49 pp.

Wilson, C. A., R. R. White, B. R. Orr, and G. R. Roybal, 1981, *Water resources of the Rincon and Mesilla Valleys and adjacent areas, New Mexico*. New Mexico State Engineer Technical Report 43, Santa Fe, New Mexico, 66 pp.

Witcher, J. C., 1995, *A geothermal resource database of New Mexico*. Southwest Technology Development Institute, Las Cruces, New Mexico, 28 pp.

Woodside, M., and B. Simerl, 1995, *Land use and nutrient concentrations and yields in selected streams in the Albemarle-Pamlico Drainage Basin, North Carolina and Virginia*. USGS Open File Report 95-457.

APPENDIX A: GROUNDWATER DATA AND RESULTS

Table A-1. Alpha matrix (connectivity and head dependent flow relations) for 51-zone Albuquerque Basin compartmental model [ft^2/day].

Zone	1	2	3	4	5	6	7	8	9	10	11	12	13	14	15	16	17
1	0	3500	0	47721	0	0	0	0	0	0	0	0	0	0	0	0	0
2	3500	0	1429	0	95882	0	0	0	0	0	0	0	0	0	0	0	0
3	0	1429	0	0	0	3E+05	0	0	0	0	0	0	0	0	478.9	0	0
4	47721	0	0	0	31737	0	10520	0	0	0	0	0	0	0	0	0	0
5	0	95882	0	31737	0	15630	34374	0	3045	0	0	0	0	0	0	0	0
6	0	0	3E+05	0	15630	0	0	17819	0	16703	0	0	0	0	0	0	0
7	0	0	0	10520	34374	0	0	6721	0	0	0	0	0	0	0	0	0
8	0	0	0	0	0	17819	6721	0	0	0	0	0	1868	14221	0	0	0
9	0	0	0	0	3045	0	0	0	0	7487	0	0	0	0	0	0	0
10	0	0	0	0	0	16703	0	0	7487	0	0	0	0	0	0	0	0
11	0	0	0	0	0	0	0	0	0	0	0	25.53	9790	0	0	0	0
12	0	0	0	0	0	0	0	0	0	0	25.53	0	0	25360	737.5	0	0
13	0	0	0	0	0	0	0	1868	0	0	9790	0	0	2804	0	0	0
14	0	0	0	0	0	0	0	14221	0	0	0	25360	2804	0	0	0	0
15	0	0	478.9	0	0	0	0	0	0	0	0	737.5	0	0	0	750.1	0
16	0	0	0	0	0	0	0	0	0	0	0	0	0	0	750.1	0	3220
17	0	0	0	0	0	0	0	0	0	0	0	0	0	0	0	3220	0
18	0	0	0	0	0	7522	0	0	0	0	0	0	0	36728	4E+05	0	0
19	0	0	0	0	0	0	0	0	0	0	0	0	0	0	0	5E+05	0
20	0	0	0	0	0	0	0	0	0	0	0	0	0	0	0	0	3E+06
21	0	0	0	0	0	0	0	0	0	0	0	0	4247	8160	0	0	0
22	0	0	0	0	0	0	0	0	0	0	0	0	0	1387	0	0	0
23	0	0	0	0	0	0	0	0	0	0	0	0	0	0	0	0	0
24	0	0	0	0	0	0	0	0	0	0	0	0	0	0	0	0	0
25	0	0	0	0	0	0	0	0	0	0	0	0	0	0	0	0	0
26	0	0	0	0	0	0	0	0	0	0	0	0	0	0	0	0	0
27	0	0	0	0	0	0	0	0	0	0	0	0	0	0	0	0	0
28	0	0	0	0	0	0	0	0	0	0	0	0	0	0	0	0	0
29	0	0	0	0	0	0	0	0	0	0	0	0	0	0	0	0	0
30	0	0	0	0	0	0	0	0	0	0	0	0	0	0	0	0	700
31	0	0	0	0	0	0	0	0	0	0	0	0	0	0	0	0	0
32	0	0	0	0	0	0	0	0	0	0	0	0	0	0	0	0	0
33	0	0	0	0	0	0	0	0	0	0	0	0	0	0	0	0	0
34	0	0	0	0	0	0	0	0	0	0	0	0	0	0	0	0	0
35	0	0	0	0	0	0	0	0	0	0	0	0	0	0	0	0	0
36	0	0	0	0	0	0	0	0	0	0	0	0	0	0	0	0	0
37	0	0	0	0	0	0	0	0	0	0	0	0	0	0	0	0	0
38	0	0	0	0	0	0	0	0	0	0	0	0	0	0	0	0	0
39	0	0	0	0	0	0	0	0	0	0	0	0	0	0	0	0	0
40	0	0	0	0	0	0	0	0	0	0	0	0	0	0	0	0	0
41	0	0	0	0	0	0	0	0	0	0	0	0	0	0	0	0	0
42	0	0	0	0	0	0	0	0	0	0	0	0	0	0	0	0	0
43	0	0	0	0	0	0	0	0	0	0	0	0	0	0	0	0	0
44	0	0	0	0	0	0	0	0	0	0	0	0	0	0	0	0	0
45	0	0	0	0	0	0	0	0	0	0	0	0	0	0	0	0	0
46	0	0	0	0	0	0	0	0	0	0	0	0	0	0	0	0	0
47	0	0	0	0	0	0	0	0	0	0	0	0	0	0	0	0	0
48	0	0	0	0	0	0	0	0	0	0	0	0	0	0	0	0	0
49	0	0	0	0	0	0	0	0	0	0	0	0	0	0	0	0	0
50	0	0	0	0	0	0	0	0	0	0	0	0	0	0	0	0	0
51	0	0	0	0	0	0	0	0	0	0	0	0	0	0	0	0	0

Table A-1. Alpha matrix (connectivity and head dependent flow relations) for 51-zone Albuquerque Basin compartmental model [ft^2/day] (continued).

Zone	18	19	20	21	22	23	24	25	26	27	28	29	30	31	32	33	34
1	0	0	0	0	0	0	0	0	0	0	0	0	0	0	0	0	0
2	0	0	0	0	0	0	0	0	0	0	0	0	0	0	0	0	0
3	0	0	0	0	0	0	0	0	0	0	0	0	0	0	0	0	0
4	0	0	0	0	0	0	0	0	0	0	0	0	0	0	0	0	0
5	0	0	0	0	0	0	0	0	0	0	0	0	0	0	0	0	0
6	7522	0	0	0	0	0	0	0	0	0	0	0	0	0	0	0	0
7	0	0	0	0	0	0	0	0	0	0	0	0	0	0	0	0	0
8	0	0	0	0	0	0	0	0	0	0	0	0	0	0	0	0	0
9	0	0	0	0	0	0	0	0	0	0	0	0	0	0	0	0	0
10	0	0	0	0	0	0	0	0	0	0	0	0	0	0	0	0	0
11	0	0	0	0	0	0	0	0	0	0	0	0	0	0	0	0	0
12	0	0	0	0	0	0	0	0	0	0	0	0	0	0	0	0	0
13	0	0	0	4247	0	0	0	0	0	0	0	0	0	0	0	0	0
14	36728	0	0	8160	1387	0	0	0	0	0	0	0	0	0	0	0	0
15	4E+05	0	0	0	0	0	0	0	0	0	0	0	0	0	0	0	0
16	0	5E+05	0	0	0	0	0	0	0	0	0	0	0	0	0	0	0
17	0	0	3E+06	0	0	0	0	0	0	0	0	0	700	0	0	0	0
18	0	13173	0	0	0	0	0	0	1934	5416	0	0	0	0	0	0	0
19	13173	0	57557	0	5298	0	0	0	0	12161	0	0	0	0	0	0	0
20	0	57557	0	0	0	0	2092	0	0	0	38966	0	0	0	0	0	21074
21	0	0	0	0	3991	812.5	0	0	0	0	0	0	0	0	0	0	0
22	0	5298	0	3991	0	3986	7479	0	0	0	0	0	0	0	0	0	0
23	0	0	0	812.5	3986	0	0	1050	0	0	0	0	0	0	0	0	0
24	0	0	2092	0	7479	0	0	5517	0	0	0	0	0	0	0	0	0
25	0	0	0	0	0	1050	5517	0	0	0	0	0	0	0	0	0	0
26	1934	0	0	0	0	0	0	0	0	0	0	0	0	0	0	0	0
27	5416	12161	0	0	0	0	0	0	0	0	14399	4016	0	0	0	0	0
28	0	0	38966	0	0	0	0	0	0	14399	0	2960	0	0	0	0	0
29	0	0	0	0	0	0	0	0	0	4016	2960	0	0	0	0	0	0
30	0	0	0	0	0	0	0	0	0	0	0	0	0	1836	0	0	2E+05
31	0	0	0	0	0	0	0	0	0	0	0	0	1836	0	1612	0	0
32	0	0	0	0	0	0	0	0	0	0	0	0	0	1612	0	952.5	0
33	0	0	0	0	0	0	0	0	0	0	0	0	0	0	952.5	0	0
34	0	0	21074	0	0	0	0	0	0	0	0	0	2E+05	0	0	0	0
35	0	0	0	0	0	0	0	0	0	0	0	0	0	2E+06	0	0	6141
36	0	0	0	0	0	0	0	0	0	0	0	0	0	0	3E+05	0	0
37	0	0	0	0	0	0	0	0	0	0	0	0	0	0	0	3E+05	0
38	0	0	0	0	0	0	10646	0	0	0	0	0	0	0	0	0	78761
39	0	0	0	0	0	0	0	1049	0	0	0	0	0	0	0	0	0
40	0	0	0	0	0	0	0	0	0	0	0	0	0	0	0	0	0
41	0	0	0	0	0	0	0	0	0	0	0	0	0	0	0	0	0
42	0	0	0	0	0	0	0	0	0	0	0	0	0	0	0	0	0
43	0	0	0	0	0	0	0	0	0	0	0	0	0	0	0	0	0
44	0	0	0	0	0	0	0	0	0	0	1559	2155	0	0	0	0	16495
45	0	0	0	0	0	0	0	0	0	0	0	0	0	0	0	0	0
46	0	0	0	0	0	0	0	0	0	0	0	0	0	0	0	0	0
47	0	0	0	0	0	0	0	0	0	0	0	0	0	0	0	0	0
48	0	0	0	0	0	0	0	0	0	0	0	0	0	0	0	950.8	0
49	0	0	0	0	0	0	0	0	0	0	0	0	0	0	0	0	0
50	0	0	0	0	0	0	0	0	0	0	0	0	0	0	0	0	0
51	0	0	0	0	0	0	0	0	0	0	0	0	0	0	0	0	0

Table A-1. Alpha matrix (connectivity and head dependent flow relations) for 51-zone Albuquerque Basin compartmental model [ft^2/day] (continued).

Zone	35	36	37	38	39	40	41	42	43	44	45	46	47	48	49	50	51
1	0	0	0	0	0	0	0	0	0	0	0	0	0	0	0	0	0
2	0	0	0	0	0	0	0	0	0	0	0	0	0	0	0	0	0
3	0	0	0	0	0	0	0	0	0	0	0	0	0	0	0	0	0
4	0	0	0	0	0	0	0	0	0	0	0	0	0	0	0	0	0
5	0	0	0	0	0	0	0	0	0	0	0	0	0	0	0	0	0
6	0	0	0	0	0	0	0	0	0	0	0	0	0	0	0	0	0
7	0	0	0	0	0	0	0	0	0	0	0	0	0	0	0	0	0
8	0	0	0	0	0	0	0	0	0	0	0	0	0	0	0	0	0
9	0	0	0	0	0	0	0	0	0	0	0	0	0	0	0	0	0
10	0	0	0	0	0	0	0	0	0	0	0	0	0	0	0	0	0
11	0	0	0	0	0	0	0	0	0	0	0	0	0	0	0	0	0
12	0	0	0	0	0	0	0	0	0	0	0	0	0	0	0	0	0
13	0	0	0	0	0	0	0	0	0	0	0	0	0	0	0	0	0
14	0	0	0	0	0	0	0	0	0	0	0	0	0	0	0	0	0
15	0	0	0	0	0	0	0	0	0	0	0	0	0	0	0	0	0
16	0	0	0	0	0	0	0	0	0	0	0	0	0	0	0	0	0
17	0	0	0	0	0	0	0	0	0	0	0	0	0	0	0	0	0
18	0	0	0	0	0	0	0	0	0	0	0	0	0	0	0	0	0
19	0	0	0	0	0	0	0	0	0	0	0	0	0	0	0	0	0
20	0	0	0	0	0	0	0	0	0	0	0	0	0	0	0	0	0
21	0	0	0	0	0	0	0	0	0	0	0	0	0	0	0	0	0
22	0	0	0	0	0	0	0	0	0	0	0	0	0	0	0	0	0
23	0	0	0	0	0	0	0	0	0	0	0	0	0	0	0	0	0
24	0	0	0	10646	0	0	0	0	0	0	0	0	0	0	0	0	0
25	0	0	0	0	1049	0	0	0	0	0	0	0	0	0	0	0	0
26	0	0	0	0	0	0	0	0	0	0	0	0	0	0	0	0	0
27	0	0	0	0	0	0	0	0	0	0	0	0	0	0	0	0	0
28	0	0	0	0	0	0	0	0	0	1559	0	0	0	0	0	0	0
29	0	0	0	0	0	0	0	0	0	2155	0	0	0	0	0	0	0
30	0	0	0	0	0	0	0	0	0	0	0	0	0	0	0	0	0
31	2E+06	0	0	0	0	0	0	0	0	0	0	0	0	0	0	0	0
32	0	3E+05	0	0	0	0	0	0	0	0	0	0	0	0	0	0	0
33	0	0	3E+05	0	0	0	0	0	0	0	0	0	0	950.8	0	0	0
34	6141	0	0	78761	0	0	0	0	0	16495	0	0	0	0	0	0	0
35	0	16024	0	0	0	2E+05	0	0	0	0	8794	0	0	0	0	0	0
36	16024	0	10111	0	0	0	0	50668	0	0	0	20383	0	0	0	0	0
37	0	10111	0	0	0	0	0	0	13360	0	0	0	11638	0	5442	0	0
38	0	0	0	0	4651	4406	0	0	0	0	0	0	0	0	0	0	0
39	0	0	0	4651	0	2164	512.8	0	0	0	0	0	0	0	0	0	0
40	2E+05	0	0	4406	2164	0	10433	6775	0	0	0	0	0	0	0	0	0
41	0	0	0	0	512.8	10433	0	465.4	879.1	0	0	0	0	0	0	201.7	0
42	0	50668	0	0	0	6775	465.4	0	4857	0	0	0	0	0	0	0	0
43	0	0	13360	0	0	0	879.1	4857	0	0	0	0	0	0	0	38597	0
44	0	0	0	0	0	0	0	0	0	0	12079	0	0	0	0	0	0
45	8794	0	0	0	0	0	0	0	0	12079	0	6504	0	0	0	0	0
46	0	20383	0	0	0	0	0	0	0	0	6504	0	4957	0	0	0	0
47	0	0	11638	0	0	0	0	0	0	0	0	4957	0	0	0	0	1341
48	0	0	0	0	0	0	0	0	0	0	0	0	0	0	1E+05	0	0
49	0	0	5442	0	0	0	0	0	0	0	0	0	0	1E+05	0	4934	6536
50	0	0	0	0	0	0	201.7	0	38597	0	0	0	0	0	4934	0	0
51	0	0	0	0	0	0	0	0	0	0	0	0	1341	0	6536	0	0

Table A-2. Zone bottom elevations [ft above mean sea level], areal extent [km^2], and initial heads [ft].

Zone	Bottom Elevation [ft amsl]	Area [km^2]	Jan1975 Heads [ft]
1	5159.2	16	5239.7
2	5129.3	29	5209.5
3	5079.1	64	5158.4
4	2860.7	80	5252.6
5	2277.4	87	5219.1
6	-728.1	137	5162.5
7	1465	107	5227.4
8	-2661	183	5174.9
9	3899.2	79	5292.9
10	2617.8	94	5206.4
11	5316	83	5430.4
12	5083.4	41	5172.1
13	3182.4	305	5368.9
14	-68.441	231	5134.6
15	4987.3	100	5066.3
16	4918.4	56	4992
17	4887.2	74	4945.3
18	-751.43	182	5070.5
19	-6335.4	88	4988.1
20	-5916	106	4942.7
21	2519.3	122	5163.5
22	-966.25	206	5024.1
23	1635.3	153	5037.6
24	-2834.3	68	4955.1
25	1066.9	104	4965.2
26	2522.2	54	5226.9
27	780.59	36	4990.9
28	-2424	85	4928.8
29	3135.5	92	5020.5
30	4845.7	73	4920.3
31	4792.4	120	4874.2
32	4734.2	172	4819.2
33	4673.5	109	4756
34	-3002.2	108	4916
35	-4230.1	202	4874.1
36	-3833.2	265	4820.4
37	-1637.1	194	4759.5
38	-1127.3	67	4919.6
39	2358.3	116	4916
40	-2968.1	272	4873.5
41	-1289.6	756	4875
42	-4500.1	272	4822.2
43	-3190.2	213	4776
44	-2977.6	100	4922.5
45	-415.52	139	4894.1
46	-458.59	258	4836.3
47	1364.6	205	4791
48	4627.7	69	4707.2
49	1888.4	140	4713.2
50	1817.5	104	4774.2
51	3417.6	65	4727.5

Table A-3. Calibration parameters for river, irrigation canal, and reservoir leakage.

SW Reach	GW Zone# or Reservoir	Riverbed K/Thickness [day-1]	Riverbed Elevation [ft amsl]
CTI2SFP	2	0.1	5213
CTI2SFP	3	0.1	5159
Jemez	11	0.25	5430
Jemez	12	0.25	5185
SFP2ALB	15	0.1	5069
SFP2ALB	16	0.1	4993
SFP2ALB	17	0.02	4938
ALB2BDO	30	0.1	4916
ALB2BDO	31	0.1	4873.5
ALB2BDO	32	0.1	4820
ALB2BDO	33	0.1	4755
BDO2SA	48	0.1	4704
	Cochiti Reservoir	0.0006	5339
	Jemez Reservoir	0.0012	5129

Table A-4. Calibration parameters for flow to drains.

SW Reach	GW Zone#	K [ft/day]	Characteristic distance (x_i in Equation 3-15) [mile]	Drain Bed Elevation [ft amsl]
CTI2SFP	2	5	0.45	5208
CTI2SFP	3	5	0.55	5154
SFP2ALB	15	5	0.005	5064
SFP2ALB	16	5	0.2	4988
SFP2ALB	17	5	0.01	4933
ALB2BDO	30	5	0.05	4911
ALB2BDO	31	5	0.25	4868.5
ALB2BDO	32	5	0.2	4815
ALB2BDO	33	5	0.6	4750
BDO2SA	48	5	1.1	4699

Table A-5. Calibration parameters for riparian evapotranspiration from aquifer.

SW Reach	GW Zone#	Surface Elevation [ft amsl]
CTI2SFP	2	5221
CTI2SFP	3	5161.5
Jemez	11	5436
Jemez	12	5187
SFP2ALB	15	5072
SFP2ALB	16	4997
SFP2ALB	17	4941
ALB2BDO	30	4921
ALB2BDO	31	4879
ALB2BDO	32	4824
ALB2BDO	33	4763.5
BDO2SA	48	4716.5

Table A-6. Zone bottom elevations [ft above mean sea level], areal extent [km^2], and initial heads [feet above mean sea level] for the spatially aggregated Espanola Basin groundwater model.

Zone	Bottom Elevation [feet amsl]	Area [$mile^2$]	1975 Head [feet amsl]
1	355	74	5955
2	96	76	5696
3	401	44	6001
4	320	23	5920
5	96	52	5696
6	256	41	5856
7	611	77	6211
8	-111	90	5489
9	406	28	6006
10	963	70	6563
11	143	25	5743
12	551	77	6151
13	930	35	6530
14	5400	22	5600
15	5185	16	5385
16	5480	5	5680

Table A-7. Alpha matrix (connectivity and head-dependent flow relations) for 16-zone Espanola Basin compartmental model [ft^2/month].

Zone	1	2	3	4	5	6	7	8
1	0	0.00862	0	0.15229	0.0019	0	0	0
2	0.00862	0	0.0168	0	0.11299	0.02227	0.00673	0
3	0	0.0168	0	0	0	0	0.00533	0
4	0.15229	0	0	0	0.02389	0	0	0
5	0.0019	0.11299	0	0.02389	0	0.01754	0	0.01814
6	0	0.02227	0	0	0.01754	0	0.01527	0.0216
7	0	0.00673	0.00533	0	0	0.01527	0	0
8	0	0	0	0	0.01814	0.0216	0	0
9	0	0	0	0	0	0.05093	0	0.00922
10	0	0	0	0	0	0	0.01322	0
11	0	0	0	0	0	0	0	0.00806
12	0	0	0	0	0	0	0	0
13	0	0	0	0	0	0	0	0
14	0	0.0883	0	0	0.00104	0	0	0
15	0	0	0	0	0.01518	0	0	0.06972
16	0	0.23003	0	0	0	0	0.00116	0

Zone	9	10	11	12	13	14	15	16
1	0	0	0	0	0	0	0	0
2	0	0	0	0	0	0.0883	0	0.23003
3	0	0	0	0	0	0	0	0
4	0	0	0	0	0	0	0	0
5	0	0	0	0	0	0.00104	0.01518	0
6	0.05093	0	0	0	0	0	0	0
7	0	0.01322	0	0	0	0	0	0.00116
8	0.00922	0	0.00806	0	0	0	0.06972	0
9	0	0.01131	0	0.04091	0	0	0	0
10	0.01131	0	0	0.01298	0.06373	0	0	0
11	0	0	0	0.00466	0	0	0	0
12	0.04091	0.01298	0.00466	0	0.01615	0	0	0
13	0	0.06373	0	0.01615	0	0	0	0
14	0	0	0	0	0	0	0	0.00155
15	0	0	0	0	0	0	0	0
16	0	0	0	0	0	0.00155	0	0

Table A-8. Calibration parameters for stream-aquifer interactions in spatially aggregated Espanola Basin groundwater model.

SW Reach	In GW Zone	Riverbed Conductance [feet^2/s]	Stream Stage [feet amsl]
Rio Grande north of Otowi	14	0.169	From SW model
Rio Grande south of Otowi	15	6.54	From SW model
Pojoaque River	16	0.5	5671.2
Rio Nambe & Rio Tesuque	7	0.039	6092.8

Table A-9. Head-dependent boundary flow parameters for spatially aggregated Espanola Basin groundwater model.

Zone	Flow Description	Boundary Head [feet amsl]	Alpha Parameter [feet^2/day]
1	N boundary constant H	6119	392.3
2	N boundary constant H	5640.9	3562.7
3	N boundary constant H	5995.9	4194.9
14	N boundary constant H	6551	1.3
8	To Alb basin zone 1	Alb basin zone 1	265.2
8	To Alb basin zone 4	Alb basin zone 4	5656.8
11	To Alb basin zone 4	Alb basin zone 4	44.4

Table A-10. Alpha matrix (connectivity and head-dependent flow relations) for 12-zone Socorro Basin compartmental model [acre/month]. SB signifies the south boundary, which is assumed to be Elephant Butte Reservoir for all southern zones (3, 10-12).

Zone	1	2	3	4	5	6	7	8	9	10	11	12	SB
1	0	0.7188	0	0	38.633	0	0	0	0	0	0	0	0
2	0.719	0	1.0625	0	0	0	0	33.367	0	0	0	0	0
3	0	1.0625	0	0	0	0	0	0	0	0	13.5	0	1.3333
4	0	0	0	0	6.075	0	0.4219	0	0	0	0	0	0
5	38.63	0	0	6.075	0	9.675	0	0.1771	0	0	0	0	0
6	0	0	0	0	9.675	0	0	0	0.1194	0	0	0	0
7	0	0	0	0.4219	0	0	0	6.3917	0	0	0	0	0
8	0	33.367	0	0	0.1771	0	6.3917	0	0	0	0.2708	0	0
9	0	0	0	0	0	0.1194	0	0	0	0	0	0	0
10	0	0	0	0	0	0	0	0	0	0	1.4907	0	3.0962
11	0	0	13.5	0	0	0	0	0.2708	0	1.4907	0	0	0.25
12	0	0	0	0	0	0	0	0	0	0	0	0	0
SB	0	0	1.3333	0	0	0	0	0	0	3.0962	0.25	0	0

Table A-11. Calibration parameters for low flow conveyance channel surface water – aquifer interactions, and riparian evapotranspiration. These values were found by calibration with all other source terms set to steady state values.

	Sub-Reach	GW Zone #	LFCC char dist [mile]	Shallow Aquifer Ksat [ft/day]	LFCC Bed Elevation [ft amsl]	Riverbed K/Thick [day^{-1}]	Riverbed Elevation [ft amsl]	Canal bed K/Thick [day-1]	Canal bed Elevation [ft amsl]	Surface Elevation [ft amsl]
Shallow Aquifer Zone	SA2BDA	1	3	65	4576.1	0.1	4583	0.1	4590	4586
	BDA2SM	2	3	65	4495.4	0.1	4501	NA	NA	4505.5
	SM2EB	3	3	65	4456.1	0.1	4430	NA	NA	4473

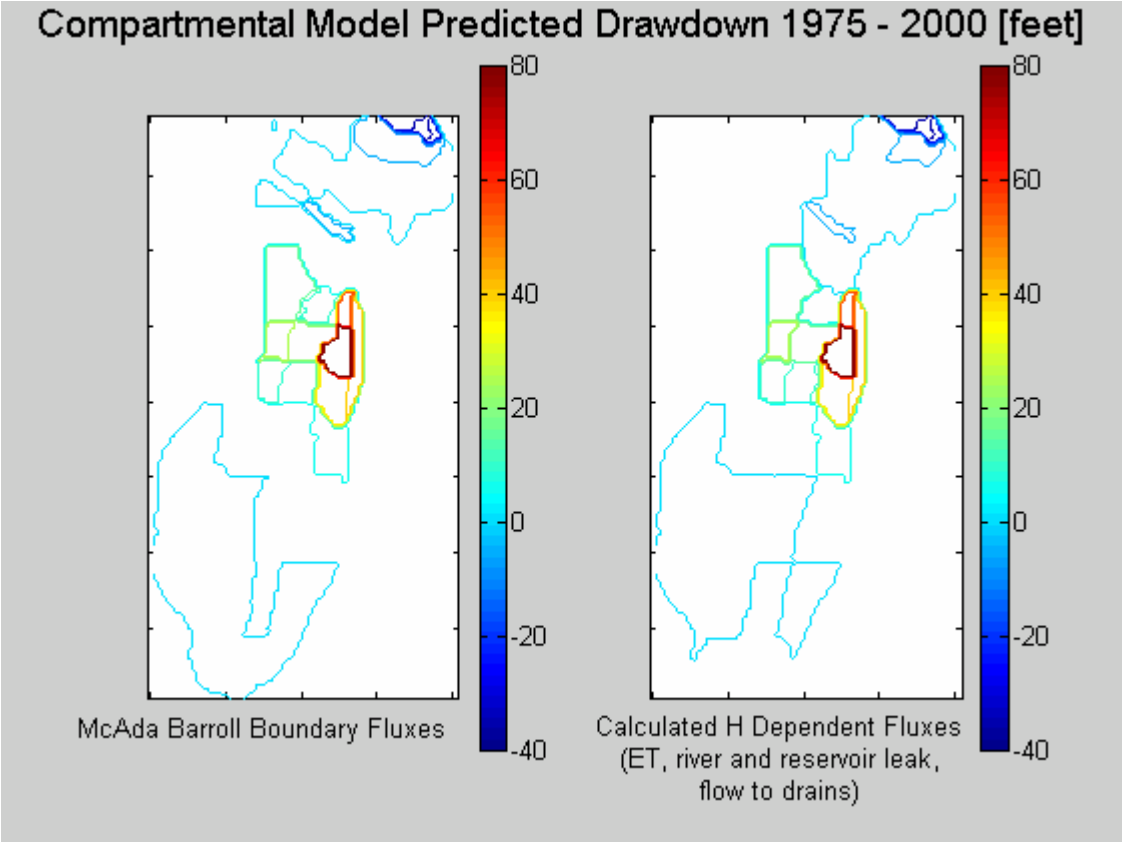

Figure A-1. Comparison of drawdown in models with head-dependent fluxes calculated internally by 51-zone model. Differences in zero level contour location are not important.

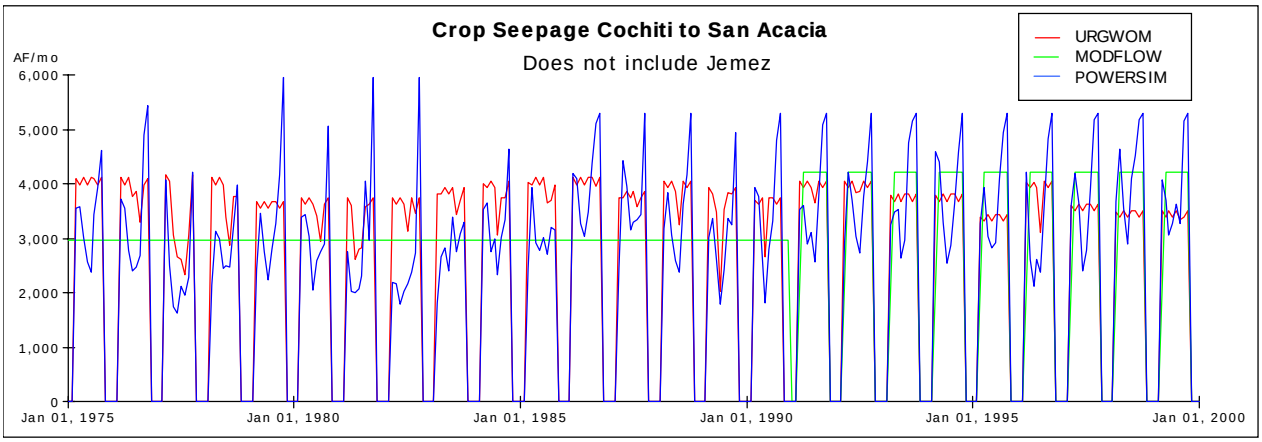

Figure A-2a. Crop seepage to the groundwater system for the Rio Grande reaches from Cochiti to San Acacia as modeled by the coupled monthly timestep model, the URGWOM surface water model, and the McAda and Barroll (2002) regional groundwater model.

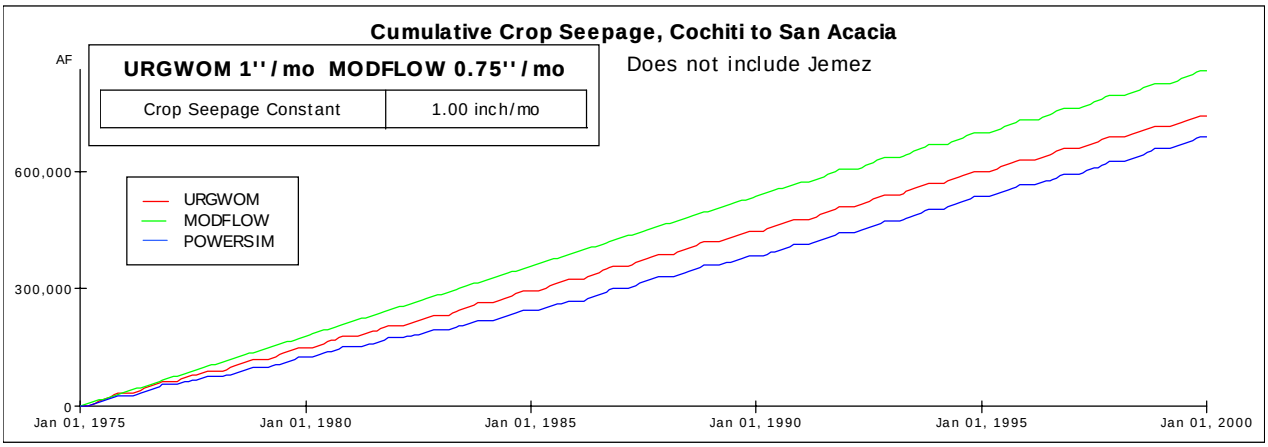

Figure A-2b. Cumulative crop seepage to the groundwater system for the Rio Grande reaches from Cochiti to San Acacia as modeled by the coupled monthly timestep model, the URGWOM surface water model, and the McAda and Barroll (2002) regional groundwater model.

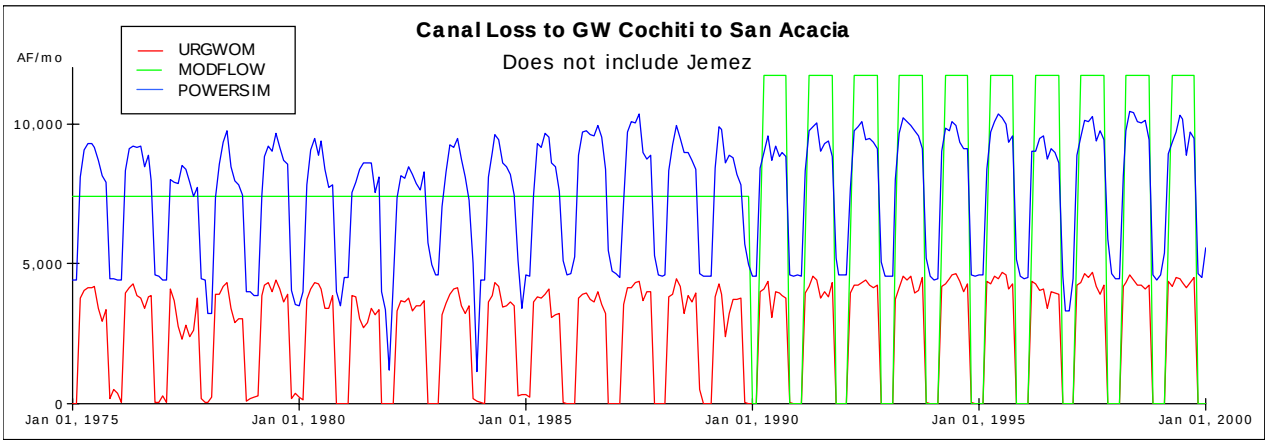

Figure A-3a. Canal seepage to the groundwater system for the Rio Grande reaches from Cochiti to San Acacia as modeled by the coupled monthly timestep model, the URGWOM surface water model, and the McAda and Barroll (2002) regional groundwater model.

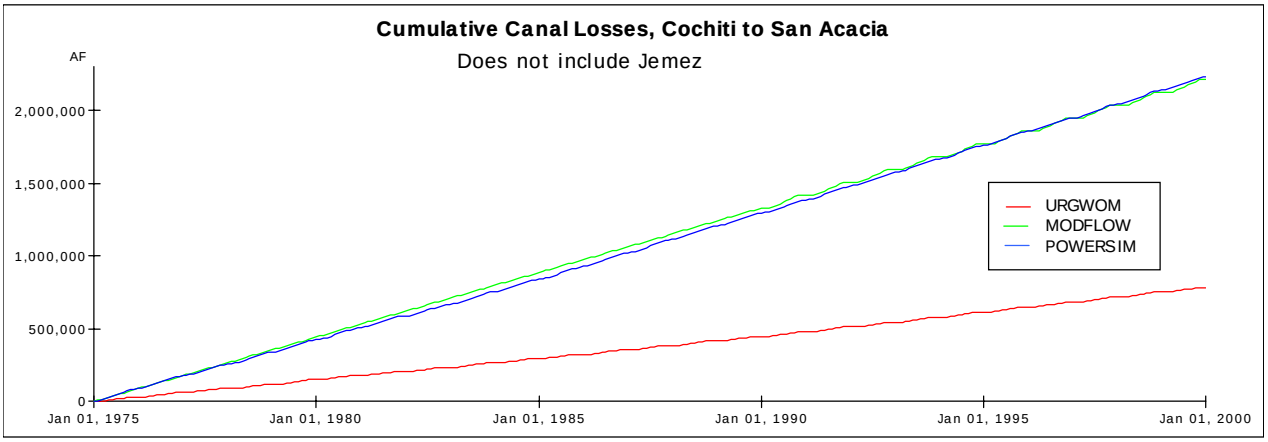

Figure A-3b. Cumulative canal seepage to the groundwater system for the Rio Grande reaches from Cochiti to San Acacia as modeled by the coupled monthly timestep model, the URGWOM surface water model, and the McAda and Barroll (2002) regional groundwater model.

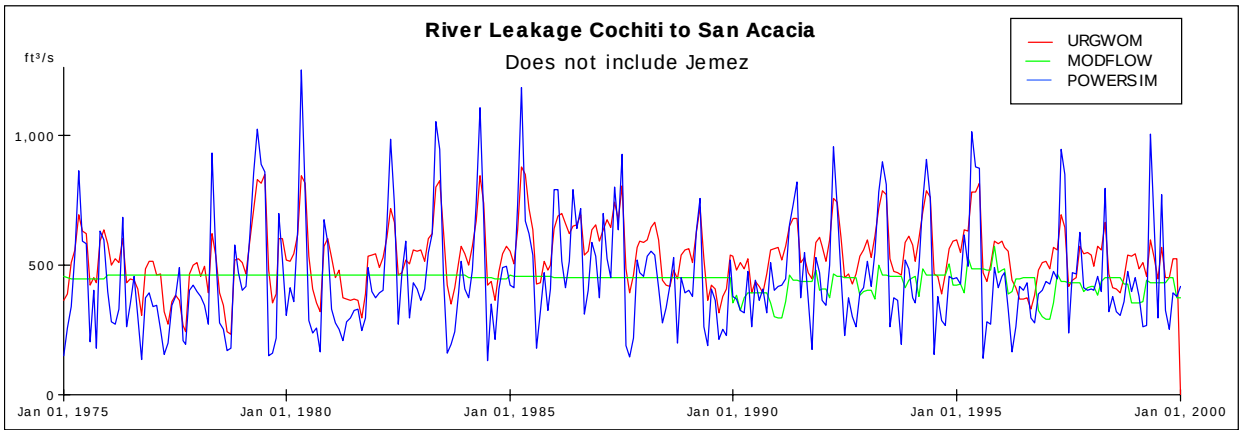

Figure A-4a. River leakage to the groundwater system for the Rio Grande reaches from Cochiti to San Acacia as modeled by the coupled monthly timestep model, the URGWOM surface water model, and the McAda and Barroll (2002) regional groundwater model.

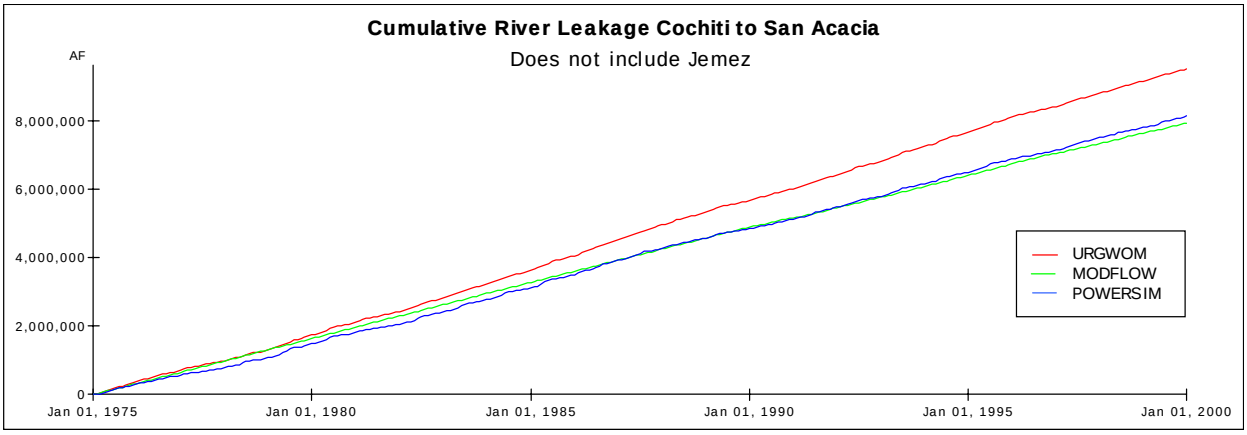

Figure A-4b. Cumulative river leakage to the groundwater system for the Rio Grande reaches from Cochiti to San Acacia as modeled by the coupled monthly timestep model, the URGWOM surface water model, and the McAda and Barroll (2002) regional groundwater model.

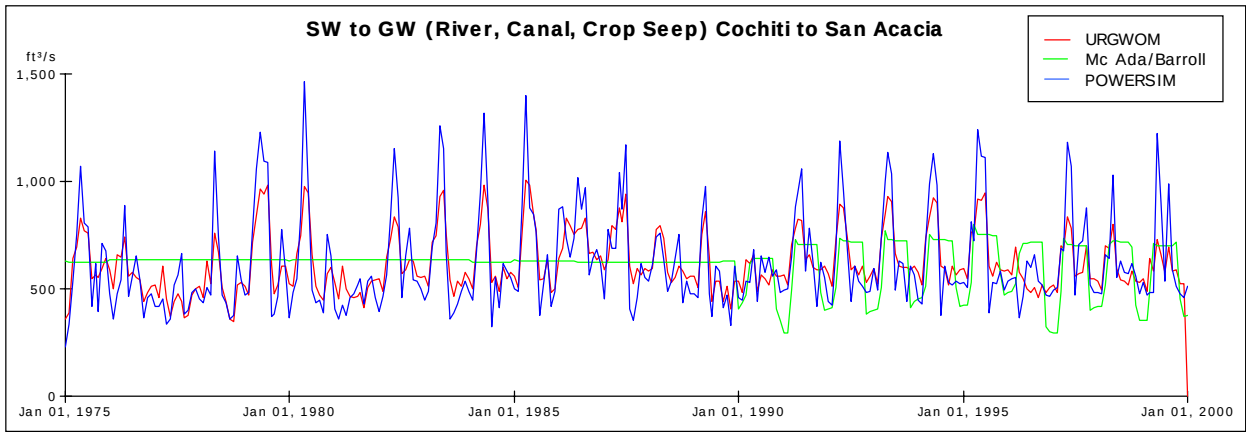

Figure A-5a. Fluxes to the groundwater system from the surface water system for the Rio Grande reaches from Cochiti to San Acacia as modeled by the coupled monthly timestep model, the URGWOM surface water model, and the McAda and Barroll (2002) regional groundwater model.

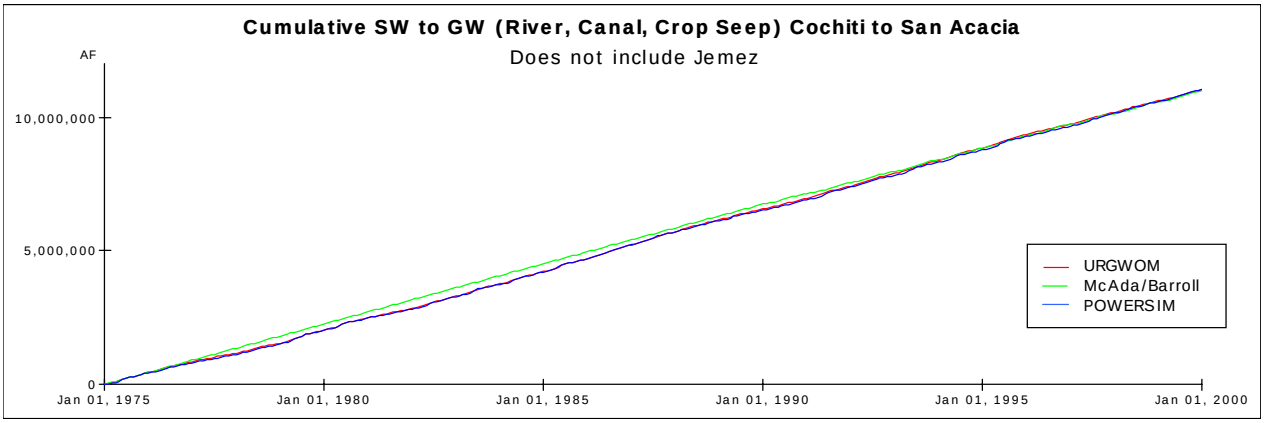

Figure A-5b. Cumulative fluxes to the groundwater system from the surface water system for the Rio Grande reaches from Cochiti to San Acacia as modeled by the coupled monthly timestep model, the URGWOM surface water model, and the McAda and Barroll (2002) regional groundwater model. Same as Figure 3-19.

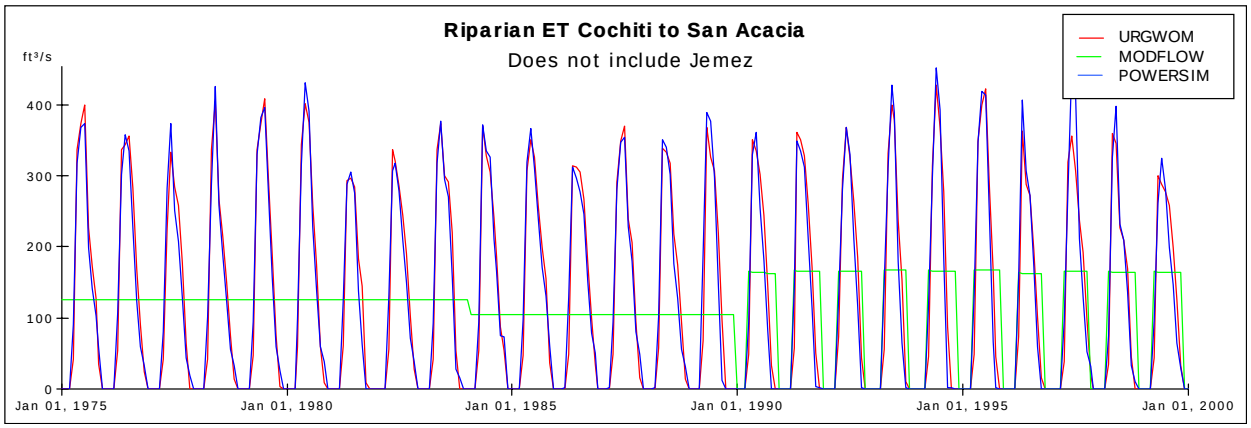

Figure A-6a. Riparian ET 1975–1999 for Rio Grande reaches from Cochiti to San Acacia as modeled by the coupled monthly timestep model, the URGWOM surface water model, and the McAda and Barroll (2002) regional groundwater model. Same as Figure 3-17.

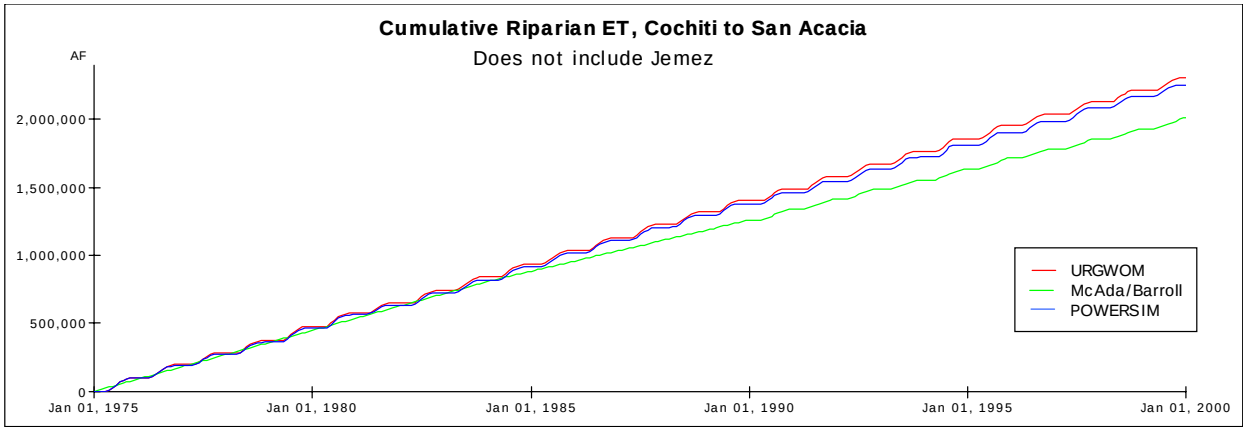

Figure A-6b. Cumulative riparian ET 1975–1999 for Rio Grande reaches from Cochiti to San Acacia as modeled by the coupled monthly timestep model, the URGWOM surface water model, and the McAda and Barroll (2002) regional groundwater model.

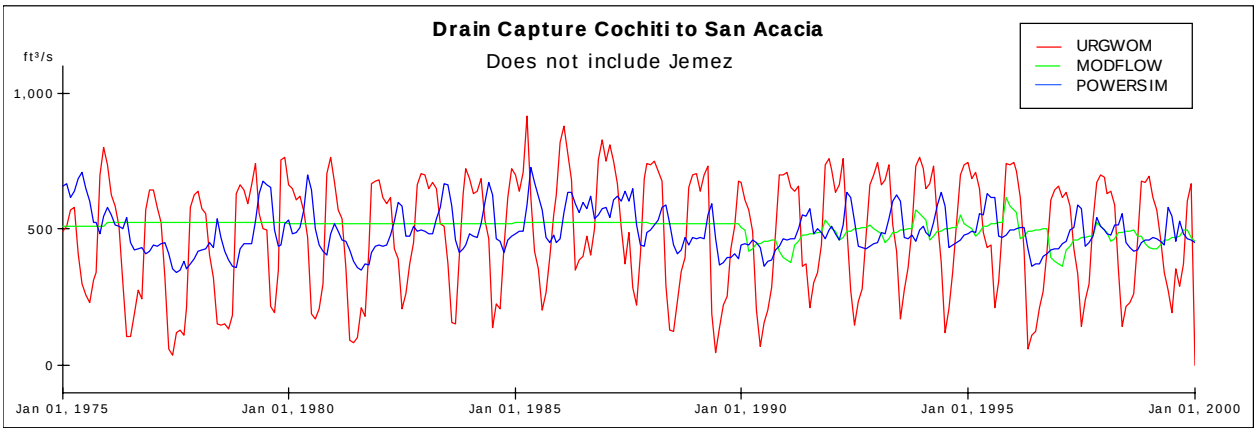

Figure A-7a. Losses from the groundwater system via drain flows for the Rio Grande reaches from Cochiti to San Acacia as modeled by the coupled monthly timestep model, the URGWOM surface water model, and the McAda and Barroll (2002) regional groundwater model.

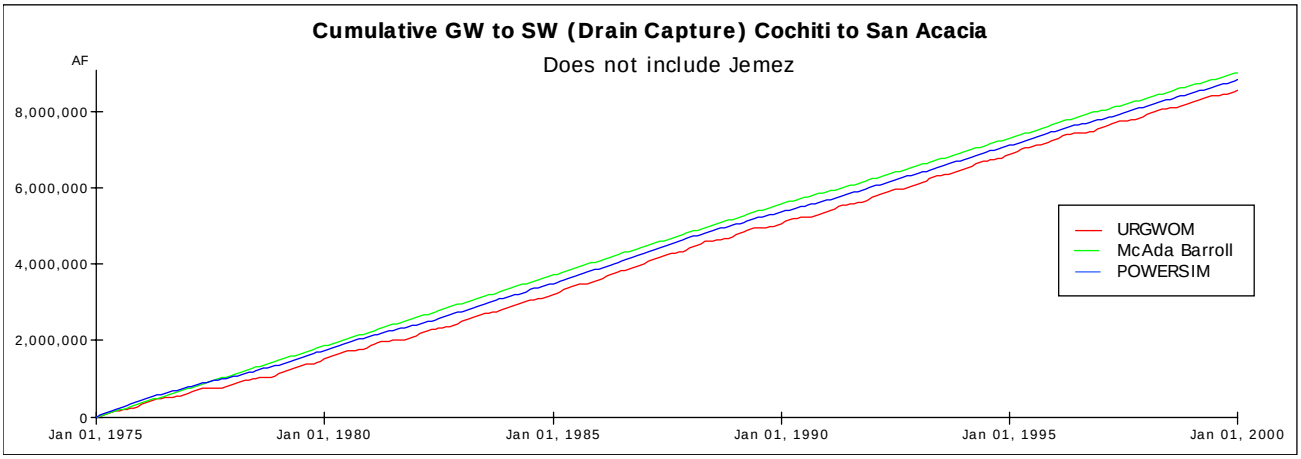

Figure A-7b. Cumulative losses from the groundwater system via drain flows for the Rio Grande reaches from Cochiti to San Acacia as modeled by the coupled monthly timestep model, the URGWOM surface water model, and the McAda and Barroll (2002) regional groundwater model.

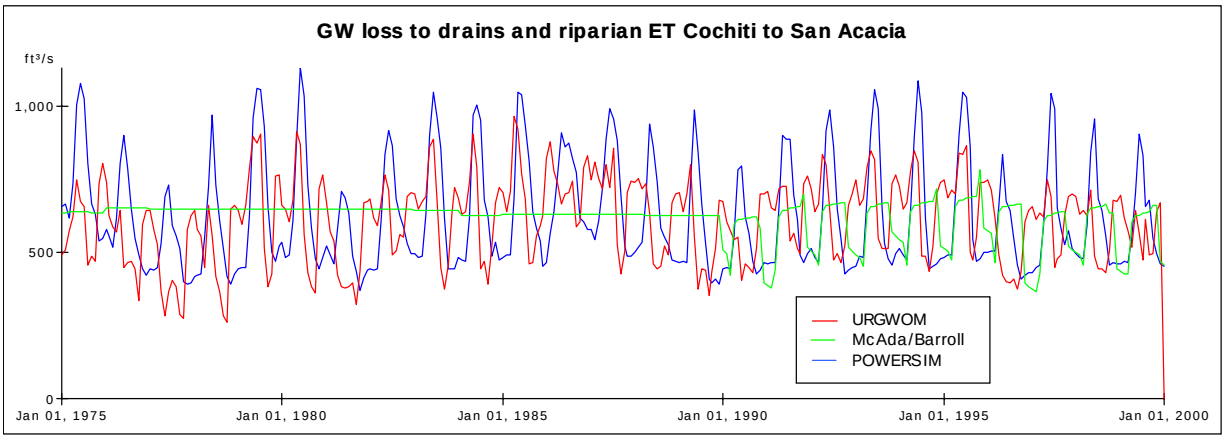

Figure A-8a. Fluxes out of the groundwater system via drains and riparian ET for the Rio Grande reaches from Cochiti to San Acacia as modeled by the coupled monthly timestep model, the URGWOM surface water model, and the McAda and Barroll (2002) regional groundwater model.

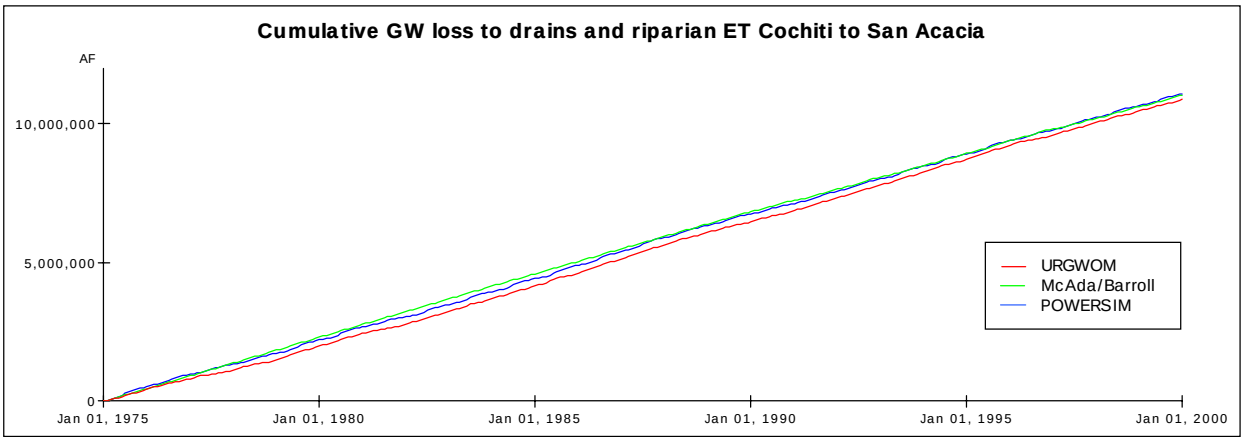

Figure A-8b. Cumulative fluxes out of the groundwater system via drains and riparian ET for the Rio Grande reaches from Cochiti to San Acacia as modeled by the coupled monthly timestep model, the URGWOM surface water model, and the McAda and Barroll (2002) regional groundwater model. Same as Figure 3-20.

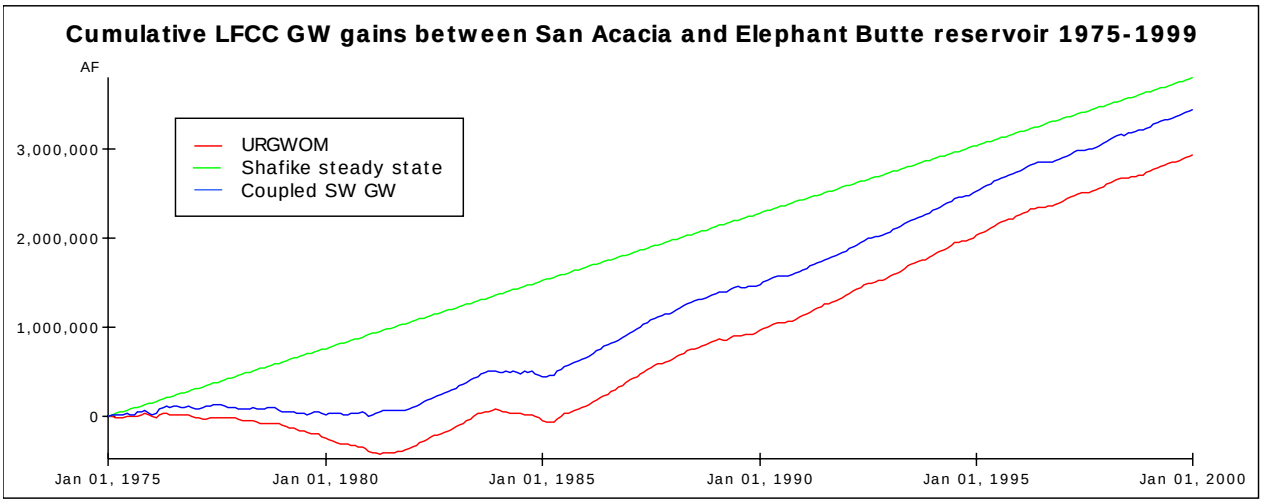

Figure A-9. Cumulative fluxes out of the groundwater system to the low flow conveyance channel for Rio Grande reaches from San Acacia to Elephant Butte as modeled by the coupled monthly timestep model, the URGWOM surface water model, and steady state values reported by Shafike (2005).

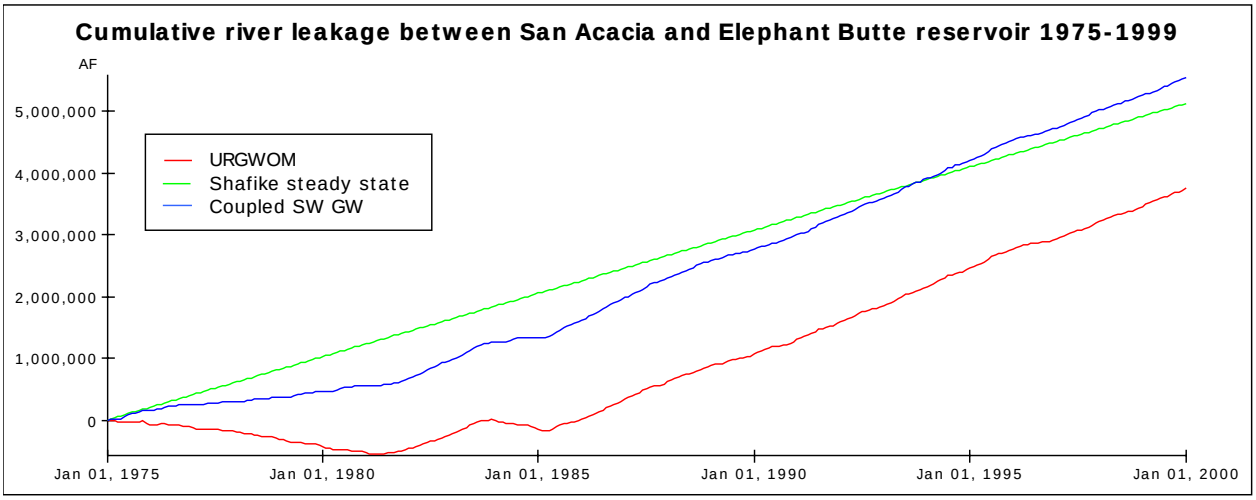

Figure A-10. Cumulative river leakage for Rio Grande reaches from San Acacia to Elephant Butte as modeled by the coupled monthly timestep model, the URGWOM surface water model, and steady state values reported by Shafike (2005).

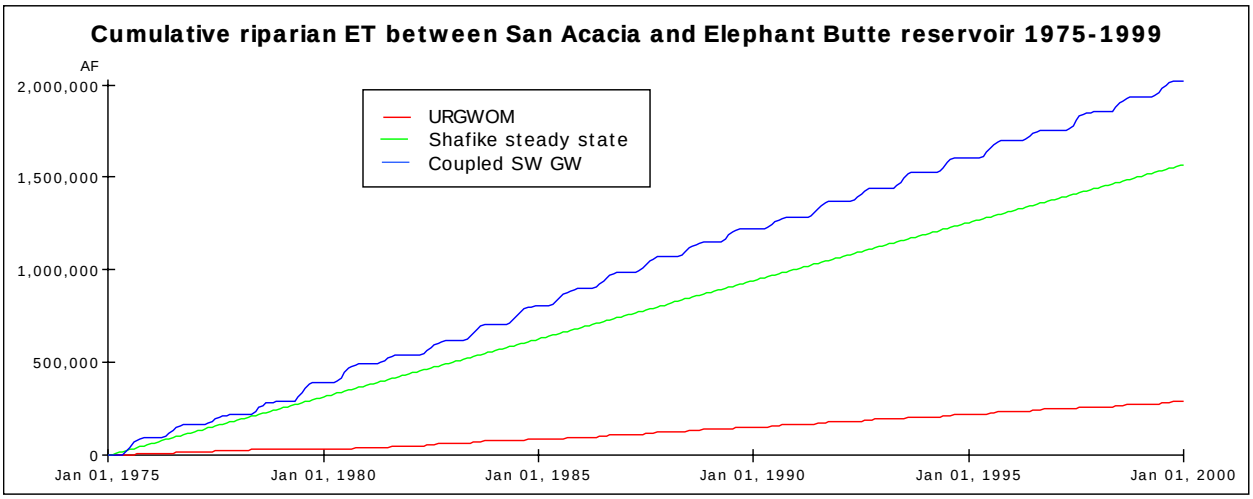

Figure A-11. Cumulative riparian evaportranspiration for Rio Grande reaches from San Acacia to Elephant Butte as modeled by the coupled monthly timestep model, the URGWOM surface water model, and steady state values reported by Shafike (2005).

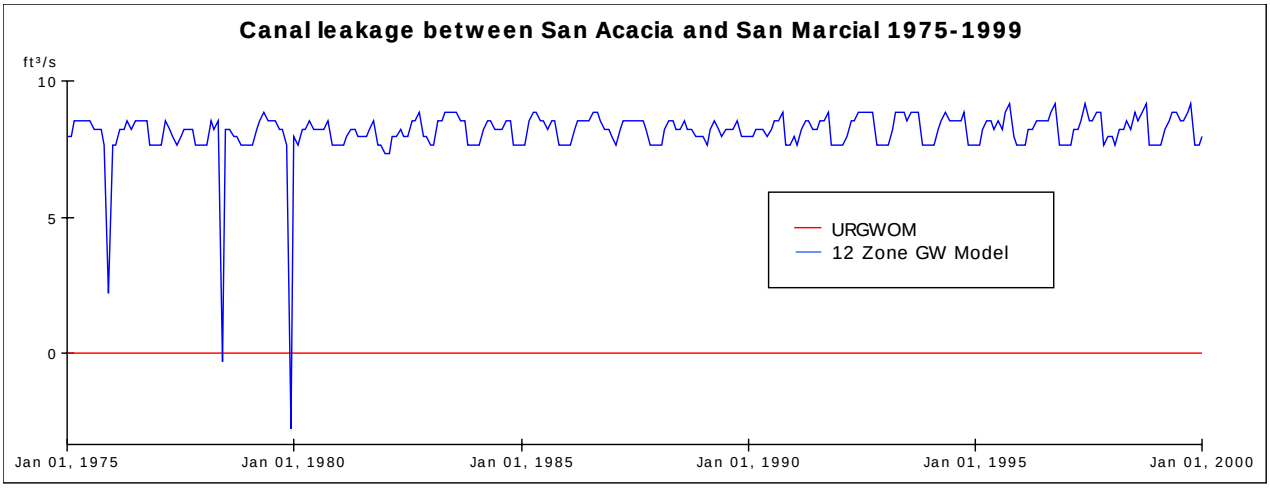

Figure A-12. Irrigation canal leakage between San Acacia and San Marcial as modeled by the coupled monthly timestep model. URGWOM does not track canal leakage in this reach.

APPENDIX B. ECONOMIC DATA AND RESULTS

Table B-1. Prices received by producer.

Year	Alfalfa ($ per ton)	Pasture Grass ($ per ton)	Grains ($ per bushel(	Corn ($ per bushel)	Miscellaneous Vegetables ($ per hundred weight)	Chile ($ per hundred weight)
1975	112	54	3.52	2.66	13	24.7
1976	112	63.5	3.02	2.33	13	24.7
1977	112	58.5	2.18	2.16	13	24.7
1978	112	64	2.85	2.45	13	24.7
1979	112	69	3.95	2.82	13	24.7
1980	112	86.5	3.8	3.44	13	24.7
1981	112	84	3.67	2.88	13	24.7
1982	112	75	3.39	3.07	13	24.7
1983	112	90	3.38	3.39	13	24.7
1984	112	99	3.37	3.03	13	24.7
1985	112	80	2.9	2.49	13	24.7
1986	112	74.5	2.25	1.87	13	24.7
1987	112	89	2.28	2.17	13	24.7
1988	112	102	3.45	2.71	13	24.7
1989	112	89.5	3.68	2.63	13	24.7
1990	114	90	2.79	2.51	13	24.7
1991	110	84.5	2.85	2.68	13	24.7
1992	100	76.5	3.1	2.41	13	24.7
1993	105	84	2.8	2.61	13	24.7
1994	123	93	3.3	2.51	13	24.7
1995	116	92.5	4.5	3.19	13	24.7
1996	129	98.5	5.1	3.19	13	24.7
1997	127	97	3.25	2.74	13	24.7
1998	120	97	2.65	2.26	13	24.7
1999	116	94	2.4	2.07	16	24.7
2000	124	102	2.7	2.18	9.25	24.7
2001	126	107	2.75	2.29	14.4	29.7
2002	143	117	3.45	2.57	12.5	29.2
2003	148	122	3.2	2.6	12.5	29.2
2004	153.92	126.88	3.33	2.7	13	30.37
2005	160.08	131.96	3.46	2.81	13.52	31.58
2006	166.48	137.24	3.6	2.92	14.06	32.84
2007	173.14	142.73	3.74	3.04	14.62	34.15
2008	180.07	148.44	3.89	3.16	15.2	35.52
2009	187.27	154.38	4.05	3.29	15.81	36.94
2010	194.76	160.56	4.21	3.42	16.44	38.42
2011	202.55	166.98	4.38	3.56	17.1	39.96
2012	210.65	173.66	4.56	3.7	17.78	41.56
2013	219.08	180.61	4.74	3.85	18.49	43.22
2014	227.84	187.83	4.93	4	19.23	44.95
2015	236.95	195.34	5.13	4.16	20	46.75

Table B-1. Prices received by producer (continued).

Year	Alfalfa ($ per ton)	Pasture Grass ($ per ton)	Grains ($ per bushel(	Corn ($ per bushel)	Miscellaneous Vegetables ($ per hundred weight)	Chile ($ per hundred weight)
2016	246.43	203.15	5.34	4.33	20.8	48.62
2017	256.29	211.28	5.55	4.5	21.63	50.56
2018	266.54	219.73	5.77	4.68	22.5	52.58
2019	277.2	228.52	6	4.87	23.4	54.68
2020	288.29	237.66	6.24	5.06	24.34	56.87
2021	299.82	247.17	6.49	5.26	25.31	59.14
2022	311.81	257.06	6.75	5.47	26.32	61.51
2023	324.28	267.34	7.02	5.69	27.37	63.97
2024	337.25	278.03	7.3	5.92	28.46	66.53
2025	350.74	289.15	7.59	6.16	29.6	69.19

Table B-2. Per acre costs in 2004$.

Year	Alfalfa	Pasture Grass	Corn	Grains	Miscellaneous Vegetables	Chile Peppers
1975	141.93	70.9	153	126.4	612.5	612.5
1976	140.7	70.3	151.7	125.3	607.2	607.2
1977	144.4	72.1	155.7	128.6	623.2	623.2
1978	146.6	73.2	158.1	130.6	632.7	632.7
1979	148.3	74	159.9	132.1	639.8	639.8
1980	145.8	72.8	157.2	129.9	629.1	629.1
1981	143.5	71.7	154.7	127.9	619.3	619.3
1982	149.1	74.5	160.7	132.8	643.3	643.3
1983	160.4	80.2	172.9	142.9	692.1	692.1
1984	174.6	87.3	188.2	155.5	753.3	753.3
1985	189.3	94.6	204	168.6	816.6	816.6
1986	204	102	219.8	181.7	880.1	880.1
1987	218.5	109.3	235.5	194.6	942.8	942.8
1988	231.1	115.6	249.1	205.8	997.3	997.3
1989	244.1	122.1	263.1	217.3	1053.2	1053.2
1990	255	127.5	274.8	227	1100.2	1100.2
1991	265	132.5	285.6	235.9	1143.3	1143.3
1992	277.1	138.6	298.6	246.7	1195.5	1195.5
1993	291.3	145.7	314	259.4	1257	1257
1994	303.6	151.8	327.2	270.3	1310	1310
1995	319.9	159.9	344.8	284.8	1380.3	1380.3
1996	335.2	167.6	361.3	298.4	1446.4	1446.4
1997	350.2	175.1	377.5	311.7	1511.1	1511.1
1998	367.6	183.8	396.3	327.2	1586.2	1586.2
1999	385.7	192.9	415.8	343.3	1664.4	1664.4
2000	404.4	202.3	436	360	1745.1	1745.1
2001	421.5	210.8	454.4	375.2	1818.7	1818.7
2002	439.5	219.8	473.8	391.3	1896.5	1896.5
2003	461	230.5	497	410.4	1989.2	1989.2
2004	477	238.45	514.2	424.6	2058	2058
2005	496.1	248	534.8	441.6	2140.3	2140.3
2006	515.9	257.9	556.2	459.3	2225.9	2225.9
2007	536.5	268.2	578.4	477.7	2314.9	2314.9

Table B-3. Birding study summary information.

Authors	Date	Title	Activities	Applicable	Location	Comments	Mean	95% CI	Median	VT or FT?
Loomis & Creel	Jan-92	Recreation benefits of increased flows in California's San Joaquin and Stanislaus Rivers	Angling, wildlife viewing, waterfowl hunting.		San Joaquin Valley - San Joaquin and Stanislaus rivers	Area includes ntl wildlife refuges, wildlife mgt areas, San Joaquin River & tributaries, and Kings River. Values for current conditions. Also values for increased flows, but these values are not broken down by recreational activity.	expected annual use value/person for wildlife viewing = $128			VT
Eubanks &Stoll (Fermata Inc.)	Oct-99	Avitourism in Texas: Two studies of birders in Texas and their potential support for the proposed World Birding Center	birding		Lower Rio Grande Valley (Texas)	Difficult to determine total WTP, as current expenditures and additional WTP are measured differently (one is per person and the other is per trip). GTCBT = ?; RGVB = some festival. Perhaps not very useful, as study areas and values are not well defined.	current expenditures: GTCBT = $981.99/person RGVB = $976.40/person additional WTP: GTCBT = $214.03/trip RGVB = $205.09/trip			VT
Eubanks, Ditton, Stoll (Fermata Inc.)		Platte River nature recreation study - Executive Summary: The economic impact of wildlife watching on the Platte River in Nebraska	wildlife watching, primarily birding	Bosque	Platte River (Nebraska)	http://www.fermatainc.com/basic/eco_nebplatte.html Sandhill Cranes Current expenditures and additional WTP are measured differently (one is per person and the other is per year), but # of trips/yr is also provided. People come from all over world.	current expenditures = $336/person additional WTP = $192.75/year average # trips = 3.5 total WTP = $400.25/trip			VT

Table B-3. Birding study summary information (continued).

Authors	Date	Title	Activities	Applicable	Location	Comments	Mean	95% CI	Median	VT or FT?
Hvenegaard, Butler, & Drystofiak	1989	Economic values of bird watching at Point Pelee National Park, Canada	birding	Bosque	Point Pelee National Park (Canada)	Is a small national park. Premier birding location in North America during the month of May.	WTP = $480/trip or $142/day			VT
William R. Clark (author); [Diamond & Filion (eds.)]	1987	Economics and marketing of 'Canada's Capistrano', *in* The value of birds: Based on the proceedings of a symposium and workshop held at the XIX World Conference of the International Council for Bird Preservation	birding	Bosque (?)	Canada		net benefits per visit (Pembroke swallows attraction) = $5.06 (1986$)			VT
Kaval & Loomis	2003	Updated outdoor recreation use values with emphasis on national park recreation	birding	(need to look at original studies to determine applicability)	US	Values are based upon four US studies conducted in NE and SE. Values for broken out by activity per person per day, and are in 1996 dollars.	mean = $24.67 min = $4.83 max = $65.38	se = $6.96		VT
Connelly & Brown	1988	Estimates of nonconsumptive wildlife use on Forest Service and BLM lands	nonconsumptive wildlife use		US	Estimates of # of trips, # of days, & # of hrs on trips to BLM and FS land, by state (and forest service region). Estimate of net econ value/trip. *Too broad & general to be useful (?)*				N/A

Table B-3. Birding study summary information (continued).

Authors	Date	Title	Activities	Applicable	Location	Comments	Mean	95% CI	Median	VT or FT?
La Rouche (USFWS)	2001	Birding in the United States: A demographic and economic analysis. Addendum to the 2001 National Survey of Fishing, Hunting and Wildlife-Associated Recreation	wildlife watching		US	84% of away-from-home wildlife watchers are birders. Demographic characteristics provided.	CS = $134/day or $488/yr for viewing wildlife outside the state; CS = $35/day or $257/yr for viewing wildlife in state	outside state: $415-561 (annual) $110-158 (daily) inside state: $233-282 (annual) $32-39 (daily)		VT
Montana Birding & Nature Trail Steering Committee	2004	Adding it up: Economic value of birding wildlife viewing to Montana	birding; wildlife watching		Montana	Univ. Montana website: biology.umt.edu/landbird/birdtrail/Adding_it_up.pdf	CS = $134/day for viewing wildlife outside the state CS = $35/day for viewing wildlife in state			VT
Hay	1988	Net economic values of non-consumptive wildlife-related recreation	observing, photographing, or feeding wildlife		US (broken out by state)	Mean values for away-from-home activities. Includes both within state and outside of state trips.	Mean net economic values per day - (see Table 1)		Median net economic values per day - (see Table A.1)	VT
Rosenberger & Loomis	2000	Benefit transfer of outdoor recreation use values	wildlife viewing							
Aiken & La Rouche	2003	Net economic values of non-consumptive wildlife-related recreation in 2001: Addendum to the 2001 National Survey of Fishing, Hunting and Wildlife-Associated Recreation	wildlife watching		New Mexico	Per day CS values are given for NM residents. Sample size is too small to yield reliable results for non- NM residents.	mean = $42	se = $8		VT

Table B-3. Birding study summary information (continued).

Authors	Date	Title	Activities	Applicable	Location	Comments	Mean	95% CI	Median	VT or FT?
Cooper & Loomis (authors); Dinar & Zilberman (eds.)	1991	Economic value of wildlife resources in the San Joaquin Valley: Hunting and viewing values, *in* The Economics and Management of Water and Drainage in Agriculture	bird viewing	general areas (?)	California	Provides net WTP per trip based upon # of birds seen per trip. Average number of trips/year = 3	**Net WTP/trip:** current conditions (# birds seen = 28): $37.33 50% more birds (# birds seen = 42): $45.00 100% more birds (# birds seen = 56): $46.67			
Crandall, Colby, & Rait	1992	Valuing riparian areas: A southwestern case study	birders, nature lovers, escapees from desert heat	Bosque del Apache	Hassayampa River Preserve, Arizona	TCM analysis of trips for which primary purpose was to visit Hassayampa; # visits as a fn of cost, age, income. CVM based upon change in flow from intermittent to perennial.	**TCM:** CS = $97/visitor See equation on p.94 **CVM:** indiv. WTP = $65			

Table B-4. NAICS sector with associated job type distribution.

20 NAICS Sectors	Management Occupations	Business and Financial Operations Occupations	Computer and Mathematical Occupations	Architecture and Engi-neering	Life, Physical, and Social Science Occupations	Community and Social Services	Legal Occupations	Education, Training, and Library
Ag, forestry, fishing, hunting	0.01750	0.00430	0.00090	0.00020	0.00470	0.00000	0.00000	0.00030
Mining	0.05800	0.03870	0.01260	0.04470	0.03040	0.00000	0.00530	0.00000
Utilities	0.05660	0.06480	0.03120	0.08500	0.01710	0.00000	0.00170	0.00010
Construction	0.04860	0.02740	0.00110	0.00970	0.00040	0.00000	0.00020	0.00000
Manufacturing	0.04970	0.02990	0.01900	0.05590	0.01050	0.00000	0.00040	0.00010
Wholesale trade	0.05700	0.03790	0.02670	0.01090	0.00490	0.00000	0.00040	0.00000
Retail trade	0.02450	0.01090	0.00400	0.00030	0.00030	0.00000	0.00010	0.00040
Transportation and warehousing	0.03020	0.01830	0.00470	0.00440	0.00070	0.00000	0.00040	0.00020
Information	0.06340	0.04730	0.13370	0.02260	0.00890	0.00010	0.00190	0.00520
Finance and insurance	0.07570	0.21010	0.05020	0.00080	0.00510	0.00050	0.01020	0.00020
Real estate	0.09110	0.04450	0.00580	0.00180	0.00230	0.00080	0.00400	0.00030
Professional and technical services	0.07310	0.11170	0.13370	0.12020	0.04520	0.00120	0.08390	0.00300
Management of companies	0.16290	0.16030	0.09010	0.02760	0.01770	0.00960	0.01010	0.00350
Administration and waste services	0.02960	0.03110	0.01620	0.00920	0.00300	0.00120	0.00240	0.00330
Education	0.04370	0.01660	0.01360	0.00180	0.01240	0.02040	0.00020	0.59380
Health and social services	0.03500	0.01280	0.00480	0.00040	0.00530	0.05470	0.00030	0.03080
Arts, entertainment and recreational services	0.03590	0.01780	0.00270	0.00060	0.00250	0.00030	0.00020	0.01750
Accommodations and food services	0.02660	0.00340	0.00020	0.00000	0.00010	0.00000	0.00000	0.00010
Other services	0.04830	0.04890	0.00700	0.00200	0.00320	0.02610	0.00180	0.02070
Government/public administration, and non-NAICS	0.05390	0.08690	0.02180	0.03020	0.03070	0.04980	0.02790	0.02210

Table B-5. NAICS sector with associated job type distribution.

20 NAICS Sectors	Arts, Design, Entertainment, Sports, and Media	Health Care Practitioner and Technical Occupations	Health Care Support Services	Protective Services	Food Preparation and Serving Related	Building and Grounds Cleaning and Maintenance	Personal Care and Service Occupations	Sales and Related Occupations
Ag, forestry, fishing, hunting	0.00070	0.00100	0.00100	0.00130	0.00010	0.01520	0.01360	0.00730
Mining	0.00060	0.00400	0.00000	0.00100	0.00030	0.00300	0.00000	0.01300
Utilities	0.00400	0.00230	0.00000	0.00640	0.00010	0.00550	0.00000	0.01730
Construction	0.00100	0.00020	0.00000	0.00080	0.00030	0.00670	0.00020	0.01980
Manufacturing	0.00570	0.00110	0.00010	0.00130	0.00270	0.00680	0.00010	0.02960
Wholesale trade	0.00830	0.00280	0.00030	0.00090	0.00080	0.00490	0.00020	0.25950
Retail trade	0.00840	0.02570	0.00290	0.00450	0.03140	0.00860	0.00570	0.54160
Transportation and warehousing	0.00080	0.00080	0.00010	0.00310	0.00210	0.00650	0.02950	0.01850
Information	0.15680	0.00040	0.00000	0.00190	0.01480	0.00410	0.01820	0.12940
Finance and insurance	0.00330	0.00520	0.00040	0.00210	0.00030	0.00290	0.00010	0.12310
Real estate	0.00620	0.00360	0.00270	0.01590	0.01140	0.08060	0.01090	0.24390
Professional and technical services	0.04250	0.01960	0.01020	0.00160	0.00050	0.00650	0.00410	0.04400
Management of companies	0.01480	0.01280	0.00450	0.00650	0.00860	0.01390	0.00710	0.05950
Administration and waste services	0.00500	0.02460	0.01290	0.07990	0.01500	0.19780	0.00750	0.06300
Education	0.01540	0.01860	0.00270	0.00890	0.03810	0.04500	0.01580	0.00270
Health and social services	0.00170	0.33300	0.19100	0.00460	0.03380	0.02920	0.06630	0.00310
Arts, entertainment and recreational services	0.09370	0.00450	0.00290	0.04270	0.17170	0.10260	0.26020	0.08050
Accommodations and food services	0.00170	0.00020	0.00000	0.00570	0.78830	0.05370	0.01260	0.03270
Other services	0.01900	0.00270	0.00640	0.01190	0.02630	0.03000	0.17700	0.06020
Government/public administration, and non-NAICS	0.00600	0.04180	0.01550	0.19630	0.01110	0.02560	0.02810	0.00760

Table B-6. NAICS sector with associated job type distribution.

20 NAICS Sectors	Office and Admin Support Occupations	Farming, Fishing, and Forestry Occupations	Construction and Extraction Occupations	Installation, Maintenance, and Repair Occupations	Production Occupations	Transportation and Material Moving Occupations
Ag, forestry, fishing, hunting	0.05670	0.68150	0.00190	0.02240	0.03120	0.13820
Mining	0.09620	0.00050	0.36340	0.08140	0.09610	0.15010
Utilities	0.21590	0.00070	0.06100	0.27060	0.13680	0.02300
Construction	0.09640	0.01500	0.66750	0.06970	0.01260	0.03730
Manufacturing	0.09770	0.00240	0.01870	0.05030	0.52410	0.09390
Wholesale trade	0.23560	0.00920	0.00400	0.06790	0.05820	0.20930
Retail trade	0.16340	0.00160	0.00390	0.05330	0.02940	0.07900
Transportation and warehousing	0.29710	0.00050	0.00510	0.05920	0.01280	0.50510
Information	0.23540	0.00000	0.00110	0.09790	0.02900	0.02790
Finance and insurance	0.50610	0.00000	0.00030	0.00230	0.00050	0.00060
Real estate	0.23400	0.00070	0.01410	0.14780	0.00610	0.07150
Professional and technical services	0.25780	0.00060	0.00810	0.00880	0.01530	0.00820
Management of companies	0.30030	0.00250	0.00790	0.02340	0.02000	0.03630
Administration and waste services	0.21850	0.00370	0.03500	0.02325	0.08740	0.13040
Education	0.10720	0.00030	0.00360	0.01275	0.00180	0.02450
Health and social services	0.16900	0.00010	0.00120	0.00790	0.00730	0.00750
Arts, entertainment and recreational services	0.09580	0.00290	0.00540	0.03660	0.00320	0.02000
Accommodations and food services	0.03790	0.00000	0.00040	0.00840	0.00740	0.02010
Other services	0.15280	0.00030	0.00360	0.17050	0.09020	0.09090
Government/public administration, and non-NAICS	0.19120	0.00250	0.04980	0.03960	0.01860	0.04300

Table B-7. SOC job types and skill-level distribution.

SOC Job Type	Unskilled	Blue Collar	White Collar	Professional
Management Occupations	0.0789	0.0562	0.7495	0.1154
Business and Financial Operations Occupations	0.2364	0.0442	0.6416	0.0778
Computer and Mathematical Occupations	0.0649	0.0000	0.8980	0.0372
Architecture and Engineering Occupations	0.1566	0.2766	0.5327	0.0341
Life, Physical, and Social Science Occupations	0.2382	0.1854	0.1558	0.4206
Community and Social Services Occupations	0.1087	0.1858	0.0596	0.6460
Legal Occupations	0.0814	0.2657	0.0444	0.6086
Education, Training, and Library Occupations	0.1091	0.0326	0.5550	0.3033
Arts, Design, Entertainment, Sports, and Media Occupations	0.1049	0.3442	0.5509	0.0000
Healthcare Practitioners and Technical Occupations	0.0640	0.2985	0.4587	0.1788
Healthcare Support Occupations	0.0645	0.9271	0.0085	0.0000
Protective Service Occupations	0.0739	0.9262	0.0000	0.0000
Food Preparation and Serving Related Occupations	0.0119	0.9881	0.0000	0.0000
Building and Grounds Cleaning and Maintenance Occupations	0.0214	0.9786	0.0000	0.0000
Personal Care and Service Occupations	0.0504	0.9496	0.0000	0.0000
Sales and Related Occupations	0.0532	0.9078	0.0464	0.0000
Office and Administrative Support Occupations	0.0338	0.9611	0.0052	0.0000
Farming, Fishing, and Forestry Occupations	0.0532	0.9432	0.0036	0.0000
Construction and Extraction Occupations	0.0289	0.9711	0.0000	0.0000
Installation, Maintenance, and Repair Occupations	0.0469	0.9531	0.0000	0.0000
Production Occupations	0.1006	0.8994	0.0000	0.0000
Transportation and Material Moving Occupations	0.0289	0.9511	0.0200	0.0000

Table B-8. Test for accuracy of methods.

20 NAICS Sectors	Summed Skill-Level Weights from Table 4-2	Summed SOC Weights from Appendix Table 4-1 (a, b, c)
Ag, forestry, fishing, hunting	1.00005	1.00000
Mining	0.99940	0.99930
Utilities	1.00023	1.00010
Construction	1.01505	1.01490
Manufacturing	1.00022	1.00000
Wholesale trade	1.00163	0.99970
Retail trade	1.00392	0.99990
Transportation and warehousing	1.00024	1.00010
Information	1.00096	1.00000
Finance and insurance	1.00091	1.00000
Real estate	1.00181	1.00000
Professional and technical services	1.00013	0.99980
Management of companies	1.00034	0.99990
Administration and waste services	1.00042	0.99995
Education	0.99987	0.99985
Health and social services	0.99982	0.99980
Arts, entertainment and recreational services	1.00080	1.00020
Accommodations and food services	0.99974	0.99950
Other services	1.00025	0.99980
Government/public administration, and non-NAICS	1.00006	1.00000

Table B-9. Urban demand and population assumptions.

1. Assume representative consumer. Aggregate demand is number of households times individual demand.
2. Number of households is a stock that increases as the population increases.
3. Assume people per household follows a trajectory similar to the last ten years for ten years, then assume people per household is geld constant. (This can be altered and used as a scenario for quality of life).
4. The Census records information about types of households. Specifically:
    a) 1-Unit detached
    b) 1-Unit attached
    c) 2-Unit
    d) 3 or 4 Units
    e) 5-9 Units
    f) 10-19 Units
    g) 20+ Units
    h) Mobile homes
5. Assume that a, b, c, and h have lawns and follow in the individual demand functions estimated by month.
6. Assume d, e, f, and g are apartment-dweller equivalents and have a base water demand proxied by the January demand. An alternative is to assume a constant per person per day use. Assume that the difference between the number of households recorded in the Census and the number of residential accounts the water utility has is the number of residences that are on wells (less the number of residences in the county that do not have any plumbing. Assume those residences on wells use the total legal amount of water per year. Assume the percentage of household structure type remains constant at the 2000 breakout: 74% single (or duplex) dwelling, 26% apartments.
7. Assume vacancy rates remain at the current rates.

Table B-10. Housing type (data from Census).

Demand Type	Housing Type	1990 (units)	% of Total 1990	Sum	2000 (units)	% of Total 2000	Sum 2000	% Change (1990 to 2000)	Average Annual % Change
Varies by Month	Single-detached	116,812	0.58	0.74	144,388	0.60	0.74	0.24	0.024
	Single-attached	11,121	0.06		13,727	0.06		0.23	0.023
	2-Units	4,163	0.02		4,372	0.02		0.05	0.005
	Mobile Homes	15,869	0.08		15,582	0.07		-0.02	-0.002
Base Demand (January Proxy)	3-4 units	12,728	0.06	0.26	13,368	0.06	0.26	0.05	0.005
	5-9 units	7,800	0.04		9,930	0.04		0.27	0.027
	10-19 units	9,331	0.05		10,662	0.04		0.14	0.014
	20+ units	23,411	0.12		26,752	0.11		0.14	0.014
	TOTAL HOUSING UNITS	201,235	1.00	1.00	23,074	1.00	1.00	0.19	0.019

Table B-11. Occupied and vacancy rates.

	1990	% of Total 1990	2000	% of Total 2000
Total Units	201,235		239,074	
Owner-Occupied	112,589	0.56	140,634	0.59
Rental	72,993	0.36	80,302	0.34
Vacant	15,653	0.08	18,138	0.08
Homeowner Vacancy	0.017		0.018	
Rental Vacancy	0.102		0.115	

Table B-12. Average number of people per household.

Type	1990	2000	Change
Own	2.73	2.61	0.12
Rent	2.28	2.22	0.06

DISTRIBUTION

6 The University of New Mexico
Department of Economics
Attn: Janie Chermak
David Brookshire
Kristine Grimsrud
Jennifer Thacher
Craig Broadbent
Jason Hanson
1915 Roma NE/Economics Building
Albuquerque, NM 87131-1101

2 New Mexico Tech
Attn: Enrique Vivoni
Carlos Aragon
Department of Earth and Environmental Sciences
801 Leroy Place, MSEC 244
Socorro, NM 87801

1 Cockerill Consulting
Attn: Kristan Cockerill
207 Cecil Miller Rd #2
Boone, NC 28607

1 University of Chicago
Attn: Don Coursey
Graduate of Public Policy Studies, 130 Harris
5801 South Ellis
Chicago, IL 60637

1 Heather Hallett
4801 San Mateo Lane NE, Apt. 178
Albuquerque, NM 87109

2	MS9018	Central Technical Files	8944
2	MS 0123	LDRD Office	011
1	MS 0370	George Backus	433
1	MS 0701	Peter Davies	6700
1	MS 0706	Peter Kobos	6312
1	MS 0735	John Merson	6310
1	MS 0735	Marissa Reno	6313
1	MS 0735	Ray Finley	6313
1	MS 0735	Ron Pate	6313

1	MS 1104	Marjorie Tatro	6200
1	MS 1110	William Hart	1415
1	MS 1138	Stephen Conrad	6322
1	MS 1138	Thomas Corbet, Jr.	6322
5	MS 1350	Vincent Tidwell	6313
1	MS 1350	Len Malczynski	6313
1	MS 1350	Howard Passell	6313
1	MS 1350	Jesse Roach	6313
1	MS 1350	William Peplinski	6313
2	MS0899	Technical Library	4536